CSIR-IIIM

वार्षिक प्रतिवेदन
Annual Report
2012-2013

सीएसआइआर–भारतीय समवेत औषध संस्थान, जम्मू–180001 (भारत)
CSIR-Indian Institute of Integrative Medicine
(Council of Scientific and Industrial Research)
JAMMU-180001 (INDIA)

CONTENTS

CONTENTS

DIRECTORS REPORT

I take pleasure in presenting this Annual Report of CSIR-Indian Institute of Integrative Medicine, Jammu and Srinagar which covers the highlights of the R&D work carried during 2012-13. This year augured very good and important for this institute as 9 research projects were approved by CSIR for IIIM for the 12th Five Year Plan period. Out of these IIIM is the nodal institute for the following two important projects.

1. ***Medicinal chemistry for Stem Cell Biology***
2. ***Nurturing a new PAN-CSIR drug pipe line: high intensity preclinical, clinical studies on lead candidates.***

During this period IIIM applied for nine product patents and published 124 research papers with average impact factor steadily increasing over the years from 2.0 to 2.9.

IIIM Jammu is also committed to establish a TECHVIL at Bhalessa, district Doda, in J&K which is about 262 kilometers from Jammu. It is proposed to improve the quality of life of the people living in this remote area, Increase the avenues for their self employment and income generation by cultivating low volume high value essential oil bearing plants in the small land holdings owned by them. IIIM already has for the first time in Jammu region, started the cultivation of lavender plantation, which is coming up very nicely.

For the promotion and usage of Hindi language in day to day official work, besides religiously conducting two meetings of TOLIC in a year, IIIM has also started the publication of an annual Hindi Journal "**GYANVARTA**" which has been highly appreciated by the concerned.

The following details in this report shall present to you the flavor of R&D work being carried out in this institute

(Ram Vishwakarma)

1.BIODIVERSITY AND APPLIED BOTANY

1.1 Glutathione regulates enzymatic antioxidant defence with differential thiol content in perennial pepperweed and helps adapting to extreme environment

Tarandeep Kaur, Hilal A. Bhat, Anuj Raina, Sushma Koul and Dhiraj Vyas

Perennial pepperweed (*Lepidium latifolium* Linn.) is a preferred 'phytofood' that is available for the longest period of a year in Ladakh. A study was undertaken to identify the mechanism of redox homeostasis and understand factors responsible for its biochemical superiority during low temperatures. Results reveal that despite the stressful environment at higher altitude, the cellular conditions are more reducing for this plant (Fig.1). The reducing environment is maintained by significant induction of GSH rather than changes in its oxidation state, which changes the redox potential by 12 mV. Lower ratio of NADP?/NADPH and induction of new antioxidative isozymes at Leh (3,505 m) suggest crucial role of redox regulation in adaptation. These new proteins have higher thiol content and could provide an efficient redox sensing mechanism in *Lepidium latifolium* that respond through GSH/NADPH redox buffers. *In vitro* feeding experiment suggested that GSH plays an important role in induction of antioxidant enzymes, which may not be the direct consequence of H_2O_2 accumulation. It needs to be further investigated whether its responsive redox metabolism has some role in its invasive growth in riparian plains of America. Our results suggest that *L. latifolium* has a responsive redox homeostasis which is achieved through GSH and/or NADPH redox couples (Fig.2). This helps the plant against low temperature-mediated photo-oxidative damage by activating more PSI reaction centres and channelizes their metabolic energy through the most efficient route. The adjustment of redox status, leads to induction of proteins with higher thiol content suggesting their increased dependence on redox regulation. There could be other factors such as soil quality, seed dispersal, their germination and other biotic considerations (associated microbiome, pests and herbivores) that are important for long-term adaptation under different environments.

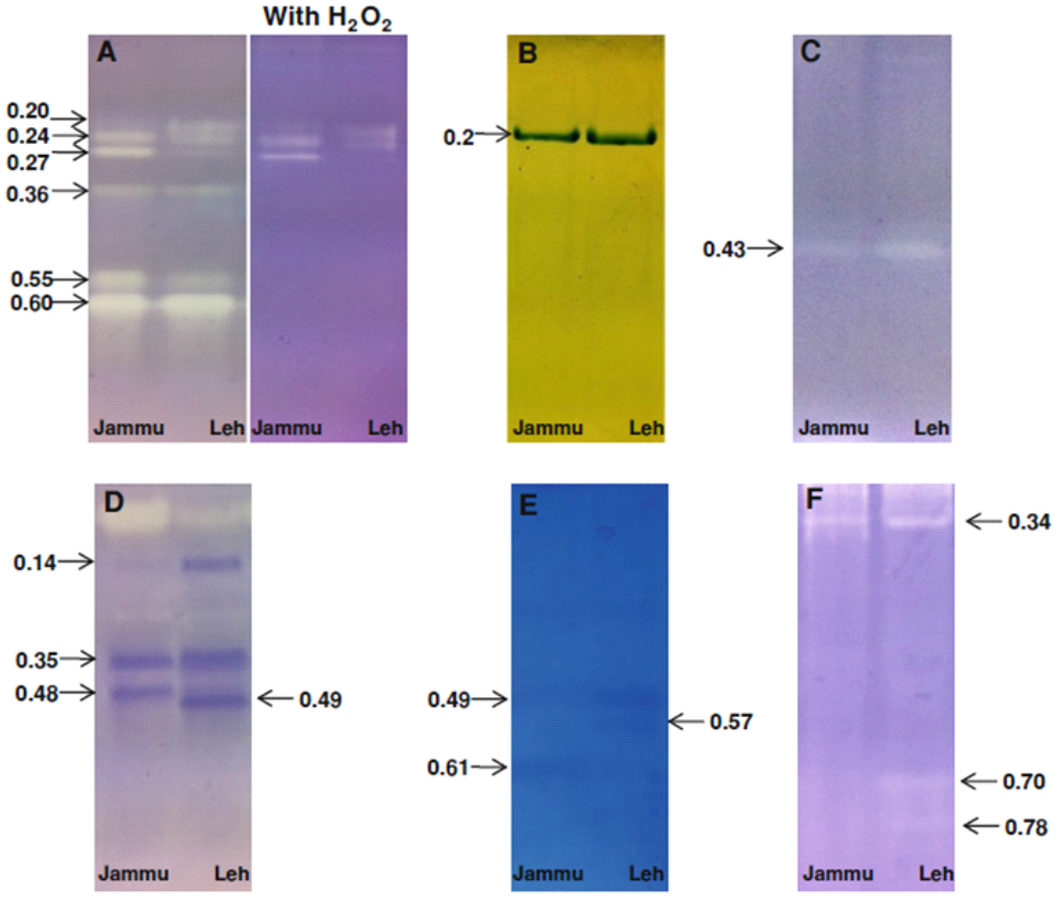

Figure 1 : *Zymogram pattern of various redox regulating and antioxidant enzymes in leaves grown at Leh (3,505) and Jammu (305 m) arrow indicates isozymes and their corresponding Rf.Pannel represent Superoxide dismutase (a), catalase 9b), ascorbate peroxidase (c), glutathione reductase (d), dehydroascorbate reductase (e) and ascobate oxidase (f)*

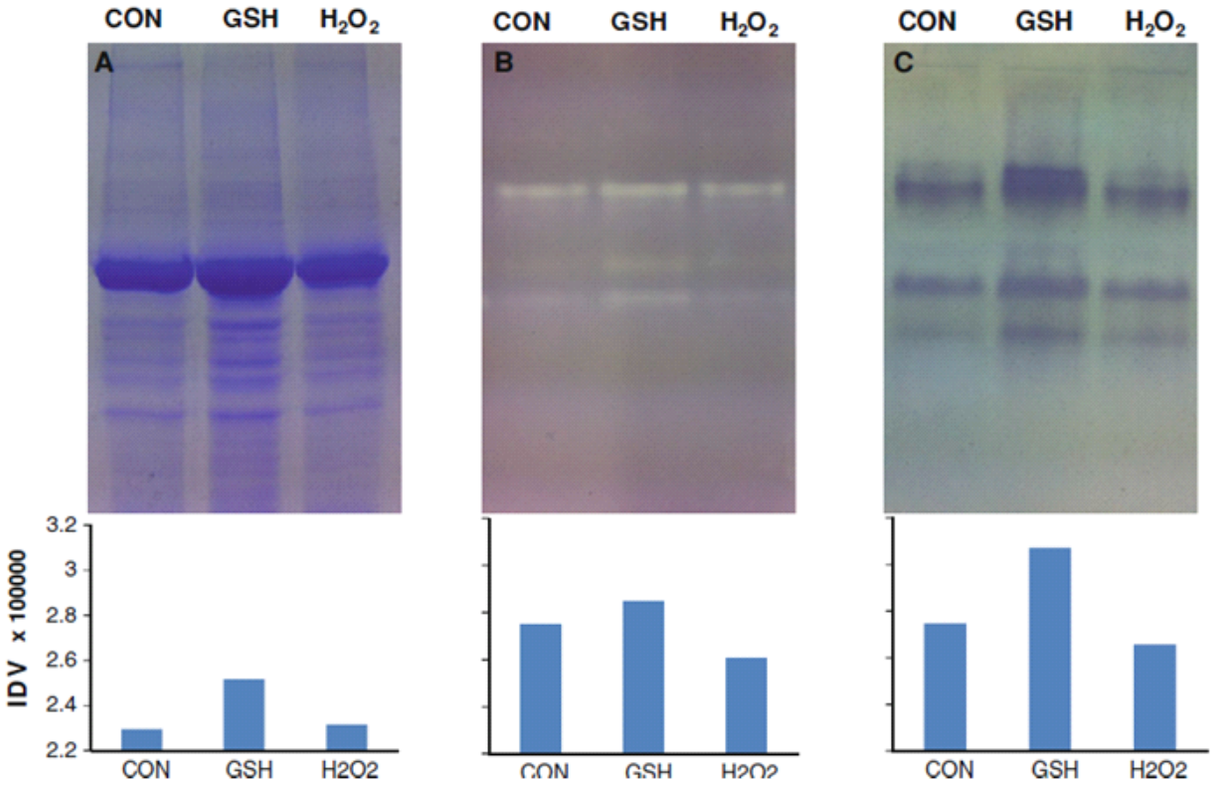

Figure 2 : PAGE analysis of (a) total protein under denaturating conditions, (b) SOD staining under native conditions and (c) GR staining under native conditions

1.2 Reproductive biology of *Withania ashwagandha* sp. novo (Solanaceae)

Bilal Ahmad Mir, Arun Kumar and Sushma Koul

Withania ashwagandha Kaul (Solanaceae) is an annual plant species of immense medicinal importance. It is a repository of a large number of pharmacologically active secondary metabolites known as withanolides. Evidence for the delimitation of the species from *W. somnifera* has been provided by our group using multidisciplinary approaches. Knowledge of reproductive biology of medicinal plants is crucial for improvement, effective conservation and management plans to evolve genetically superior varieties. Study was conducted on the floral biology, pollination behavior and breeding system of *W. ashwagandha* in natural populations grown at our experimental field under near natural conditions (Fig.1). Flowering (peak) takes place during April–July and anthesis occurs between 08:00 and 11:00 h. The period of stigma receptivity coincides with anther dehiscence. Fruit set on pollination treatments ranged from 90.8% (passive autogamy), 72% (assisted autogamy), 30.30% (xenogamy), and 56.50% (geitonogamy) through 50.40% (open pollination). Xenogamy brings about very low fruit set, seed-set and seed germination percentages. It is inferred that *W. ashwagandha* is predominantly an autogamous and self-compatible species. Self-compatibility is mainly accomplished due to close proximity of stigma and anthers. A high percentage of fruit and seed set in controlled self pollination experiments in *W. ashwagandha* confirmed its self-compatible nature. Results of pollination experiments also confirm absence of apomixis. The floral architecture especially relative size and close proximity of stigma and anthers predispose the species for self pollination. The species shows rare occurrence in natural habitats; it needs conservation via 'in situ' as well as 'ex situ' methods. Large scale cultivation in its natural habitat on one hand and limited exploitation for the market demand on the other is the only option for conservation. Breeding experiments of this medicinally important plant species (especially xenogamy) will open new dimensions for genetic improvement of crop in future. Further, the information generated by the present study will help in development of hyperproductive varieties with respect to withanolides content and root biomass by inter varietal crosses besides being useful for studying the chemogenetic inheritance of withanolides.

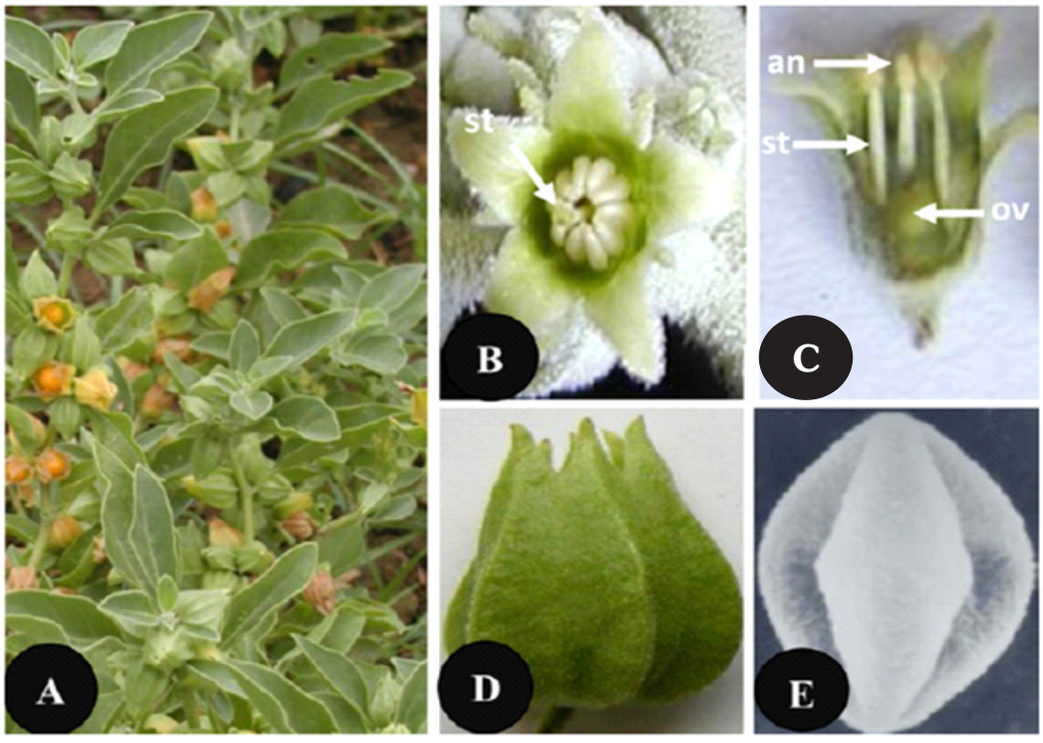

Figure 1 : *Withania ashwagandha* (A) Fruiting twig with orange berries, (B) single flower Showing arrangement of pistil, stamen and greenish receptive stigma, (C) LS of flower two days after anthesis , (D) Elongated fruiting calyx and (E) Scanning electron micrograph of pollen

1.3 Divergence in essential oil composition among thirty one core collections of *Ocimum sanctum* L. grown under sub-tropical region of Jammu

Kitchlu S, G Ram and A Ahuja

Evaluation of thirty one core collections of *Ocimum sanctum* L. synonyms *O. tenuiflorum* L. collected from different ecological regions representing contrasting environment of India was carried out. All the collections were grown under sub-tropical region of Jammu, India (Fig.1). Study revealed wide range of variability in quantitive and qualitative attributes of oil. Essential oil content ranged between 0.16% ± 0.01% - 0.55% ± 0.08% showing the presence of fifteen constituents. Methyl eugenol (1.54% - 93.16%) and Eugenol (0.06% - 70.41%), were the major constituent. The other major con- stituent of the oil was *β*-Caryophyllene (4.60% - 33.77%) which was detected in almost all the collections. Borneol, Copane, *α* Caryophyllene were other constituents detected in almost all the accessions. *α* selinene was detected in traces in only three accessions (OS-01, OS-03, OS-50) and *β*-selinene was detected in four accessions (OS-01, OS-03, OS-50, OS-72. Accession OS-70 collected from Patna, showed distinct chemical profile having *β*-Elemene (32.81%), *β*-Cary- ophyllene (16.37%), Germacrene-D (18.05%), *β*-Ocimene (17.69%) and Copane (5.738%). Being distinct in oil profil- ing, Patna collection was designated as distinct chemotype. Collections OS-50 from Gwalior from Central India and OS-59 from Rajkot Western India have been identified as methyl eugenol (93.16%) and eugenol (70.41%) rich geno- types. The data collected provided useful information with respect to composition of essential oil among core collection evaluated representing various agro-climatic zones.

Figure 1 : *Ocimum sanctum* : Vegetative Phase & Reproductive Phase

2.PLANT BIOTECHNOLOGY

2.1 Using differential display PCR to explore Cytochrome P450 diversity and expression in different tissues of *Coleus forskohlii*

Praveen Awasthi, Irshad Ahmad Rather, Yashbir S. Bedi, Ram Vishwakarma and Sumit G. Gandhi

Coleus forskohlii is a perennial herb from mint family, which grows in subtropical climates, and is well known for its blood pressure lowering activity. Chemoprofiling of *C. forskohlii* has found accumulation of several labdane diterpenes in its roots, where forskolin is the major bioactive constituent. It is a potent reversible activator of adenylate cyclase. It has a very unique chemical structure, with eight chiral centers and diverse functional groups. Not much information is available regarding its biosynthesis; only two genes involved in biosynthesis of common upstream intermediates of the terpenoid pathway have been cloned from *C. forskohlii*. Chemical structures of advanced intermediates of forskolin biosynthesis suggest that about 4-5 Cytochrome P450 monooxygenases could be involved in catalyzing the final reactions. Cytochrome P450 monooxygenases (CYPs) are Heme proteins, involved in various biosynthetic and detoxicative pathways in plants. CYP enzymes are encoded by a highly divergent gene superfamily.

Here we have used differential display reverse transcription PCR using degenerate primers designed in conserved Heme binding region of CYPs. cDNA samples prepared from different tissues of *C. forskohlii*, such as root, leaf and stem were used as template. Amplicons, in the size range of 300-750 base pairs, displaying differential expression pattern (Fig. 1), were picked for sequencing and further analysis by BlastX. Since degenerate primers were used for amplification, as expected some of the sequenced clones were not homologous to CYPs. Table 1 summarizes the sequencing results and closest match obtained from BlastX analysis.

A1.1c and A1.2q were found to be homologous to Flavone synthase, while A3.2e was homologous to Flavanoid 3' monooxygenase. Both these enzymes play an important role in metabolism of flavanoids. C 3.1d, C3.2C were homologous to CYP71D and CYP76C family proteins, respectively. CYP71D members catalyze specific steps in the synthesis of indole alkaloids, sesquiterpenoids, cyclic terpenoids and flavanoids. CYP76C proteins are involved in processes such as ascorbate and aldarate metabolism, coumarine and phenylpropanoid biosynthesis, fluorene degradation, gamma-Hexachlorocyclohexane degradation, limonene and pinene degradation.

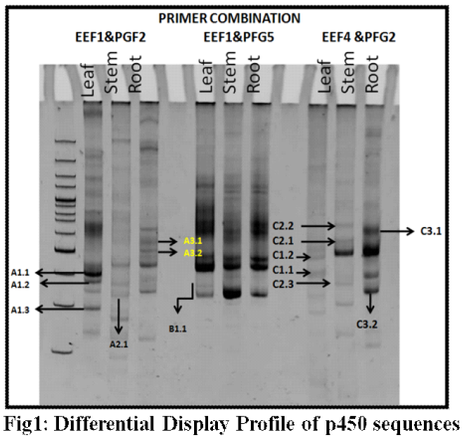

Fig1: Differential Display Profile of p450 sequences

Table 1: Analysis of sequences of obtained from differential display RT-PCR

Sequence Codes	Tissue expression pattern seen on 8%PAGE			BLASTX Result
	LEAF	STEM	ROOT	
A1.1c	+	-	-	**Flavone synthase**
A1.2q	+	-	-	**Flavone synthase**
A1.3c	+	-	-	**Photosystem II**
A2.1c	-	+	-	**Hypothetical protein**
A3.1a	-	-	+	**No significant match**
A3.2e	-	-	+	**Flavonoid 3' Monoxygenase**
B1.1b	+	-	-	**No significant match**
B1.2b	+	-	-	**No significant match**
C1.1a	+	-	-	**Hypothetical protein**
C1.2a	+	-	-	**Hypothetical protein**
C2.1a	-	+	-	**Hypothetical protein**
C2.2c	-	+	-	**Esterase**
C2.3c	-	+	-	**Hypothetical protein**
C3.1d	-	-	+	**CYP71D**
C3.2c	-	-	+	**CYP76C4**

2.2 Cloning and characterization of Flavone synthase gene from *Coleus forskohlii*

Praveen Awasthi, Irshad Ahmad Rather, Yashbir S. Bedi, Ram Vishwakarma and Sumit G. Gandhi

Flavonoids are one of the most intensively studied plant secondary metabolites. More than 10,000 flavonoids have been identified so far. Flavonoids have diverse biological applications; as a sunscreen for plants, protection against UV and phytopathogens, signaling between the plants and its environment, as floral pigment, etc. *Coleus forskohlii* is a perennial herb from mint family, which grows in subtropical climates. Traditional medicinal uses of *C. forskohlii* include treatment of digestive disorders, skin ailments, genito-urinary disorders, respiratory problems, gastric pain, circulatory and heart ailments, hypertension etc. Two flavones namely 4,7-dimethoxy-5,6-dihydroxy flavone and chrysoplenetin have been reported from *C. forskohlii* until now. Flavone synthase, an enzyme involved flavonoid metabolism, catalyzes the following reaction:

$$\text{flavanone} + \text{2-oxoglutarate} + O_2 \rightleftharpoons \text{flavone} + \text{succinate} + CO_2 + H_2O$$

Full length cytochrome P450 sequences were cloned from *C. forskohlii*. One clone was found to be homologous to Flavone synthase, which we have designated *CfFNS*. A phylogenetic tree of CYP sequences was plotted, as expected *CfFNS* clusters with CYPs involved in flavanoid biosynthesis, while other CYPs, such as those involved in terpenoid metabolism, abscisic acid metabolism, brassinosteroid metabolism and glucosinolate metabolism form separate clades (Fig. 1).

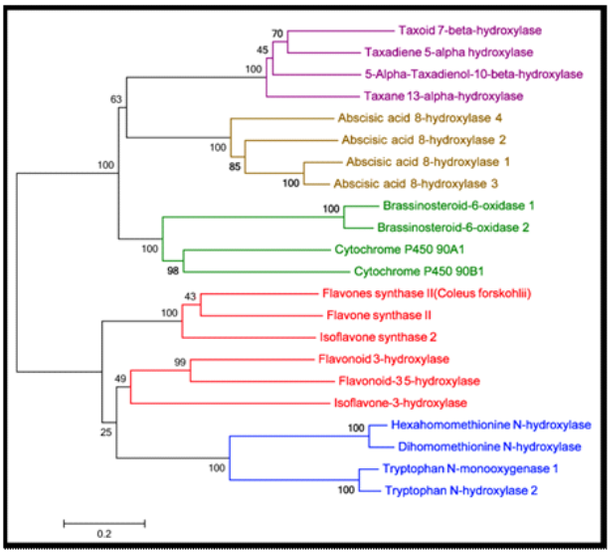

Figure 1: Phylogenetic tree of plant CYP proteins involved in various metabolic processes.

Full length cDNA of *CfFNS* is 1776 bp in size, with ORF of 1530 bp and having 73 bp 5'UTR and 173 bp 3'UTR. It encodes a protein of 509 amino acid with theoretical molecular weight of 57.542KDa and pI: 8.49. *CfFNS* shows maximum identity of 82.8% with FNS of *Perilla frutescens* followed by 82.5% with FNS of *Ocimum basilicum* (Fig. 2).

	Coleus forskohlii	*Ocimum basilicum*	*Perilla frutescens*	*Torenia spp.*	*Antirrhinum majus*	*Picrorhiza kurroa*
Coleus forskohlii		82.5	82.8	72.9	73.1	66.3
Ocimum basilicum	90.6		80.3	73.4	74.7	66.4
Perilla frutescens	91	89.2		75.9	75.8	66.2
Torenia spp.	85.2	85.4	86.7		77	66.5
Antirrhinum majus	86.4	86.5	87	87.7		71.1
Picrorhiza kurrooa	77.2	76.7	77.1	77.7	80.4	

% Identity % Similarity

Figure 2: Identity and Similarity matrix of closest homologs of *CfFNS*

Expression profiling of *CfFNS* in different tested tissues of *C. forskohli* plants shows that it is predominantly expressed in leaves and leaf bud. Treatment of *C. forskohlii* plants with chemical elicitors such as methyl jasmonate and salicylic acid, plant hormones such as abscisic acid, herbicide such as 2,4-Dichlorophenoxyacetic, mechanical treatments such as UV-A irradiation and wounding, lead to strong induction of *CfFNS* compared to controls (Fig. 3). FNS of *Medicago trancatula* was also shown to be induced by methyl jasmonate.

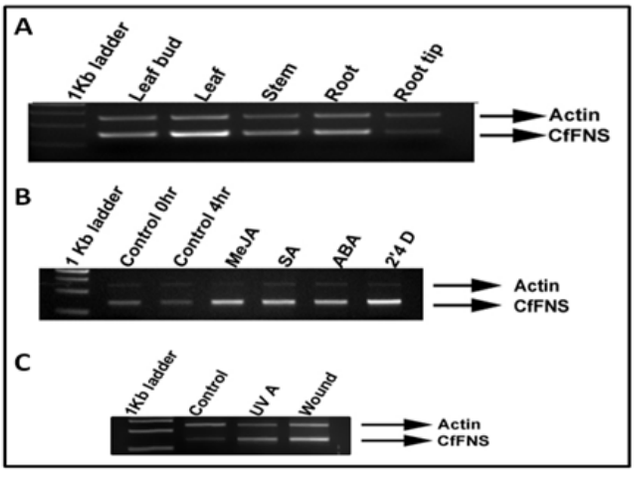

Figure 3: Expression analysis of *CfFNS*

2.3 Cloning and characterization of Flavonoid 3' Hydroxylase gene from *Coleus forskohlii*

Praveen Awasthi, Irshad Ahmad Rather, Yashbir S. Bedi, Ram Vishwakarma and Sumit G. Gandhi

In plants, flavonoids serve an important function of providing yellow or red/blue pigmentation to petals, thus helping to attract pollinators. Apart from floral pigmentation, flavonoids play role in UV filteration, symbiotic nitrogen fixation, signaling between plant and its environment, etc. Flavonoids have been shown to have anti-oxidant, anti-allergic, anti-inflammatory, anti-microbial, anti-cancer and anti-diarrheal activities. More than 10,000 flavonoids have been identified so far. Two flavones have been reported from *C. forskohlii* until now, namely 4,7-dimethoxy-5,6-dihydroxy flavones and chrysoplenetin. Flavones are a class of flavonoids, based on the backbone of 2-phenylchromen-4-one. Flavonoid 3' Hydroxylase (F3'H), a cytochrome P450 enzyme, also known as flavonoid 3' monooxygenase, catalyzes the following reaction:

flavonoid + NADPH + H^+ + O_2 ⇌ 3'-hydroxyflavonoid + $NADP^+$ + H_2O

Full length cytochrome P450 sequences were cloned from *C. forskohlii*. One clone was found to be homologous to Flavonoid 3' Hydroxylase, which we have designated *Cf*F3'H. A phylogenetic tree of CYP sequences was plotted, as expected *Cf*F3'H clusters with CYPs involved in flavanoid biosynthesis, while other CYPs, such as those involved in terpenoid metabolism, abscisic acid metabolism, brassinosteroid metabolism and glucosinolate metabolism form separate clades (Fig. 1)

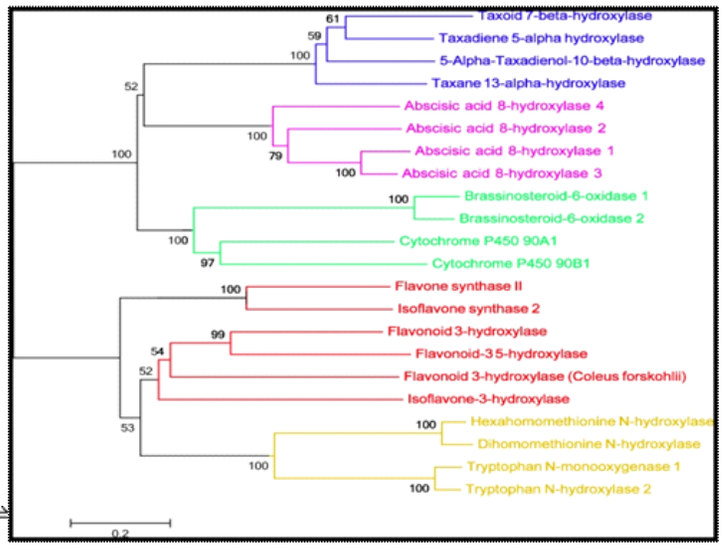

Figure 1: Phylogenetic tree of plant CYPs protein involved in different Biosynthetic Metabolism.

Full length cDNA of *CfF3'H* is 1701bps in size, with ORF of 1521bps and having 35 bps 5'UTR and 145bps 3'UTR. It encodes a protein of 506 amino acid with theoretical molecular weight of 56.04KDa and pI: 8.14. *CfF3'H* shows maximum identity of 72% with *F3'H* of *Vitis vinifera* (Fig. 2).

Expression profiling of *CfF3'H* in different tested tissues of *C. forskohli* plants shows that it is predominantly expressed in leaves and leaf bud. Treatment of *C. forskohlii* plants with chemical elicitors such as methyl jasmonate and salicylic acid, plant hormones such as abscisic acid, herbicide such as 2,4-Dichlorophenoxyacetic, mechanical treatments such as UV-A irradiation and wounding, lead to strong induction of *CfF3'H* compared to controls (Fig. 3).

	Coleus forskohlii	*Solanum lycopersicum*	*Solanum lycopersicum*	*Fragaria vesca*	*Vitis vinifera*	*Solanum lycopersicum*
Coleus forskohlii		64.9	63.5	63.6	63.8	61.6
Solanum lycopersicum	78.5		88.6	72.4	73.2	81.1
Solanum lycopersicum	78.7	94.1		72.4	74.6	80.7
Fragaria vesca	76.7	85.5	86.2		75.8	67.8
Vitis vinifera	75.9	86.4	87.3	88		68.7
Solanum lycopersicum	77.1	92.3	91.7	84.3	84.7	

% Identity % Similarity

Figure 2: Identify and Similarity matrix of closest homologs of *CfF3'H*

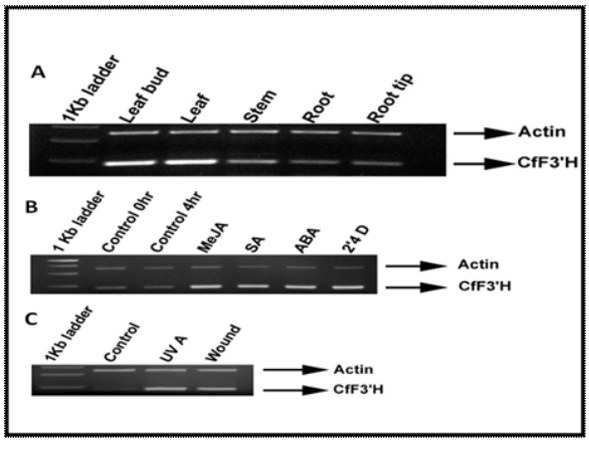

Figure 3: Expression analysis of *CfF3'H*

2.4 Cloning and characterization of 4-coumarate: coenzyme A ligase gene from Coleus forskohlii

Vidushi Mahajan, Praveen Awasthi, Irshad Ahmad Rather, Yashbir S. Bedi, Ram Vishwakarma and Sumit G. Gandhi

4-Coumarate CoA Ligase (4CL) is one of the important key enzymes of general phenyl propanoid metabolism, which provides the precursor molecules for a large variety of important plant secondary products such as lignin, flavonoid etc. It catalyzes the activation of 4-coumarate and various other cinnamic acid derivatives to the corresponding thiol esters in two-step reaction via an adenylate intermediate. Thio reaction represents the last step in a short series of biochemical conversions, known as phenyl- propanoid metabolism leading from phenylalanine to the activated cinnamic acid derivatives. These derivatives are precursors for the biosynthesis of a large variety of plant secondary metabolites.

The reaction catalysed by 4CL is:

ATP + 4-coumarate + CoA

⟶ AMP + diphosphate + 4-coumaroyl-CoA

Here we have cloned full length 4CL gene from *Coleus forskohlii* and named it *Cf*4CL. *Cf*4CL is 1893 bps in size, with ORF of 1640 bps and having 69 bps 5'UTR and 187 bps 3'UTR (Figure 1). It encodes a protein of 509 amino acid with theoretical molecular weight of 62.855 KDa and pI: 4.85. *Cf*4CL shows maximum identity of 86.4% with 4CL of *P.fortunei* followed by 83.1% with 4CL of *M.officinaliis* (Fig. 2). A phylogenetic tree was constructed to understand the molecular relatedness of *Cf*4CL with its homologs from other plant species (Fig. 3). Complete nucleotide and protein sequence is shown in figure 4.

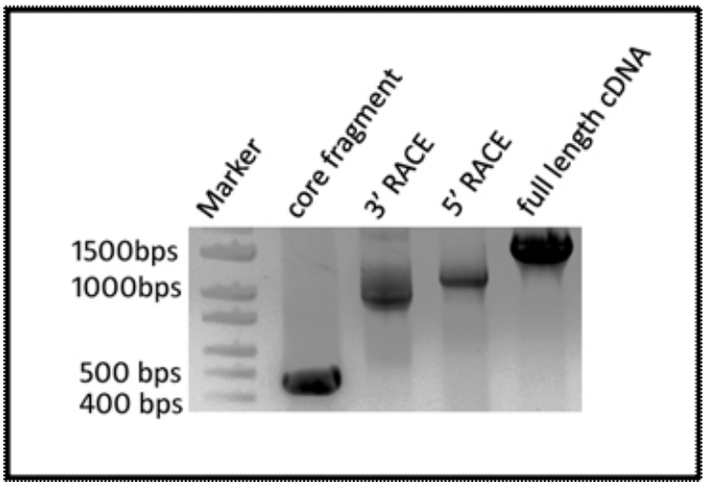

Figure 1: Gel picture showing PCR amplicons of core fragment, 5'RACE, 3' RACE and full length gene of *Cf4CL*

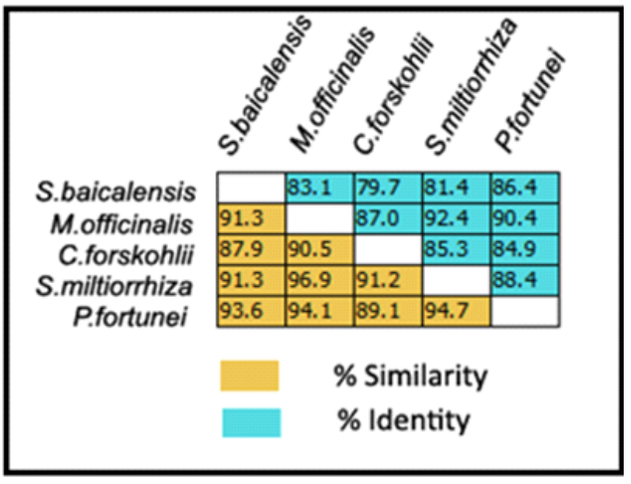

Figure 2: Identity and Similarity matrix of *Cf*4CL with its closest homologs from other plant species.

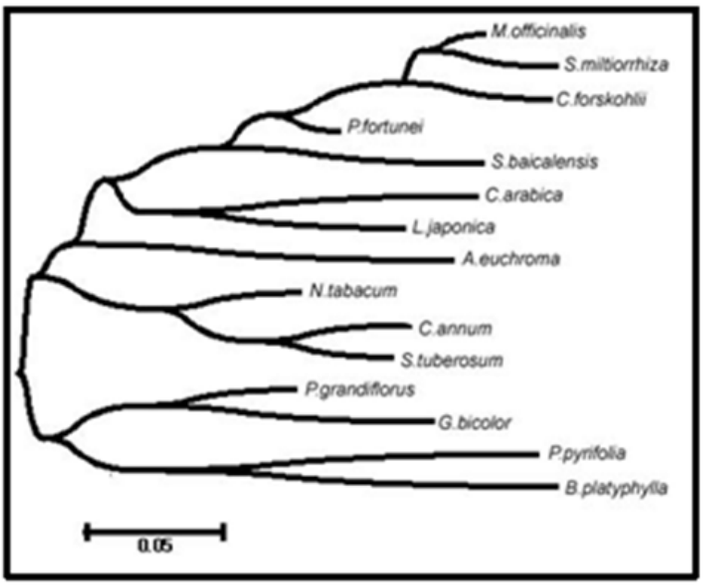

Figure 3: Phylogenetic tree showing relatedness of *Cf*4CL with other plant 4CLs proteins.

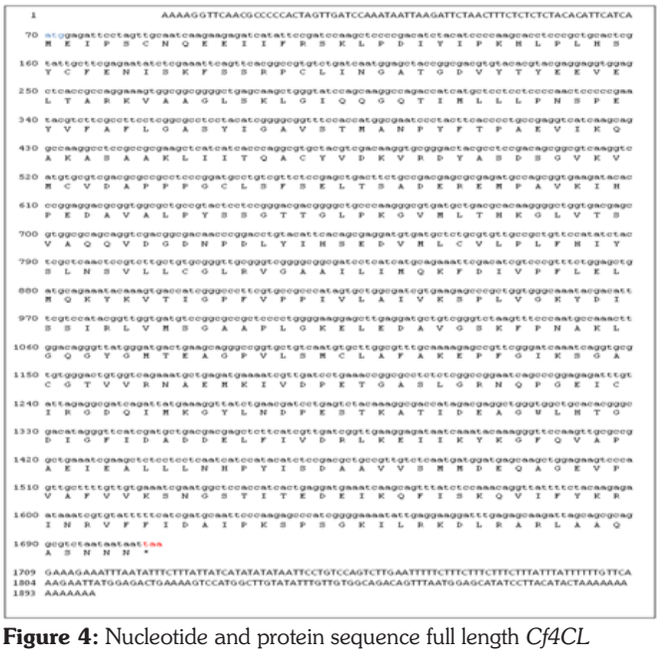

Figure 4: Nucleotide and protein sequence full length *Cf4CL*

2.5 Cloning and characterization of Chalcone Synthase gene from *Coleus forskohlii*

Vidushi Mahajan, Praveen Awasthi, Irshad Ahmad Rather, Yashbir S. Bedi, Ram Vishwakarma and Sumit G. Gandhi

Flavonoids are a class of secondary metabolites in plants that are involved in many important functions like floral pigmentation, UV filteration, symbiotic nitrogen fixation, signaling between plant and its environment etc. More than 10,000 flavonoids have been identified so far. Two flavones have been reported from *C. forskohlii* until now, namely 4,7-dimethoxy-5,6-dihydroxy flavones and chrysoplenetin. CHS (Chalcone Synthase) catalysis serves as the initial step for flavonoid biosynthesis. Chalcone synthase catalyzes a stepwise reaction of three acetate residues from malonyl-CoA with 4 -coumaroyl-CoA to yield the intermediate naringenin-chalcone. Naringenin chalcone serves as the precursor for synthesis of all flavonoids.

CHS catalyzes the following reaction:

3 malonyl CoA + coumaroyl CoA

⟶ naringenin chalcone + CO2 + 3CoA

CHS is constitutively expressed and is ubiquitous in all plants. However, its expression is known to increase on exposure to light/ UV light, pathogens, elicitors and wounding.

Here we have cloned full length CHS gene from Coleus forsohlii and named it as *Cf*CHS. *Cf*CHS is 1595 bps in size, with ORF of 1173 bps and having 244 bps 5'UTR and 177 bps 3'UTR (Fig. 1). It encodes a protein of 509 amino acid with theoretical molecular weight of 45.280KDa and pI: 5.36. *Cf*CHS shows maximum identity of 94.6% with CHS of *A.rugosa* followed by 94.1% with CHS of *P.frutescens* (Fig. 2). A phylogenetic tree was constructed to understand the relatedness of *Cf*CHS with its homologs in other plant species (Fig. 3). Complete nucleotide and protein sequence is shown in figure 4.

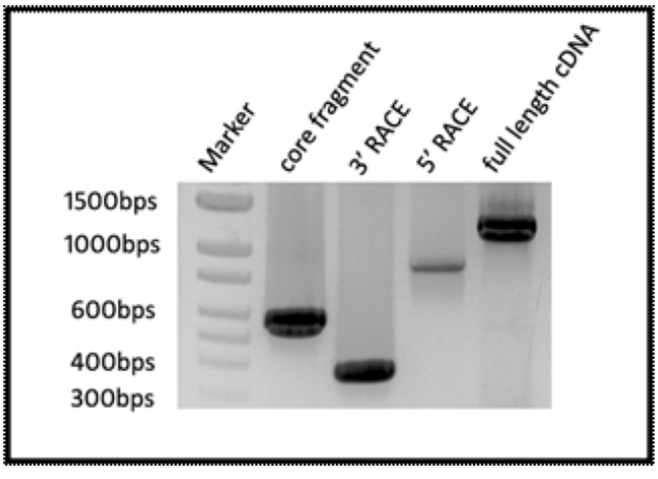

Figure 1: Gel image showing PCR amplicons of core fragment, 5'RACE, 3' RACE and full length gene of *CfCHS*

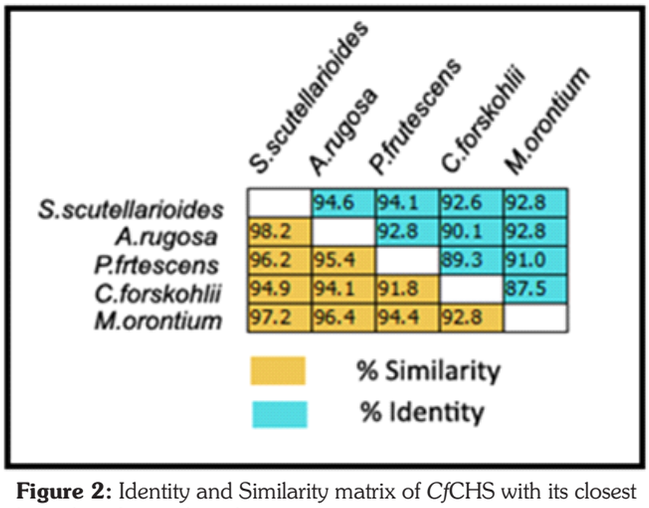

Figure 2: Identity and Similarity matrix of *Cf*CHS with its closest homologs from other plant species

Figure 3: Phylogenetic tree showing relatedness of *Cf*CHS with its homologs from other plant.

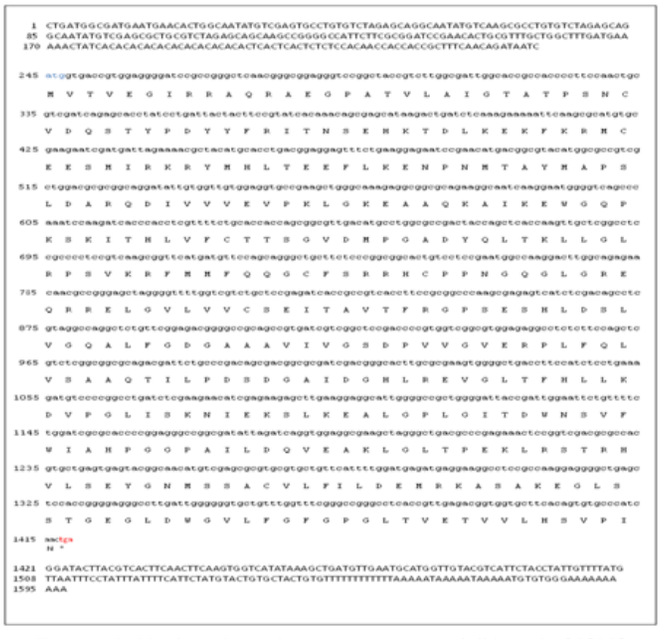

Figure 4: Nucleotide and protein sequence full length *CfCHS*

2.6 Production of rohitukine in leaves and seeds of *Dysoxylum binectariferum*: an alternate renewable resource

Vidushi Mahajan, Neha Sharma, Sunil Kumar, Vikram Bhardwaj, Asif Ali, R.K. Khajuria, Yashbir.S.Bedi, Sumit Gandhi and Ram Vishwakarma

Plant derived natural products have been the single largest source of clinically useful anti-cancer compounds. It is noteworthy that more than 60% of currently used anti-cancer drugs are natural products, their analogues or derivatives.

Flavopiridol, a recently approved drug for treatment of chronic lymphocytic leukaemia (CLL) is a potent inhibitor of cyclin dependent kinases (CDKs). Most cancers exhibit mutations in ATM and/or P53 genes, resulting in multiple defects in the G1 and G2 checkpoint controls of mitotic cell cycle. Flavopiridol mediated inhibition of CDKs blocks cell cycle progression and induces apoptotic cell death. Apart from inhibiting CDKs, flavopyridol also suppresses bcl2 expression, thus promoting apoptosis.

Flavopiridol possesses a hybrid chemical structure composed of flavone and piperidyl moieties. Though, it is a completely synthetic molecule, the basis of its unique structure is a chromone alkaloid natural product: Rohitukine. Rohitukine was first reported from trunk bark of *Amoora rohituka*, followed by its discovery, in considerably higher amounts, in the trunk bark of *Dysoxylum binectariferum*. Both these plants belong to the family Meliaceae, and are native to India, China and other parts of Asia. Rohitukine was originally identified as the component responsible for anti-inflammatory and immunomodulatory activities. During structure-activity relationship (SAR) studies, a derivative, flavopiridol, emerged as a tyrosine kinase inhibitor and possessed potent growth inhibitory activity against breast and lung carcinoma cell lines. It was earlier submitted to a screen for potential inhibitors of Epithelial Growth Factor Receptor (EGFR) and Protein Kinase A (PKA), though eventually it became evident that its anti-cancer activity was far more potent than its affect on EGFR and PKA. Search for its true molecular target revealed its potent inhibitory activity against CDKs10.

Trunk bark of *D.binectariferum* is the widely used source for isolation of rohitukine for the synthesis of potential anti-cancer drug flavopiridol (Sanofi) and P-276-00 (Piramal). The extraction of trunk bark is destructive for the tree and eventually leads to its death. This being a slow growing tree species, an alternate renewable resource for extraction of rohitukine would be more nature friendly. Crude extracts were prepared from different parts of tree such as leaves, young stems, fruits and seeds. Rohitukine content in all the tissues was quantified by HPLC (Fig. 1). Further, we isolated pure rohitukine from leaves of *D.binectariferum* (Fig. 2), which is a renewable resource and doesn't damage the tree or put its existence to danger. ^{1}H NMR was recorded in MeOD (Fig. 3) to confirm that the extracted compound is pure rohitukine only.

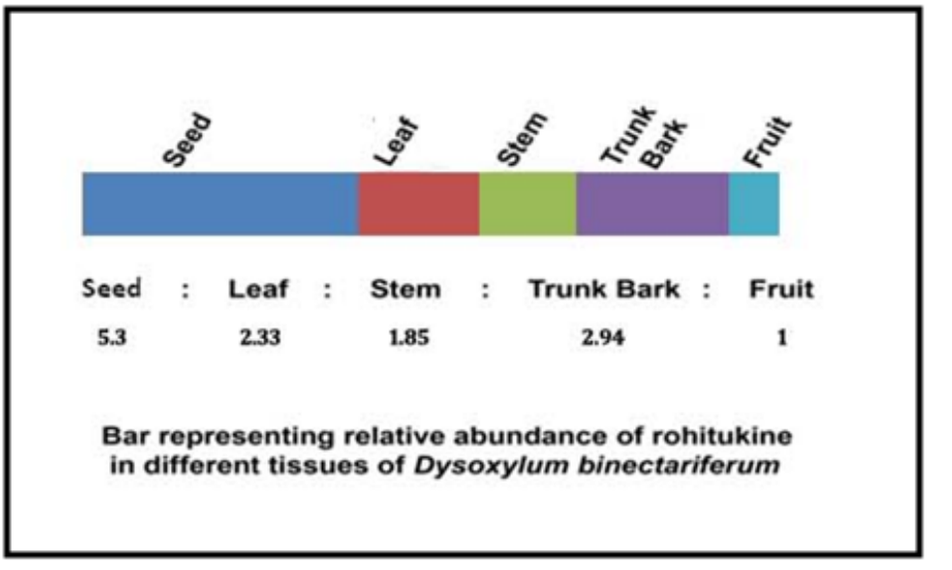

Figure 1: Distribution of rohitukine in different parts of the tree *Dysoxylum binectariferum*.

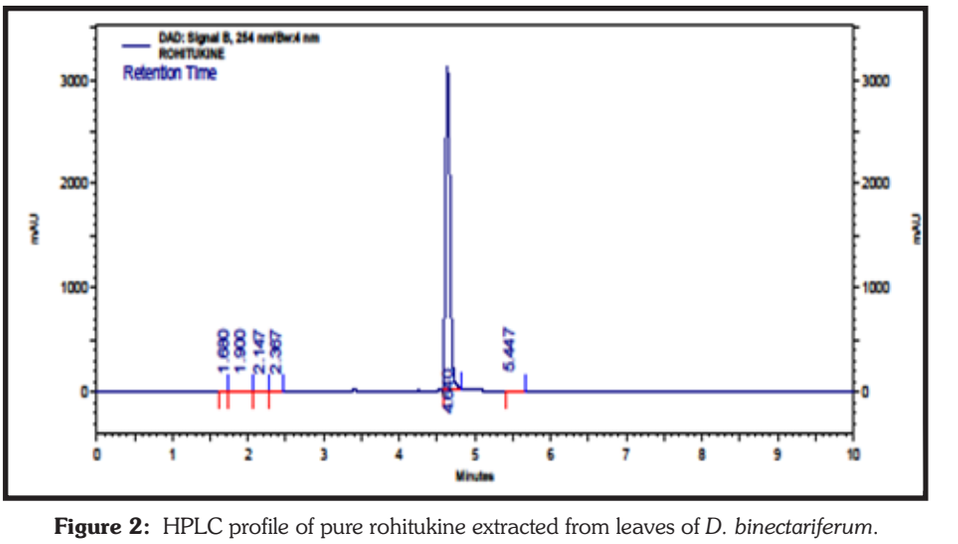

Figure 2: HPLC profile of pure rohitukine extracted from leaves of *D. binectariferum*.

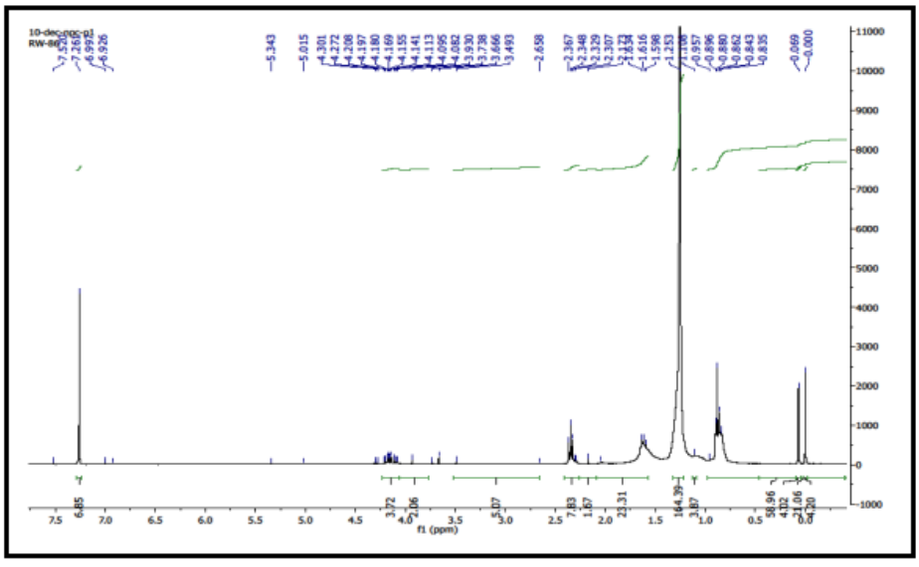

Figure 3: NMR of pure rohitukine in MeOD.

2.7 Role of MYC2, a bHLH Transcription Factor on the Artemisinin biosynthetic pathway in *Artemesia annua* L.

Nazia Abbas, Irshad Ahmad Rather, Sumit G. Gandhi, Ram Vishwakarma and Yashbir S. Bedi.

Malaria, the world's most severe disease caused by *Plasmodium falciparum* infection, has caused more than a million deaths annually (Greenwood and Mutabingwa, 2002). Although many efforts have been made to control malaria, no apparent result has been obtained except the artemisinin combination therapies recommended by the world health organization (WHO) (Graham *et al*., 2010). Engineering metabolic pathways of *A. annua* plants holds a great potential for increasing artemisinin production (Ro *et al*., 2006). In comparison with the great progress made in cloning enzymes of the artemisinin pathway and engineering the pathways in microorganisms (Bouwmeester *et al*., 1999; Ro *et al*., 2006; Teoh *et al*., 2006; Zhang *et al*., 2008; Teoh *et al*., 2009), relatively little information is available about the regulatory mechanisms of artemisinin biosynthesis in plants. MYC2 originally isolated as JIN1 (jasmonate insensitive 1) is a bHLH transcription factor and plays the most versatile role in various signal transduction pathways. It acts as a point of cross-talk among light, Abscissic acid (ABA) and Jasmonic acid (JA) signaing pathways (Berger *et al*., 1996; Abe *et al*., 2003; Lorenzo *et al*., 2004; Anderson *et al*., 2004; Yadav *et al*.,). Recently Yu *et al* (2012) have shown that two JA-responsive transcriptional factors AaERF1 and AaERF2 from *A. annua* bind to the cis-elements of *ADS* and *CYP71AV1* promoters and positively regulate artemisinin biosynthesis. Considering positive role of JA on artemisinin biosynthesis as well as cross talk of MYC2 with JA, the regulatory role of MYC2 in artemisinin biosynthetic pathway is quite obvious.

So far in this study we have cloned the core fragment of the *MYC2* from the *Artemesia annua*. The sequence of Arabidopsis *MYC2* (AT1G32640) was used as a query sequence for a BLAST search on GenBank. The search returned an *A. annua* EST (expression sequence tags) (EY106094.1) which was from the leaf cDNA library. Based on the sequence, a pair of primers Aa*MYC2*F and Aa*MYC2*-R were designed, synthesized, and used to amplify the partial sequence of a putative *MYC2* transcription factor from *A. annua*. The 623bps sequence of the Aa*MYC2* was amplified (Fig 1.) and cloned in pTZ57R/T (Fig. 2). Further to isolate the full length of Aa*MYC2*, 5'prime and 3'prime RACE will be performed and the work is under progress.

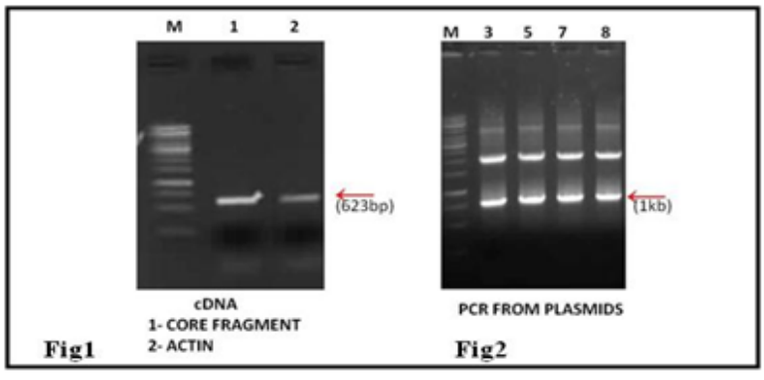

Figure 1: The core fragment of *AaMYC2* amplified with the gene specific primers AaMYC2 FP and *AaMYC2* RP. From the figure lane M- shows 1kb DNA ladder, lane1- 623bps core fragment of AaMYC2 and lane 3- 640bps actin. **Figure 2:** Shows 1000bps fragment of *AaMYC2* cloned in PTZ57R/T and amplified by *M13* Forward and reverse primers.

Expression Analysis of *AaMYC2* in response to different phytohormones

It is well known that the phytohormones of jasmonate (JA), salicylic acid (SA), and abscisic acid (ABA) aid plants in survival from the biotic and abiotic stresses by triggering a de novo synthesis of protective metabolites and proteins (Wolucka et al., 2005; Tuteja, 2007; Yuan and Lin, 2008; Browse, 2009). Recent reports showed that JA treatment of *A. annua* plants resulted in enhanced artemisinin production (Baldi and Dixit, 2008; Wang et al., 2010), possibly by stimulating both the glandular trichome formation and the sesquiterpene accumulation in glandular trichome (Maes et al., 2011). However, transcription factors involved in JA regulation of artemisinin biosynthesis have not been reported.

The expression of *AaMYC2* under the influence of Methyl jasmonate, 2,4D and NaCl was investigated using semi-quantitative PCR. For this study 8 week old plant of *Artemesia annua* was treated with 100µM of Methyl jasmonate, 2,4D and NaCl for 4 hours. The total RNA was isolated and the expression of *AaMYC2* was studied. The figure 3 below clearly depicts the expression profile of *AaMYC2,* which is upregulated in the presence of Methyl jasmonate, 2,4D and NaCl as compared to wild type mock plants i.e, without any treatment. The results are in accordance with the previous results as shown in case of *Arabidopsis* by Boter et al., 2004; Abe et al., 2003. Thus from the above study at the primary stage we can speculate that MYC2 can be the possible transcription factor regulating the Artemeisinin accumulation in the glandular trichomes in *Artemesia annua*.

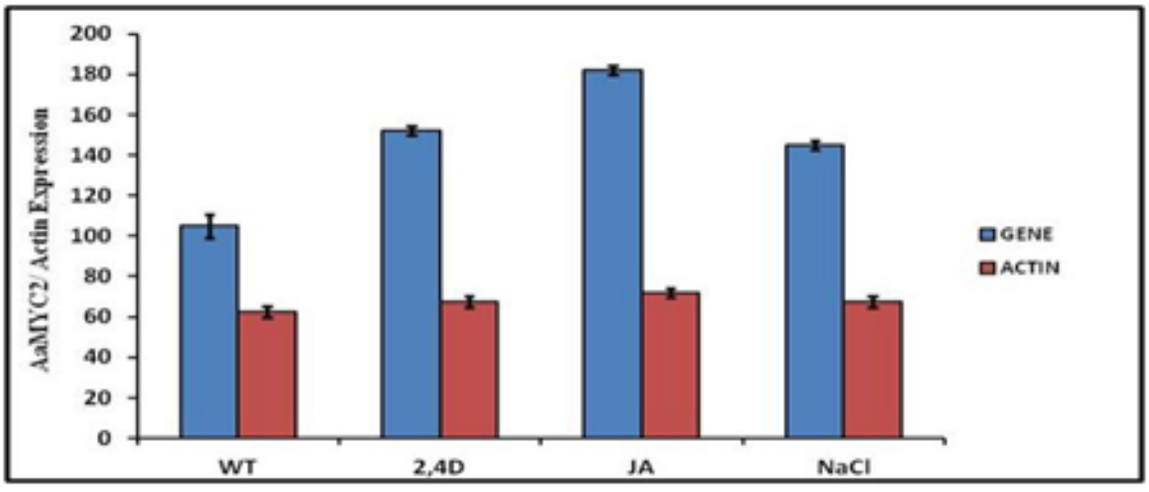

Figure 3: Quantitative analysis of 364 bp fragment of *Aa MYC2* with respect to actin in response to various hormones.

In-vitro regeneration of *Artemesia annua* from leaf explants for transgenic Development:

One of the main experiment of our project is the genaration of RNAi transgenic lines of *MYC2* in *Artemisia annua* and analysis of transgenes with respect to affect of MYC2 knockdown on artemisinin biosynthesis. For the *in-vitro* regeneration of *Artemesia annua*, seeds of *A. annua* were surface-sterilized and sown in germination medium MS (Murashige and Skoog, 1962) basal medium with the addition of sucrose 3% and 0.7% agar. When they had reached 5 cm in length, the germinated seedlings were collected and the leaves were cut into 0.5-cm-diameter discs and used as the explants for regeneration. The Leaf discs were horizontally placed in Petri dishes containing MS (Murashige and Skoog, 1962) medium fortified with various combinations and concentrations of different growth regulators *viz.,* BAP and NAA for callus induction. The callus so generated is now grown on different concentrations of NAA and BAP for the further rooting and shooting (Fig.4).

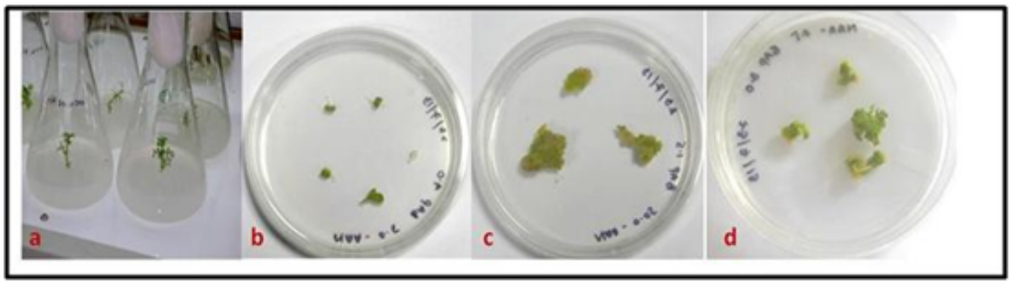

Figure 4: *In-vitro* regeneration of *Artemesia annua*

a, Tissue culture raised plantlets of *Artemesia annua* from the seeds. **b,** Leaf explants of *Artemesia annua* grown on MS media supplemented with NAA (0.5mg/L) and BAP (4mg/L). **c,** Callus regenerated from the leaf explants after 40 days incubation. **d,** Shootlet regenerated from the callus on medium suplemented with NAA (0.5mg/L) and BAP (3mg/L).

2.8 Molecular cloning and characterization of two genes (squalene synthase and lupeol synthase) associated with terpenoid biosynthesis in *Glycyrrhiza glabra*

Pankaj Pandotra, Suphla Gupta, Ajai P Gupta, Ashok Ahuja and Ram Vishwakarma

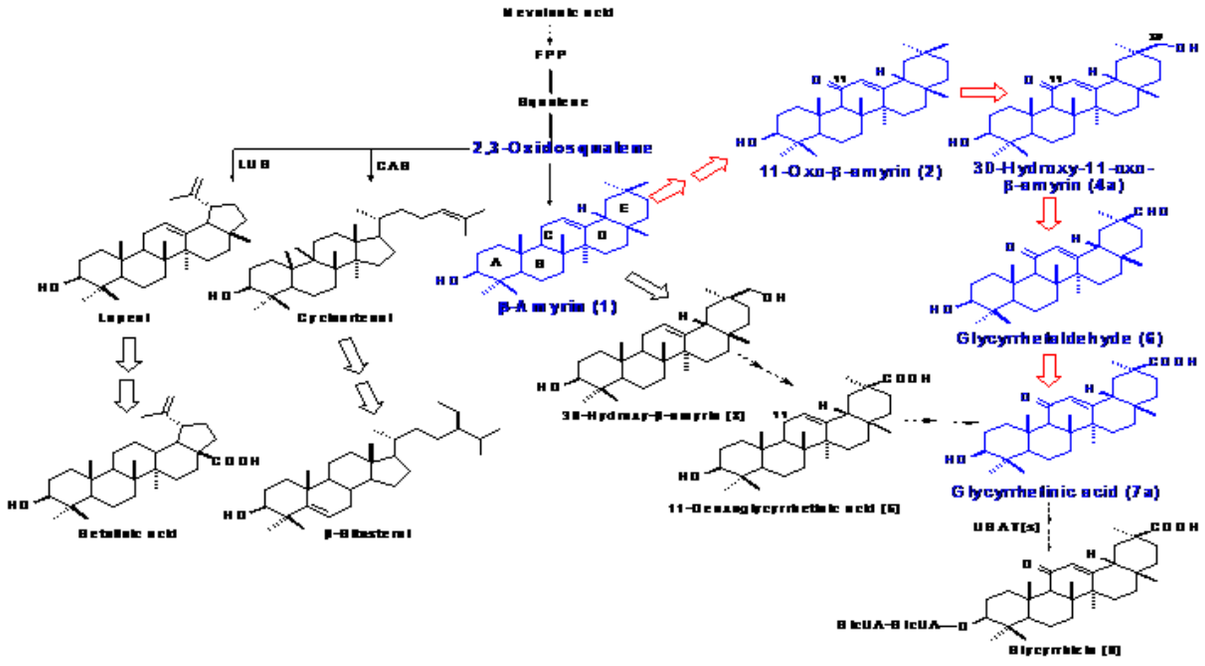

Figure 1: Scheme of proposed pathway for biosynthesis of Glycyrrhizin

Triterpenoid Saponins are bioactive compounds produced by plants generally for defence. In recent times, their use in drug discovery has attracted lots of attention. Glycyrrhizin is one such tri-terpenoid saponin produced by *Glycyrrhiza species* (*glabra* and *uralensis*). The biosynthesis of Glycyrrhizin *in planta* is largely unknown. Current ideas of saponin biosynthesis in plants consider them to be derived from metabolites of phytosterol anabolism. In this, squalene synthase, a membrane bound protein, catalyzes the linking of two Farnesyl diphosphate units to form squalene, which subsequently gets epoxygenated to form squalene epoxidase- the last common precursor of tri-terpenoid saponins. Full length of Squalene synthase gene was cloned from *Glycyrrhiza glabra*. We adopted reverse transcription polymerase chain reaction (RTPCR) strategy using degenerate primers. Using these primers, a core fragment of 650 bp was amplified which was used for designing specific primers for doing 5` and 3` RACE to clone full length of the target gene. The cDNA of the cloned give was approximately 1.5 kb (1473bp) length encoding a protein of 412 aminoacid residue with predicted molecular weight of 46.4kD . The BLAST analysis of the sequence showed maximum similarity (100%) with *Glycyrrhiza glabra* squalene synthase 2 (d86410.1) and 99% identity with SS2 of *Glycyrrhiza uralensis* sequences already deposited in NCBI. The analysis showed the presence of putative conserved domains for Isoprenoid biosynthesis-C 1 Superfamily.

The predicted 3Dstructure (I-TASSER)of squalene synthase gene is shown in Figure 2.

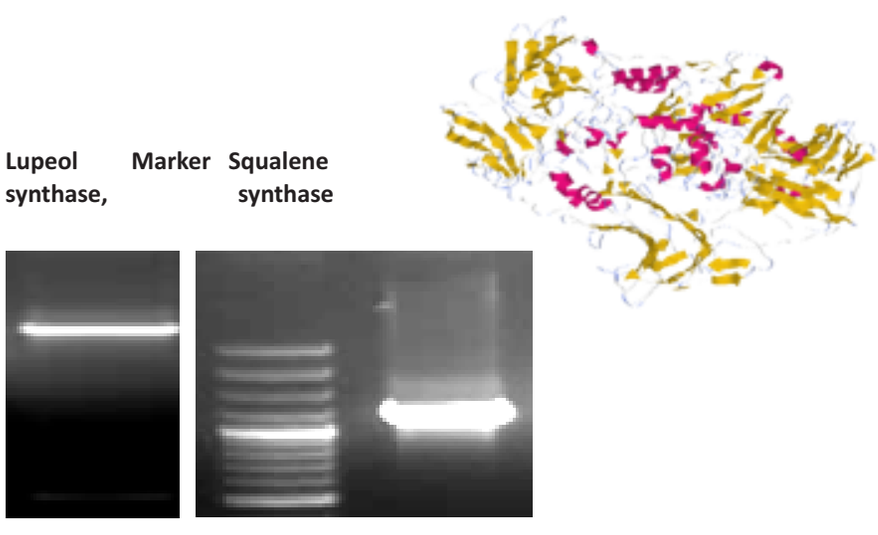

Figure 2: (a) Full-length genes: Squalene synthase and Lupeol synthase; (b) predicted 3 Dstructure (I-TASSER) of squalene synthase gene

Oxidosqualene cyclase (OSCs) catalyzes the cyclization of 2,3 oxidosqualene, a common intermediate of both sterols and triterpenoids, into array of tri terpenoids. Lupeol synthase, an oxidocyclase, catalyzes it into Lupeol which is the precursor of betulinic acid. The gene was cloned and characterized from *Glycyrrhiza glabra* using degenerate primers and following RT-PCR methodology. The 750 bp long core fragment obtained was cloned in pTZ5R/T vector and sequenced following standard molecular biology protocols. The gene specific primers designed were used to get 5` and 3` ends using Rapid Amplification of cDNA Ends which were cloned and sequenced. The sequence showed 99% homology with Lupeol synthase gene of *Glycyrrhiza glabra* (Q764T8.1) and *uralensis* species (BAL41371.1). The cloned cDNA encoded a 86.7 kD protein of 758 amino acid residue having putative conserved domains of IsopreneC2 like Superfamily. The gene belongs to Terpene cyclase/mutase family containing 4 PFTB repeats.

2.9 Regeneration of *Glycyrrhiza glabra* plants through various *in vitro* pathways.

Suphla Gupta, Pankaj Pandotra, Ram A Vishwakarma and Ashok Ahuja

A complete procedure for plant regeneration utilizing various regeneration pathways has been standardized that has provided basis for functional genomics studies (Fig.1). *In vitro* organogenesis from root culture systems and subsequent stolon formation producing glycyrrhizin was established in *Glycyrrhiza glabra.* This was the first report of stolon proliferation *in vitro* in *G. glabra. De novo* proliferation of shoot differentiation for clonal mass propagation was achieved using excised roots, obtained from *in-vitro* grown plantlets. Root tissue has advantage of being highly regenerative, easy to maintain and manipulate to get true-to-type regenerates. The procedure of *de novo* organogenesis involved root induction in *in-vitro* grown shoots using rooting medium (1/2 MS +0.1mg/L NAA) followed by excision of the roots and culturing them back in shooting medium (1/2 MS+ 2% sucrose + 1mg/ml BA + 0.25mg/ml NAA) to produce profuse shoots and complete plant. Proximal or middle section of the root was found to be more proliferative to shoot differentiation which subsequently regenerated to give plantlets. Miniature plantlets were successfully acclimatized and hardened under green house conditions before being transferred to field. Regeneration potential of root cultures to undergo organogenesis to differentiate plants was comparatively better in terms of frequency of shoot morphogenesis from mature stolons.

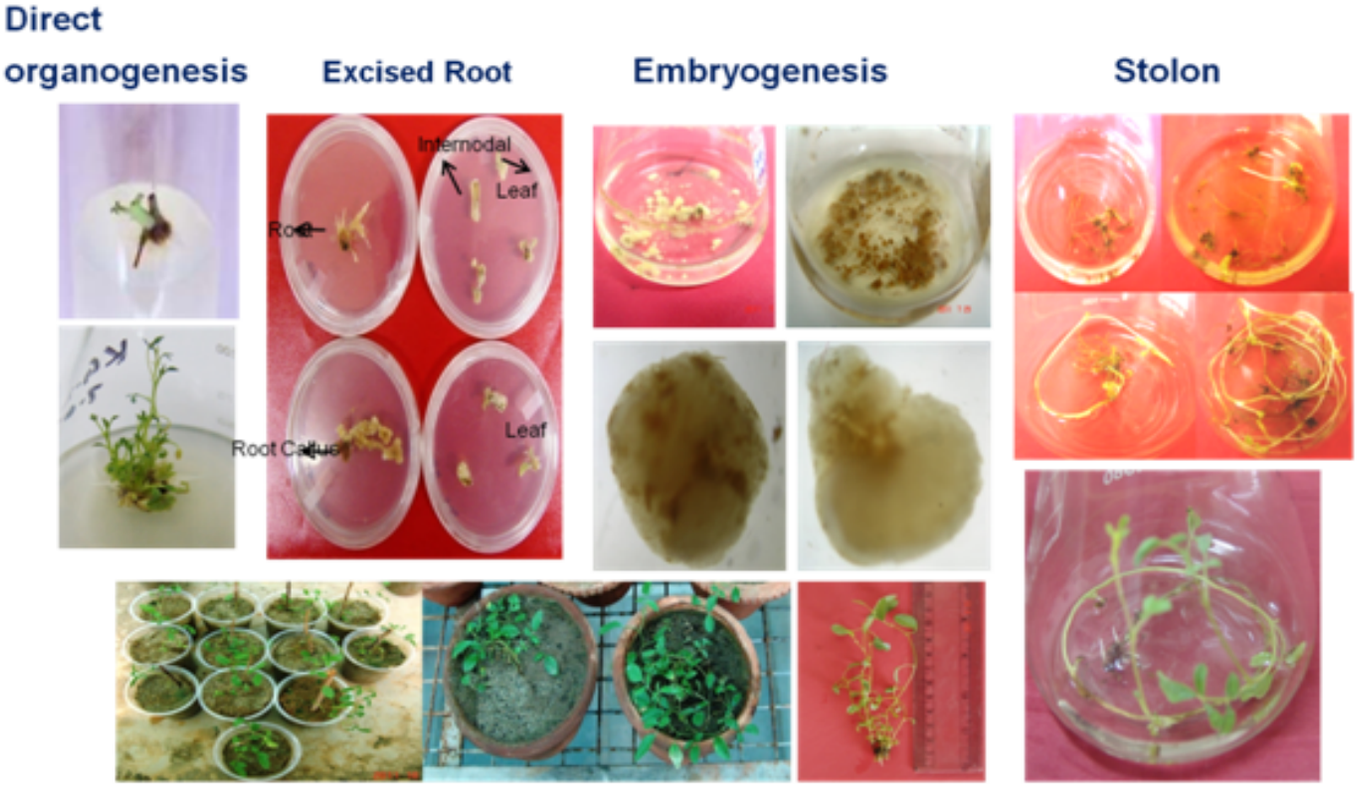

Figure 1 : Regeneration of *Glycyrrhiza glabra* plants through various *in vitro* pathways

Conventionally, rhizome of *G. glabra* is actual propagating material, which is being uprooted for drug purposes, resulting in shortage of the material for cultivation purposes.

As such the present described procedure, where root cultures have been utilized for regeneration of plantlets would provide attractive alternative approach for rapid micro-cloning and studying glycyrrhizin biosynthesis of elite clones.

Besides, Encapsulation" strategy for propagation and conservation of selected clones of G glabra was also standardized (Fig. 2). A reliable protocol for *in vitro* propagation of shoot tips of Glycyrrhiza glabra using alginate method was standardized. Artificial (Synthetic) seed production along with micropropagation can solve many problems with regeneration of *Glycyrrhiza glabra*, which produces non-viable seeds with great difficulty. The explants shoot tips and axillary budsmd, nodal segments were used from *in vitro* cultures for encapsulation. Different concentrations of sodium alginate and calcium chloride were tried to get round to spherical shape and fast and better germination of artificial seeds. A gelling matrix of 2% sodium alginate and 100 mM calcium chloride was found most suitable for the formation of firm, clear and isodiametric ideal beads (Fig. 2). It was further noticed that no effect of the duration of sodium alginate treatment on bead formation was observed. However, timing of $CaCl_2$ treatment proved to be crucial with 100 mM $CaCl_2$, treatment time of 15 min was most suitable for isodiametric bead formation. The procedure developed in this study is easy to handle and produced high levels of shoot formation. Thus, the protocol is applicable for long-term storage of shoot tips of *Glycyrrhiza glabra.*

Figure 2: Encapsulated alginate entrapped shoot apices of *Glycyrrhiza glabra*

2.10 Metabolite profiling of various *in vitro* raised cultures of *Glycyrrhiza glabra*

Pankaj Pandotra, Suphla Gupta, Ajai P Gupta, M K Verma, Ashok Ahuja and Ram A Vishwakarma

In-vitro culture lines of different morphogenetic nature were employed for studying the metabolome in *Glycyrrhiza* plant. Comparative metabolite profiling of *in-vitro* raised culture lines carried out, showed distinct profile with high chemical heterogeneity (Fig. 1). This pointed out role of morphogenesis in glycyrrhizin biosynthesis. Glycyrrhizin and glycyrrhitinic acid were the major identified constituents. Tissue culture systems initiated during the work carried out were found to be ideal material for genomic studies. The developed culture lines of different morphogenetic nature (root culture, stolons and *in vitro* raised plants) were utilized for molecular cloning and expression analysis of key regulatory genes involved in the biosynthesis of glycyrrhizin (Fig. 1).

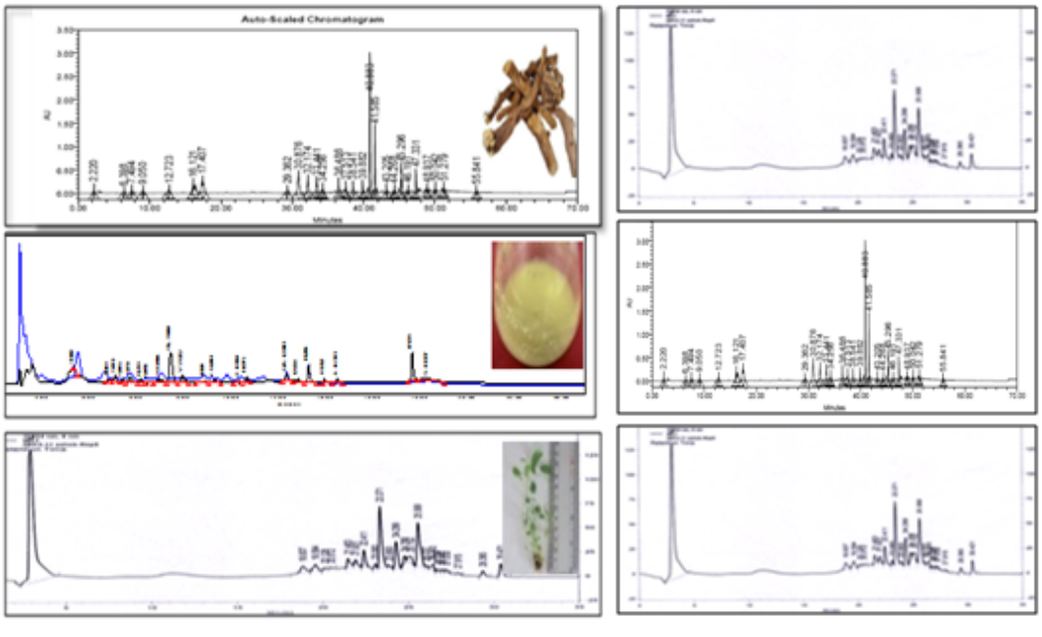

Figure 1: Differential terpenoid array in cultured tissues of *Glycyrrhiza glabra*

2.11 Cloning and functional characterization of three branch point oxidosqualene cyclases from *Withania somnifera* (L.) Dunal

Niha Dhar, Satiander Rana, SumeerRazdan, Wajid W. Bhat, Rekha S. Dhar, Ram Vishwakarma and Surrinder K. Lattoo

Oxidosqualene cyclases (OSCs) positioned at a key metabolic sub-dividing junction execute the indispensable enzymatic cyclizations of 2, 3-oxidosqualene for varied triterpenoid biosynthesis. Branch-point like these present favourable gene targets for redirecting metabolic fluxes towards specific secondary metabolites. However, detailed information regarding the candidate OSCs covering different branches and their regulation is necessary for desired genetic manipulation. *Withania somnifera* (*Ws*), a medicinal plant of immense repute is known to synthesize a large array of pharmacologically important steroidal lactone triterpenoids called withanolides. Withanolides, sterols, and suite of triterpenoids are elaborated *via* common 30-carbon intermediate 2, 3-oxidosqualene involving a highly regio and stereo- specific step carried by a family of genes called OSCs. This division is supposed to constitute a key sub-dividing point leading to the division of 2, 3-oxidosqualene between cycloartenol synthase which leads to the formation of cycloartenol that acts as the precursor to phytosterols and to withanolides and other array of OSCs that shape a range of diverse triterpenoids (Fig. 1).Such branch point genes become prospective candidates for perturbation which may impact respective branch flux by redirecting the precursor pool towards desired secondary metabolite and concurrently decrease the flux through competitive pathways.

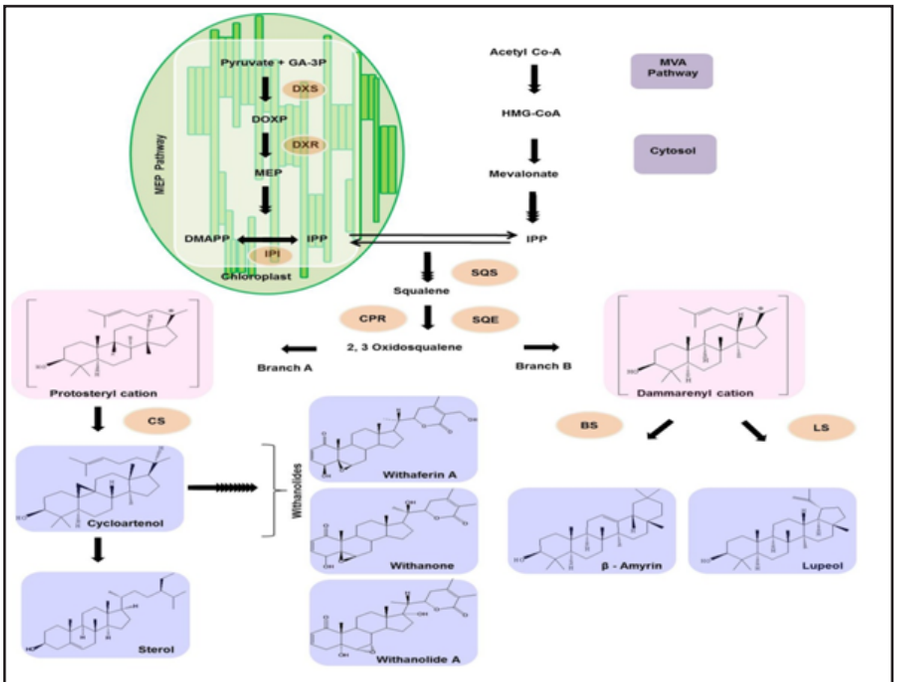

Figure 1: Scheme of proposed withanolide biosynthesis pathway

In an attempt to redirect the fluxes, we first functionally characterized three *W. Somnifera* OSCs namely cycloartenol synthase (*Ws*OSCS/CS), β-amyrin synthase (*Ws*OSC/BS) and lupeol synthase (*Ws*OSC/LS). Full length ORFs of these three *Ws*OSCs have been reported in our earlier studies. The three *Ws*OSCs were heterologously expressed in *Schizosaccharomyces pombe*. Extracts were prepared by DCM method and subjected to LC-MS analyses which confirmed their mono-functionality on being compared to their respective standards and negative control (empty vector) as shown in Fig.2.

Further, to elucidate the transcriptional regulation of the three *W. somnifera* OSCs *via* their respective promoters, upstream region of each gene was

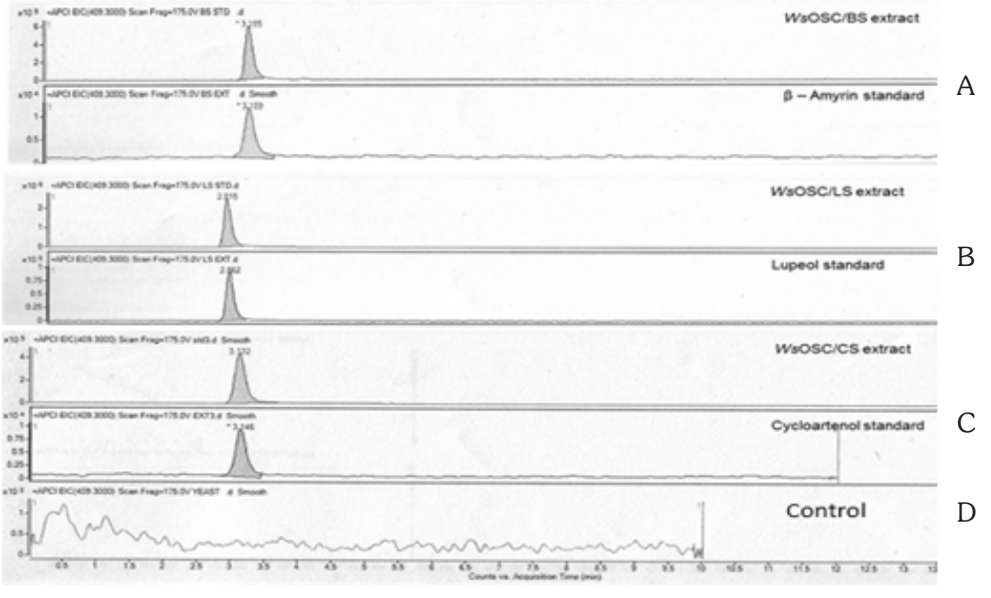

Figure 2: Extracted ion chromatogram (EIC) of standards β-amyrin, lupeol and cycloartenol and*S. pombe* cells transformed with expression constructs (A) pDS472aB, (B) pDS472aL, (C) pDS472aC and empty vector (D) pDS472a.

isolated using genome walking strategy and searched for various putative *cis*-regulatory elements using *in silico* tools *viz.* PLACE and Plant Care databases. Among these, three regulatory elements were selected to investigate their mediation in elicitor responsiveness with an aim to study the inducible nature of the promoters. These included 1) bZIP protein-binding motifs TGACG/CGTCA present in all the three promoters responsible for MeJA responsiveness 2) GARE-motif (TCTGTTG) involved in GA_3 responsiveness, identified in *Ws*OSC/BS and *Ws*OSC/LS promoters; 3) Box-W1, a fungal elicitor responsive element with a consensus sequence of TTGACC scanned in promoters of *Ws*OSC/BS and *Ws*OSC/LS (Fig. 3).

Endogenous plant-derived elicitor treatment of MeJA (0.1mM), GA_3 (1mM) and exogenous microbe-derived YE (0.1%w/v) treatments were supplemented to liquid cultures of *W. Somnifera*. In this context, promoter analysis was evaluated with regard to withanolide production and *Ws*OSCs gene expression levels. The three elicitors acted as both positive and negative regulators for the three OSCs. Differential transcript profiles were clearly reflected in relation to elicitor treatment with discernible changes in withanolide concentrations. Microbe derived exogenous YE elicitor played a role of negative regulator for the two competitive OSCs of *Ws*OSC/CS which are *Ws*OSC/BS and *Ws*OSC/LS while as *Ws*OSC/CS showed no change in its expression in response to YE (Fig. 4). However, there was significant increase in withanolide concentration with YE in comparison to MeJA and GA_3 treatments (Fig. 5). The down regulation of *Ws*OSC/BS and *Ws*OSC/LS is possibly indicative of decrease in the division of common substrate among the three branch OSCs.

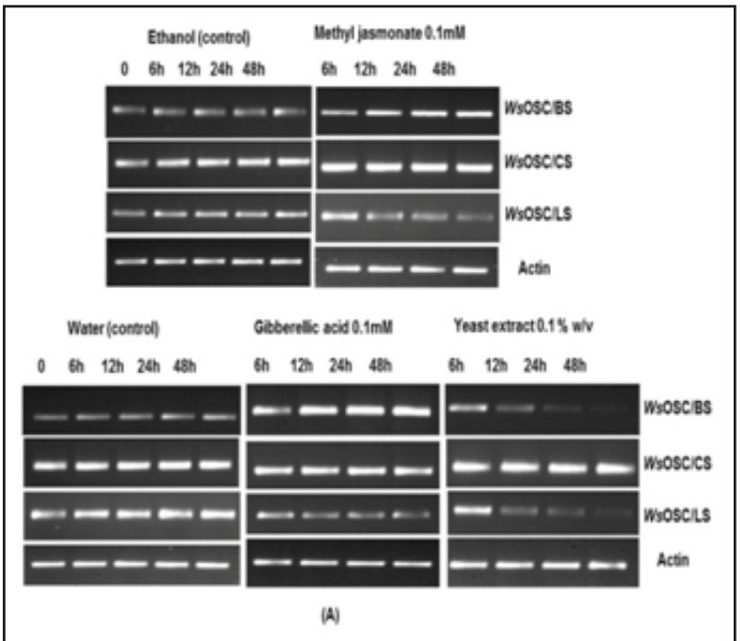

Figure 4: Transcript profiles of *Ws*OSCs in response to elicitor treatments. (A) Time courses of *Ws*OSC/BS, *Ws*OSC/LS and *Ws*OSC/CS expression in micropropagated *Withania somnifera* elicited by methyl jasmonate (MeJA; 0.1 mM), gibberellic acid (GA_3; 0.1 mM) and yeast extract (YE; 0.1% w/v). Actin was kept as endogenous control.

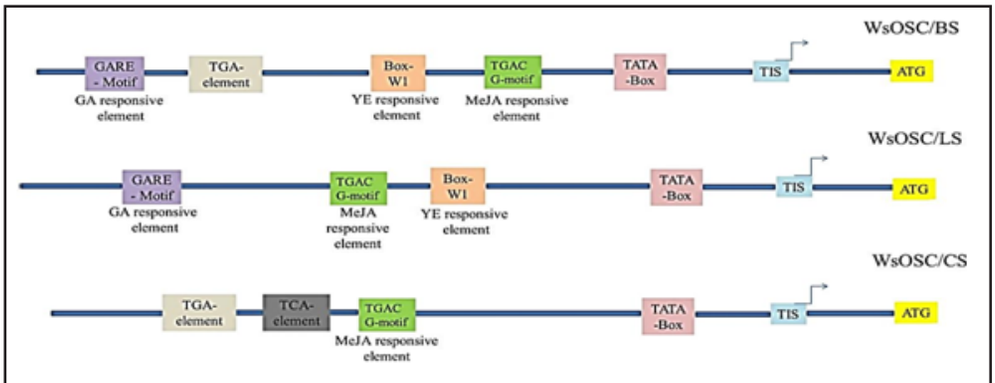

Figure 3: Upstream regions of WsOSC/BS, WsOSC/LS and WsOSC/CS comprising of important stress related conserved *cis*-motifs

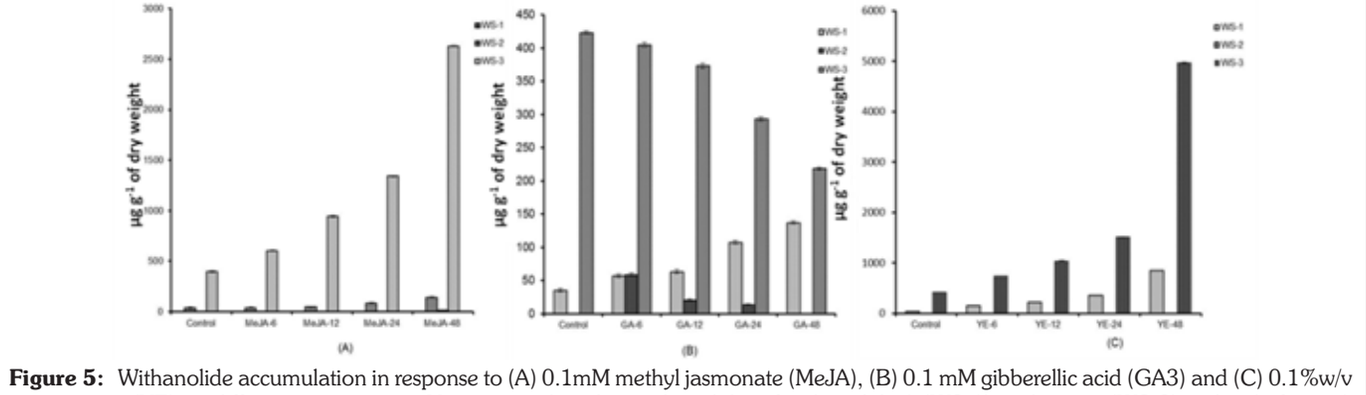

Figure 5: Withanolide accumulation in response to (A) 0.1mM methyl jasmonate (MeJA), (B) 0.1 mM gibberellic acid (GA3) and (C) 0.1%w/v yeast extract (YE) at different time courses. Variation in three key withanolides of withanolide A (WS-1), withanone (WS-2) and withaferine A (WS-3) was confirmed by HPLC analysis at 6, 12, 24 and 48 h. All values obtained were means of triplicate with standard errors. Time course accumulation of WS-1 and WS-3 was statistically significant at $p<0.01$ level.

2.12 NADPH-Cytochrome P450 reductase: Molecular cloning and functional characterization of two paralogs from *Withania somnifera* (L.) Dunal

Satiander Rana, Niha Dhar, Sumeer Razdan, Wajid W. Bhat, Rekha S. Dhar, Ram Vishwakarma and Surrinder K. Lattoo

Withania somnifera (L.)Dunal a highly reputed medicinal plant synthesizes large array of steroidal lactone triterpenoids called withanolides. Although, its chemical profile and pharmacological activities have been studied extensively during the last two decades but limited attempts have been made to decipher the biosynthetic route and identification of key regulatory genes involved in withanolides biosynthesis. Principally, withanolides (C-30) are synthesized *via* both mevalonate (MVA) and non-mevalonate (DOXP) pathways. The head-to-tail condensation of isopentenyl pyrophosphate (IPP) leads to formation of farnesyl diphosphate (FPP) which is the main precursor for triterpenoids. Cytochrome P450 reductase is most imperative redox partner of multiple P450s involved in primary and secondary metabolite biosynthesis. Cytochrome P450 enzymes belong to one of the largest and most functionally diverse protein super-families which is pivotal in various metabolic molecular circuitries. Presence of multiple CPRs in plants may reflect the diversity of P450s and seem primarily to confront the high demand of electron supply during biotic and abiotic stress or differential expression at various stages of plant development.

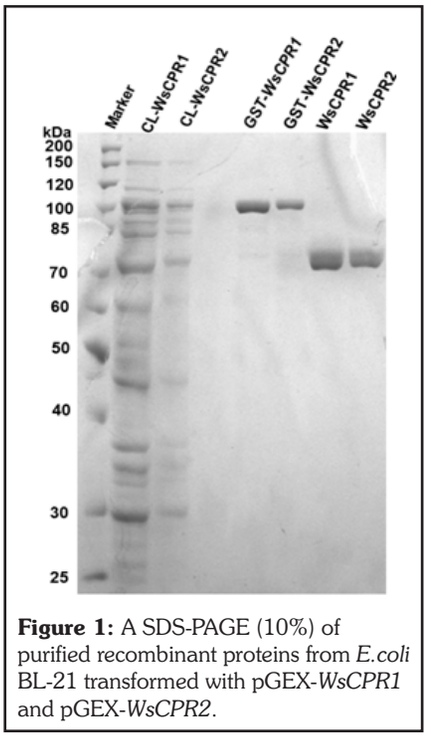

Figure 1: A SDS-PAGE (10%) of purified recombinant proteins from *E.coli* BL-21 transformed with pGEX-*WsCPR1* and pGEX-*WsCPR2*.

As a part of on-going endeavour to investigate various pathway genes in withanolide biosynthesis, we have already cloned and expressed two paralogs of CPR (NCBI GenBank*Acc No. WsCPR1*: HM036710 and *WsCPR2*: GU808569) in *E. Coli*. In an attempt to carry this work forward, we have used the principle of affinity chromatography and purified recombinant fusion CPR proteins having GST-tags using glutathione sepharose beads (Fig. 1).

Purified WsCPR1 and WsCPR2 were used for functional characterization by enzyme assay method wherein NADPH was used as electron donor for reducing its substrate cytochrome *c* where WsCPR1 was observed to possess higher specific activity of7.56±0.06 μmol min $^{-1}$ mg $^{-1}$ while asspecific activity of WsCPR2 was 6.83±0.06 μmol min $^{-1}$ mg $^{-1}$. For kinetic studies of WsCPRs, the enzyme and NADPH were kept constant whereas the concentration of cytochrome *c* was taken in increasing order (Fig. 2). As the substrate concentration was increased, the amount of products produced also increased. V_{max} of each purified protein was also calculated. This was explained by Michaelis-Menten plot. The apparent K_m value for WsCPR1 was 5.06±0.30 μM which showed its high affinity towards cytochrome *c* while for WsCPR2 K_m value was 6.48±0.33 μM.

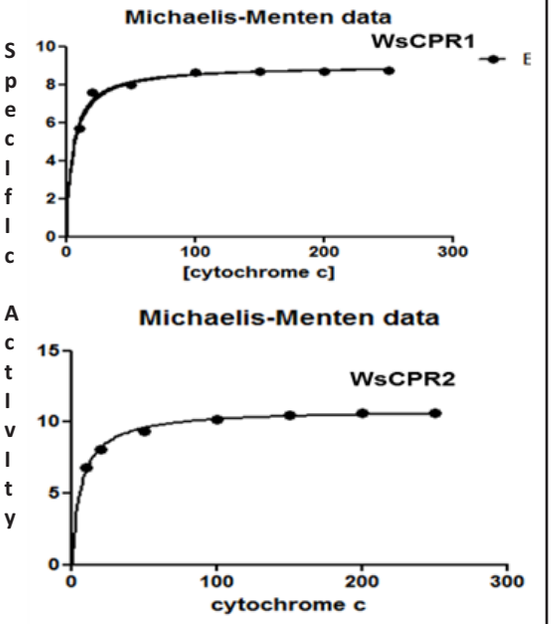

Figure 2: Enzyme kinetics of WsCPR1 and WsCPR2

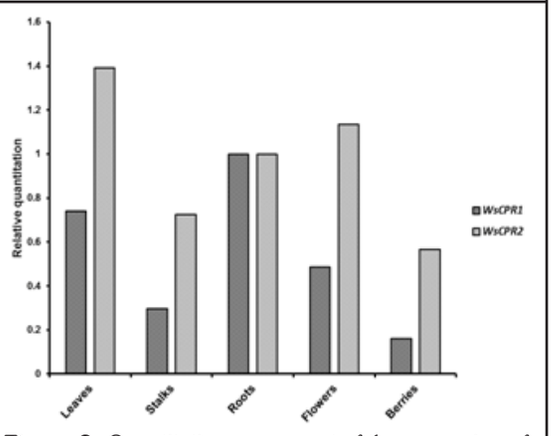

Figure 3: Quantitative assessment of the expression of *WsCPR1* and *WsCPR2* in different tissues of *Withania somnifera*.

Tissue specific expression showed that *WsCPR1* and *WsCPR2* expressed constitutively with varying expression levels in different tissues as depicted in Figure 3. *WsCPR2* was found to be transcribing more in all tissues in comparison to *WsCPR1*. However, highest expression of CPR1 was observed in roots among all the tissues (Fig. 3). The expression pattern of *WsCPR2* is in agreement with the higher content of withanolides in leaves of *W. somnifera* as reported earlier and

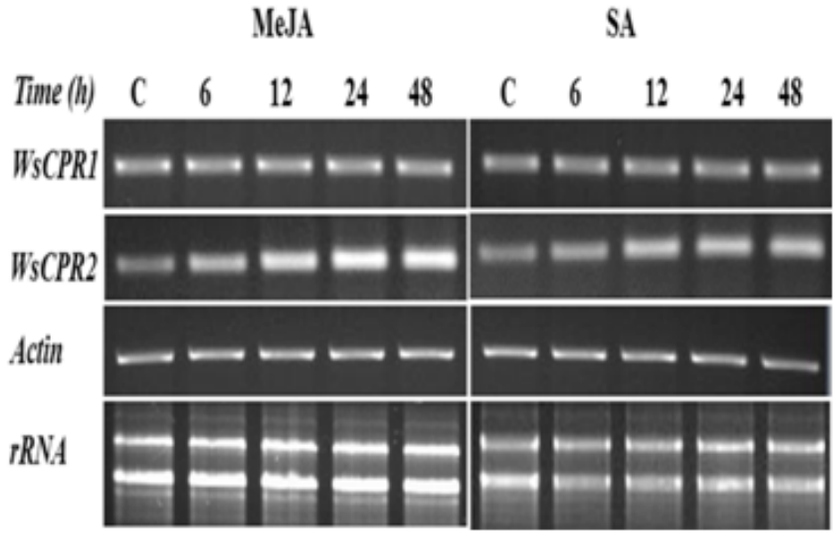

Figure 4: Time courses of *WsCPR1* and *WsCPR2* expression in micropropagated *Withania somnifera* induced MeJA and SA

probably indicates their involvement to meet the high metabolite flux, withanolides extracted from the treated samples were subjected to HPLC analysis. There was increase in WS-1, WS-2 and WS-3 over a period of time in response to elicitor treatments (Fig. 5). In MeJA treated samples there was a significant increase in WS-3 (396.37±0.44–2629.397±0.41 μg g^{-1} of dry weight) while as WS-2 accumulated meagrely (13.818±0.14 μg g^{-1} of dry weight) after 48 h. SA treated samples showed more increase in WS-1 (117.768 ± 0.44 – 257.546 ± 0.29 μg g^{-1} of dry weight) with no traces of WS-2.

To determine the gene copy number and further validation of two paralogs of CPR in *W. somnifera*, southern blot analysis was carried out under high stringency conditions using DIG-labelled full length probes for *WsCPR1* and *WsCPR2*.The results obtained suggest that *Withania* genome contains two paralogs of P450 reductase and single allele for both *WsCPR1* and *WsCPR2*(Fig. 6).

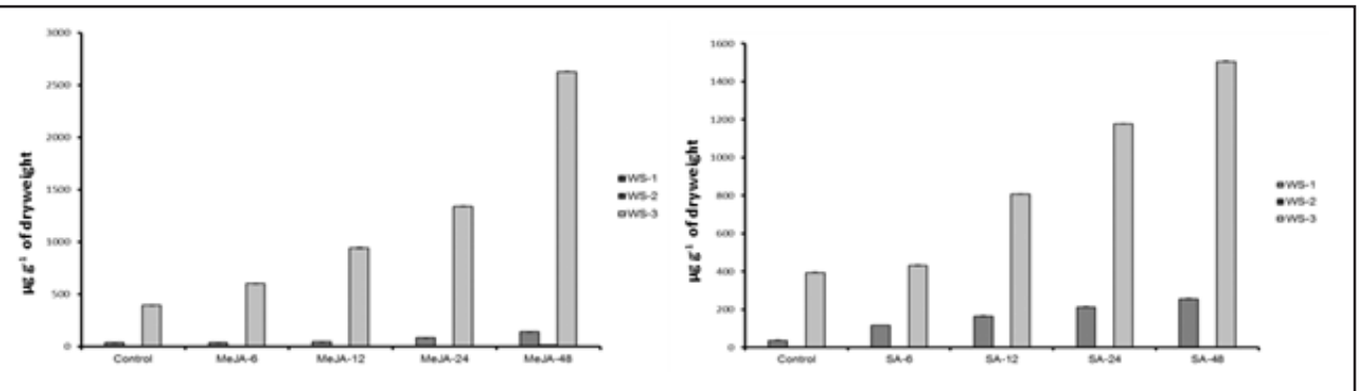

Figure 5: Effect of MeJA and SA treatment on withanolides accumulation at different time intervals

reductive demand of different P450 monooxygenases for driving the biosynthesis of withanolides.

Elicitor treatments with MeJA and SA resulted in induction of *WsCPR2* while the expression of *WsCPR1* remained unchanged. The elicitors strongly enhanced the transcript level of *WsCPR2* which had a positive influence on withanolides accumulation (Fig. 4). To establish a correlation between expression profiles and

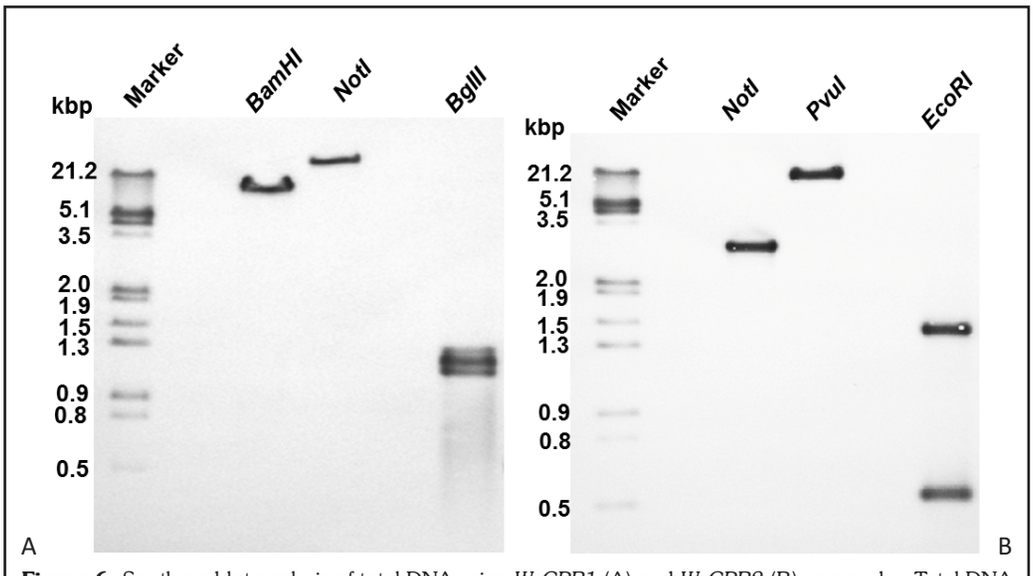

Figure 6: Southern blot analysis of total DNA using *WsCPR1* (A) and *WsCPR2* (B) as a probe. Total DNA (30 μg) isolated from *Withania somnifera* was digested with the indicated restriction enzymes, The digested samples were electrophoresed on 0.8 % agarose gel, blotted onto nylon membrane and subjected to hybridisation using DIG-labelled ORF of *WsCPR1* and *WsCPR2* as probes. First lane contains molecular markers with indicated molecular weight on the left side.

2.13 Dynamics of withanolide biosynthesis in relation to temporal expression pattern of metabolic genes in *Withania somnifera* (L.) Dunal: A comparative study in two morpho-chemovariants

Niha Dhar, Satiander Rana, Wajid W. Bhat, Sumeer Razdan, Shahzad A. Pandith, Shabnam Khan, Prabhu Dutt, Rekha S. Dhar, Ram Vishwakarma and Surrinder K. Lattoo

Withania somnifera (L.)Dunal (Solanaceae) commonly known as ashwagandha enjoys tremendous popularity as a traditional medicinal plant since antiquity. Most of its remedying significance has been attributed to a class of molecules called withanolides which are a novel group of C-28 steroidal lactones built on an intact or rearranged ergostane framework in which C-22 and C-26 are oxidised to form a six membered δ-lactone ring. In recent years there have been some reports pertaining to tissue-specific site of synthesis and accumulation of withanolides in *W.somnifera*. The literature presents ambiguity vis-à-vis *de novo* synthesis and translocation of withanolides. Tissue-specificity does not necessarily reveal the general trend of plant secondary metabolism as secondary metabolites are spatially and temporally synchronized in terms of biosynthesis, accumulation and translocation. In many instances few get structured and stored at the same location in the plant, while as others get reallocated from the site of synthesis to other tissues of the plant. Noticeable variations in secondary metabolites are also evident in plant life cycle encompassing various phenophases/ontogenetic stages from vegetative to reproductive growth phase. Dynamics of withanolide biosynthesis in respect to these various contours has not been studied yet.

As a step towards this, we have examined the alteration in withanolide biosynthesis at different temporal phases of plant development in leaf and root tissue of two distinct varieties of *W.somnifera* to provide a qualitative and quantitative insight in to the synthesis and reallocation of withanolides.

The material for present study comprised of open pollinated seeds of two distinct varieties of *W. Somnifera* designated as WS-Y-08 (25-30 cm tall with yellow berries) and WS-R-06 (100-125 cm tall with red berries). These two accessions differ appreciably in their capacity to synthesize and accumulate different withanolides. The root and leaf tissues from the two varieties were used as a source material for high performance liquid chromatography (HPLC) analysis of withanolide-A (WS-1), withanone (WS-2) and withaferin A (WS-3)and RNA extraction and cDNA preparation. Sampling from WS-Y-08 and WS-R-06 was performed at five ontogenetic stages of plant growth. These stages included vegetative (S-I), flowering (S-II), fruit-set (S-III), fruit-maturation (S-IV) and over-maturation (S-V) stages during seed to seed life cycle of the plant. Expression profiles of five genes namely squalene synthase (*Ws*SQS), squalene epoxidase (*Ws*SQE), cyloartenol synthase (*Ws*CAS), cytochrome P450 reductase 1 (*Ws*CPR1) and cytochrome P450 reductase 2 (*Ws*CPR2) were studied using semi-quantitative PCR method at five developmental phases.

HPLC based chemoprofiling of WS-Y-08 and WS-R-06 revealed significant differences in the concentration of the three key withanolides in leaf and root tissues at different phenophases. However, the metabolite dynamics through different developmental phases in the two accessions did not

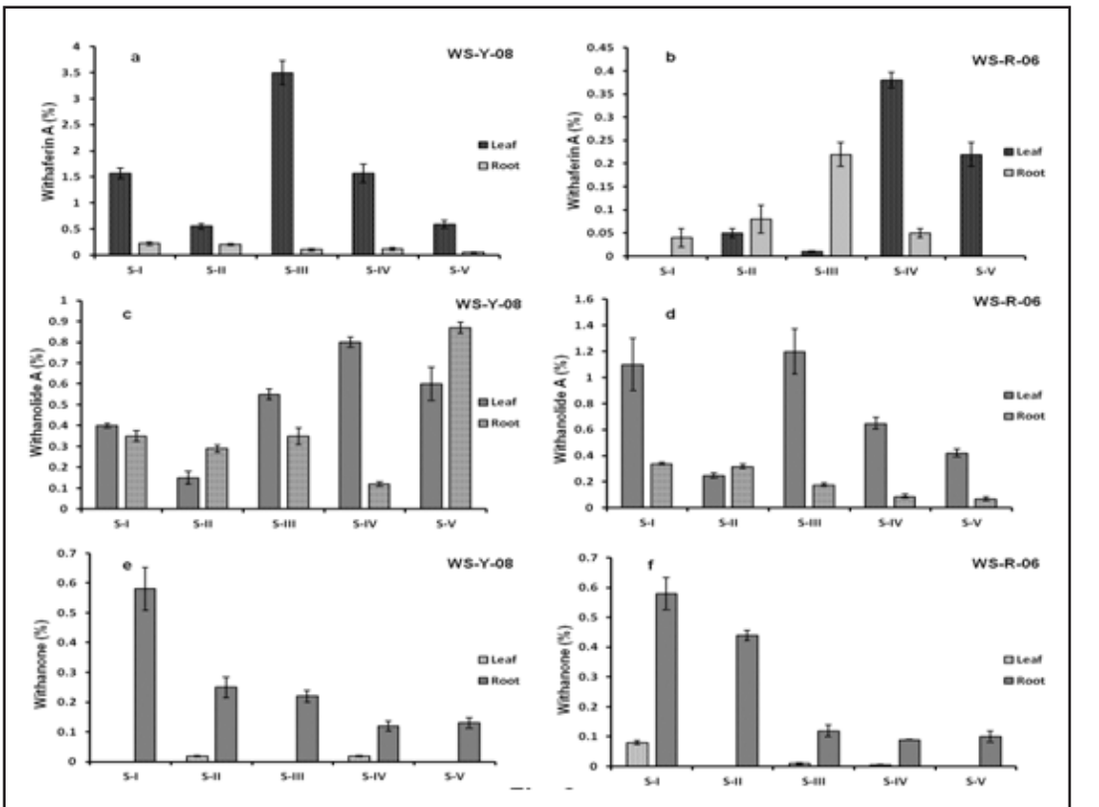

Figure 1: Withanolide A (WS-1), withanone (WS-2) and withaferine A (WS-3) accumulation at vegetative (S-I), flowering (S-II), fruit-set (S-III), fruit-maturation (S-IV) and over-maturation stages (S-V).

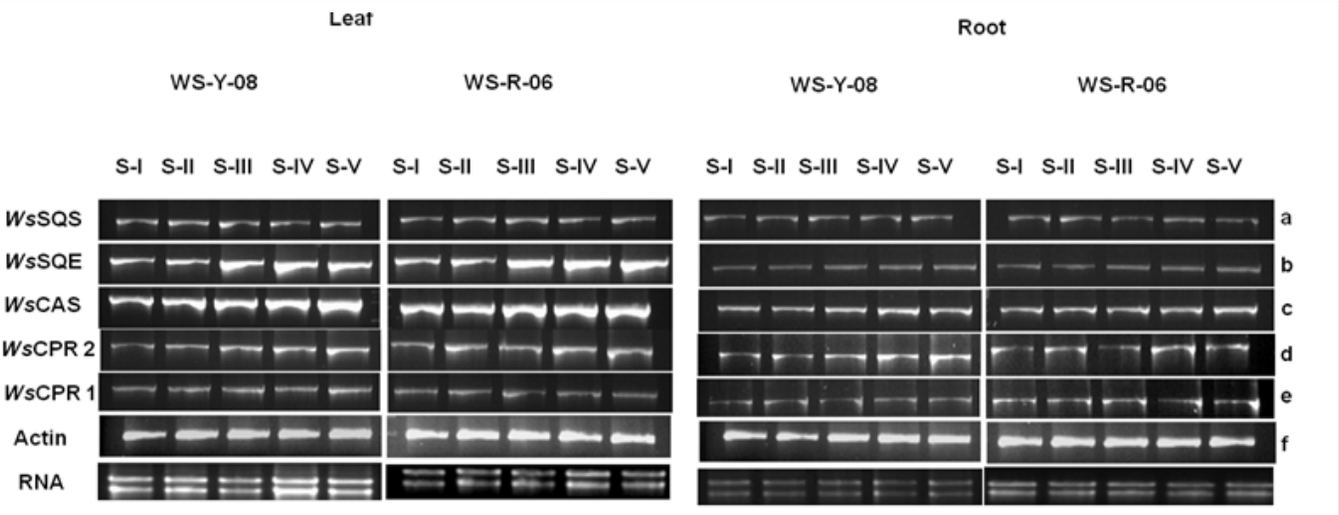

Figure 2: Comparative expression levels of *Ws*SQS, *Ws*SQE, *Ws*CAS, *Ws*CPR1 and *Ws*CPR2 at vegetative (S-I), flowering (S-II), fruit-set (S-III), fruit-maturation (S-IV) and over-maturation (S-V) stages in *Withania somnifera*.

present any congruence in the pattern of metabolite accumulation (Fig. 1).

The relative transcript profiles of identified genes at different developmental stages showed appreciable variation in leaf and root tissues of WS-Y-08 and Ws-R-06 (Fig. 2). Expression level of all the five genes was significantly higher in leaves of both the varieties as compared to the roots.

These studies presented that the dynamics of accumulation of withanolides and the transcriptomic abundance of various key pathway genes during ontogenesis are synchronized. Comparative quantitative and qualitative chemoprofiles of leaf and root tissues revealed no correspondence between the pattern of accumulation in the two tissues, thus apparently pointing towards *de novo* tissue-specific synthesis of withanosteroids in *W.somnifera*.

2.14 A phenylalanine ammonia-lyase ortholog (*PkPAL*) from *Picrorhiza kurrooa* Royle ex. Benth: Molecular cloning, promoter analysis and response to biotic and abiotic elicitors

Wajid W.Bhat, Sumeer Razdan, Satiander Rana, Niha Dhar, Shahzad Pandith, Parvaiz Qazi, Rekha S. Dhar, Ram Vishwakarma and Surrinder K. Lattoo

Phenylalanine ammonia-lyase (PAL) is the first key enzyme in the phenylpropanoid pathway leading to the accumulation of many phenylpropanoid metabolic products, such as flavonoids, coumarins, phenolics and others. Present knowledge about the biosynthesis of picrosides, and the genes and enzymes involved, is however limited. Although some recent work has been started which is mainly aimed at unravelling the pathway of picroside biosynthesis, the biosynthetic pathways for the production of picrosides and related iridoid glycosides in *P. kurrooa* still remains to be poorly understood.The biosynthesis of picrosides, pharmacologically active iridoid glycosides of *P. Kurrooa*, involves the synthesis of iridoid moiety from isoprenoid pathway through a series of oxidation and cyclization steps followed by condensation of a glucose moiety, and addition of phenylpropanoid pathway derived phenolic acid moieties like cinammic acid, vanillic acid, etc. Cloning and characterization of the genes involved in picroside biosynthetic pathway is of significant relevance to manipulate the copious production of iridoid glycosides *in planta*. Since this plant is highly endangered and endemic to North-Western Himalayas, it would be of immense value to explore the heterologous production of picrosides in bacteria or yeast through synthetic biology approaches. The aim of the present study, therefore, was to characterize an ortholog of phenylalanine ammonia lyase from *P. kurrooa*. A homology based strategy was employed to identify phenylalanine ammonia-lyase gene from *P. kurrooa*, taking advantage of the highly conserved amino acid motifs present in plant PALs. Two forward degenerate primers were designed based on amino acid sequences in the conserved regions of plant PALs. RT-PCR generated a 505bp fragment that was homologous with other plant PAL genes. Subsequently, 3′ and 5′ RACE PCR generated 971bp

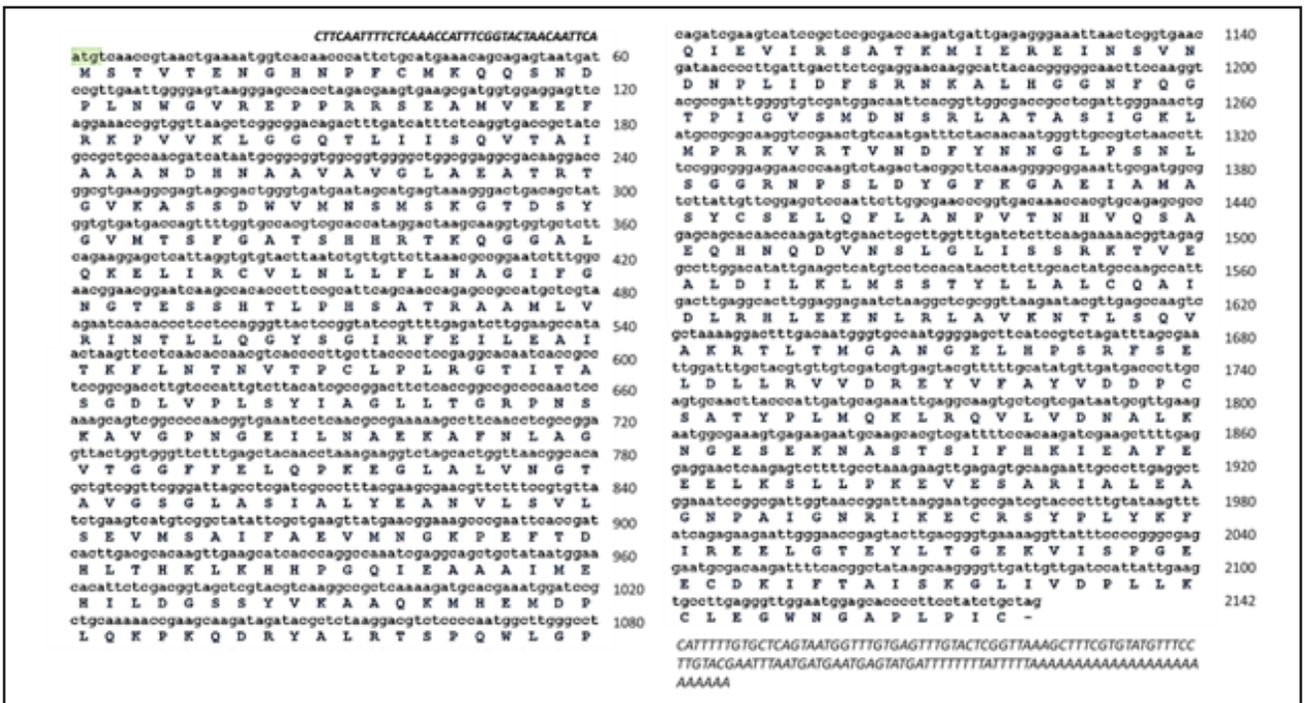

Figure 1: Nucleotide and the deduced amino acid sequence of *PKPAL*. 5´ UTR and 3´ UTR are underlined. The dash marks the translation termination codon.

fragment and 878bp fragment, respectively. From overlapping sequences of three fragments, the 2,312 bp full-length *PkPAL* cDNA was constructed and identified. Sequence analyses indicated that it contains an open reading frame (ORF) of 2,142 bp encoding for 713 amino acid residues. It was flanked by 38 bp 5′untranslated region (UTR) and 132 bp3′untranslated region (UTR) (Fig. 1).The nucleotide sequence of full length cDNA of phenylalanine ammonia-lyase identified from *P. kurrooa* was submitted to NCBI GenBank under accession number JQ996410and designated as *PkPAL*.

RT-PCR analysis indicated that *PkPAL* expressed in a constitutive manner in the tissues of leaf, inflorescence and rhizome, with the maximum expression in leaves (Fig. 2). Plant samples were collected from three different altitudinal gradients of Kashmir Himalayan range. RNA was extracted from leaf and rhizome tissues and analysed for transcript abundance. There was a positive correlation between the altitude and the expression level of *PkPAL* (Fig. 3). The expression level of *PkPAL* was highest in sample collected from Dhanwas location at an altitude of 3500 m (above sea level) followed by Yarikhah (altitude 2400 m) and the expression of *PkPAL* was lowest in the sample originally collected from Sonamarg location but habituated and cultivated at a lower altitude of Srinagar (altitude 1730 m).

Using genome walking strategy, we isolated 718 bp 5´ upstream regions of *PkPAL*. The predicted transcription start site (TSS, +1) correlated well with the 5´ RACE analysis and is located at 45 bp upstream of the ATG start codon using PlantProm (Fig. 4).

To find the expression profile of *PkPAL* in response to various elicitors, and to

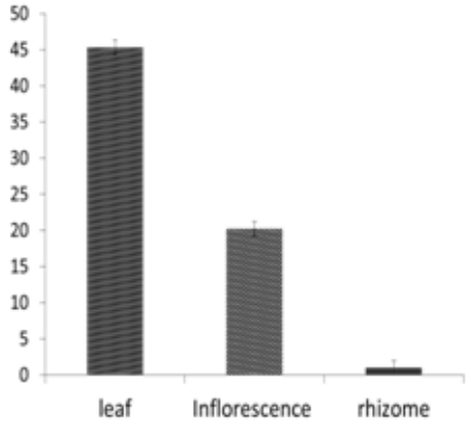

Figure 2: Expression characteristics of *PkPAL* in different tissues, including leaf, rhizome and inflorescence.

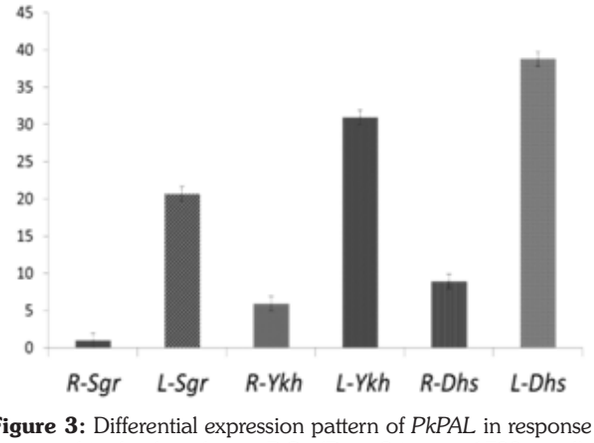

Figure 3: Differential expression pattern of *PkPAL* in response to varying altitudinal gradients. *R-Sgr*(Root-Srinagar; 1730 m asl), *L-Sgr*(Leaf-Srinagar; 1730 m asl), *R-Ykh*(Root-Yarikhah; 2400 m asl), *L-Ykh*(Leaf-Yarikhah; 2400 m asl), *R-Dhs*(Root-Dhanwas; 3500 m asl), *L-Dhs*(Leaf-Dhanwas; 3500 m asl).

corroborate these results with the identified important *cis*-regulatory elements, transcripts were assayed in response to MeJA, SA, UV-B and 2,4-D. In the present study, MeJA exogenous application of 2, 4-D in comparison to the effect of MeJA or SA (Figure 5c). *PkPAL* showed 6-fold increase after 6 h of induction, followed by a steady decrease in the followed by a steady decrease up to 48 h post-induction (Figure 5d).

Starting from the crystal structure of *P. crispum* PAL (PDB: 1w27), the three-

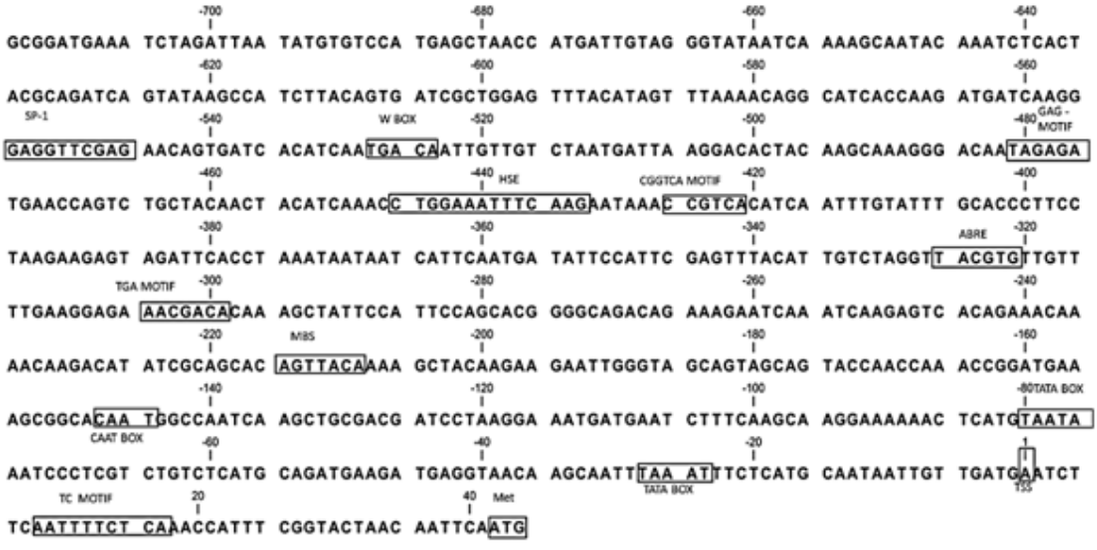

Figure 4: Nucleotide sequences of the *PkPAL* gene promoter. Numbering starts from the predicted transcription start site. The putative core promoter consensus sequences and the motifs with significant similarity to the previously identified *cis*-acting elements are boxed and the names are given.

up-regulated the expression of *PkPAL* significantly and the mRNA level peaked at 6 h, with about 30-fold increase. Afterwards, a decrease in *PkPAL* transcript level was seen at 12 h which continued up to 48 h. The time course of *PkPAL* expression is depicted in Figure 5a. In the present study, SA elicited differential transient increase in accumulation of *PkPAL* transcripts. *PkPAL* showed 13-fold increase in the expression profile, 12 h post induction (Figure 5b). Transcript abundance was less obvious with transcript level. To understand the effect of UV on the expression of *PkPAL*, we treated *in vitro* raised analysed plantlets with UV-B radiations. After 3 h of induction, there was a maximum 8-fold increase in the transcript levels of *PkPAL* dimensional structure of the *PkPAL* was built (Fig. 6). Consistent with the description in *P. crispum*, *PkPAL* was composed of MIO domain, core domain and inserted shielding domain (Fig. 6).

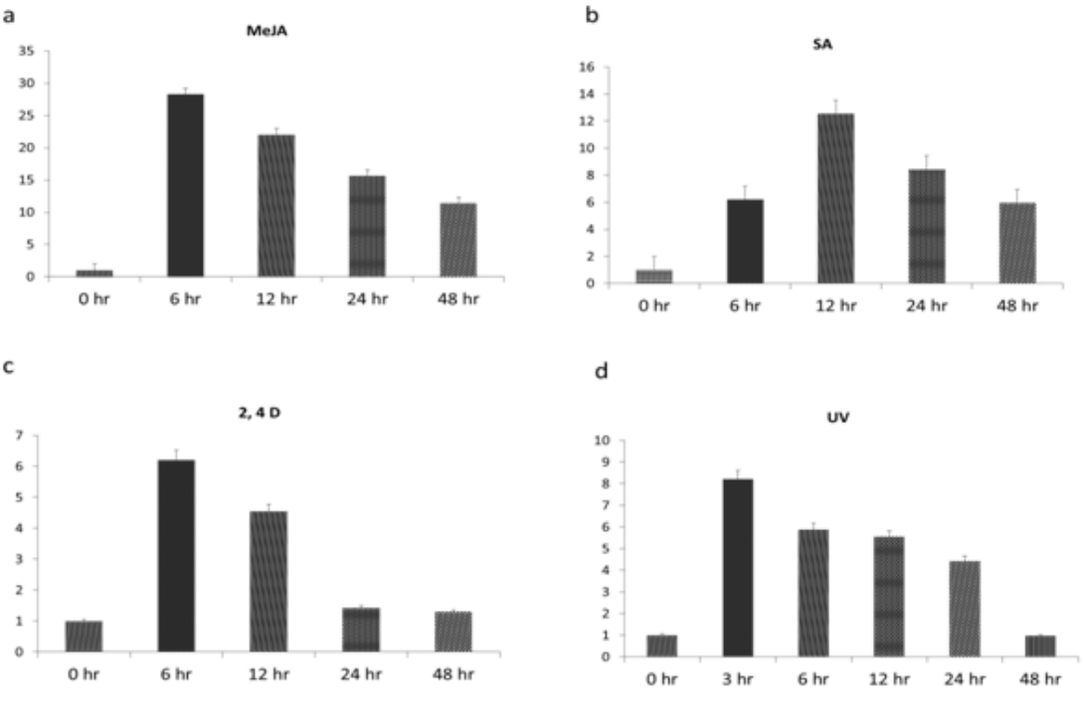

Figure 5: Time-course expression characteristics of *PkPAL* in response to methyl jasmonate (a), salicylic acid (b), 2, 4-dichlorophenoyacetic acid (c) and UV-B (d) at different time points.

Besides, *PkPAL* also contained an Ala-Ser-Gly triad which is highly conserved in plant PALs. This triad can be converted auto-catalytically, *via* internal cyclization and elimination of two water molecules, to the electrophilic prosthetic group 3, 5-dihydro-5-methylidene-4H-imidazol- 4-one (MIO), which functions as an important co-factorof PAL. The predicted structure of *PkPAL* was further refined by employing KoBa^{MIN} web server. The stereo-chemical qualities of the energy refined predicted model of *PkPAL* proteins was validated by PROCHECK server. Ramachandran plot analysis of *PkPAL* showed 88.1% residues in the most favourable region, 10.1% residues in the additional allowed region, 1.7% in the generously allowed region and 0.2% in the disallowed region.

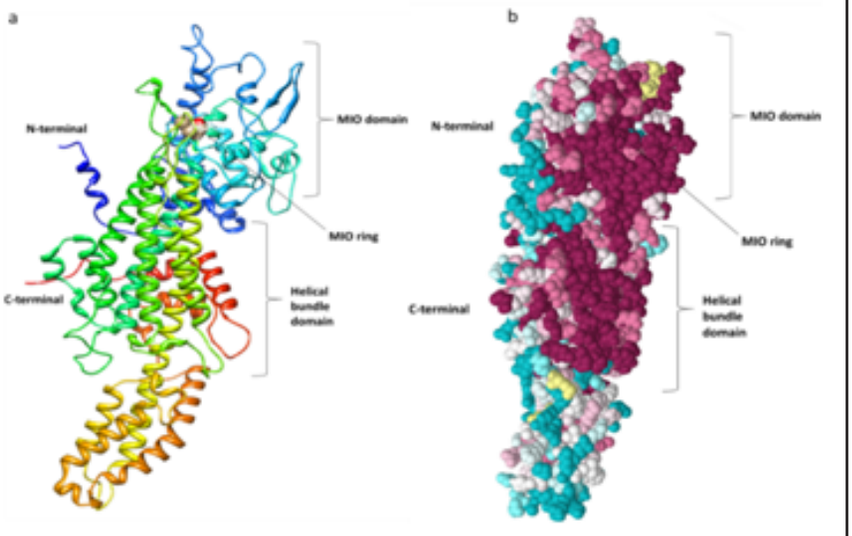

Figure 6: Three dimensional protein model and conserved residue prediction for *PKPAL*. A: Ribbon display of the 3-D structures of *PKPAL* as predicted by PHYRE2 web server, using crystal structure *Petroselinum crispum Ps*PAL1 (Protein Data Bank (PDB) id. 1w27) as template. N and C-terminal domains are shown. B: Evolutionary conserved key residue analysis of *PkPAL* identified using Consurf, an empirical Bayesian inference based web server. Residue conservation from variable to conserve is shown in blue (1) to violet (9).

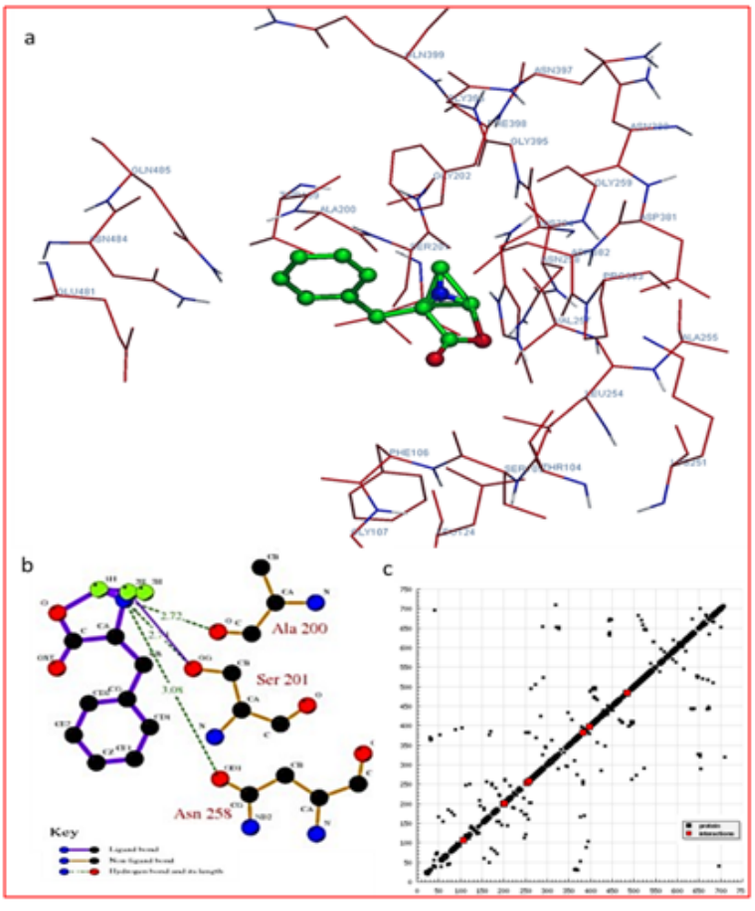

Figure 7: Schematic diagram of phenylalanine docked into the proposed active binding pocket of *PkPAL*(a). 2D representation of the interaction figure and H-bonding of phenylalanine with catalytically key residues of *PkPAL*(b). H-plot of modelled *PkPAL* showing key interacting partners of *PkPAL* that interact with phenylalanine, converting it to cinnamic acid (c).

The docking of *PkPAL* and L-phenylalanine was predicted with DockingServer (Fig. 7). Docking of the L-phenylalanine in the active site of *PkPAL* showed that it binds to the enzyme pocket with high affinity. The free energy change (ΔG) of the best pose of enzyme-ligand complex was found as -4.92 kcal/mol and the total intermolecular energy was found to be -5.23 kcal/mol. The results showed that the possible binding pocket consisted of Phe106, Gly107, Ala200, Ser201, Gly202, Asp203, Leu204, Leu254, Asn258, Phe 398, Asn380, Asp381 and Asn382, which contained the Ala-Ser-Gly triad. Purview of literature suggests that this is the only report of PAL ortholog cloned and characterized from *P. kurrooa*.

2.15 Altitudinal variability in anthraquinone constituents from novel cytotypes of *Rumex nepalensis* Spreng - a high value medicinal herb of North Western Himalayas

Umer Farooq , Shahzad A. Pandith , Manjit Inder S. Saggoo and Surrinder K. Lattoo

Rumex nepalensis Spreng (Polygonaceae) is a perennial, ascending herb distributed throughout Himalayas from Bhutan to Kashmir and also to Turkey, Java and South Africa. It owes its pharmacological significance to an active class of compounds known as anthraquinones. The occurrence of polyploid races within plant species continues to be of interest to plant systematists and biologists.*R. nepalensis* displays large incidence of polyploidy; that being the case attracted our attention. To catalogue, genetic and chemical diversity of medicinal flora of North Western Himalayas through population based studies; the present investigation included cytological, chemical and morphometric analysis of various populations. We determined the chromosome counts in corroboration with comparative chemo-profiles of the five different cytotypes of *R. nepalensis*. The investigations suggest positive correlation between ploidy level and metabolite accumulation in relation to different altitudinal gradients.

The wild growing plants of *R. nepalensis* were collected from five different locations of the Kashmir valley (J & K state, India) (Table 1).

Detailed cytological analysis of various populations of *R. nepalensis* revealed the existence of four different chromosomal races with meiotic chromosome numbers n= 20, 30, 40 and 60 in the Kashmir region (Table 1). These chromosome counts are the first ever records for this species. The occurrence of intra-specific polyploids in *R. nepalensis* is indicative of the fact that its genome is still in flux and constant evolution, possibly to enhance the adaptive and survival value of the species under varied ecological niches of Himalayan region.

S. No.	Meiotic chromosome	Cytotype (ploidy status)	Location of plant collection	Accession number (PUN)*
1	20**	Tetraploid (4x=40)	Zawoora ($33^0$43' N, $75^0$14' E; 2000 m)	57691
2	30**	Hexaploid (6x=60)	Zawoora upper reaches ($34^0$44' N, $74^0$48'E; 2300 m)	57676
3	40**	Octaploid (Y) (8x=80)	Yusmarg ($33^0$47' N, $74^0$39' E; 2600 m)	57677
4	40**	Octaploid (T) (8x=80)	Thajwas ($34^0$18' N, $74^0$48' E; 3400 m)	57660
5	60	Dodecaploid (12x=120)	Lidderwatt ($34^0$04 N, $75^0$17' E; 3500 m)	57683

Table 1: Chromosome count and ploidy status recorded in different populations of *Rumex nepalensis* from five locations of Kashmir Himalayas.

by Holmgren and Holmgren (1998)

**First chromosomal report at world level

The overall concentration of in the direction of glycosylation, like many of the plant natural products may be towards enhancing their solubility and stability for facilitating their easy storage and accumulation in plant cells.

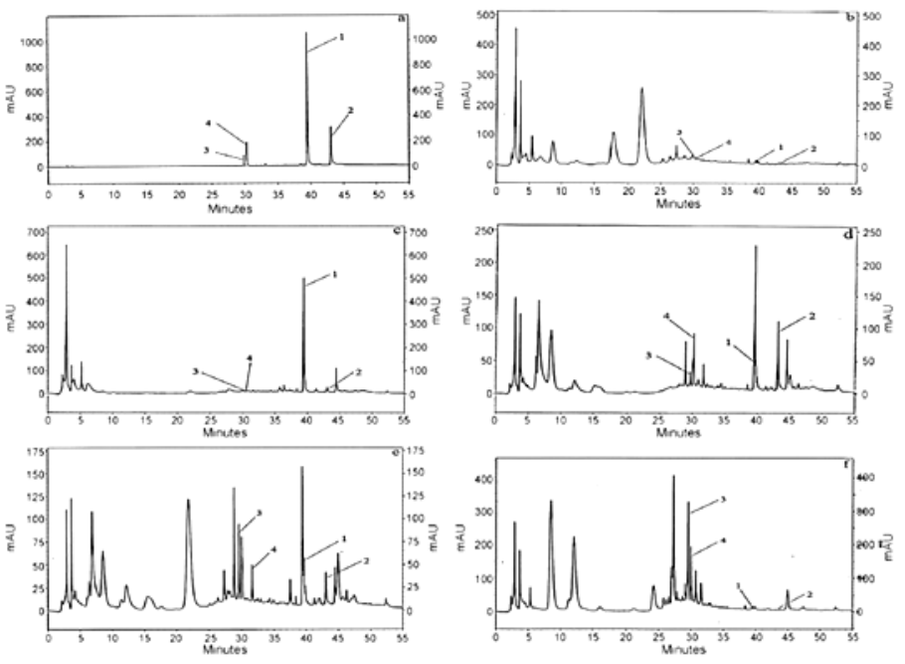

Figure 1: HPLC chromatograms of standard major anthraquinones (a) and methanolic extracts of leaves of tetraploid (b), hexaploid (c), octaploid Y (d), octaploid T (e) and dodecaploid (f) cytotypes of *R. nepalensis*. Abbreviations: 1= emodin; 2= chrysophanol; 3= emodin glycoside; 4= chrysophanol glycoside.

*Herbarium code of the Botany Department, Punjabi University, Patiala, as per "Index Herbariorum"

glycosides was found to be higher than that of their respective aglycone forms at all ploidy levels. This shuffle

There was a well marked increasing trend in the concentration of all four anthraquinone compounds from

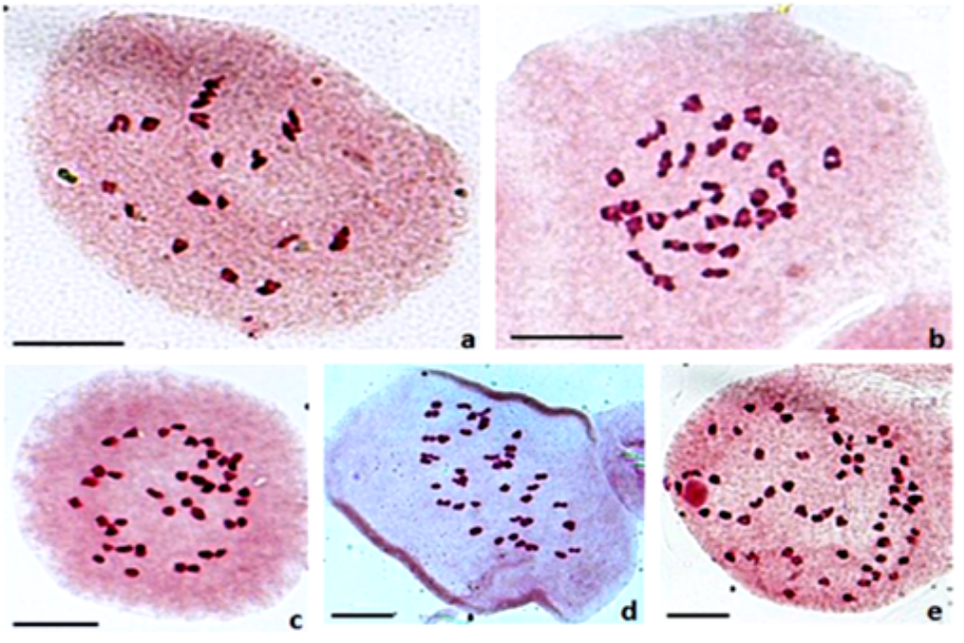

Figure 2: Meiotic chromosome numbers in five populations from different altitudinal ranges in *R. nepalensis;* A PMC at metaphase- I showing twenty bivalents (n= 20; Zawoora, 2000 m in altitude) (a); A PMC showing thirty bivalents (n= 30; Zawoora, 2300 m) (b); A PMC at metaphase- I showing forty bivalents (n= 40,Yusmarg, 2600 m) (c); A PMC at metaphase-I showing 40 bivalents (n= 40, Thajwas, 3400 m) (d); A PMC at diakinesis showing sixty bivalents (n= 60, Lidderwatt (3500 m) (e). Bar= 10 μm.

tetraploid to octaploid variants. In terms of relative percentage, anthraquinones were found to be maximum (33.95%) in the dodecaploid type and minimum (2.73%) in the tetraploid one, providing a clue towards the difference in pharmacological significance of these two cytotypes (Table 2; Fig. 3).

*Concentration of all four anthraquinones in one cytotype / total concentration in all cytotypes × 100

Morphological variations in all the populations of five different cytotypes were evaluated. Microscopic characters widely used for the identifcation of ploidy levels *viz.* pollen grain diameter and stomatal length were also analyzed (Table 3).

The present investigation thus led to the identification and existence of four novel chromosomal races wherein ploidy level ranges from tetraploidy to dodecaploidy. These polyploid races are hitherto unreported in *R. nepalensis* except for 2n= 120. Chemoprofiling based on four key anthraquinones of different cytotypes from various altitudinal gradients presented an appreciable variability in chrysophanol, emodin and their glycoside contents. The increasing pattern of metabolite accumulation broadly seems to be in conformity with the increasing altitude and ploidy status. This study has a prospect to explore desirable populations with higher content of chemical constituents for commercial and pharmacological utilization.

Table 2: Relative percentage of four key anthraquinone constituents in the leaves of five different cytotypes of *Rumex nepalensis*

Ploidy Level	Tetraploid	Hexaploid	Octaploid (Y)	Octaploid (T)	Dodecaploid
Relative percentage (%)*	2.73	8.49	28.98	25.85	33.95

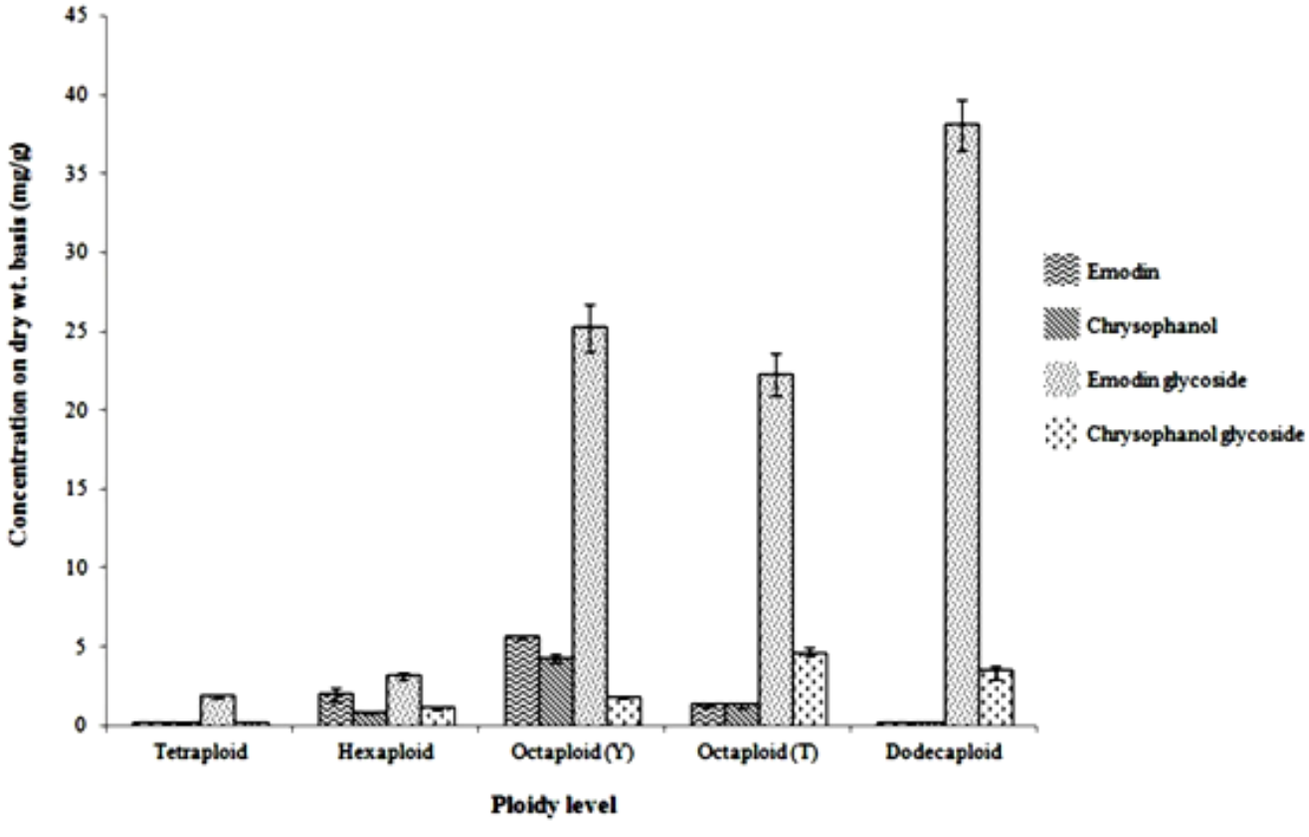

Figure 3: Graphic representation of the concentrations of key anthraquinones in five different cytotypes of *R. nepalensis.* All values obtained were means of triplicate with standard errors.

Table 3: Morphological comparison of different cytotypes in *Rumex nepalensis*

S. no.	Characters	Tetraploid cytotype 2n=40	Hexaploid cytotype 2n=60	Octaploid cytotype (Y) 2n=80	Octaploid cytotype (T) 2n=80	Dodecaploid cytotype 2n=120
1	Plant height (cm)	120-150	100-130	80-100	85-103	40-80
2	Branches/ plant	7-10	4-7	10-15	9-13	6-9
3	Leaves/ branch	12-15	3-7	4-7	5-8	4-6
4	Ochrea length (mm)	0.5-1	1-1.5	1-2	1-2	1-2
5	Petiole length (cm)	2-2.5	1-1.5	1.5-2	1-2	1-5
6	Leaf size (cm) L/B	2.5-4/1.5-2	3-5/2-3	5-6/3-3.5	4-6/3.5-4	7-10/4.5-6
7	Leaf surface	Smooth	Smooth	Hairy	Hairy	Profusely hairy
8	Inflorescence length (cm)	1-2	1.15-2.5	2-3	2-4	4-5
9	Average stomatal size	19.68×8.78 21.95×8.50	20.01×9.08 22.03×8.75	23.01×10.91 22.79×9.35	23.13×11.02 21.88×9.24	25.98×12.68 25.67×12.73
10	Pollen size (µm)	21.29×20.26	22.56×21.75	23.74×22.23	22.98×22.06	29.31×28.72
11	Habit (Herb)	Tallest	Tall	Medium	Medium	Small sized
12	Habitat	Grows on moist rich soils	Found in close area of water streams	Occurs on moist slopes	Occurs on moist slopes	Occurs in higher altitudes

2.16 Type III plant polyketide synthases: Molecular characterisation of aloesone synthase (*Re*ALS) and chalcone synthase (*Re*CHS) from *Rheum emodi* Wall Ex. Meisn.

Shahzad A. Pandith, Niha Dhar, Y.S.Bedi and Surrinder K. Lattoo

Rheum emodi (Polygonaceae), a multipurpose medicinal herb of immense therapeutic importance is distributed in the temperate and subtropical regions of Himalayas from Kashmir to Sikkim, at elevations ranging from 2000 to 4500m.The major phyto-constituents of the plant include anthraquinones (emodin, aloe-emodin, chrysophanol, rhein, physcion) and stilbenes, and their respective glycoside derivatives. These frequently occurring key constituents are reportedly known for various biological activities including antioxidant, cytotoxic, antimicrobial, antifungal, antitumor, antidiabetic, antiproliferative and immunoenhancing. They are synthesized *via* polyketide pathway which is yet to be fully elucidated.

The polyketides represent a family of highly structurally diverse compounds all produced *via* iterative decarboxylative condensations of starter and extender units. The manipulation of substrate selection in a PKS is an important aspect towards the goal of generating large libraries of unnatural natural products for biological and pharmaceutical applications. In an endeavour towards deciphering the role of some of the key genes of the polyketide pathway, we have successfully cloned two genes *viz.* aloesone synthase (*Re*ALS) and chalcone synthase (*Re*CHS). *Re*ALS and *Re*CHS are the plant-specific type III polyketide synthases which share 62% amino acid sequence identity. The former takes acetyl-CoA as a starter unit and carries out six successive condensations with malonyl-CoA to produce a heptaketide aloesone, whereas the later catalyses condensation of 4-coumaroyl-CoA with three molecules of malonyl-CoA to generate naringenin chalcone which then isomerizes to chalcone.

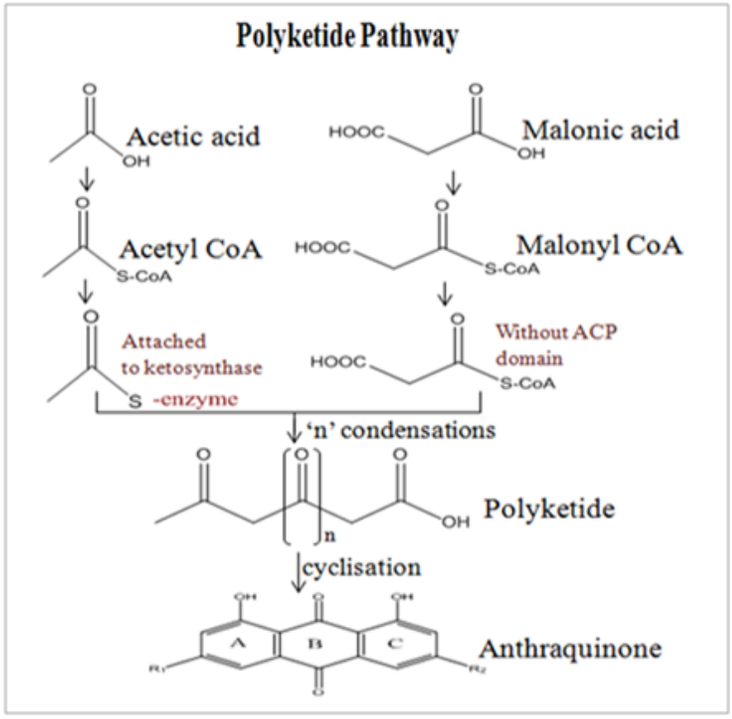

Figure 1: Polyketide pathway leading to the biosynthesis of anthraquinones. The number of condensations and the type (or presence/absence) of cyclisation reactions vary among different plant polyketide synthases. Free CoA thioesters are used for condensation reactions without the involvement of acyl carrier protein (ACP) in type III plant polyketide synthases. The pathway is operative mostly in fungi, bacteria and some higher plant families like Leguminoceae, Rhamnaceae and Polygonaceae.

The *in vitro* regenerated plants (Fig. 2) were used for total RNA isolation. The cDNA synthesis was carried out using Revert Aid Premium first strand cDNA synthesis kit.A pair of degenerate oligonucleotide primers, designed according to the conserved sequences of other related genes were usedfor the amplification of core cDNA fragments of *Re*ALS and *Re*CHS. These fragments were then cloned in pTZ57R/T InsTA cloning vector, transformed in DH5a cells and subjected to nucleotide sequencing using ABI

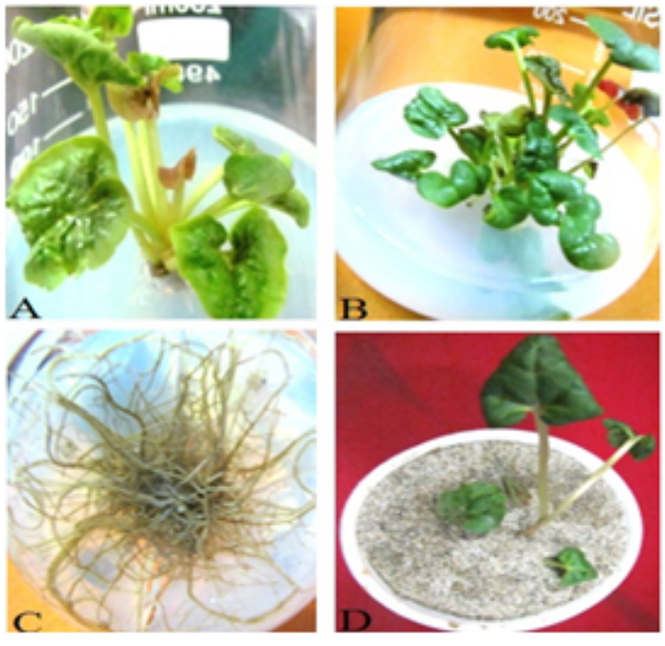

Figure 2: Leaf tissues of *In vitro* regenerated plants (A-D) were used for RNA isolation.

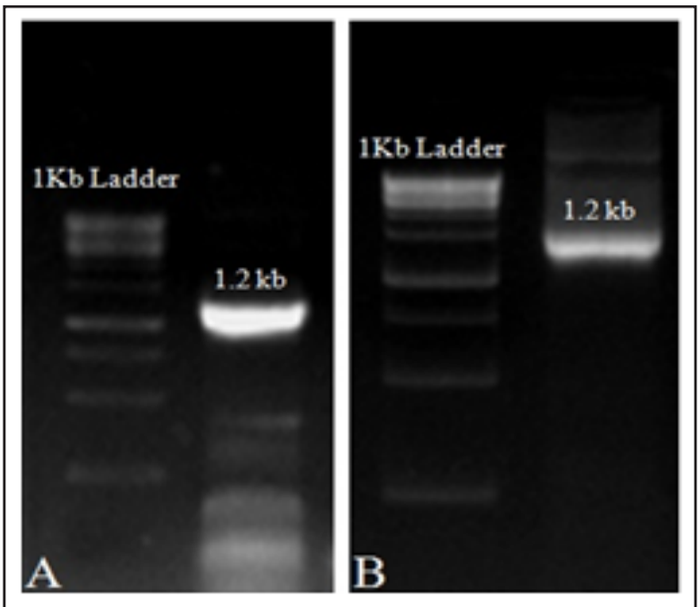

Figure 3: Full length amplified fragments of*Re*ALS (A) and *Re*CHS (B).

3130xl Genetic Analyzer. The sequences obtained were used for designing gene specific primers (GSPs) for cloning of 5'and 3' ends of the respective genes by RACE-PCR. First strand cDNA synthesis for 5' and 3' RACE was carried out using Gene Racer cDNA amplification kit. The nested amplified fragments of both 3' and 5' RACE of each of the two genes were cloned and sequenced. By comparing and aligning the sequences of the core fragments, 5' RACE and 3'

RACE products, the full-length cDNAs of *Re*ALS and *Re*CHS were generated and subsequently amplified with primers (Fig. 3).

The nucleotide sequences obtained were translated using Translate tool (http://www.expasy.ch/tools/ dna.html) and the properties of deduced amino acid sequences (Fig. 4) were estimated using ProtParam (http://www.expasy.ch/tools/prot param.html).

The open reading frames (ORFs) for *Re*ALS and *Re* CHS comprised of 1176 and 1179 nucleotide bases, respectively. These nucleotide bases confer to 391 and 392 amino acids with a predicted molecular mass of 43.33 kDa and 43.62 kDa, respectively for *Re*ALS and *Re*CHS genes. The calculated theoretical PI for *Re*ALS was 5.74 and for *Re*CHS it was 9.14. The secondary structures were determined by SOPMA (http://npsa-pbil.ibcp.fr) programme. The predicted secondary structure of *Re*ALS showed the abundance of alpha helices (47.75) and random coils (32.15 %) while as extended strands were in fewer amounts (14.42 %) (Fig. 5A). In case of *Re*CHS alpha helices (46.46 %) and random coils (30.19 %) were most predominant followed by extended strands (15.80 %), whereas beta turns were least abundant (7.55 %) (Fig. 5C).The three dimensional structures of *Re*ALS and *Re*CHS were predicted using Phyre tool (www.sbg.bio.ic.ac.uk/phyre2/) with the crystal structure of chalcone synthase from *Medicago sativa* complexed with malonyl CoA (PDB ID: 1CML) as template (Figs. 5B, 5D).

The phylogenetic trees were constructed from different amino acid sequences to ascertain the degree of evolutionary relatedness among different plant species.

Protein sequences were retrieved from the GenBank through the BLASTp algorithm at the National Centre for Biotechnology Information (NCBI) using cloned full length sequences as query and several sequences with the highest score from different were aligned using the ClustalW2 tool (http://www.ebi.ac.uk) using default parameters and a Phylogenetic tree was

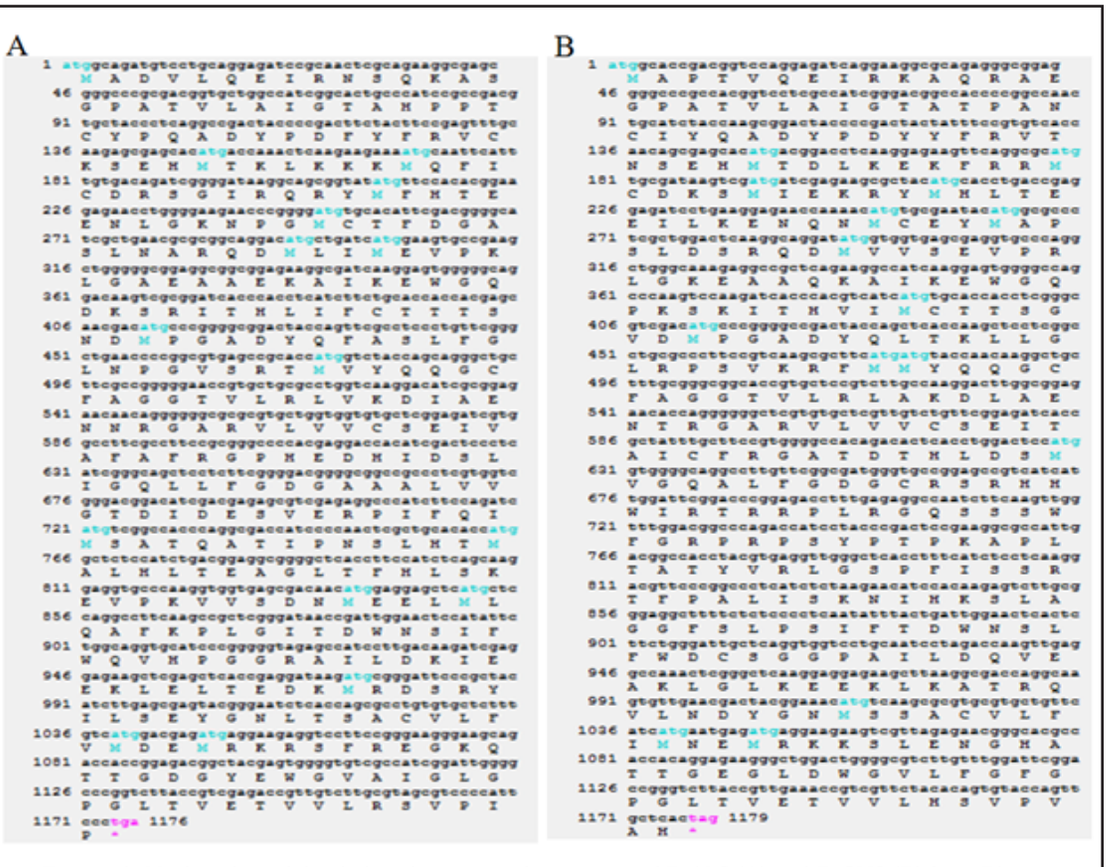

Figure 4: Nucleotide and the deduced amino-acid sequences of *Re*ALS (A) and *Re*CHS (B) from *Rheum emodi*. The stop codons at positions 1176 and 1179 are highlighted in pink.

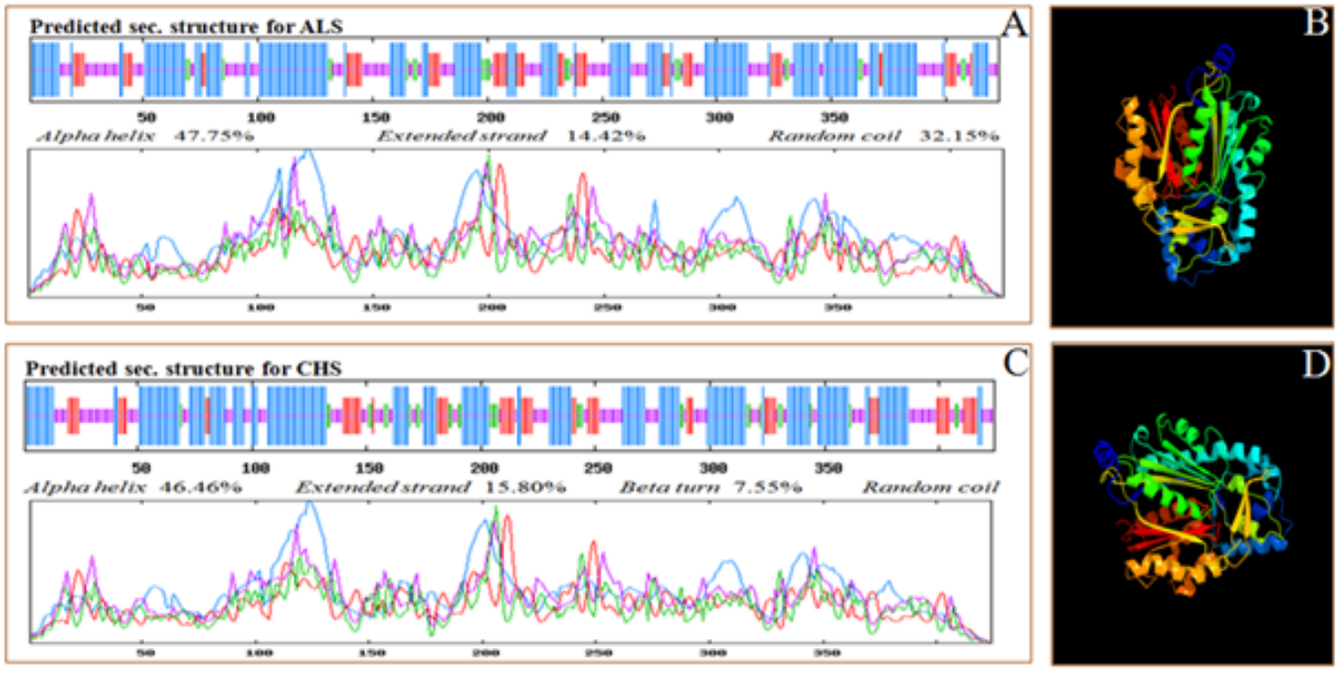

Figure 5: Protein structures based on deduced amino acid sequences: Secondary structures of *Re*ALS (A) and *Re*CHS (C) predicted by SOPMA programme; Predicted 3D protein structures of *Re*ALS (B) and *Re*CHS (D) as determined by Phyre software programme.

constructed by neighbour-joining method using the MEGA5.2 software programme (Fig's. 6 and 7).

Furthermore, the *E. coli*/yeast expression analysis and there from protein purification/functional validation of the selected genes is being pursued.

Figure 6: Phylogenetic analysis of deduced amino acid sequences. Phylogeny of *Re*ALS was inferred by the Neighbor-joining method using MEGA 5.2 software. A total of 17 protein sequences used for the analysis were from following plant species: *Rheum emodi*(KC473812);*Polygonum cuspidatum* (ACC76752.1); *Hordeumvulgare* (ACH42078.1); *Triticumaestivum* (AAQ19318.1); *Litchi chinensis* (ADB44077.1); *Aegilopstauschii* (EMT05352.1); *Citrus sinensis* (ACB47461.1); *Tricyrtishirta* (BAH16615.1); *Lonicera japonica* (AGE10597.1); *Narcissus tazetta var. chinensis* (AFM36770.1); *Acacia confusa* (AFA55180.1); *Populus alba* (ABC86919.1); *Dimocarpuslongan* (AEO36981.1); *Paeonialactiflora* (AEK70334.1); *Tulipafosteriana* (AGJ50587.1); *Vitisvinifera* (BAA31259.1); *Digitalis lanata* (CAA05512.1).

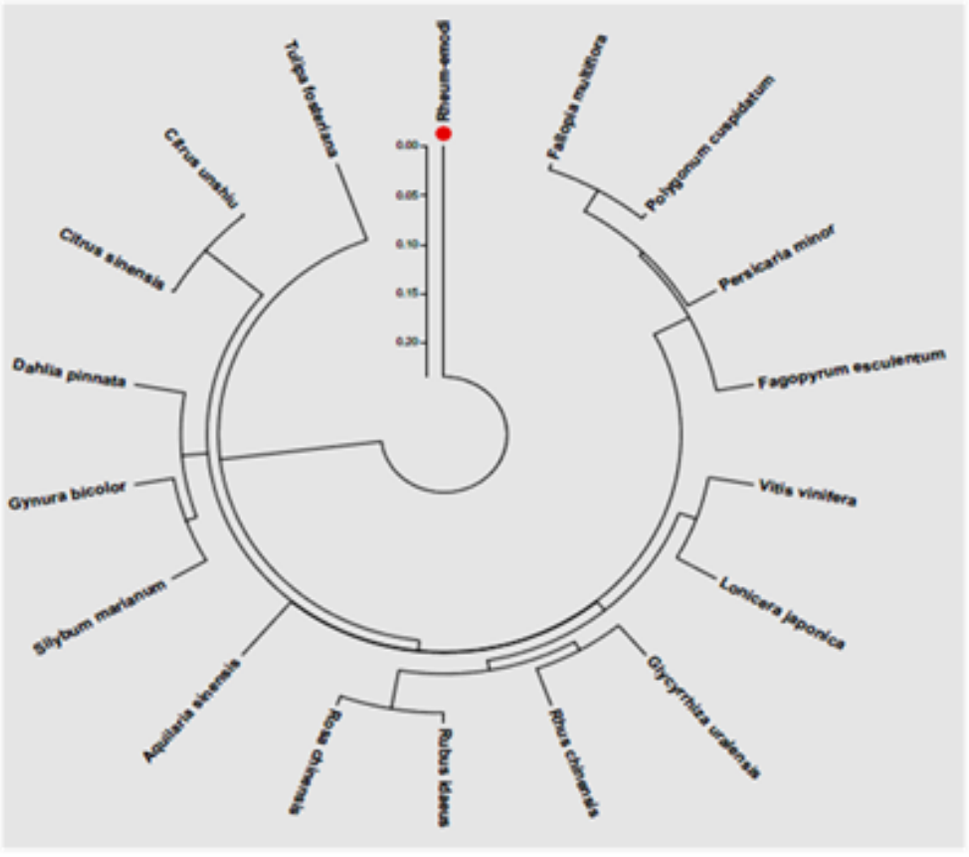

Figure 7: Phylogenetic analysis of deduced amino acid sequences. Phylogeny of *Re*CHS was inferred by the Neighbor-joining method using MEGA 5.2 software. A total of 18 protein sequences used for the analysis were from following plant species: *Rheum-emodi* (KC822472); *Fallopiamultiflora* (ADK45325.1); *Polygonumcuspidatum* (ABK92282.2); *Fagopyrumesculentum* (ADT63062.1); *Persicaria minor* (AFI98395.1); *Citrus sinensis* (ACB47461.1); *Silybummarianum* (AFK65634.1); *Gynurabicolor* (BAJ17656.1); *Citrus unshiu* (ACQ41890.1); *Vitisvinifera* (BAB84112.1); *Aquilariasinensis* (ABM73434.1); *Lonicera japonica* (AGE10597.1); *Dahlia pinnata* (BAK08888.1); *Glycyrrhiza uralensis* (ADZ45298.1); *Rhuschinensis* (AGH13332.1); *Tulipafosteriana* (AGJ50587.1); *Rubusidaeus*

2.16 Promiscuous breeding behaviour and efficient meiotic recombination guarantees high reproductive success and robust genetic variability in *Grewia asiatica* L.

Tareq A. Wani, Satiander Rana, Wajid W. Bhat, Suresh Chandra, Surinder Kitchloo and Surrinder K. Lattoo

Reproductive excellence holds the key for sustenance, flourishment, genetic improvement and evolution. The knowledge regarding the breeding system is a prerequisite to understand the efficiency or failure of a species for genetic variation and evolutionary success. The sexual systems operating in plants are varied. These vary from obligate selfing to obligate out-crossing with whole range of self-compatible to self-incompatible systems. Superimposed upon these breeding systems are protendary, protogyny, gynodiocism and andromonocism. Additionally, in most of the sexually reproducing species,recombination is the chief source of variation readily available to evolutionary forces. The rate and nature of recombination are determined by the breeding and meiotic systems, which are integral parts of the sexual cycle and together constitute the 'genetic system'. Furthermore, for optimum genetic amelioration and effective conservation of allelic and genetic variability, understanding of breeding/mating systems is imperative. The type of mating system determines how genetic information is transferred from one generation to the next and determines the genetic makeup of progenies.

*Grewia asiatica*Linn (Tillaceae), commonly known as 'Phalsa' is a multipurpose gregarious shrub, found in tropical and subtropical parts of India. It is reputed for its medicinal properties as it finds its mention in Ayurveda and in the traditional systems of medicine. The major chemical constituents of Phalsa are grewinol, flavonoids, quercetin, and naringenin from flowers, taraxa sterol, β-sitosterol, erythrodiol, β- amyrin, lupeol, betulinlupenone, friedelin and α-amyrin from the bark. Fruit pulp is a rich source of flavonoids, proteins and amino acids**.** The ripe Phalsa fruits are consumed fresh, in desserts, or processed into refreshing fruit and soft drinks. In spite of the diverse uses, the two drawbacks that restrict full exploitation of the potential uses of this species are the short shelf life of its fruits and its larger seed size. Short shelf life makes the fruits suitable only for local

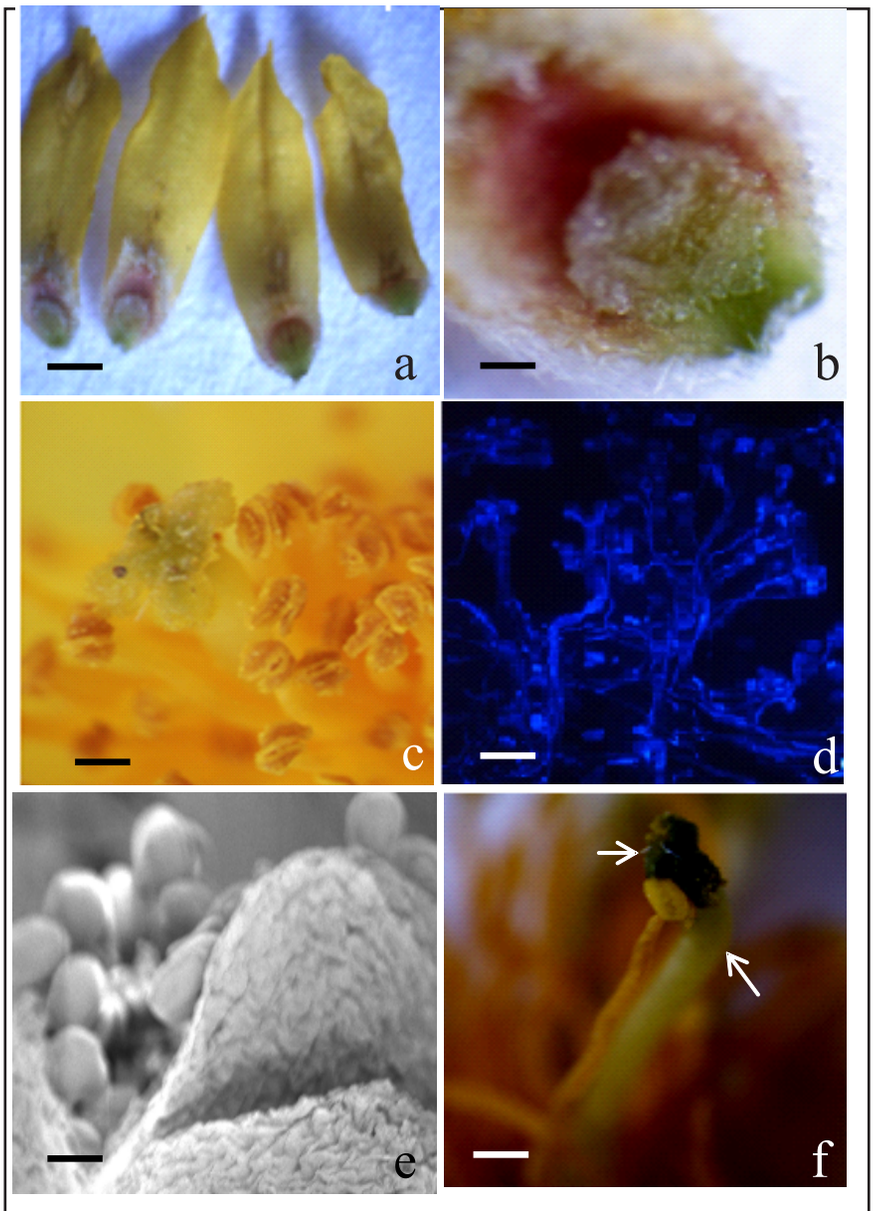

Figure 1: *Grewia asiatica*: Nectariferous petal base (a), Single nectary showing nectar exudates (b) (bars = 5 mm), Receptive stigma clogged with germinating pollen grains (c), fluorescing pollen tubes traversing through stylar canal (d) (bars = 150 μm), anther dehiscence through longitudinal slit presenting pollen grains as observed by SEM (f) (bar = 100 μm), recurved stigma adpressed with dehiscent anther provides for autonomous selfing (bar = 0.5 mm)

strategy has been envisaged for the induction of parthenocarpy *via* multipronged approaches. It includes study of genetic system, understanding

Flowering phenology, mating behaviour and meiotic system and also the biotechnological approach for the disruption of highly conserved molecular pathway of seed formation.

G. asiatica is self-compatible and is accompanied by differences in various reproductive features such as abundant pollen production (stamens- ∞), protandary and syndrome of other characters which favour autogamy, geitenogamy, xenogamy or blend of these (Table 1).The flowers are scentless. There are distinct nectaries with copious nectar secretion at the base of petals (Fig.1a,b) adsperssed with ovary base. Flowers are visited by oligolectic bees, moths, ants,lady bird beetles, butterflies etc. (Fig.2 a-f). Visiting insects are rewarded with both nectar and pollen. The insect visits commence at about 08:00 hours and continue up to 14:30 hours with peak activity between 9:30 and 11:30 hours. Reproductive phenology of the plant from floral bud initiation up to fruit set and seed dispersal was also observed and is shown in Fig.3. Flower bud initiation occurs in the 2nd week of March (2013), flowering peaks during 1st week of April, ovary maturation/fruit initiation starts from 2nd week of April, and the optimum fruit set was observed during 2nd week of May; fruit ripening commences from 4th week of May, and culminates by 2nd week of June.

marketing. While the larger seeds with respect to fruit is a disadvantage. To circumvent these drawbacks, induction of parthenocarpy or stenospermy is a viable option. Parthenocarpic fruits are seedless and tend to have longer shelf life and amenable to mechanical processing. During the present investigation, a

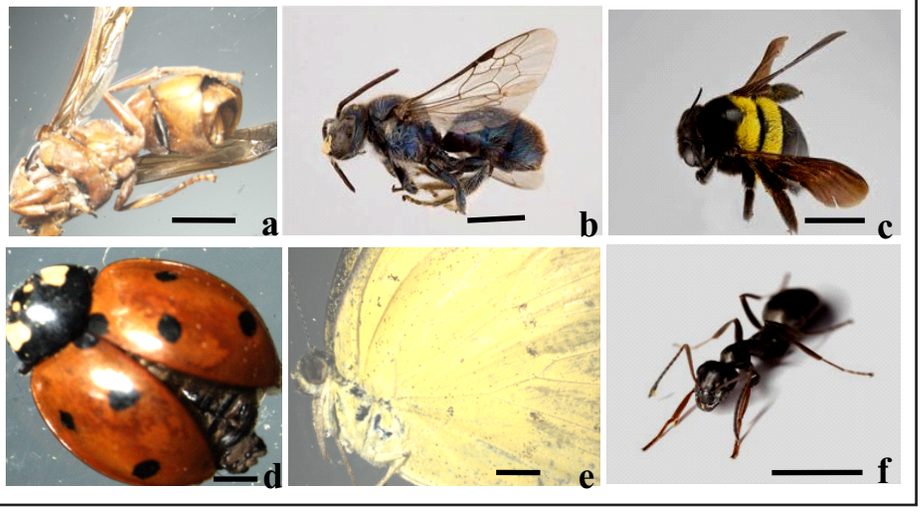

Figure 2: Frequent insect visitors facilitate adequate pollination of *Grewia asiatica*. *Apis*sp. carries the sizable pollen load (a), *Melipona* sp.(b), *Exomalopsis* sp. (c), *Coccinellidae* sp. (d), *Parnassius* sp. (e), *Formicidae*sp. (f) (bars = 5 mm).

Table 1: Summary of some morphometric traits and reproductive features of *Grewia asiatica*

Character	
Number of branches per plant	87.6±7.1*
Number of inflorescences per plant	1016.16±65.46
Number of flowers per inflorescence	10.4±0.60
Number of fruits per inflorescence	7.3±0.90
Fruit set percentage/plant	
Open pollination (natural)	71.15±9.34
Spontaneous self pollination/autogamy (bagging)	52.39±4.65
Geitenogamy	82.75±8.32
Xenogamy (manual cross-pollination)	26.67±5.76
Number of pollen grains/anther [P]	114.94±10.50
Number of ovules/flower [O]	4
Number of anthers/flower [A]	86 ± 3.2
Number of pollen grains/ flower	9884.84±95.34
Pollen/ovule ratio [P/O]	2471.21
Number of flowers per plant [Fl]	10568.80±114.65
Number of fruits per plant [Fr]	7417.96±63.23
Number of seeds per fruit [S]	1.64±0.21
Seed/ovule ratio per flower [S/O]	0.4
Fruit/flower ratio [Fr/Fl]	0.70
Pre-emergent reproductive success [Fr/Fl x S/O]	0.28

*Mean and SEM. Data were collected from an experimental trial in its fourth year of growth.

Sexual promiscuity in *G. asiatica* is manifest as a result of dichogamous nature of protandrous type and profuse visitation by pollinators. Due to non-overlapping of male and female phases, as anthers dehisce prior to stigma receptivity, the species is predisposed for both outcrossing (xenogamy) and geitenogamy. In rare instances, insignificant number (1-2%) of flowers were observed to practice auto nomous selfing as the recurved stigmatic tip is adpressed with dehisced anthers with sufficient pollen presentation (Fig. 1f)

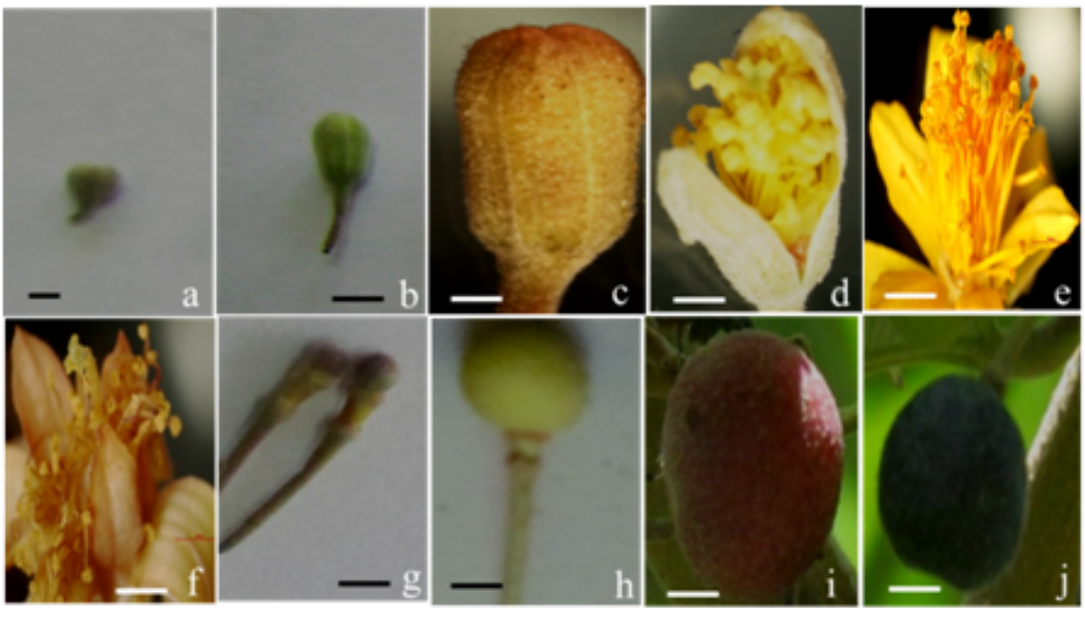

Figure 3: Reproductive phenology of *Grewia asiatica*: Early floral bud (a, b), mature floral bud (c), flower at anthesis (d), after anthesis (e), floral senescence (f), fruit initiation and maturation (g-j). Bars = 5 mm.

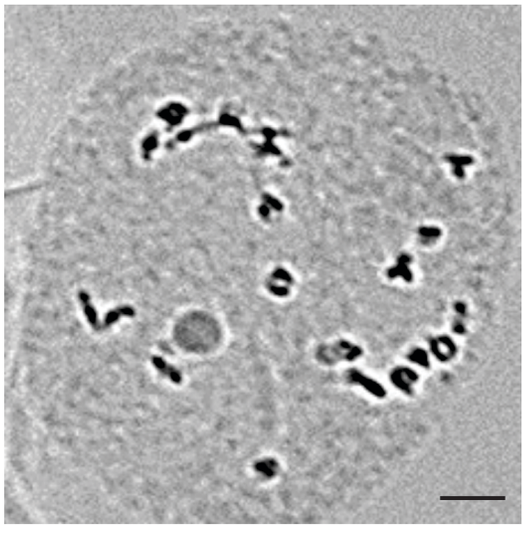

Figure 4: *Grewia asiatica*: Meiotic spread showing 19^{II} at diplotene. Bar = 10 μm.

Stigmatic secretion and germinating pollen grains adhering to stigmatic surface mark the peak stigmatic receptivity (Fig. 1c). It takes 3-5 h for pollen grains to germinate and traverse through the stylar canal to effect fertilization. (Fig. 1d).The species practices stiff pollen competition (pollen load =525.57±22.35) as there are about 131 pollen grains available to sire one seed. 1-2 ovules out of four mature into seeds. High pollen to ovule ratio(P/O) and moderate seed to ovule ratio (S/O) are in agreement with the postulates of xenogamous and autogamous behaviour of the species. Pre-emergent reproductive success (PERS) was 28% (Table 1), a critical attribute for Phalsa fruit yield optimization.

G. asiatica has a somatic chromosome count of 2n=38.The number of chiasmata per bivalent ranged from 1-3 with an average chiasmata of 1.4 per bivalent. The mean chiasmata frequency at diplotene (Fig. 4) and metaphase-I varied with an average of 26 ± 2.6and19 ± 2.0 chiasmata per meiocyte respectively (Table 2). Both, empirically and conceptually, high reproductive success and efficient genetic system has a potential to ameliorate yield and yield contributing characters in *G. asiatica.*

Table 2: Features of meiotic system in *Grewia asiatica*

Xta frequency per pmc at			
Somatic chromosome number			Recombination index
	Diplotene	Metaphase I	
38	26 ± 2.6	19 ± 2.0	45

2.17 Molecular characterization of UGT94F2 and UGT86C4, two glycosyltransferases from *Picrorhiza kurrooa*: Comparative structural insight and evaluation of substrate recognition

Wajid Waheed Bhat, Niha Dhar, Sumeer Razdan, Satiander Rana, Rukmankesh Mehra, Amit Nargotra, Rekha S. Dhar, Nasheeman Ashraf, Ram Vishwakarma and Surrinder K. Lattoo

Uridine diphosphate glycosyltransferases (UGTs) are pivotal in the process of glycosylation for decorating natural products with sugars. It is one of the versatile mechanisms in determining chemical complexity and diversity for the production of suite of pharmacologically active plant natural products. *Picrorhiza kurrooa*, a highly reputed medicinal herb is well known for its hepato-protective properties which are attributed to a novel group of iridoid glycosides known as picrosides. Although the plant is well studied in terms of its pharmacological properties, very little is known about the biosynthesis of these important secondary metabolites (Fig. 1). As previously reported, we have identified two family-1 glucosyltransferases from *P. kurrooa*. The full length cDNA of UGT86C4 (1641bp) contains an open reading frame (ORF) of 1422 bp corresponding to a protein of 473 amino acids with a calculated molecular weight of 53 kDa and an isoelectric point (pI) of 4.72. The full length cDNA of UGT94F2 (1612 bp) contains an ORF of 1455 bp encoding a protein of 484 amino acids with a calculated molecular weight of 55 kDa and pI of 5.26.The nucleotide sequence of full length cDNAs of both genes were submitted to NCBI GenBank under accession numbers JQ996408 and Jq996409.

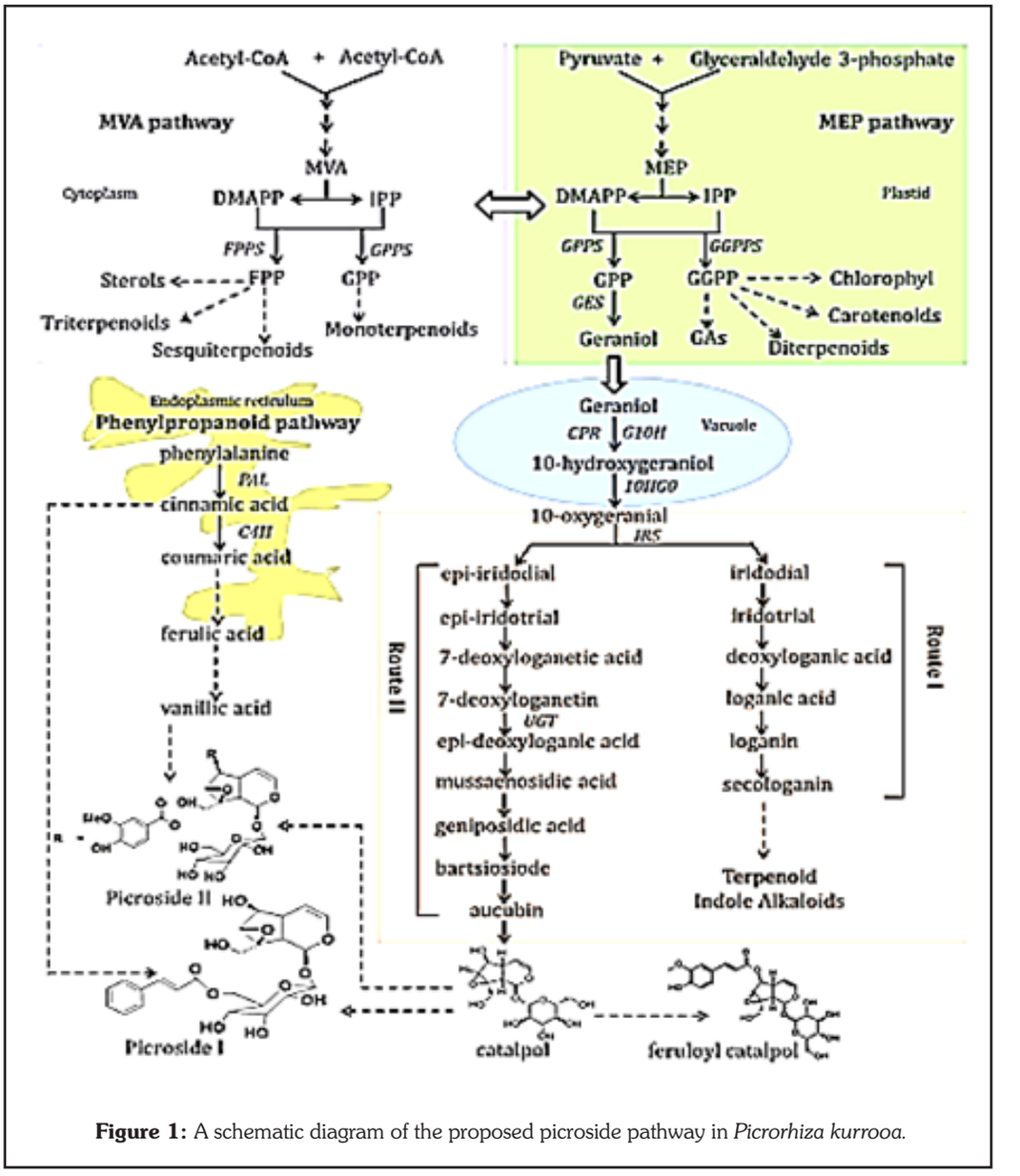

Figure 1: A schematic diagram of the proposed picroside pathway in *Picrorhiza kurrooa.*

The full length ORF of UGT86C4 and UGT94F2 were digested from the pJET-UGT86C4 and pJET-UGT94F2 gene constructs using *Bam*HI and *Not*I restriction enzymes and inserted into vector *pGEX4T-2* yielding pGEX4T2-UGT86C4and pGEX4T2-UGT94F2 respectively. The gene constructs were transformed into competent *BL21*cells and their expressions were induced by the addition of 0.2 mM IPTG at approximately OD_{600} = ~0.5. This resulted in the appearance of a new fusion polypeptide with an expected molecular mass of approximately 68 kDa when resolved on SDS-PAGE (Fig. 2)

To understand the basis for the substrate specificity of UGT86C4 and UGT94F2, protein homology models were constructed using PHYRE2 web server with the crystal structure of *Arabidopsis* UGT72B1 (pdb id. 2VCH-A) as the template.The proposed model for *Picrorhiza* UGT86C4 and UGT94F2 shares the structural features described for the Family-1 UGTs by adopting the so-called GT B-fold formed by the C-terminal and N-terminal domains separated by an inter-domain linker and consists of two N- and C-terminal domains with similar Rossmann-like

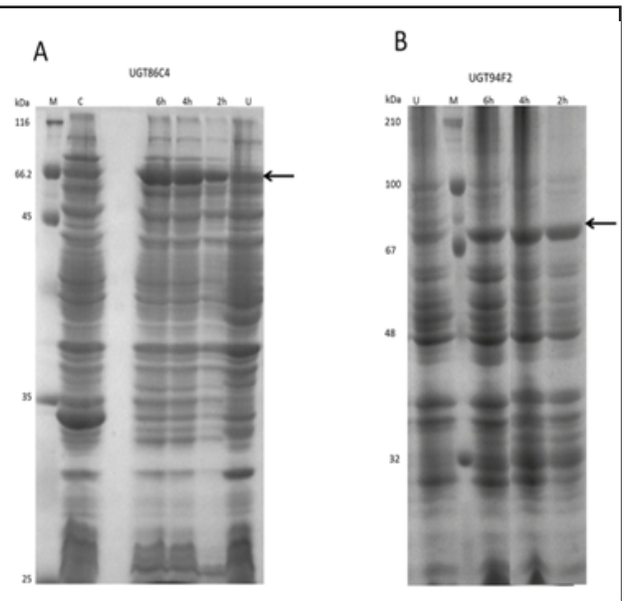

Figure 2: Time-course heterologous expression of UGT86C4 (A) and UGT94F2 (B) in *E. coli*.

folds (Fig. 3).

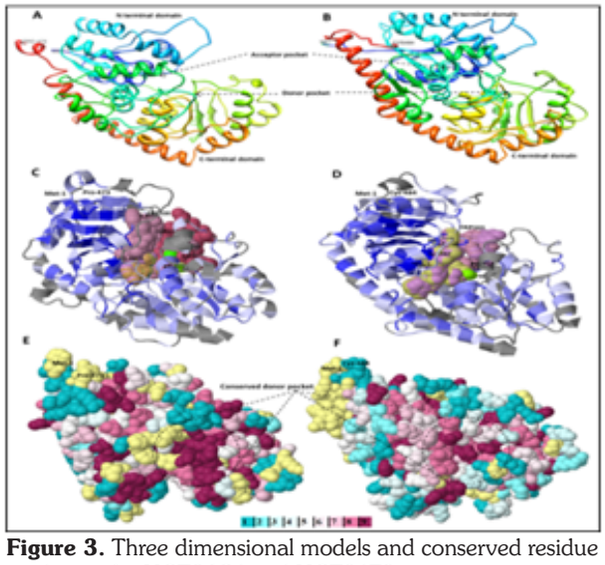

Figure 3. Three dimensional models and conserved residue prediction for UGT86C4 and UGT94F2

Docking experiments were initially performed using iridotrial, 7-deoxyloganetic acid, 7-deoxyloganetin, apigenin, kaempferol and naringenin (Figure 4 and 5). Based on the docking and Prime MMGBSA results of UGT86C4, the docking studies of the ligand dataset i.e., iridotrial, 7-deoxyloganetic acid, 7-deoxyloganetin, apigenin and naringenin showed similar binding affinity except for kaempferol where the binding affinity was comparatively higher. Kaempferol is quite suitably placed within the proposed binding pocket of UGT86C4 as shown in Figure 4A. It is proposed to involve in five H-bond formation with Asp122 (1.81 Å), Lys193 (2.38 Å), Ser286 (1.7 Å and 2.04 Å), Leu287 (2.08 Å) and Asn365 (1.85 Å and 1.94 Å) (Figure 6A). UGT94F2 was found to have strong binding affinity for iridoid class of compounds including iridotrial, 7-deoxyloganetic acid, 7-deoxyloganetin in comparison to apigenin, kaempferol and naringenin (Fig. 5). Out of the three iridoid moieties, UGT94F2 showed maximum binding affinity towards 7-deoxyloganetin. The compounds apigenin, kaempferol and naringenin showed very poor binding affinity towards the protein's acceptor site both in terms of dock score and binding energy parameters. The interaction of 7-deoxyloganetin, having the best binding affinity as per the docking studies, within the acceptor site of UGT94F2 is shown in (Fig. 5D). It is proposed to be involved in three H-bonds with Val146, Ser271 and Asn352. The oxygen of the pyran ring is involved in two H-bonds with Asn352 at 1.746 Å and 2.425 Å and the hydroxyl group attached to the pyranring is involved in H-bond with Val146 at 2.457 Å. Besides this, the oxygen of the carboxyl group is involved in H-bond with Ser271 at 1.829 Å. These four H-bonds appears to provide stability to the molecule within the binding pocket. It was also revealed that Ser271 and Asn352 plays pivotal role in substrate identification (Fig. 6B).

To elucidate whether the differential expression patterns of the two *Picrorhiza* UGT genes correlates with transcriptional regulation *via* their promoters, upstream region of both the UGT genes were isolated and scanned for putative *cis*-regulatory elements using the PlantCARE and PLACE databases.Using genome walking

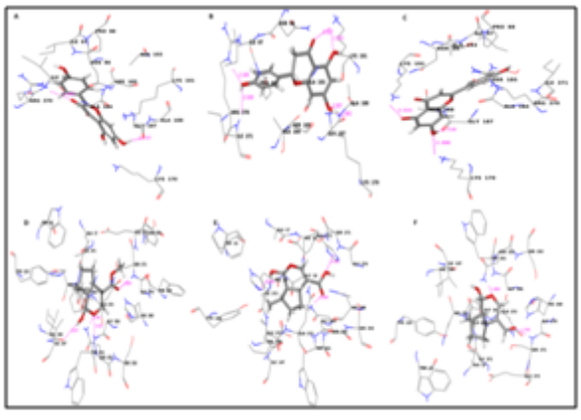

Figure 4: Molecular docking of UGT86C4. Diagram showing (A) kaempferol (B) naringenin (C) apigenin (D) 7-deoxyloganetin (E) 7-deoxyloganetic acid and (F) iridotrial docked into the proposed binding pockets of UGT86C4.

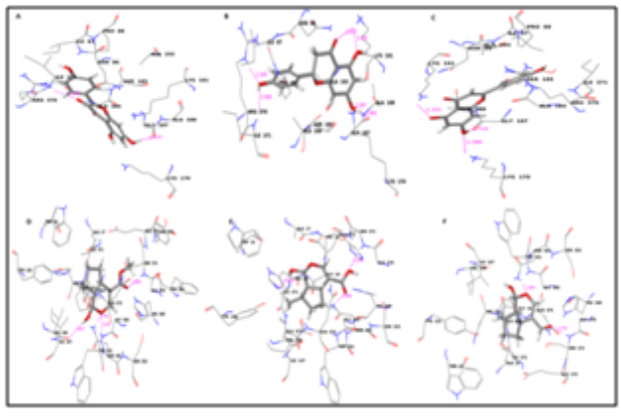

Figure 5: Molecular docking of UGT94F2. Diagram showing (A) kaempferol (B) naringenin (C) apigenin (D) 7-deoxyloganetin (E) 7-deoxyloganetic acid and (F) iridotrial docked into the proposed binding pockets of UGT94F2.

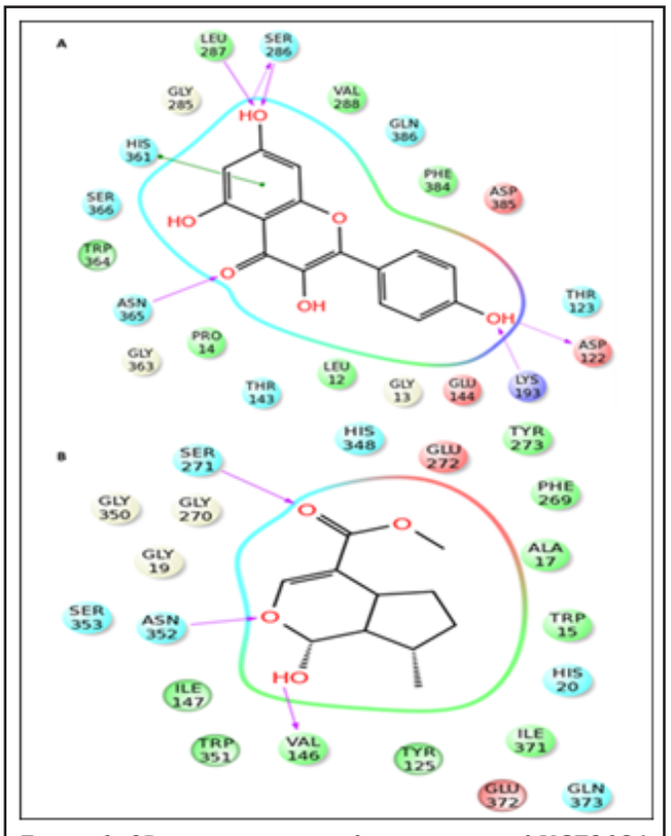

Figure 6: 2D representation of interactions of UGT86C4 and UGT94F2. 2D representation of the interaction figure (in pink) of kaempferol with UGT86C4 (A), and 2D interaction figure of 7-deoxyloganetin with UGT94F2 (B).

strategy, we isolated a 595 bp and 571 bp 5´ upstream regions of UGT86C4 and UGT94F2 genes (Fig. 7).

UGT86C4 showed highest expression in inflorescence followed by leaves and least expression was found in roots. However, spatial expression pattern of UGT94F2 showed maximum transcript abundance in leaves, followed by inflorescence and least expression was found in rhizomes (Fig. 8A). These results suggest that UGT86C4 and UGT94F2 are expressed differentialy in different plant organs hinting towards their spatial regulation. The results showed that the expression levels of both the UGTs were strongly increased by phytohormone treatments, though the expression pattern was different for different phytohormones (Fig. 8).

MeJA up-regulated the expression of both UGTs but at different time intervals after induction. UGT86C4 showed 8-fold increase in expression after 12 h of application of MeJA while UGT94F2 showed 15-fold increase in the expression after 24 h of MeJA application (Fig. 8B). With SA, our study shows differential transient increase in accumulation of UGT86C4 and UGT94F2. UGT94F2 showed maximum increase of 10-fold after 12 h of induction which corroborated well with the picroside accumulation. While as UGT86C4 showed 16-fold increase in the expression profile 6 h post induction (Fig. 8C). However in *P. kurrooa*, 2, 4-D increased the picroside levels, although the increase was less as compared to the effect of MeJa or SA.

To corroborate the expression pattern of UGT86C4 and UGT94F2 with the level of picroside accumulation in different tissues of *P. Kurrooa* including rhizomes, leaves and inflorescence were analysed for picroside accumulation using high performance liquid chromatography (Fig. 9). The picroside contents were found to vary in different tissues with leaves having maximum accumulation of picroside-I (PK-I; 5.937±0.20% DWB) followed by inflorescence (5.139±0.12% DWB) and least accumulation was found in rhizomes (4.716±0.09% DWB).

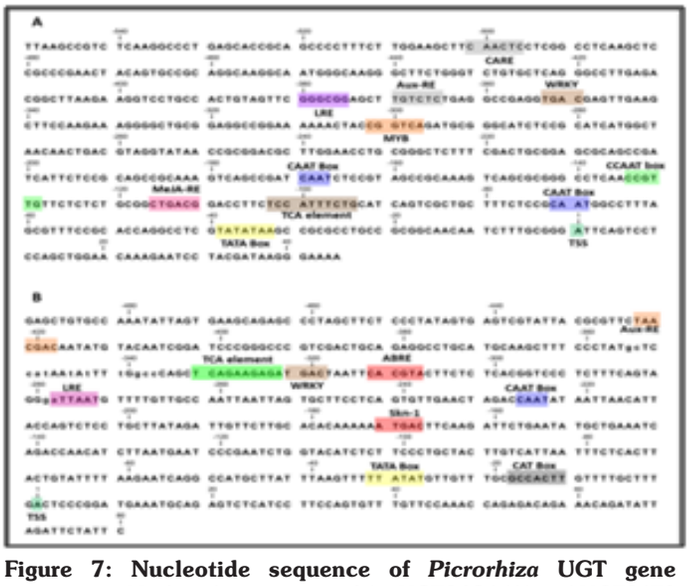

Figure 7: Nucleotide sequence of *Picrorhiza* UGT gene promoters. Nucleotide sequences of the UGT86C4 (A) and UGT94F2 (B) gene promoters. The putative core promoter consensus sequences and the motifs with significant similarity to the previously identified *cis*-acting elements are shaded and the names are given.

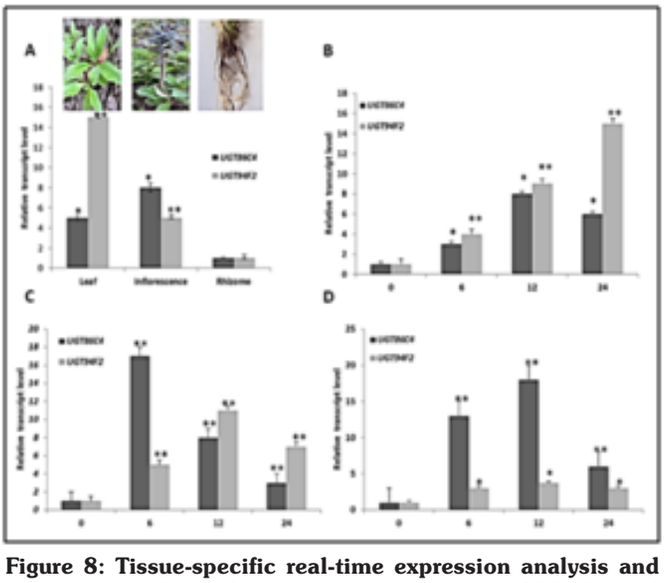

Figure 8: Tissue-specific real-time expression analysis and time-course effect of elicitor treatments on UGT86C4 and UGT94F2. Tissue-specific expression of UGT86C4 and UGT94F2 (A), time-course effect of methyl jasmonate (MeJA) (B), salicylic acid (SA) (C) and 2, 4-dichlorophenoxyacetic acid (2,4-D) (D) on the expression of UGT86C4 and UGT94F2.

However, a different trend was seen in the levels of picroside-II, wherein roots showed highest level (PK-II; 4.064±0.12%) followed by leaves (3.6615±0.12%) and least accumulation was found in case of inflorescence (3.521±0.12% DWB).

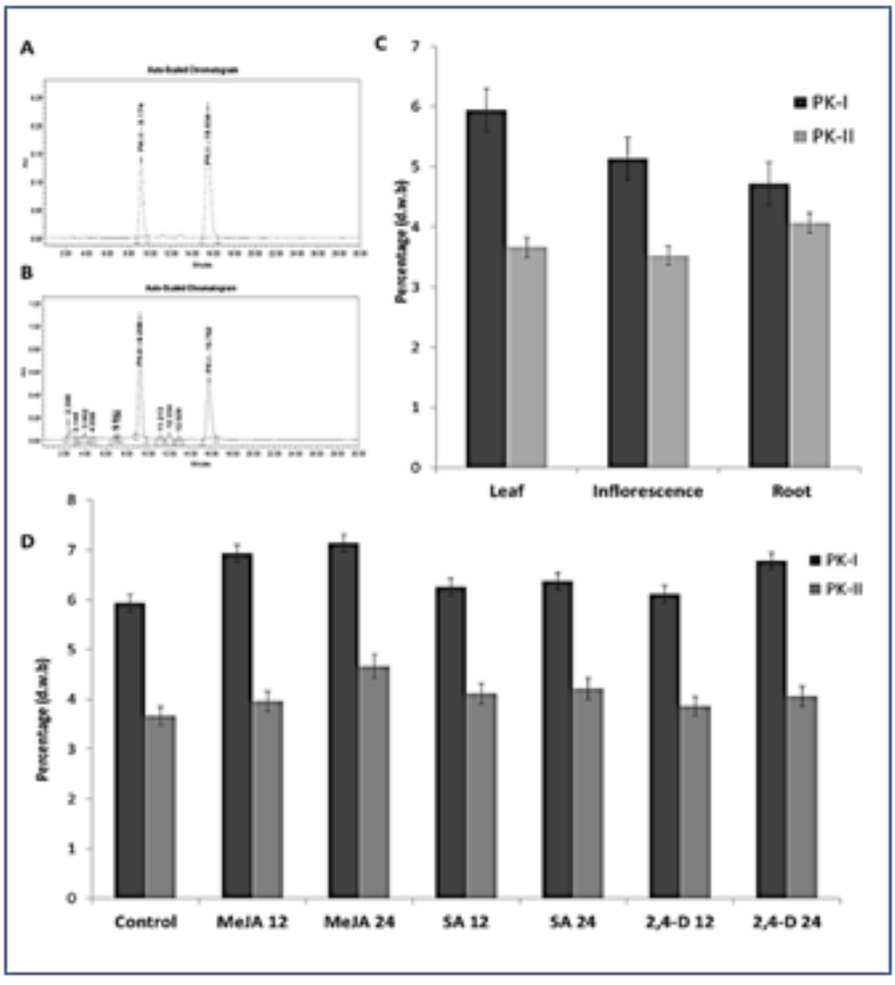

Figure 9: Tissue-specific and time-course effect of elicitor treatments on picroside accumulation. HPLC chromatogram of standard (picroside I and picroside II) at 270nm (A). HPLC chromatogram of leaf sample showing peaks of picroside I and picroside II (B). Tissue-specific accumulation of picrosides (PK-I and PK-II) in leaves, inflorescence and rhizomes of *P. kurrooa* (C). Effect of methyl jasmonate (MeJA) (B), salicylic acid (SA) (C) and 2, 4-dichlorophenoxyacetic acid (2, 4-D) (D) treatments on picrosides accumulation at different time intervals (D). HPLC analysis demonstrated the change in two key picrosides, PK-I and PK-II at 12 and 24 h after treatments of mature leaves.

3. ANTI-CANCER THERAPEUTICS AND INFLAMMATORY PHARMACOLOGY

3.1 Lead identification based on Purinyl-Quinazolinone scaffold as PI3K inhibitors

Aashiq Hussain, Abid Hamid, Shashank Kumar Singh and Ajit Kumar Saxena

Owing to its widespread activation in cancer, a growing appreciation of the therapeutic potential of inhibitors of the phosphoinositide 3-kinase (PI3K) pathway has stimulated intense interest in compounds with suitable pharmacological profiles. Keeping this in view, the analogs of tetrazolyl-quinazolinone scaffold have been designed, synthesized and its biological results for anticancer activity were evaluated. Total 29 analogs of tetrazolyl-quinazolinone scaffold were screened against 12 types of cancer cell lines of Colon, Breast, Leukemia, Lung, Prostate and Pancreas origins including normal breast epithelial cell line fR2. One of the analogs – SIP-1107 was found to be highly potent against majority of the cell lines used sparing the normal cell line. However, it was maximally active against Colo-205 (Colon cancer) with IC_{50} = 0.25±0.06μM while IC_{50} against fR2 came out to be 4μM. Then SIP-1107 was tested for enzymatic activity for PI3Kα and PI3Kδ isoforms as they have the crucial role in cancer. The IC_{50} for PI3Kα and PI3Kδ isoforms came out to be 35.76nM and 105nM respectively. SIP-1107 was further mechanically evaluated for cell cycle analysis using propidium iodide dye, apoptotic studies by annexin-V apoptosis assay and nuclear morphological changes by DAPI staining. These results demonstrates that SIP-1107 primarily does G1 phase arrest at lower concentrations of 0.1 and 0.5μM while at higher concentrations of 1, 3, 5, 7 and 9μM apoptosis was main cause of inhibition of cell proliferation. SIP-1107 was then evaluated for PI3K pathway. Fluorescence microscopy of PI3K-p85α showed its down-regulation even at 0.2μM concentration. Downstream of PI3K i,e p-Akt (Ser-473) was down-regulated as shown by fluorescence microscopy. Further downstream of Akt is transcription factor of fatty acid synthase enzyme–SREBP1 (sterol regulatory element binding protein 1) whose translocation to nucleus was down-regulated by PI3K inhibition as shown by florescence microscopy. The results of PI3K pathway inhibition was also evaluated by western blotting for PI3K-p110α and PI3K-p85 using β-actin as loading control (Fig.1).

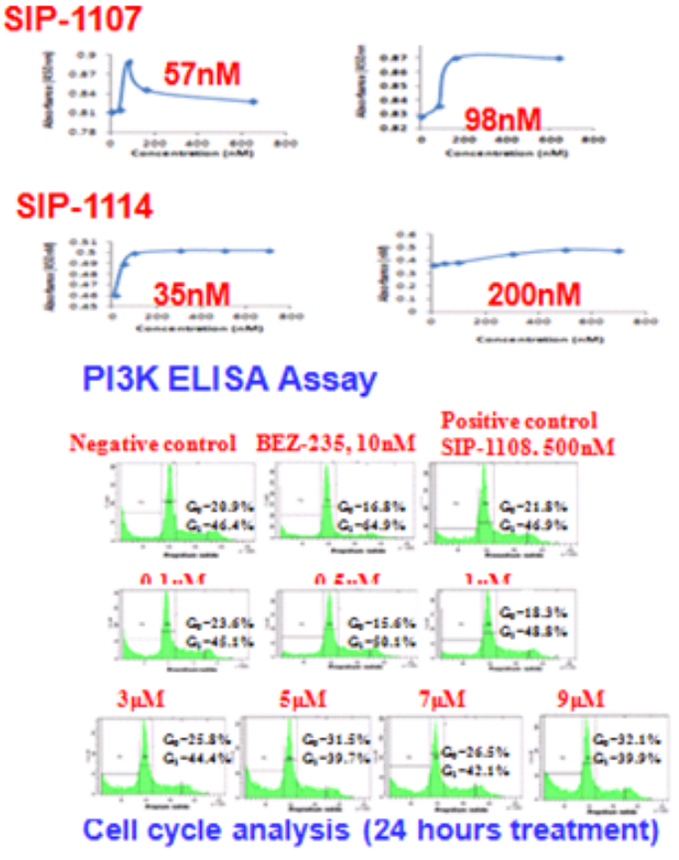

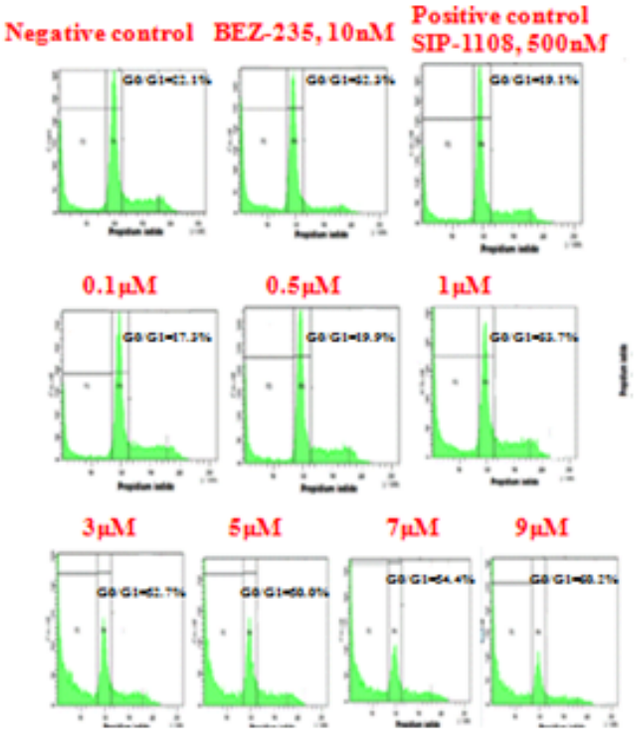

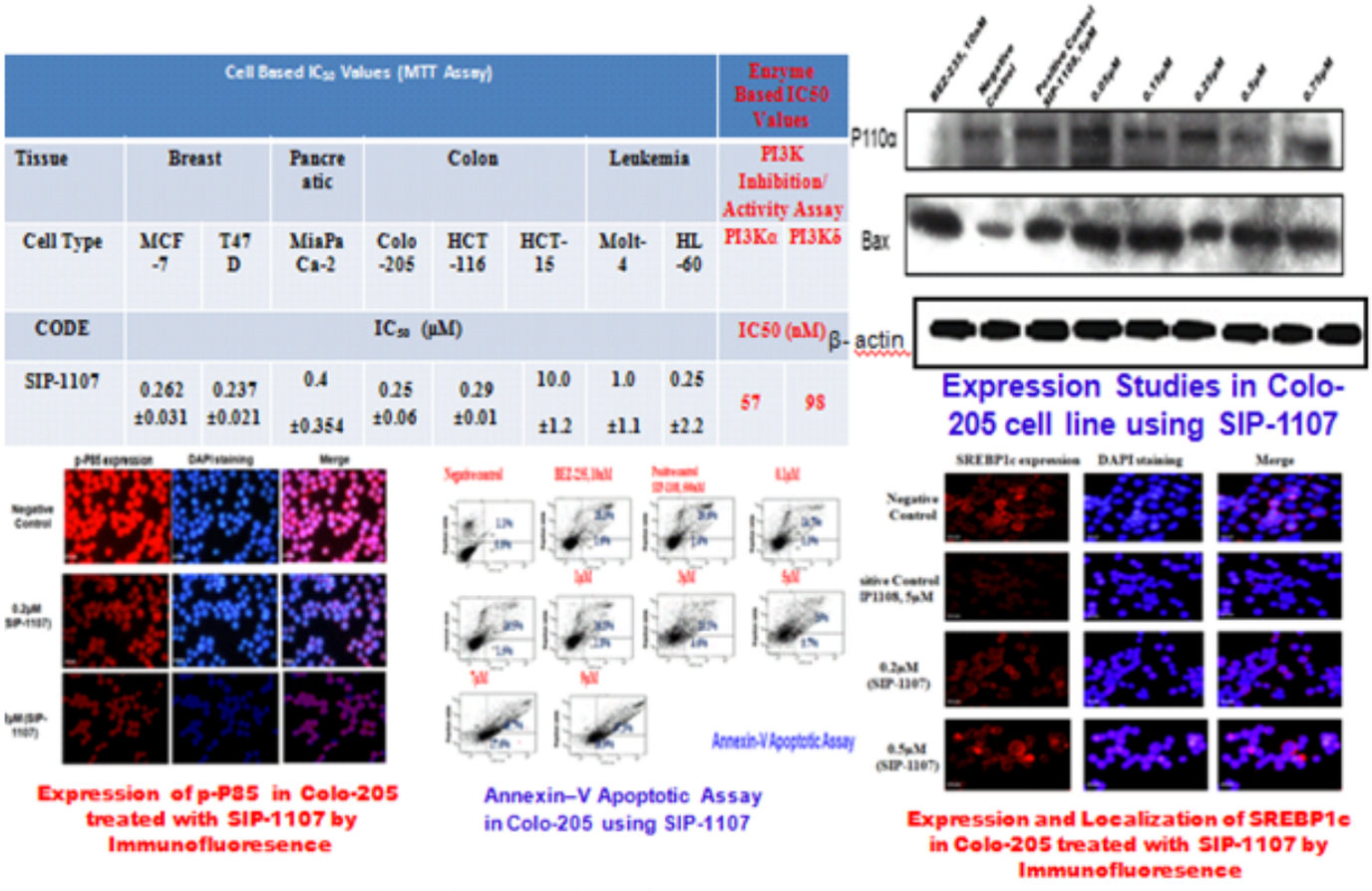

Figure 1:- Effect of Purinyl-Quinazolinone on signaling mediators

3.2 Mechanistic evaluation of 3-α-Butyrloxy-β-boswellic acid (BOBA) & 3-α-Propionyloxy-β-boswellic acid (POBA) for the possible target elucidation, inhibition against important signaling pathways and towards anticancer therapeutic strategy in colon cancer

Yasrib Qurishi, Abid Hamid, Shashank Kumar Singh, Ajit Kumar Saxena, D.M. Mondhe, P.R. Sharma and Govind Yadav

Colorectal cancer is the second leading cause of cancer deaths worldwide. Multiple genetic aberrations contribute to the development of biologically aggressive and clinically malignant colorectal carcinomas. In the present study, an approach is aimed at the inhibition of target signaling molecules that may be specifically involved in the onset and progression of colorectal cancer among several other malignancies. Therefore, the study relates to the field of therapeutics, particularly to the induction of target mediated apoptosis thereof cytotoxicity and anti-cancer activity displayed by semi-synthetic analogs of Boswellic acid from Boswellia Serrata, i.e. 3-α-Butyrloxy-β-boswellic acid (BOBA) and 3-α-Propionyloxy-β-boswellic acid (POBA) to target important signaling pathways.

The cytotoxicity data revealed that the specific differential sensitivity of colon cancer cell lines (Caco-2, HCT-15 and Colo-205) towards these substances containing the acyl derivative(s). The observation of the specificity of BOBA and POBA in the induction of cell death towards these cancerous cells was validated by using normal cells (CV-1) and more potency was observed against Caco-2 and HCT-15 cells. Considering the inhibitory potential of BOBA & POBA in cell proliferation of colon cancer cells, we further sought to decipher the target involved and understand the mechanism leading to the activation of the cell death phenomena. Since,

increasing numbers of proteins, nucleic acids and other molecular entities have been explored as therapeutic targets in cancer, so in an effort to this, major challenge was to decide which targets to pursue from an increasing pool of possible validated targets for the scaffold used in the present study. In this context, molecular docking via in silico studies for BOBA and POBA has provided us clue for few possible targets such as phosphoinositide-3-kinase (PI3K) isoforms (α, β, γ and δ), histone deacetylases (HDACs), insulin growth factor receptor (IGFR) and cyclin dependent kinases (CDKs); however, PI3K was observed to play a major role in interacting with BOBA or POBA as deduced by binding energy studies. The in vitro screening studies suggested that PI3K inhibition can be the potential target unlike HDAC. It is noteworthy to mention here that the PI3K signaling pathway is important for cellular proliferation and its deregulation has been implicated in the progression to the transformed phenotype leading to the colorectal carcinoma. Importantly, we observed a significant difference in the inhibition levels of various isoforms with PI3Kα being particularly interesting showing least IC_{50} values for these molecules. Based on in vitro, in silico and cell free PI3K inhibition studies, our data for the first time revealed that BOBA & POBA can induce colon cancer cell death possibly by targeting the PI3K signaling. It has been reported that the PI3K along with its downstream effector i.e. protein kinase B (PKB) also known as Akt over-activation in tumors triggers a cascade of responses from cell growth, proliferation, survival to motility, thus bears importance to be explored. Following BOBA and POBA treatment to Caco-2 and HCT-15 cells, we observed significant down-regulation of catalytic subunit of PI3K (PI3K:p110α) which was subsequently associated with the inhibition of phosphorylation of Akt at Ser^{473} and Thr^{308} residues by expression studies. Since, Akt also regulates various cellular events by regulating the phosphorylation of various mediators of cellular functions such as retinoblastoma and the latter is one of the important players in allowing cell cycle progression by transcription dependent means. It was observed that BOBA and POBA inhibited the phosphorylation of retinoblastoma at Ser^{795} which directly imparted its inhibitory effect on the expression of important cell cycle protein i.e. cyclin E evaluated in the study. Furthermore, the observed up-regulation of p53 is in agreement with the fact that the over-activation of p53 inhibits cyclin E/CDK 2 complex formation during the cell cycle arrest or during the pharmacological intervention such as BOBA and POBA to the colon cancer cells. Also, down-regulation of the Akt can couple to pathways that inhibit the functioning of the effector machinery such as NF-kB which is involved in cell proliferation and was found to be significantly down-regulated in Caco-2 and HCT-15 cell lines treated with either of BOBA or POBA molecule(s). The data also suggested that the inhibition of Akt pathway can induce FOXO3a mediated cell death or apoptosis (Fig. 1, 2). This can be attributed to the FOXO3a dephosphorylation which results in its nuclear translocation in the presence of down-regulated Akt on treatment of cells to BOBA or POBA. In order to ascertain the nature of the cell death induced by BOBA and POBA in colon cancer cells, the various biological endpoints associated with it revealed that the hypo-diploid sub-G_0 DNA population to be associated with the translocation of phosphatidyl serine from the inner leaflet to outer cell surface, followed by inhibition of anti-apoptotic protein i.e. Bcl-2 and activation of pro-apoptotic protein i.e. Bax with an overall increase in the Bcl-2/Bax ratio on treatment with BOBA and POBA. These events were further confirmed by the observed activation of caspase 8, caspase 9 and caspase 3 cascade as was also evident from mitochondrial membrane potential ($\Delta\Psi m$) loss. Nevertheless, the inhibitory effect on cell migration (Fig. 3) and colony formation (Fig. 4) further provided the importance of the BOBA and POBA as the possible agents in preventing the colon cancer cell metastasis and development.

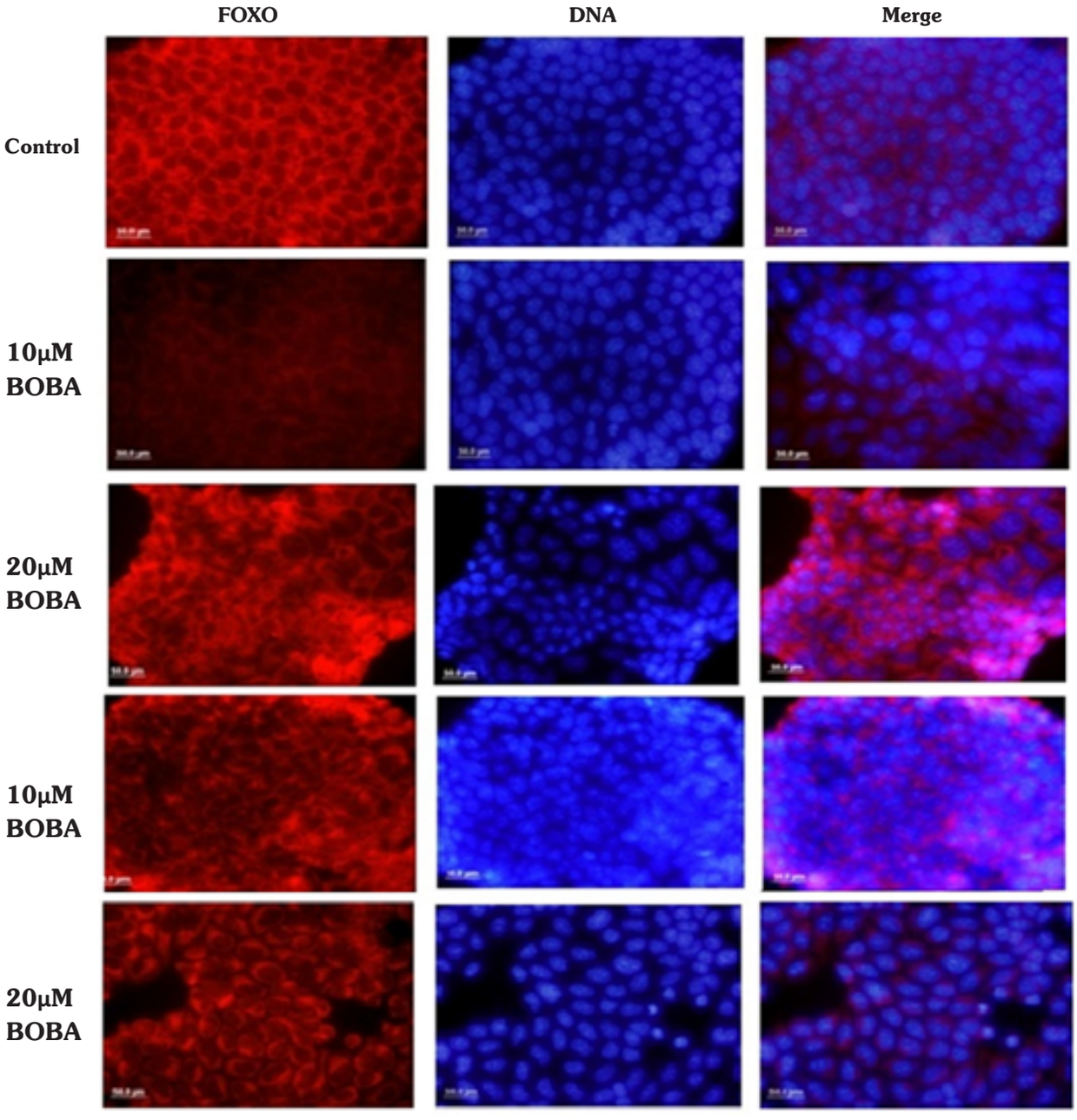

Figure 1: Immunofluorecence microscopy showing nuclear localization of endogenous FOXO3a/p-FRHRL1 (Thr 32) in HCT-15 colon cancer cell line

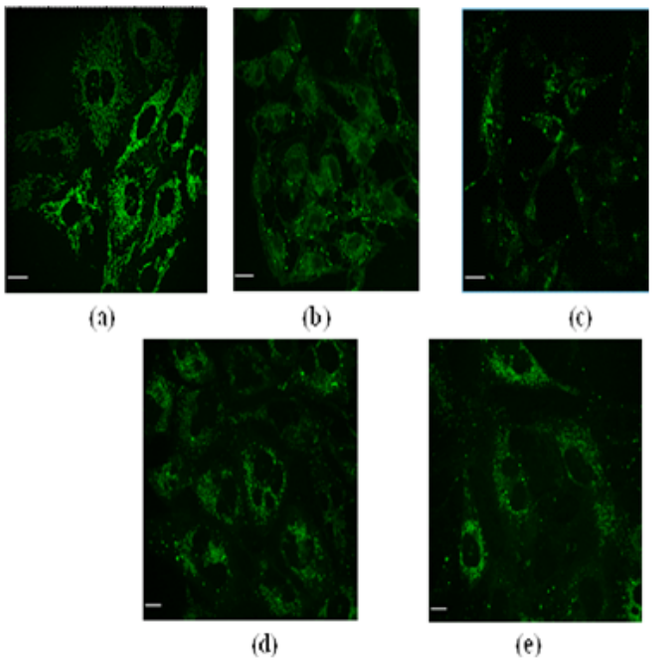

Figure 2: Measurement of mitochondrial membrane potential ($\Delta\Psi_m$) using Rh-123 dye: Caco-2 cells (a) untreated (b) treated with 20μM of BOBA and (c) treated with 30μM of BOBA, (d) treated with 20μM of POBA and (e) treated with 30μM of POBA for 24 h were stained with Rh-123 for 30 min, mounted cover slip and fluorescence observed under confocal microscopy (laser 488)

In order to further highlight the importance of PI3K/Akt mediated cancer cell apoptosis observed under *in vitro* conditions, the various in vivo tumour models such as Ehrlich Ascitic Tumour (EAT), Ehrlich Ascitic Carcinoma (EAC) and Sarcoma-180 employed in the present study also showed significant growth inhibition after BOBA or POBA treatments. Additionally, by the approach of surgical implantation in *in vivo* hollow fiber assay encapsulated with diverse cancer cell lines, the tumor inhibitions after BOBA and POBA treatment were comparable to that of the different *in vivo* models.

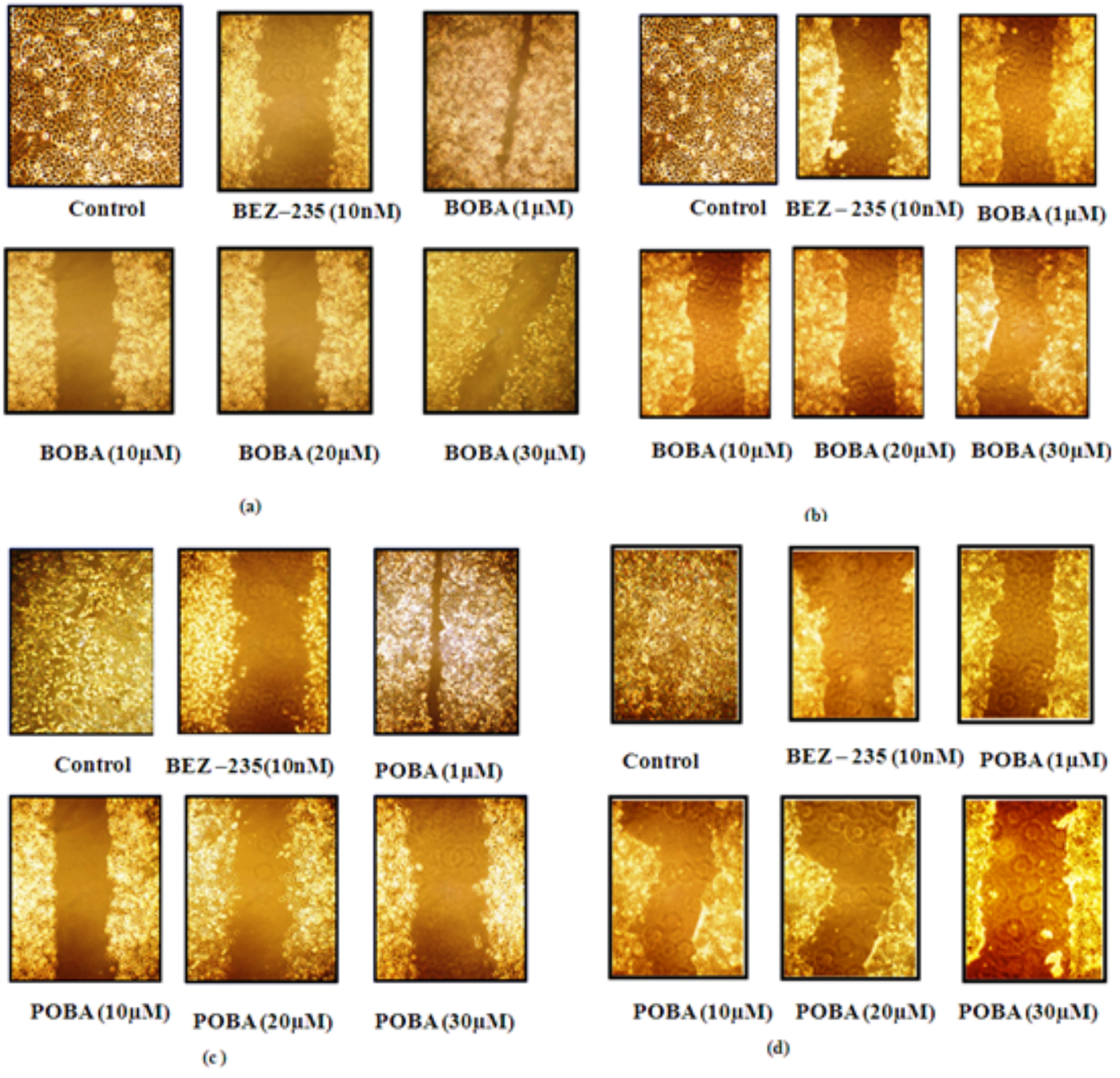

Figure 3: Effect of BOBA and POBA on cell migration: (a) BOBA treated with Caco-2 and (b) BOBA treated with HCT-15 (c) POBA treated with Caco-2 (d) POBA treated with HCT-15 cells. HCT-15 and Caco-2 ($1x10^6$/ml) in culture were treated with various concentrations of BOBA and POBA for 24h. BEZ-235, at a concentration of 10nM was used as positive control

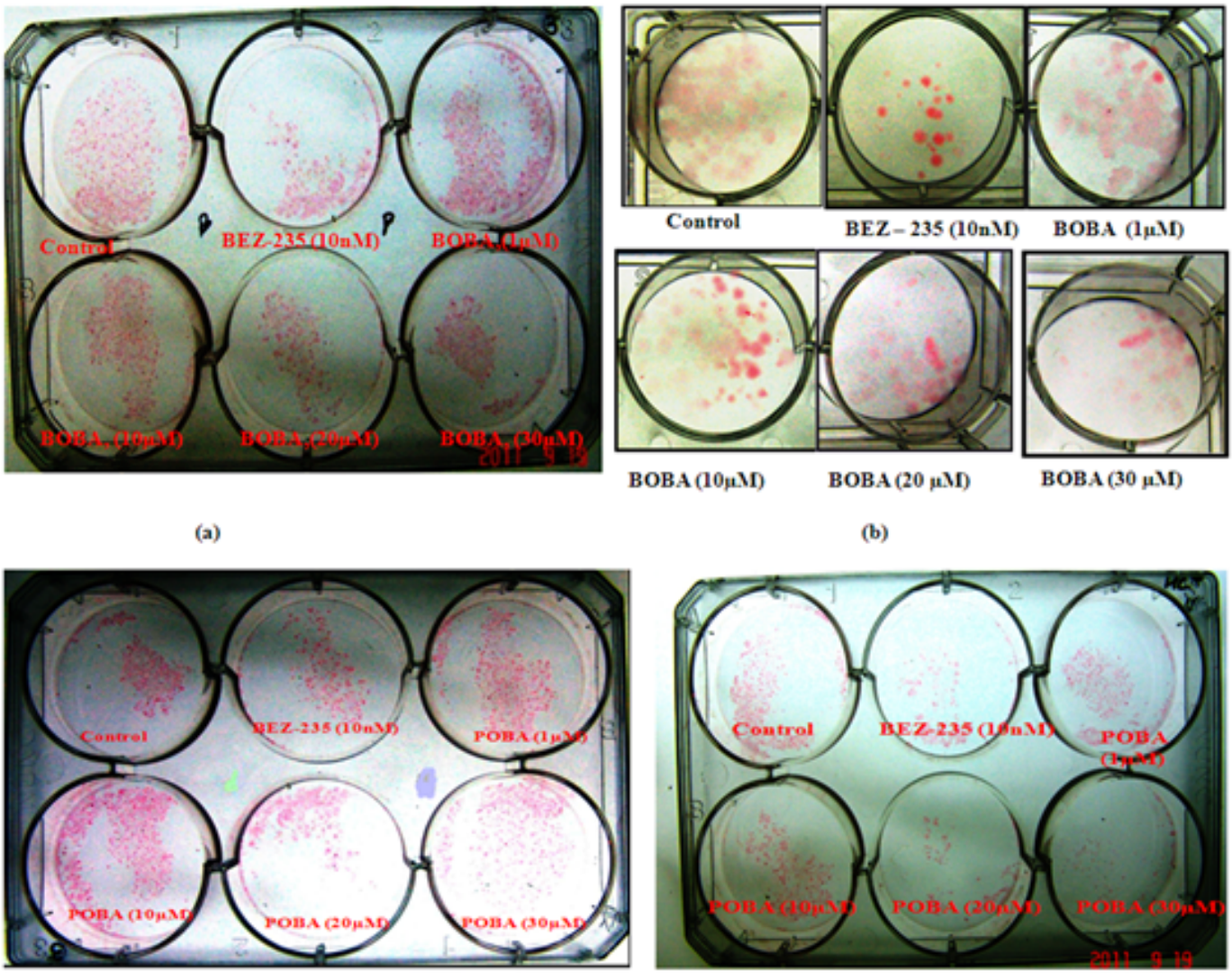

Figure 4: The use of BOBA and POBA effectively inhibits colony formation and growth of (a) Caco-2 cells treated with BOBA (b) HCT-15 cells treated with BOBA and (c) Graphical representation of BOBA treated with Caco-2 and HCT-15 (d) Caco-2 treated with POBA (e) HCT-15 treated POBA (e) Graphical representation of POBA treated Caco-2 and HCT-15 cells. The indicated cell lines at a density of approximately 200 cells/well were seeded in 6-well plates. On the second day, the cells were treated with different concentrations (1μM, 10μM, 20μM, 30μM) of either BOBA or POBA. After 12 days, the plates were stained for the formation of cell colonies with crystal violet dye. Data are representative of one of the three similar experiments carried out in triplicate.

Taken together, the study revealed the correlation between the *in vitro* evaluation, *in silico* studies and the influence on the in vivo anti-tumor activity and provided a preclinical molecular basis for the identification of naturally occurring boswellic acid based molecules as PI3K/Akt/FOXO signaling modulators for the induction of colon cancer cell death among several others. Therefore, BOBA and POBA derivatives may represent the potential agents in targeting the PI3K/Akt in the therapeutic perspective of colon cancer and may also open up a new window in the construction of multi targeted anticancer agents.

3.3 Tetrahydroazepino quinazolinone (THAPQ) as anti-proliferative agent

Asif K Qazi, Abid Hamid, Shashank Kumar Singh and Ajit Kumar Saxena

Resistance to chemotherapy represents a major obstacle in correcting colorectal carcinomas (CRC). In addition, despite recent advances in the treatment of metastatic disease, the prognosis of these patients remains poor. Moreover, the understanding of deregulation of various signaling pathways that influence cell growth, cell cycle progression, apoptosis and invasion has provided novel targets in cancer therapy. In this context, we observed for the first time that Tetrahydroazepino quinazolinone (THAPQ) exhibit potent antiproliferative activity with IC_{50} value of 12μM against HCT-116 cell line representing colon cancer. Our data revealed that THAPQ target PI3K/ NF-κB pathway which results in apoptosis. Furthermore, THAPQ induce hypo diploid sub-Go DNA besides impaired

cancer cell invasion parelled with loss of mitochondrial membrane potential. Furthermore, THAPQ treatment results morphological changes and also loss of microvillae. In conclusion, THAPQ inhibits cell cancer cell viability, suppress PI3K isoform enzyme activity, causes cell cycle arrest, alters mitochondrial membrane potential, impaired cancer cell metastasis and induce apoptosis of HCT-116 cells.

3.4 Novel histone deacetylase inhibitor molecule(s) and cancer cell death

Mudasseir Ahmad, Javid Ahmad Bhat and, Abid Hamid

Recently, histone deacetylase inhibitors have emerged as promising class of anti-tumour drugs especially against cutaneous-T cell lymphoma. Based on SAHA pharmacophore, first therapeutic HDAC inhibitor approved by FDA, a series of molecules was synthesised. Amongst 14 molecules synthesised so far, one molecule Mq1 was found to be a HDAC inhibitor with significant doc score and *in-vitro* cytotoxicity against several cancer cell lines. Mq1 causes maximum G_0/G_1cycle arrest at 5μM concentration in HL-60 cell line. Mq1 is a more potent inducer of intrinsic apoptosis than SAHA in HL-60 cell line. Mq1 induces PARP cleavage and increases the expression of cyclin D1 and decreases the expression of cyclin E1.

3.5 Betulinic acid derived substituted-1, 2, 3-triazoles as potential apoptotic agents

Rabiya Majeed, Abid Hamid and Ajit Kumar Saxena

Betulinic acid derived substituted-1, 2, 3-triazoles as potential apoptotic agents. Cytotoxic agents from nature are presently the mainstay of anticancer chemotherapy, and the need to reinforce the arsenal of anticancer agents is highly desired. Chemical transformation studies carried out on betulinic acid, through concise 1,2,3-triazole synthesis via click chemistry approach at C-3 position in ring A have been evaluated for their cytotoxic potentiation against nine human cancer cell lines. Most of the derivatives exhibited higher cytotoxic profiles than the parent molecule and two compounds (7 and 13) displayed impressive IC_{50} values (2.5 and 3.5 μM respectively) against leukemia cell line HL-60 (5-7-fold higher potency than betulinic acid). As evident from various biological end points, inhibition of cell migration and colony formation, mitochondrial membrane disruption followed by DNA fragmentation and apoptosis, is demonstrated.

3.6 Molecular association of exogenous folate and aging on hepatic DNA methylation: Implications in pathobiology of precancerous tissue

Rauf Ahmad Najar and Abid Hamid

Folic acid is an essential nutrient that is required for one-carbon biosynthetic processes and for methylation of biomolecules. Deficiency of this micronutrient leads to disturbances in normal physiology of cell. The present study deals with the regulatory mechanisms of folate uptake in liver during folate deficiency and supplementation. Male Wistar rats were fed with folate deficient and folate supplemented diet for 3 to 5 months and the molecular mechanisms of folate uptake were studied in liver. There was significant decrease of body weight between control and folate deficient for 3 months. The serum folate also validates our study with decrease of folate levels in folate deficient (FD) and increase of folate levels in folate supplemented (FS) with 2mg and 8mg and maximum increase was observed in folate supplemented with 8mg.The transport uptake of folate in liver basolateral membrane (BLM) was studied using radiolabeled 5-MTHF at different pH between 5 to 8 and maximum uptake in all subgroups was observed at pH 5.5. The uptake at pH 5.5 in control(14.33± 0.13),3M FD (18.85 ± 0.14***), 3M FD +2MFS-2mg(12.15 ± 0.49***), 3M FD +2MFS-8mg(9.31 ± 0.94***), 5M FD (26.34 ± 0.38). The characterization of the folate transport system in liver basolateral membrane (BLM) suggested it to be a carrier mediated and acidic pH dependent, with the major involvement of proton coupled folate (PCFT) transporter and folate binding protein (FBP) in the uptake. Moreover, folate deficiency increase the folate transport by altering the V_{max} and K_m, the V_{max} at 0.5μM folate concentration and increase V_{max} in FD (52.35) in comparison to control (42.69) and in case of 5M FD V_{max} (23.5 ± 0.282), 3M FD +2MFS-2mg(10.7 ± 1.97), 3M FD +2MFS-8mg(9.36 ± 0.876) that is V_{max} decreased with supplementation. The affinity of folate for folate transporters was also studied and it was observed that K_m decreased in FD (0.7857) in comparison to control (0.8146) which validates maximum uptake of folate in FD.

3.7 Enhanced anticancer potential of encapsulated solid lipid nanoparticles of TPD: A novel triterpenediol from *Boswellia serrata*

Shashi Bhushan, Vandita Kakkar, Harish Chandra Pal, Santosh Kumar Guru, Ajay Kumar, D. M. Mondhe, P. R. Sharma, Subhash Chandra Taneja, Indu Pal Kaur, Jaswant Singh and A. K. Saxena

A pentacyclic triterpenediol (TPD) from *Boswellia serrata* have significant cytotoxic and apoptotic potential in a large number of human cancer cell lines. To enhance its anticancer potential, it was successfully formulated into solid lipid nanoparticles (SLNs) by micro-emulsion method with 75% drug entrapment efficiency. SEM and TEM studies indicated that TPD-SLNs were regular, solid and spherical particles in the range of 100-200nm, the system was indicated to more or less stable upon storing up to six months. TPD-loaded SLNs showed significantly higher cytotoxic / anti-tumor potential than the parent drug. TPD-SLNs have 40-60% higher cytotoxic and apoptotic potential than the parent drug in terms of IC_{50}, extent of apoptosis, DNA damage and expression of pro-apoptotic proteins like TNF-R1, cytochrome-c and PARP cleavage in HL-60 cells. Moreover, blank SLNs did not have any cytotoxic effect on the cancer as well as in normal mice peritoneal macrophages. *In vivo* anti-tumor potential of TPD-SLNs were significantly higher than TPD alone in Sarcoma-180 solid tumor bearing mice. Therefore, SLNs of TPD successfully increased the apoptotic and anticancer potential of TPD at comparable doses (both *in vitro* and *in vivo)*. This work provides a new insight for improvising the therapeutic efficacy of TPD by adopting novel delivery strategies such as solid lipid nanoparticles (Fig.1).

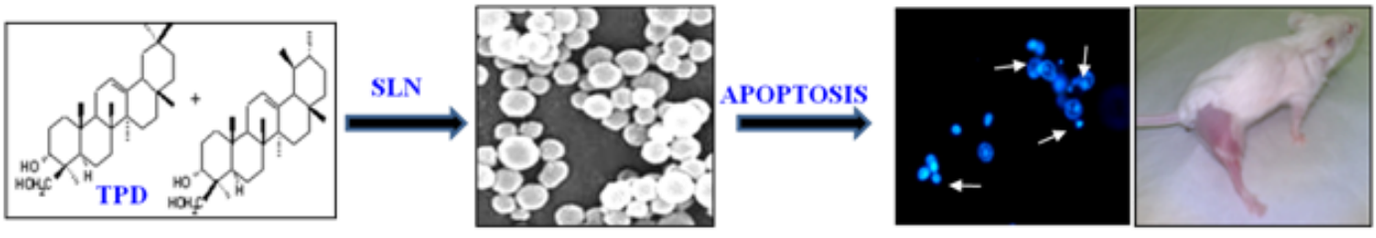

Figure 1: Enhanced anticancer potential of encapsulated solid lipid nanoparticles of TPD

3.8 Phosphodiesterases (PDEs)

Syed Sajad Hussain

Mammalian Phosphodiesterases (PDEs) are a group of enzymes transcribed from 21 genes and have been classified into 12 families (PDE1-PDE12) based on enzymatic properties, sequence homology, and sensitivity to inhibitors. These families contain many splice variants (1). PDEs hydrolyze the intracellular cyclic nucleotides (cAMP and cGMP).

Cyclic nucleotide phosphodiesterase type 5 (PDE5) is an enzyme mainly found in corpus cavernosum, heart, lung, platelets, prostate, urethra, bladder, liver, brain, and stomach. It hydrolyses the cyclic guanosine monophosphate (cGMP). A lower cGMP level in smooth muscles has been associated with many health disorders, hence making the cGMP hydrolysis a good target for inhibitors. Many PDE5 inhibitors have been approved as drugs for treating male erectile dysfunction (ED) and cardiovascular diseases and the hunt to discover new inhibitors is on in many pharmaceutical companies and academic centers. In addition PDE5 inhibitors have been shown to have some role in treating diseases like as stroke, Raynaud's disease, overactive bladder, and premature ejaculation (2,3). Sildenafil is a PDE5 inhibitor and first FDA approved oral medicine for the treatment of erectile dysfunction (approved in 1998)(4) and pulmonary arterial hypertension (PAH) (approved in 2005)(5-8). Vardenail and Tadalafil are two other PDE5 inhibitors which are approved for the treatment of ED and PAH (9,10). Recently Avanafil also made it to the list of approved drugs for treating ED by inhibiting the PDE5. The main issue with these PDE5 inhibitors is selectivity against other PDE isozymes, most notably PDE6 or PDE11 (11) hence there is continuing interest in discovering novel inhibitors which will he highly specific against PDE5.

Analogue based drug discovery is a general principle in medicinal chemistry for discovering new and

better drugs. These analogues are chemically modified but structurally similar compounds and most of these modifications involve the addition or deletion of one or more functional groups. There is a possibility that these analogues retain the corresponding pharmacological activity, however it is not uncommon to have similar structures with completely different activities. So it is imperative to check the activity of these analogues in a battery of experiments to check their efficacy against the corresponding disease.

In our recent studies our MCD colleagues made analogues of approved drugs Sildenafil and Tadalafil, in hope to discover new molecules which will be highly specific and efficient in terms of PDE5 inhibition. We developed an enzyme based *in vitro* assay system for the Phosphodiesterases, screened the analogue molecules and determined the IC50 of the active compounds. In addition we developed an already published conscious Rabbit model (12) for screening PDE5 inhibitors.

Till now we have found 4 small molecule analogues of Sildenafil which inhibit PDE5 as actively as parent molecule or even better. They show the IC50 values in the range of 2-16nM (Sildenafil IC50=3.5nM). In order to determine the specificity of these active molecules the IC50 of these four molecules against all the 11 human PDE isoforms was determined and found to be similar to that of the parent molecule especially against the most critical phosphodiesterase called PDE6. We are in a process to compare the efficiencies of all these active molecules in the conscious rabbit model.

3.9 Analysis of subcellular localization of cell signaling proteins using GFP as a fusion partner

Paramjeet Singh, Gurjinder Singh, Gayatri Jamwal, Mohd Saleem and Mohd Jamal Dar

In order to develop cell-based assays for cancer drug development, some of the proteins involved in cell-cell signalling (e.g PI3K signalling proteins) were fused with green flourescent protein (GFP). Transient expression of these fluorescent reporter proteins in HEK-293 cells was performed for the one's that include EGFR, IGF-1R, p110-beta, beta-catenin etc. Transfected HEK-293 cells were grown for 48 hours and visualized by confocal microscopy. Shown below in Fig-A is GFP (vector) expression in these HEK-293 cells. B- p110-beta shows nuclear as well as cytosolic expression (Fig 1). C- IGF-1R also shows diffused expression pattern. D- EGFR shows typical plasma membrane expression pattern. E- Beta-catenin used as a control also shows diffused expression pattern.

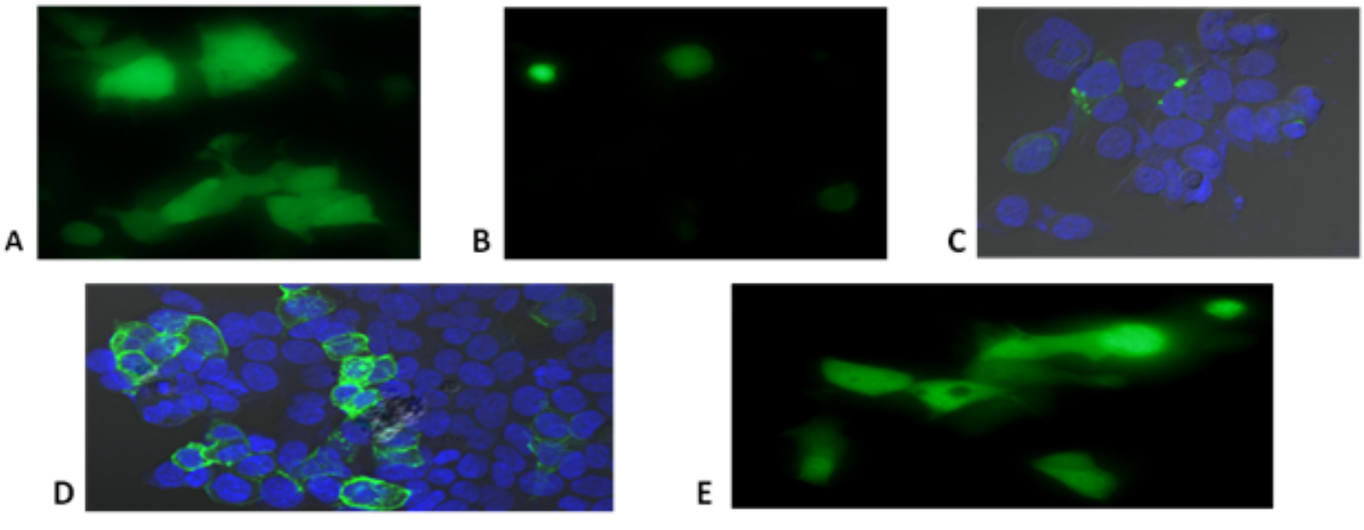

Figure 1: Subcellular Localization of Cell signaling proteins using GFP

3.10 A novel MMP-2 Inhibitor 3-azidowithaferin A (3-azidoWA) abrogates cancer cell invasion and zngiogenesis by modulating extracellular Par-4

Bilal A. Rah, Hina Amin, Khalid Yousuf , Sheema Khan, Gayatri Jamwal, Debaraj Mukherjee and Anindya Goswami

Withaferin A, a steroidal lactone from *Withania somnifera* (Aswagandha) has allured the attention of the biologists due to it's attributor pharmacological properties like anti-cancer, anti-stress, anti-convulsant, immunomodulatory and neurological effects As important anti-neoplastic agent Withaferin A exhibited anti-angiogenic potential by targeting vimentin. Recently, it has been reported that 2, 3-dihydrowithaferin A-3β -O-sulphate acts as a potent prodrug of withaferin-A. In the light of promising therapeutic prospective of Withaferin A as an anticancer molecule reported by our institute we were keen to investigate modifications of the ring A. Our chemistry group envisaged that substitution of the α-β-unsaturated carbonyl system of Witheferin A at the β -position may be a practical approach to find new activities of the modified compounds as this will obviate irreversible covalent binding in active sites by biological nucleophiles, a reason behind drug resistance in cancer treatment. Moreover, still today the actual mode of action of metastasis /angiogenesis inhibition by Withaferin A remains ambiguous.

In the present study, we have identified a highly selective MMP-2 inhibitor, 3-azidoWA, a natural product withanolide derivative from traditional medicinal plant *W. Somnifera*. Though, withanolides have been well documented for diverse biological functions, *viz,* antiproliferative, antiinvasive, radiosensitizing and antiarthritic, here, for the first time, we uncover the target specific MMP-2 inhibition by 3-azidoWA in moderately aggressive cervical and prostate cancer cells. We demonstrate here that 3-azidoWA is a potent inducer of extracellular Par-4. Although, the intracellular Par-4 induction by Withaferin A had been empowered the apoptotic induction of these class compounds in several cancers, interestingly, we have explored the role of extracellular systemic Par-4 which was robustly increased in the conditioned media due to 3-azidoWA treatment as compared to Withaferin A treatment Fig. 1 (B). Our data reveal that inhibition of MMP-2 expression and gelatinase activity by 3-azidoWA was extracellular Par-4 dependent as shown in Fig. 1.

Matrix metalloproteinases are the lead candidates to facilitate tumor invasion process by triggering a chain of signalling cascades and play crucial role not only in invasion, angiogenesis and metastasis, but also determines cancer cell transformation, growth, apoptosis and signal transduction. In the last twenty years majority of the MMP inhibitors showed lack of success in clinical trials because none of these synthetic/semi synthetic drugs were selective for specific MMP's. Thus, learning lessons from looking back at previous failed attempts necessitates developing selective MMP inhibitors that should not have cross-reaction with other MMP's. Here we demonstrate that 3-azidoWA only selectively blocked MMP-2 activity Fig. 1 (A) and thus motility and invasion of diverse cell line in extracellular Par-4 dependent manner Fig 3 (C, D). By degrading the basement membrane, MMP's are considered to accelerate cell mobility in a stationary tumor cell and promote metastasis. Mounting evidences have suggested that MMP's not only function in cancer progression and metastasis but may also contribute to steps of cancer development. These diverse activities may account for the role of MMP-2, a pivotal matrix metalloprotease that control cancer cell motility and invasion. In the present study we have illustrated that non-toxic doses of 3-azidoWA significantly inhibited the migration and invasion of HeLa and PC-3 cells when treated in a dose dependent fashion in Boyden chamber invasion assay as depicted in Fig. 2 (A,B,E,F).

In addition to degrading ECM components, MMP's were shown to confer apoptosis resistance by modulating Fas-FADD mediated death signalling and cleavage of Fas by MMP-2 resulted in decreased sensitivity of HT-29 colon carcinoma cells to Fas mediated apoptosis. Extracellular Par-4, on the other hand has been documented to exert apoptotic effect by activating downstream caspase-3. Earlier studies have shown that downregulation of MMP-2 with adenovirus mediated delivery of MMP-2 (ad-MMP-2) SiRNA reduced invasion, migration and angiogenesis in A549 cells *in vitro* and inhibited tumor growth and metastasis *in vivo*. Further the authors also revealed that Ad-MMP-2 mediated tumor growth inhibition occurred through cleavage of caspases -8,-9 and -3, and activation of FAS-mediated signaling pathway. Consisting with that finding, we demonstrate here 3-azidoWA as well as TRAIL mediated inhibition of MMP-2 in cervical and prostate cancer cell line through induction of extracellular Par-4 which has been shown to induce extrinsic apoptotic pathway by FADD-caspase-8-caspase-3 activation (Fig. 3. A, B). Interestingly, we have observed that ectopically over expressed GFP-Par-4 which secreted spontaneously in the conditioned media, significantly inhibited MMP-2 within 48 h of post transfection (Fig. 3. F). Moreover, 3-azidoWA treatment caused activation of caspase-3 and downregulate MMP-2 expression compared to vehicle treated cells and inhibition of caspase-3 activation by caspase inhibitor could not restore the MMP-2 expression level. Hence, that inhibition of MMP-2 by 3-azidoWA was apoptosis independent

(Fig 4). To address the rational discrimination of 3-azidoWA for controlling cell motility versus apoptosis we carefully choose a range of drug concentrations and observed that 0.5μM 3-azidoWA did not contribute to DNA fragmentation (data not shown) but altered cell motility. Therefore, there may be a logical explaination that at a low dose (0.5 μM) 3-azidoWA inhibited MMP-2, but had no effect on cleaved caspase-3 activation, but at the dose level of 1uM, not only MMP-2 activity was strongly downregulated but also caspase-3 mediated apoptotic machinery might be upregulated via extracellular Par-4. Thus it can be possible that low dose of 3-azidoWA induced basal secretion of extracellular Par-4 that might be utilized to downregulate MMP-2 and additional increase of 3-azidoWA /prolong drug treatment might add excess pool of secretory Par-4 in the conditioned media that accelerates apoptosis by extrinsic pathway. But, how the intracellular Par-4 level is correlated with extracellular Par-4 secretion due to 3-zidoWA treatment is under current investigation in our laboratory.

Consisting with the previous report we have noticed a dose dependent increase in extracellular Par-4 level when HeLa/PC-3 cells were treated with TRAIL and tunicamycin with fairly high concentration (300ng/ml TRAIL and 1uM tunicamycin), which also inhibited MMP-2 gelatinolytic activity (Fig 1. D,E). Therefore, for the first time our results suggest that extracellular Par-4 (causal effects of multiple agents) modulate MMP-2 activity. In view of finding the role of 3-azidoWA induced extracellular Par-4, that escalated gradually with increasing concentration of 3-azidoWA, we found the concomitant weaken MMP-2 band in the zymogram (having equal loading control BSA), that resembled anti-invasive property of conditioned media containing secretory Par-4 and when these extracellular Par-4 in the conditional media was depleted with Par-4 neutralizing antibody, HeLa cells invaded through the membrane of the Boyden chamber and MMP-2 level was restored. Additionally, for further verification we diminished extracellular Par-4 secretion with BFA and found that depletion of extracellular Par-4 due to Brefeldin A treatment restored MMP-2 level compared to untreated control. The inhibition of MMP-2 secretion by Brefeldin A might overcome by some mechanism need to be elucidated in future. This data vividly suggest the role of extracellular Par-4 mediated motility inhibition stimulated by 3-azidoWA.

Angiogenesis is a crucial step in tumor progression and invasion regulated by VEGF. MMP-2 plays a pivotal role in this process. Interestingly, our *in vivo* results reveal 3-azidowithaferin A is capable of suppressing VEGF-bFGF induced neovessel formation *in vivo*. Note the treatment with increasing concentration of 3-azidowithaferin A almost abolished the new blood vessel formation in the plugs containing VEGF and bFGF (Fig 5A, B). Due to the importance of TIMP-1 in cancer cells invasion, and angiogenesis, we have demonstrated that 3-azidowithaferin A treatment augmented the expression of TIMP-1 which is a modulator of MMP-2 expression in both cell lines, in dose dependent manner. Moreover, MAPK and PI3K/Akt pathways also contribute pivotal role in tumor development and angiogenesis. Therefore, we investigated the effect of 3-azidoWA on the activities of MAPK and PI3K/Akt signaling pathways. The results of our studies suggest that treatment with 3-azidoWA inhibited internal ERK and Akt phosphorylation in both HeLa and PC-3 cells in a dose dependent manner (Fig. 6), suggesting that the signaling pathways mediated by MAPK, PI3K/Akt were suppressed by 3-azidoWA. Collectively, these results suggest that 3-azidoWA suppressed *in vivo* angiogenesis in mice by blocking ERK, Akt phosphorylation and amplified TIMP-1 expression.

In conclusion, we have illustrated a novel pathway of 3-azidoWA induced MMP-2 inhibition, mediated through pro-apoptotic secretory protein Par-4, secreted by a classical BFA sensitive pathway. We have verified the possibility of apoptotic induction and abrogation of metastasis could be controlled independently /collaboratively by 3-azidoWA. Interestingly we disclose that 3-azidoWA mediated MMP-2 inhibition is apoptosis sovereign. Taken together this report unveils a therapeutic potential of 3-azidoWA, derivative of dietary compound withaferin A to inhibit motility ability of cervical and prostate cancer cells through matrix metalloproteinase-2 and induction of extracellular Par-4, which has broader aspects of controlling tumorigenesis

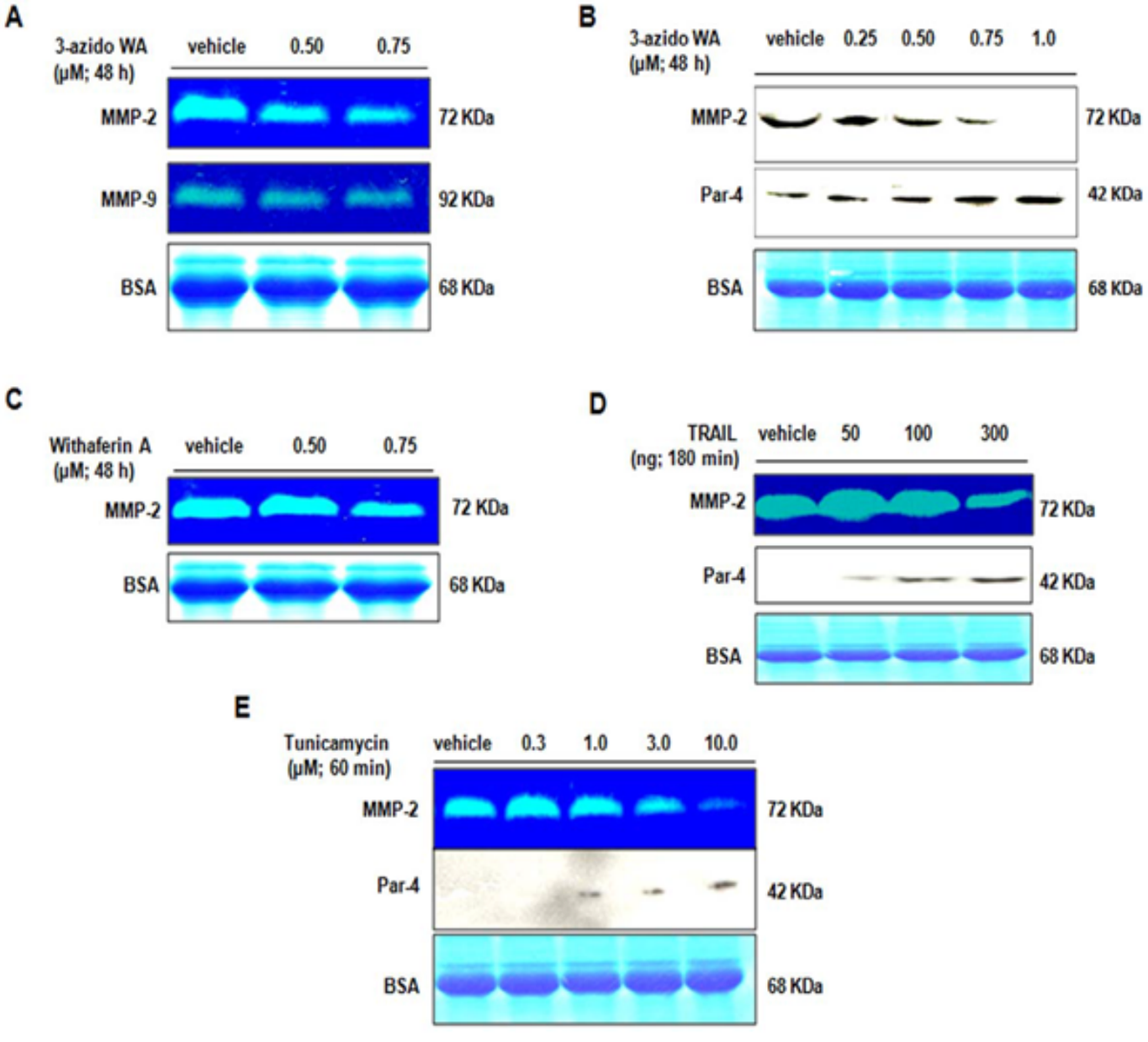

Figure 1: 3-azidowithaferin induces extracellular Par-4 secretion and inhibits MMP-2. (A) HeLa cells were left untreated or treated with 0.50 μM and 0.75 μM of 3-azidoWA for 48 h, conditioned media was analyzed for MMP-2 & -9 gelatinase activity. (B) HeLa cells were left untreated or treated with 0.25, 0.50, 0.75 and 1μM 3-azidowithaferin A for 48 hrs , conditioned media obtained was employed for western blot analysis followed by Coomassie blue staining to reveal the 68 kDa BSA band for loading control. (C) HeLa cells were treated with various concentration of parent withaferin A for 48 h and the activity of MMP-2 was determined by gelatin zymography. (D) & (E) HeLa cells were treated with TRAIL for 180 minutes and with tumicamycin for 60 minutes (as indicated). Conditioned media were subjected to gelatin zymography analysis for MMP-2 activity and Western blot analysis for extracellular Par-4 , followed by coomassie blue staining for loading control

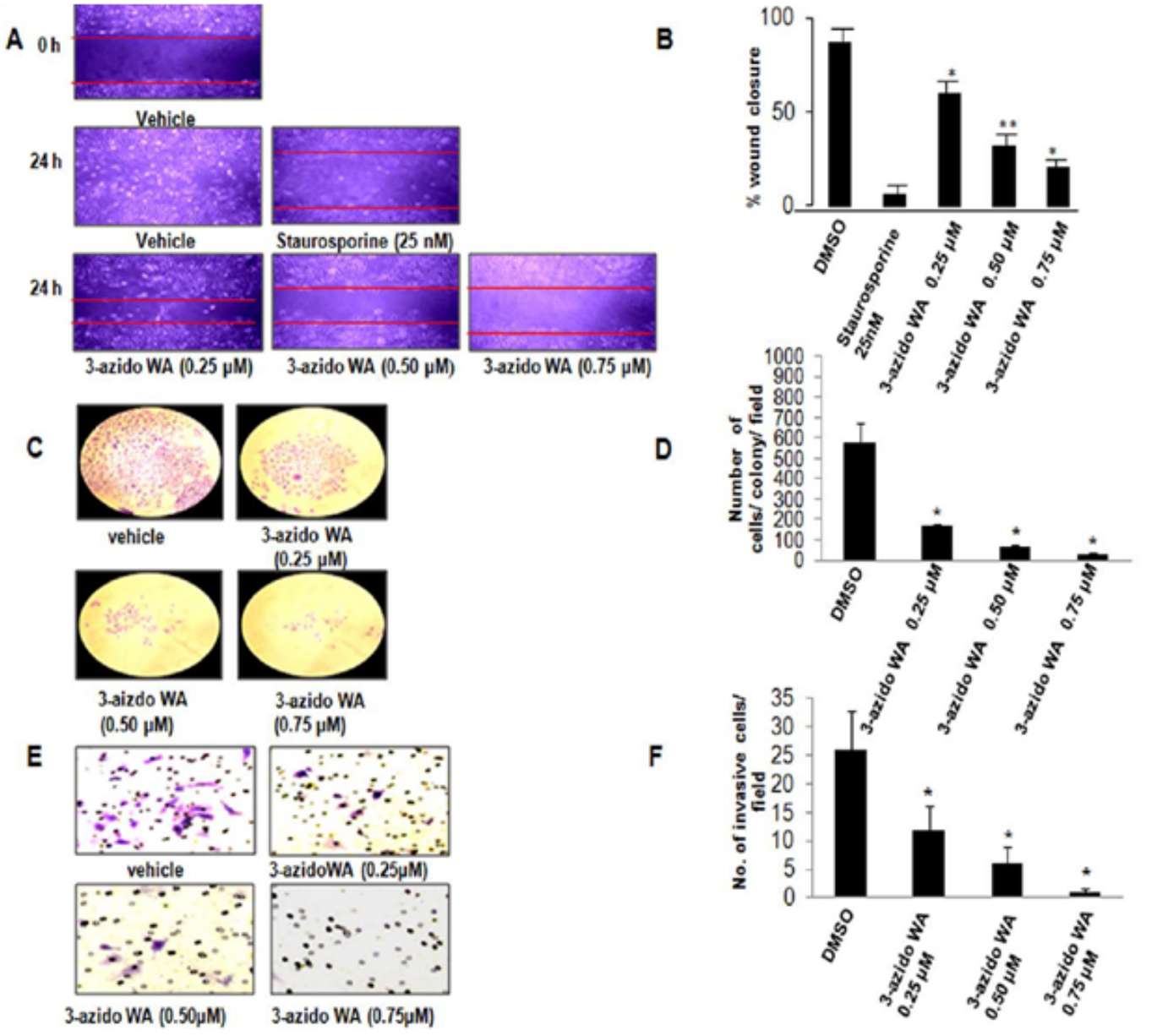

Figure 2: 3-azidowithaferin A inhibits motility, invasion and colony formation ability of HeLa cells. (A) HeLa cells ($0.5x10^5$ cells/well) were grown to confluence in six well tissue culture plate and scratched with sterile tip, 3-azidoWA was added to cultures as indicated. Scratched areas were photographed (magnification 100x) at zero hour and then subsequently again 24 h later to assess the degree of wound healing. (B) The scratched areas were quantified in three random fields in each treatment, and data were calculated from three independent experiments. (C) HeLa ($1x10^3$) cells/well were cultured and treated with various concentration of compound 3-azidoWA for 5 days at 37^0C and then stained with crystal violet (for details see materials and methods), numbers of stained colonies were counted, photographed (100x) and (D) data were calculated from three independent experiments. Columns mean; bars SD of three independent experiments. * P< 0.05, **P< 0.01 compared with untreated control. (E) Cell migration was determined via the modified Boyden chamber assay as described in Materials and Methods. HeLa cells ($2x\ 10^5$) were seeded in top chamber in the presence or absence of 0.25, 0.50, and 0.75 μM of 3-azidoWA. Cells were allowed to migrate for 24 h, at which point migratory cells on the bottom half of the insert membrane were stained with 0.1% crystal violet and counted under 200x magnification. (F) Invasive cells were counted using image software as the number of migrated cells per high-power field (HPF). Five fields were counted in triplicate (n = 3) from each insert. Cell images were obtained using microscope Nikon Eclipse E200 inbuilt with camera. Columns, mean; bars SD of three independent experiments. * P< 0.05, **P< 0.01 compared with untreated control.

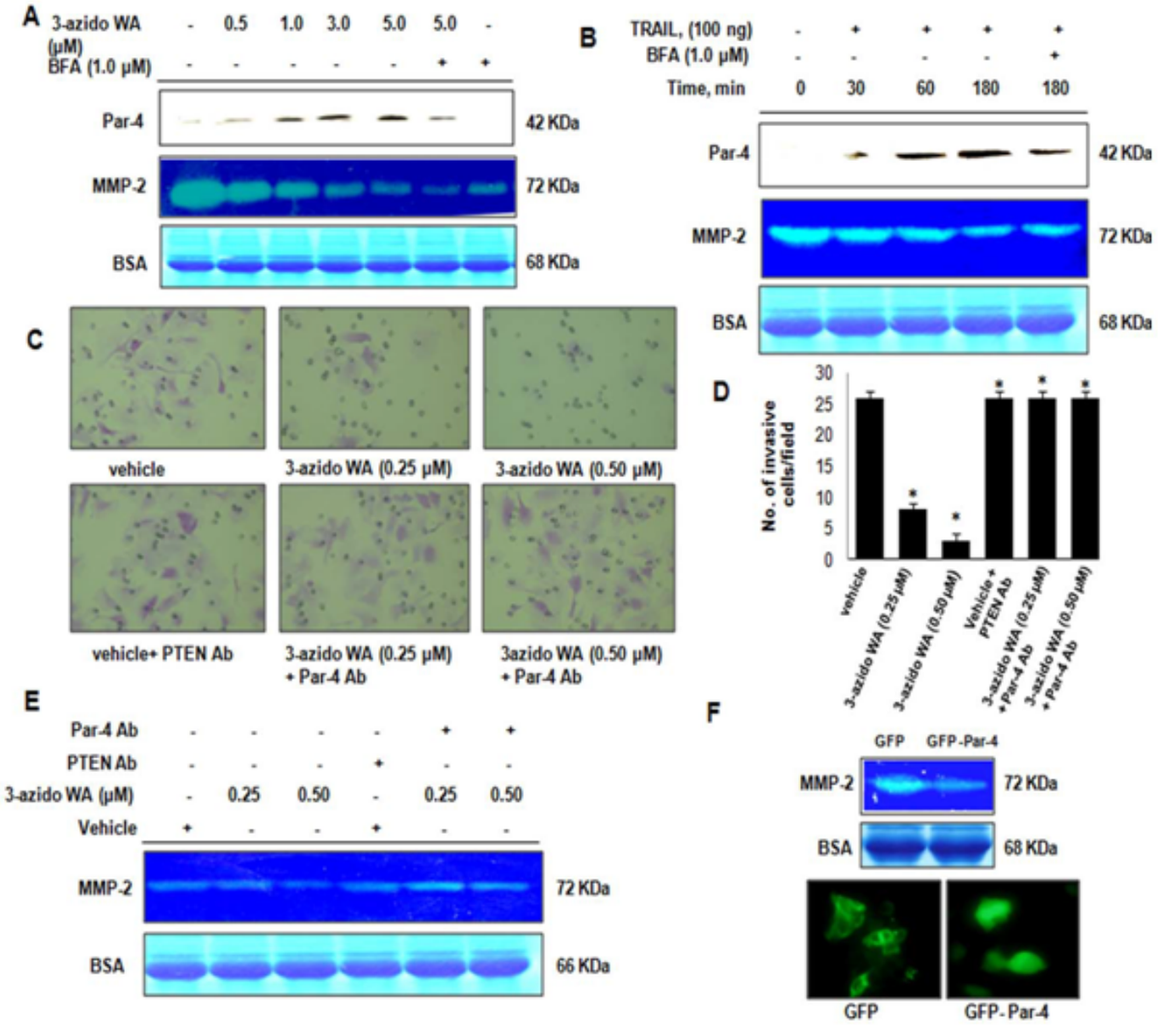

Figure 3: 3-azidoWA induced extracellular Par-4 abrogates invasion of PC-3 cells. (A) PC-3 Cells were left untreated or pretreated with BFA (1.0 μM) for 120 min, then treated with 3-azidoWA as indicated for 48 hours. Conditioned media were prepared, and subjected to gelatin zymography for MMP-2 activity and western blot (WB) analysis for Par-4, followed by Coomassie blue staining for loading control. (B) PC-3 cells were left untreated or pretreated with BFA (1.0 μM) as indicated, then exposed to TRAIL (as indicated). Conditioned media were prepared, and subjected to gelatin zymography for MMP-2 and western blot (WB) analysis for Par-4. (C) & (D) Cell migration was determined by the modified Boyden chamber assay as described in materials and methods. HeLa cells (2x 10^5 cells/well) were seeded in top chamber in the presence of 0.25 and 0.50 μM of 3-azidoWA along with untreated in upper and lower lane. Cells were allowed to migrate for 24 h, at which point migratory cells on the bottom half of the insert membrane were stained with 0.1% crystal violet and counted under 200x magnification and in lower lanes Par-4 antibody was added in 0.25 and 0.50 μM 3-azidowithaferin A treatment group and control PTEN antibody was added in untreated group and further incubated for 24 h. Migratory cells were counted using image software as the number of migrated cells per high-power field (HPF). Five fields were counted in triplicate from each insert of three independent experiments (SD. *, $P < 0.05$). Migrated cell images were obtained using microscope Nikon Eclipse E200 inbuilt camera (200x magnification). (E) Zymography was performed from conditional media collected from cells treated with 3-azidoWA (0.25 and 0.50μM) along with untreated and 3-azidowithaferin A (0.25 and 0.50 μM) + Par-4 antibody, corresponding untreated + PTEN antibody. Coomassie stain of BSA confirms equal loading (lower band). .(F) PC-3 cells were transiently transfected with GFP and GFP-Par4, 48 h post-transfection conditioned media were analyzed through gelatin zymography , followed by coomassie blue staining to reveal the 68 kDa BSA band for loading control and green fluorescence protein expressions were checked under fluorescence microscope and photographed (100x).Columns, mean; bars SD of three independent experiments. * $P < 0.05$, compared with untreated control.

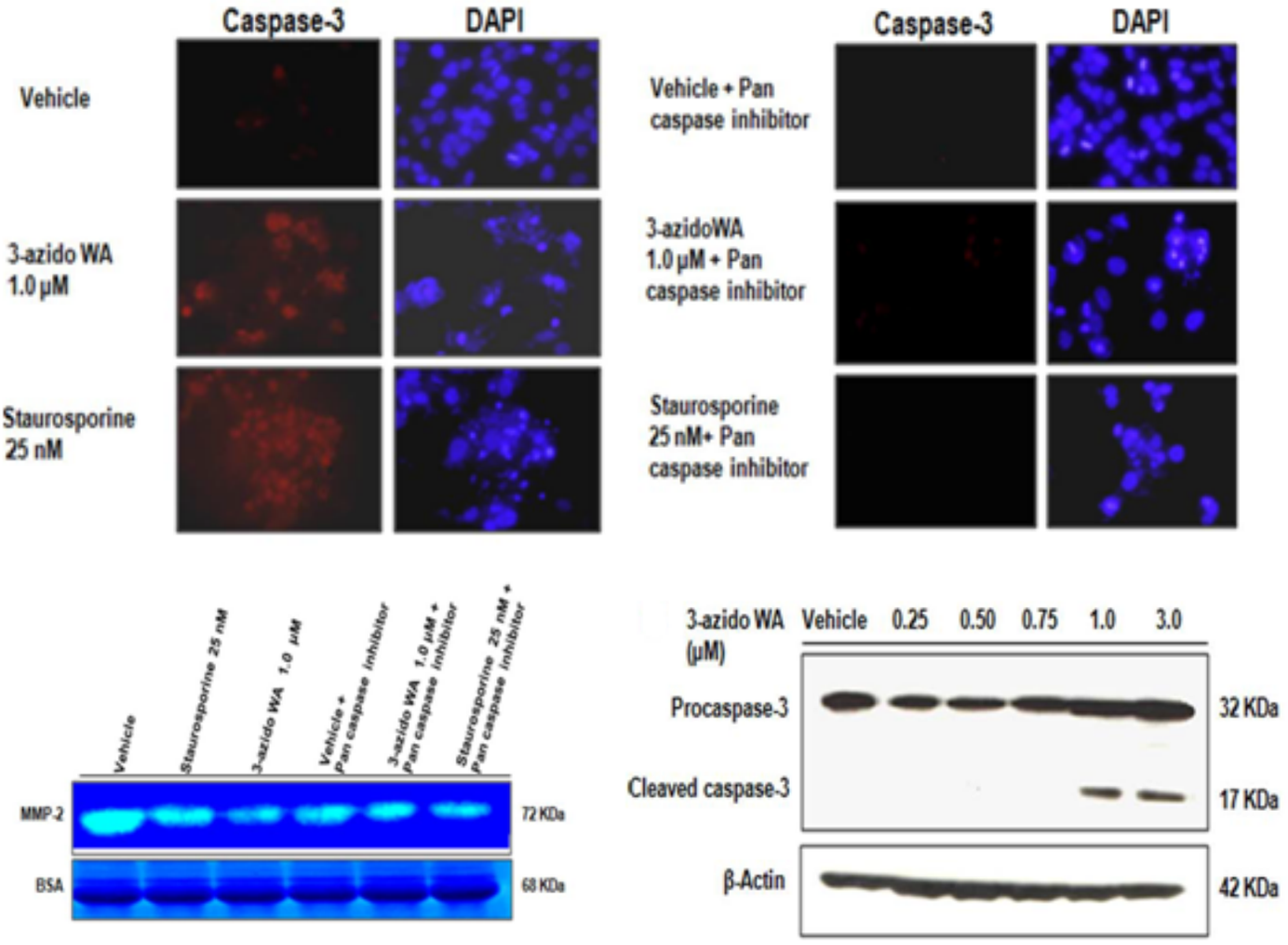

Figure 4: 3-azidowithaferin induce MMP-2 inhibition is apoptosis independent. (A) HeLa cells (0.5×10^6 cells/well) were plated in cover slip in 6 well tissue culture plate and were treated with 1μM 3-azidoWA along with vehicle and staurosporine (25nM) in presence (right panel) and absence (left panel) of Pan caspase inhibitor. After 24 h treatment cells were washed, fixed and immunostained with caspase-3 antibody (Texas red), counterstained with DAPI (blue) to score apoptotic nuclei and analyzed random fields with Zeiss LSM-510 metaconfocal microscope and images were captured at 63x magnification.. (B) Conditional media collected from above experimental group were employed for MMP-2 activity by zymography.

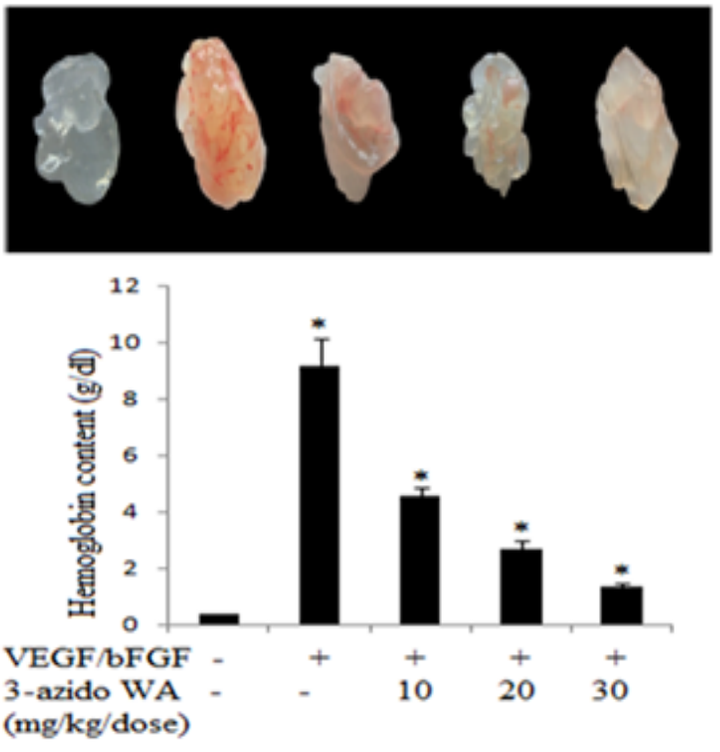

Figure 5: (A) The macroscopic appearance of angiogenesis in Matrigel plugs. C57/BL6J mice were injected subcutaneously into the right flank of abdomen with matrigel supplemented with 250 ng/mL VEGF-A and 500 ng/mL bFGF. After 7th day of injection of matrigel, animals were treated with different doses of 3-azidoWA for 8th, 9th and 10th day successively and sacrificed on 11th day to remove matrigel plugs. Matrigel plugs from control (without VEGF-A and bFGF), treated (with VEGF-A and bFGF) and 3-azidoWA (10 mg/kg/d, i.p., 20 mg/kg/d, i.p. and 30 mg/kg/d, i.p.) exposed were compared. (B) Hemoglobin content of the matrigel plugs. Matrigel plugs were removed and homogenized in 10mM PBS.Hemoglobin estimation was analyzed with Drabkin's reagent. * P< 0.05, compared with untreated control.

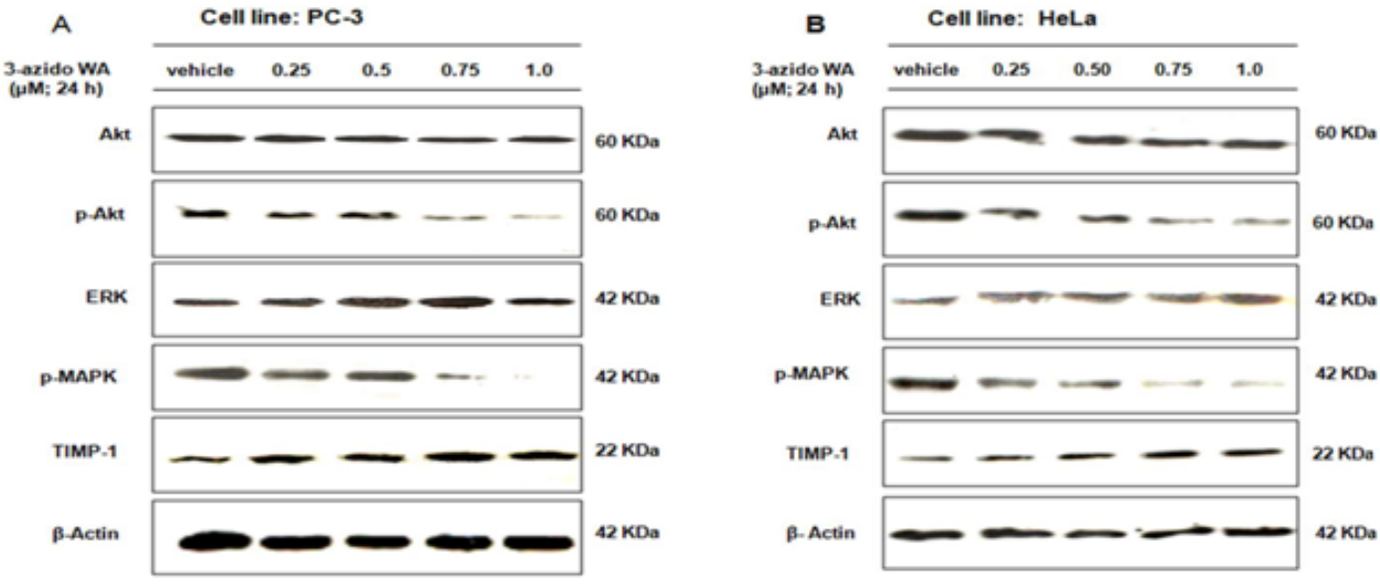

Figure 6: Effect of 3-azidowithaferin A on phosphorylation of Akt, ERK and expression of TIMP-1. (A) HeLa and PC-3 cells were treated with increasing concentrations of 3-azidoWA as indicated, phosphorylated and total Akt, ERK expressions were determined by Western blotting. TIMP-1 expression was verified by same method.

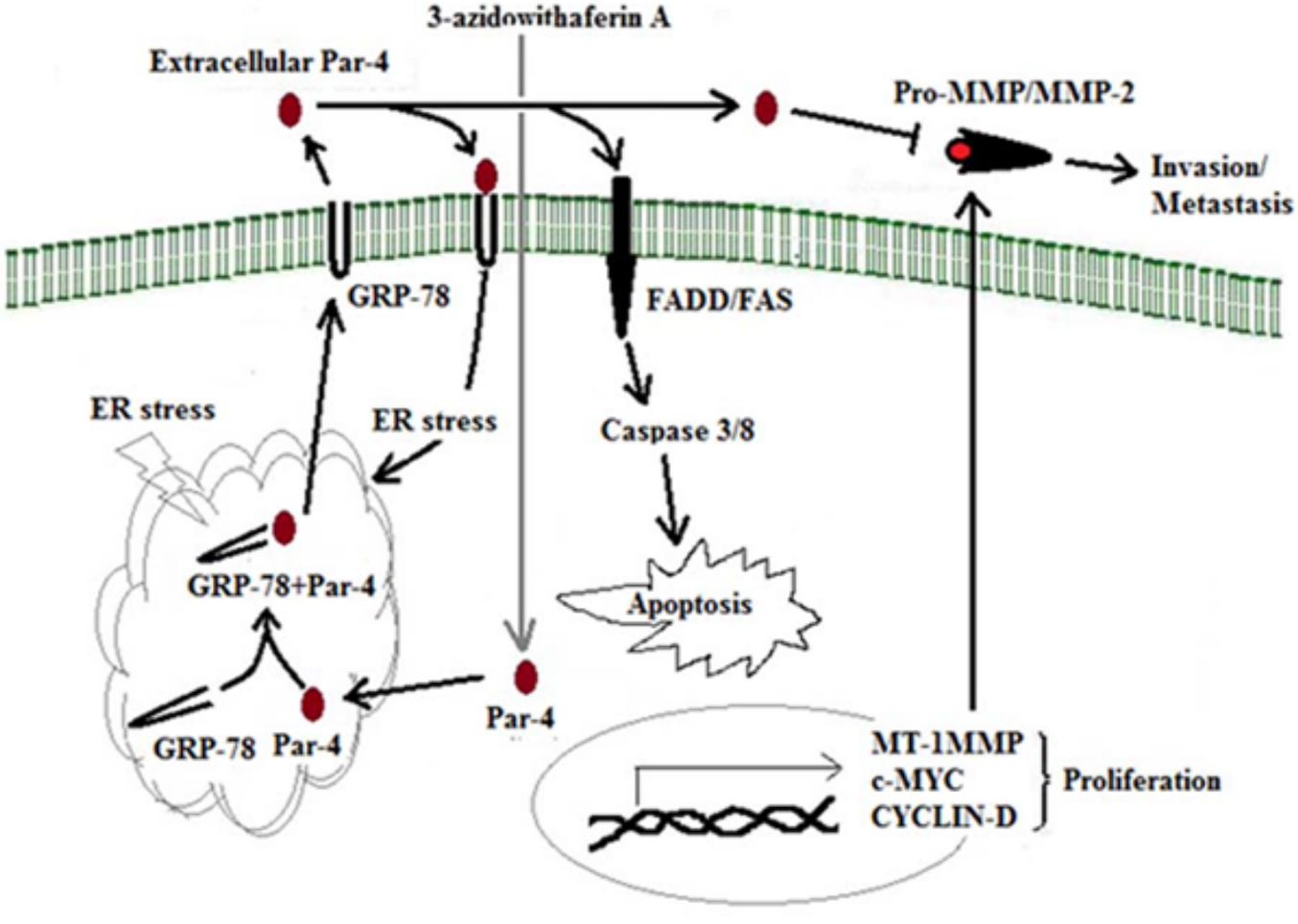

Figure 7: Schematic represents the extracellular Par-4 induction due to 3-azidoWA could abrogate invasion

3.11 Design and synthesis of novel N,N'-glycoside derivatives of 3,3'-diindolylmethanes as potential antiproliferative agents

Deepak K. Sharma, Bilal A. Rah, Mallikharjuna R. Lambu, Altaf Hussain, Syed K. Yousuf, Anil K. Tripathi, Baldev Singh, Gayatri Jamwal, Zabeer Ahmed, Nayan Chanauria, Amit Nargotra, Anindya Goswami and Debaraj Mukherjee

3,3' Diindolylmethane (DIM), a chemopreventive agent, derived from Brassica food plants (cabbage, broccoli, Brussels sprouts, cauliflower), which could protect against tumorigenesis in multiple organs (forestomach, mammary gland, uterus, liver). It induces Par-4 in L3.6pl and Colo-357 pancreatic cancer cells. DIM induced apoptosis in breast cancer cells occurs through the mitochondrial pathway by inhibiting Akt and NF-κB pathways. 3,3'-diindolylmethane is a strong mitochondrial H^+-ATPase inhibitor, and stimulates mitochondrial reactive oxygen species (ROS) production, which is responsible for p21 upregulation. DIM derived compounds also induce several characteristic markers of ER stress including GRP78 and C/EBP homologous transcription factor (CHOP/GADD153). These stress-related responses are accompanied by upregulation of the death receptor DR5 and activation of extrinsic and intrinsic pathways of apoptosis. Studies have also shown that DIM could inhibit the growth of tumors through the induction of apoptosis and G1 cell cycle arrest in human breast cancer cells and prostate cancer cells.3,3'-Diindolylmethane was found to have low bioavailability, what have limited its possible widespread use. Recent reports show that the highly absorbable microencapsulated formulation of 3,3'-diindolylmethane is in I/III phases of clinical trials for treatment of cervical displasia and prostate cancer. These make the bis-indoles an important class of anticancer chemotherapeutics and potential source of medicinal lead compounds.

In view of the great potential of DIMs as potent chemotherapeutic agents against a wide variety of cancers, the 3,3'-diindolylmethane scaffold has been the subject of synthetic manipulations with the aim of carrying out SAR studies on analogues for anticancer activity. The bioactive analogues of DIM were then glycosylated to improve potency, as the glycosyl component plays a significant role in most of the secondary metabolites isolated from natural sources.

Keeping all these aspects in view, we designed novel analogues of bisindolylmethanes for our present study, bringing in three modifications in the structure: (i) keeping bisindolylalkane as a core and using different electron donating or withdrawing group substituted aryl rings and alkyl groups, (ii) varying the substitution on the aromatic portion of indole, and (iii) using two identical sugar components with both nitrogens of a bisindolylalkane moiety (in contrast to rebeccamycin and staurosporin in which a single sugar component is attached to one or both indoles of an indolocarbazole moiety).

Here we demonstrate the anti-proliferative activities of synthetic derivatives of DIM by MTT assay in three cancer cell lines, A549 (non small cell lung carcinoma), HeLa (cervical cancer cell line), and MCF-7 (breast cancer) as shown in Table 1. Some of the compounds show promising anti-proliferative activity having IC_{50} below 5μmol, with compound **7d** exerting the highest anti-proliferative activity having IC_{50} 1.3μmol on A549, 0.3 μmol on HeLa, and 0.9 μmol on MCF-7 cell lines in comparison to values of 10, 12, 14 nmol respectively noted with positive control staurosporine. Thus, our current investigation strongly underscores the anti-proliferative (Fig. 1 and 3) and anti-metastatic (Fig. 2) role of **7d**, which could induce apoptosis in three different cell lines by upregulating pro-apoptotic protein Par-4 and concomitantly diminishing the expression of pro-survival protein Bcl-2 . The pro-apoptotic potential of intracellular Par-4 was increased in presence of **7d** and triggered apoptosis in all three cell lines. As Par-4 has been found to bind to chaperone protein GRP78, it is tempting to suggest that the excess amount of Par-4 consequent upon **7d** treatment could translocate GRP78-Par-4 into the cell membrane to activate the extrinsic FAS-FADD - caspase-8 pathway (Fig. 4). Interestingly, the docking study (Fig. 5) and western blot analysis revealed **7d** as a more competent blocker of GRP78 and could induce Par-4 better than the other DIM compounds. Thus compound **7d** might exert a dual effect of simultaneous inhibition of GRP78 in the ER lumen and utilizing a pool of Par-4-GRP78 complex to exert apoptotic effects. The therapeutic implication of induction of secretion of Par-4 and downregulation of GRP-78 due to **7d** treatment of diverse cancer cells is currently under investigation (unpublished data). Nevertheless, the compounds of this structural class appear amenable to further modifications and will prove useful for the design of new anticancer agents.

Table 1: Cytotoxic Effects of Compounds 1a-7d on A549, HeLa and MCF7 Human Cancer Cells

Compound	IC_{50} (µmol) [b]		[a]
	A-549	HeLA	MCF-7
1a	40.0 ± 0.436	21.8 ± 0.026	22.2 ± 0.226
2a	7.5 ± 0.010	0.9 ± 0.095	5.5 ± 0.144
2b	9.0 ± 0.100	4.0 ± 0.010	3.5 ± 0.017
2c	8.0 ± 0.100	3.9 ± 0.095	2.8 ± 0.037
2d	10.0 ± 0.265	5.5 ± 0.010	2.3 ± 0.044
2e	100.0 ± 0.100	64.5 ± 0.557	89.0 ± 0.026
2f	100.0 ± 0.100	63.2 ± 0.090	77.5 ± 0.035
2g	12.0 ± 0.265	6.1 ± 0.100	7.8 ± 0.027
2h	10.0 ± 0.608	5.1 ± 0.100	2.8 ± 0.084
2i	25.0 ± 0.361	12.8 ± 0.006	24.9 ± 0.095
2j	5.5 ± 0.100	3.2 ± 0.190	4.1 ± 0.190
2k	8.5 ± 0.200	4.3 ± 0.156	7.1 ± 0.008
2l	8.5 ± 0.100	4.8 ± 0.026	3.5 ± 0.046
2m	5.6 ± 0.010	1.5 ± 0.075	3.2 ± 0.173
2n	5.5 ± 0.020	1.5 ± 0.100	3.1 ± 0.155
2o	6.5 ± 0.044	3.9 ± 0.111	3.6 ± 0.200
2p	3.5 ± 0.095	1.3 ± 0.090	5.5 ± 0.046
3a	8.5 ± 0.017	4.2 ± 0.180	4.0 ± 0.090
4a	>100	>100	>100
4b	>100	>100	>100
4c	>100	>100	22.5± 0.263
4d	12.5 ± 0.010	35.0 ± 0.430	5.8 ± 0.090
5a	>100	>100	23.6± 0.436
5b	>100	>100	27.1± 0.205
5c	>100	>100	23.6± 0.0.158
5d	26.0 ± 0.300	7.0 ± 0.191	2.5± 0.115

6a	24.0 ± 0.100	70.0 ± 0.210	>100
6b	24.0 ± 0.300	70.0 ± 0.150	>100
6c	8.0 ± 0.076	3.5 ± 0.080	>100
6d	17.0 ± 0.070	10.0 ± 0.105	>100
7a	2.7 ± 0.010	32.0 ± 0.173	53.2 ± 0.061
7b	2.5 ± 0.026	27.0 ± 0.046	51.1 ± 0.098
7c	2.4 ± 0.080	30.0 ± 0.165	66.7 ± 0.098
7d	1.3 ± 0.030	0.3 ± 0.015	0.9 ± 0.008

[b]IC50 values are indicated as the mean ±SD of three independent experiments.

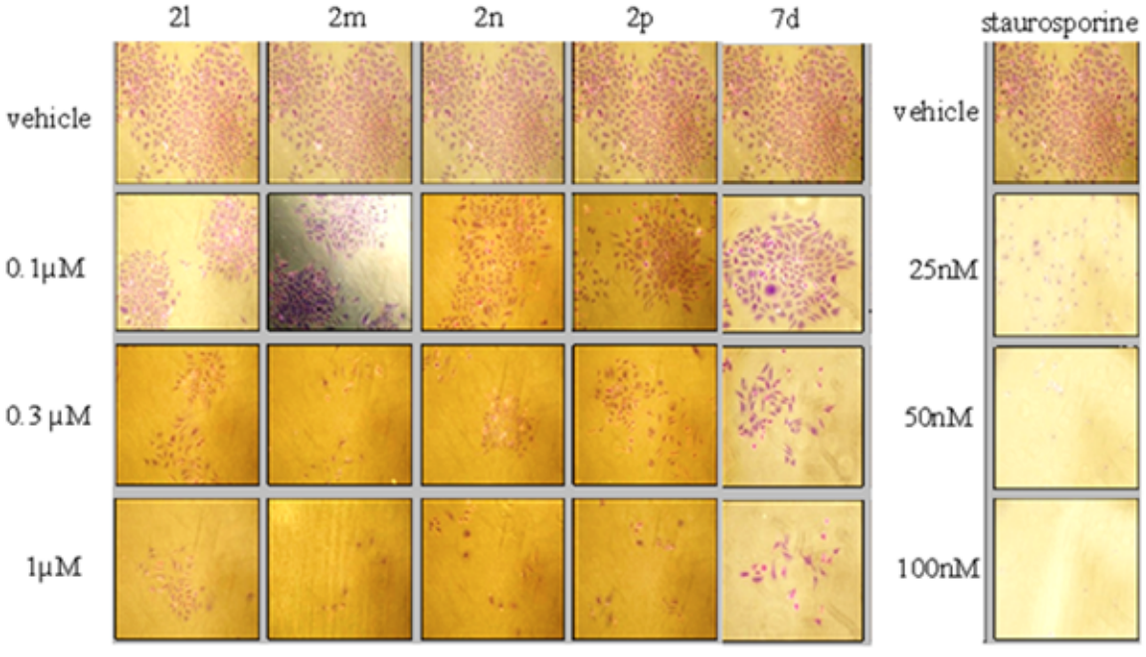

Figure 1: Colony formation inhibition: 1×10^3 HeLa cells were plated in 6-well plate and left treated with vehicle (left first column), or with 0.1 μmol, 0.3 μmol, 1 μmol of **2l**, **2m**, **2n**, **2p**, and **7d** for 5days and then stained with crystal violet. (Magnification x10)

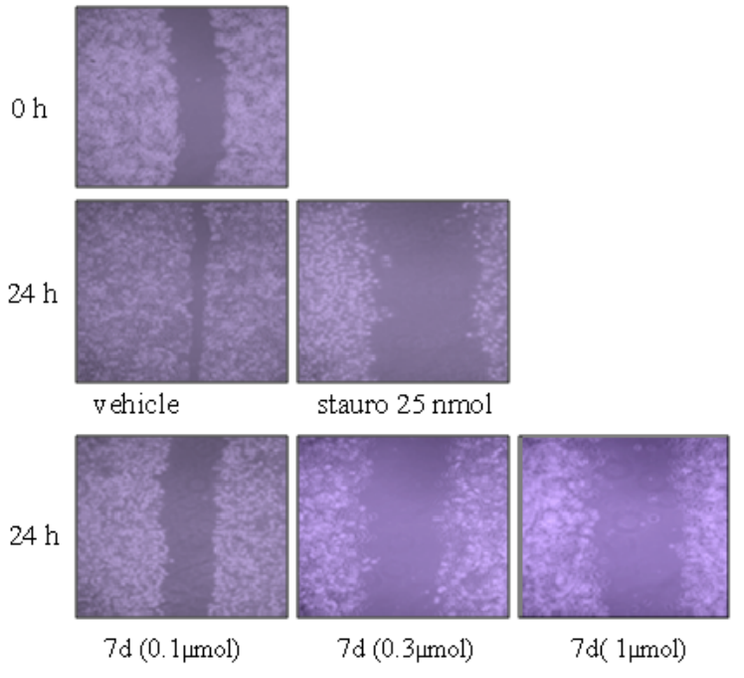

Figure 2: Cells (5.5×10^5) grown to confluence were scratched with a plastic pipette tip (200 μL) to create a wound and then washed to remove detached cells. Compound **7d** (0.1, 0.3, or 1μmol) was added to cultures as indicated. Cultures were photographed at zero h and then subsequently again at 24 h to assess the degree of wound healing (Magnification x10).

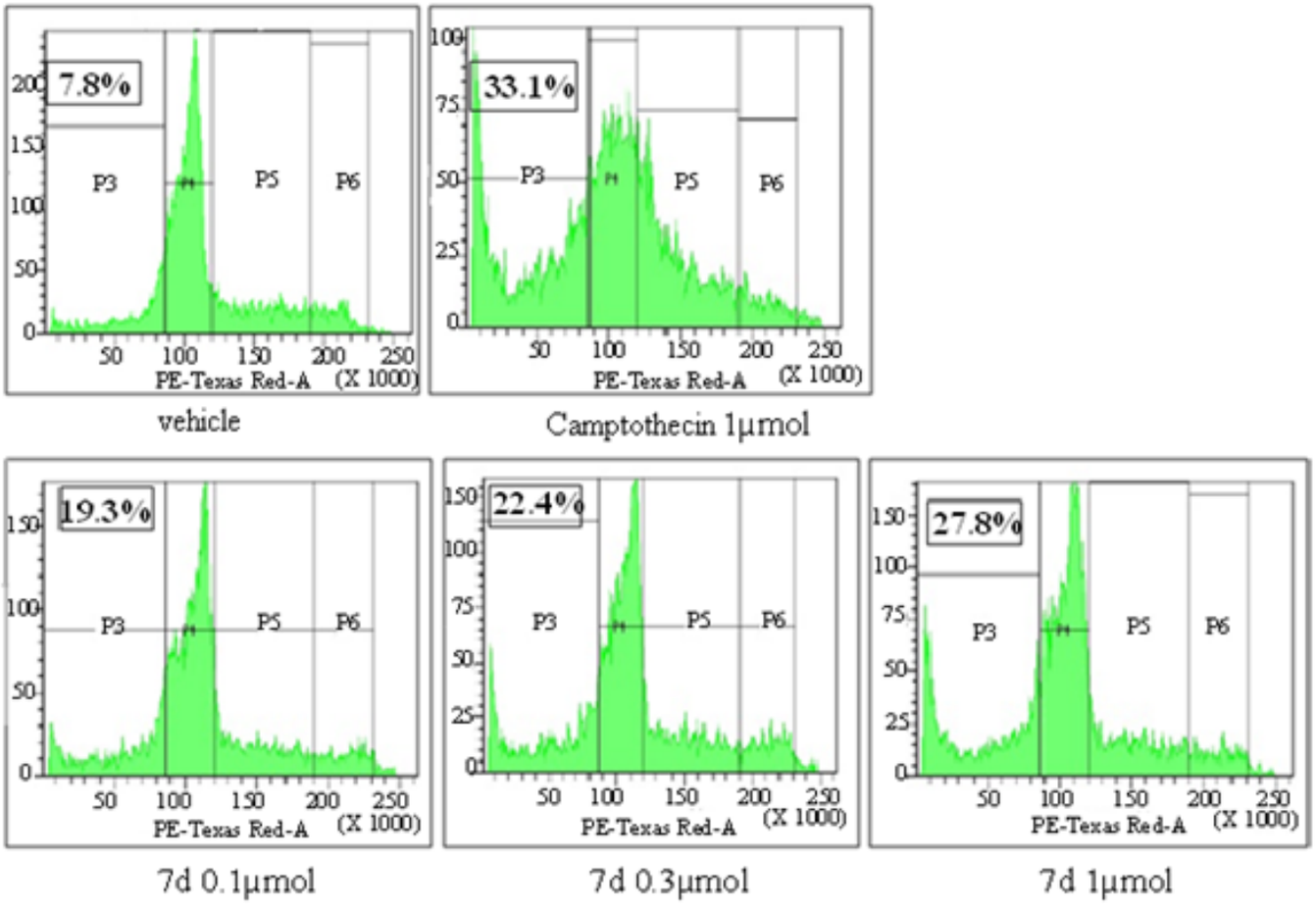

Figure 3: HeLa cells ($5x10^5$) were treated with DMSO vehicle and **7d** (0.1, 0.3, and 1μmol), and subjected to cell cycle analysis for 24 h along with positive control camptothecin. There is significant percentage of cells in sub-G1, which increases with increase in concentration of **7d**.

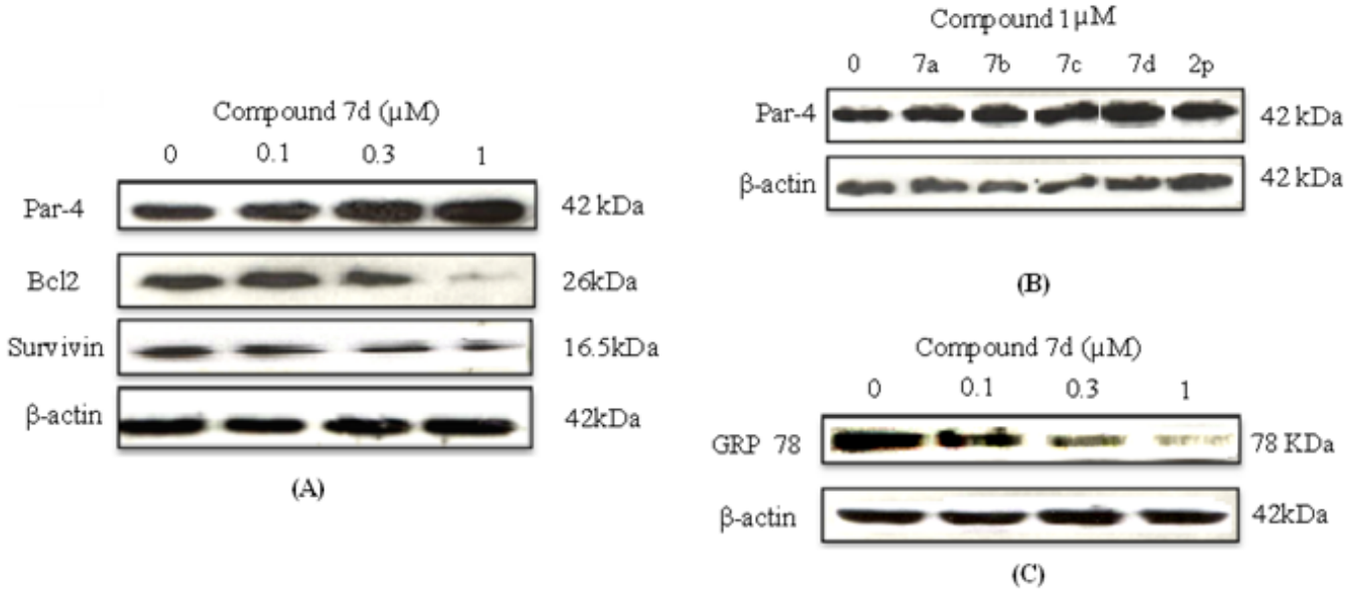

Figure 4: Western blot analysis showed that (A) compound **7d** induces tumor suppressor protein Par-4 and significantly decreases the expression of anti-apoptotic proteins Bcl-2, survivin in dose dependent manner; at 1 μmol concentration, there is almost complete suppression of Bcl-2, (B) comparison of Par-4 induction by 2p and glycoside derivatives at 1 μmol concentration which shows that compound 7d induce Par-4 maximally, (c) compound **7d** decreases the expression of anti-apoptotic proteins GRP-78 in dose dependent manner; at 1 μmol concentration, there is almost complete suppression of GRP-78, in HeLA cell line.

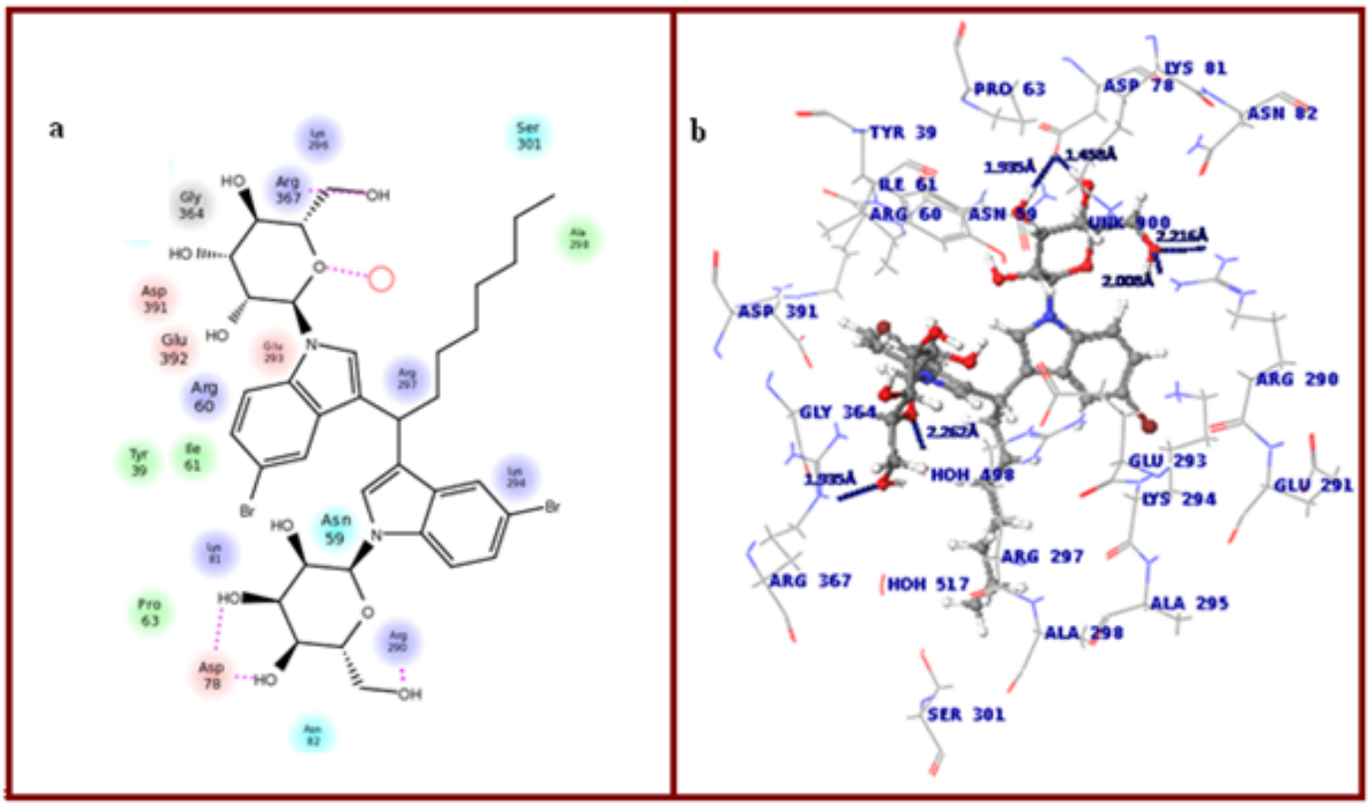

Figure 5: Views of functional motifs of compound **7d** binding with GRP-78 (a, left) and docked inside the GRP-78 binding cleft (b, right).

3.12 A new cytotoxic quinolone alkaloid and a pentacyclic steroidal glycoside from the stem bark of *Crataeva nurvala*: Study of anti-proliferative and apoptosis inducing property

Sadhna Sinha, Priyanka Mishra, Hina Amin, Bilal Rah, Debasis Nayak, Anindya Goswami, Naresh Kumar, Ram Vishwakarma and Sabari Ghosal

Plant secondary metabolites and their semi-synthetic derivatives continue to play an important role in cancer chemopreventive studies. Few anticancer agents amongst a broad arsenal of naturally occurring compounds currently undergoing clinical trials include podophyllotoxin, camptothecin, vinblastine and paclitaxel. Considerable efforts have also been paid to generate promising lead compounds through high throughput screening (HTS) protocols, combinatorial chemistry and bioinformatics tools. However, natural products have an edge as they are evolved for some special biological purpose and exhibit remarkable HTS hit rates, much higher than to be expected. Usually these compounds possess unique built-in chirality which promotes most effective binding to complex proteins and other three-dimensional biological receptors. Hence, the best way to find new leads amid unexplored chemical space is to turn to those natural product scaffolds that are unrepresented. *Crataeva nurvala* Buch. Ham. (Capparaceae), an important medicinal plant of Ayurvedic and Unani system of medicine has been studied mainly with the stem bark part for obstructive and nonobstructive uropathies. It is also used for the treatment of prostate enlargement and bladder sensitivity. Phytochemical studies showed that it contained lupeol, betulinic acid, b-sitosterol, stigmasterol and cabadicine as major chemical constituents of the plant. Lupeol had been reported to reduce the deposition of calcium oxalate, the most common stone forming constituent in animals. It also possessed anticancer, antitumor, anti-Q2 arthritic, anti-inflammatory, hepatoprotective, and cardioprotective activities . In this study we demonstrate that a new cytotoxic quinolone alkaloid (Fig.1 a) and a pentacyclic steroidal Glycoside (Fig.1 b) from the stem bark of *Crataeva nurvala* could block the migration of cervical and prostate cancer cells and prevent their colony formation ability as well.

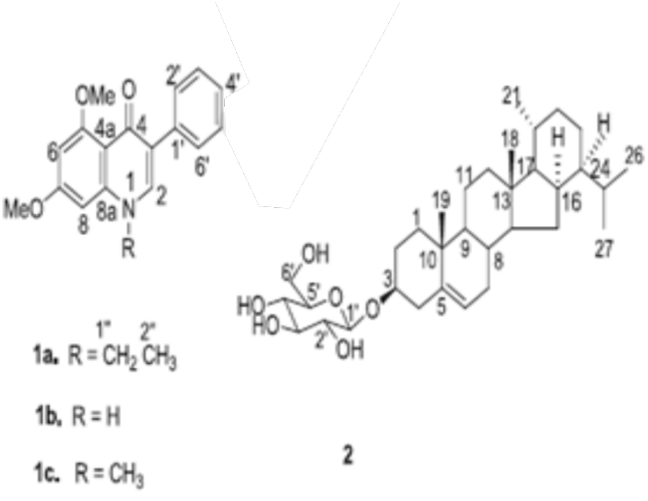

Fig. 1. Chemical structures of crataemine (**1a**), 1-unsubstituted (**1b**) and 1-Me (**1c**) substituted derivatives of **1a** and crataenoside (**2**).

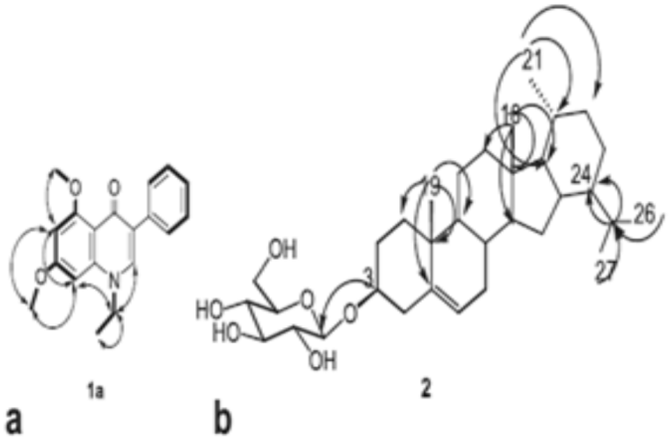

Fig. 2. 2D NMR correlations of **1a** and **2**. (a) Showing HSQC and COSY correlations of **1a** in bold lines and important NOESY correlations by arrows. (b) Showing HSQC and COSY correlations in bold lines and important HMBC correlations by arrows.

Initially, MTT assay was performed to define the optimum concentration at which the compounds were nontoxic to cells. The cancer cells treated with 50 μM concentration of 1a and 80 μM of 2 (IC_{50} values) affect the viability of HeLa and PC-3 (data not shown) cells significantly. To test the effect of 1a and 2 on growth kinetics of cancer cells, colony formation assay were performed in a dose dependent manner as shown in Figs. 3a and 4a respectively. Sub-lethal doses of the compounds decreased colony formation ability of HeLa and PC-3 (data not shown) cells in statistically significant manner ($P < 0.05$). To examine the effect of the compounds on cell migration, wound healing assay was performed on confluent monolayers of HeLa and PC-3 cells. The vehicle DMSO treated cells (control) were able to completely fill in the cleared area, whereas treatment with 50 and 80 μM of 1a and 2 significantly ($P < 0.05$) inhibited the migration of HeLa (Figs. 3b and 4b) and PC-3 (data not shown) cells, thereby reducing their migration capability. The experimental data strongly demonstrated that both 1a and 2 could block the migration of HeLa and PC-3 cells in a dose dependent manner. To further elucidate the underlying mechanism for cytotoxicity of 1a and 2 we performed apoptosis studies on HeLa and PC-3 (data not shown) cells. After treating the cells with different concentrations of the compounds, the percentage of apoptotic cells was assessed by propidium iodide staining, followed by flow cytometric analysis (Fig. 2 c and Fig. 3 c). Interestingly, compounds 1a and 2 observed 76.8% and 63.5% apoptotic cells at 50 μM and 80 μM concentrations compared to 68.6% with 1 μM concentration of positive control camptothecin. By using 4,6-diamidino-2- phenylindole (DAPI) staining we observed that 1a and 2 induced apoptosis in HeLa cells within 24 h of incubation as compared to positive control staurosporine as shown in Figs. 2 d and 3 d respectively. The data indicated the occurrence of early apoptosis with chromatin condensation around the nuclear periphery, accompanied by nuclear size reduction (white arrow heads). Thus, the data provides an anticancer potential of 1a and 2 seems to provide a substantial support for the use of these compounds in cancer therapy.

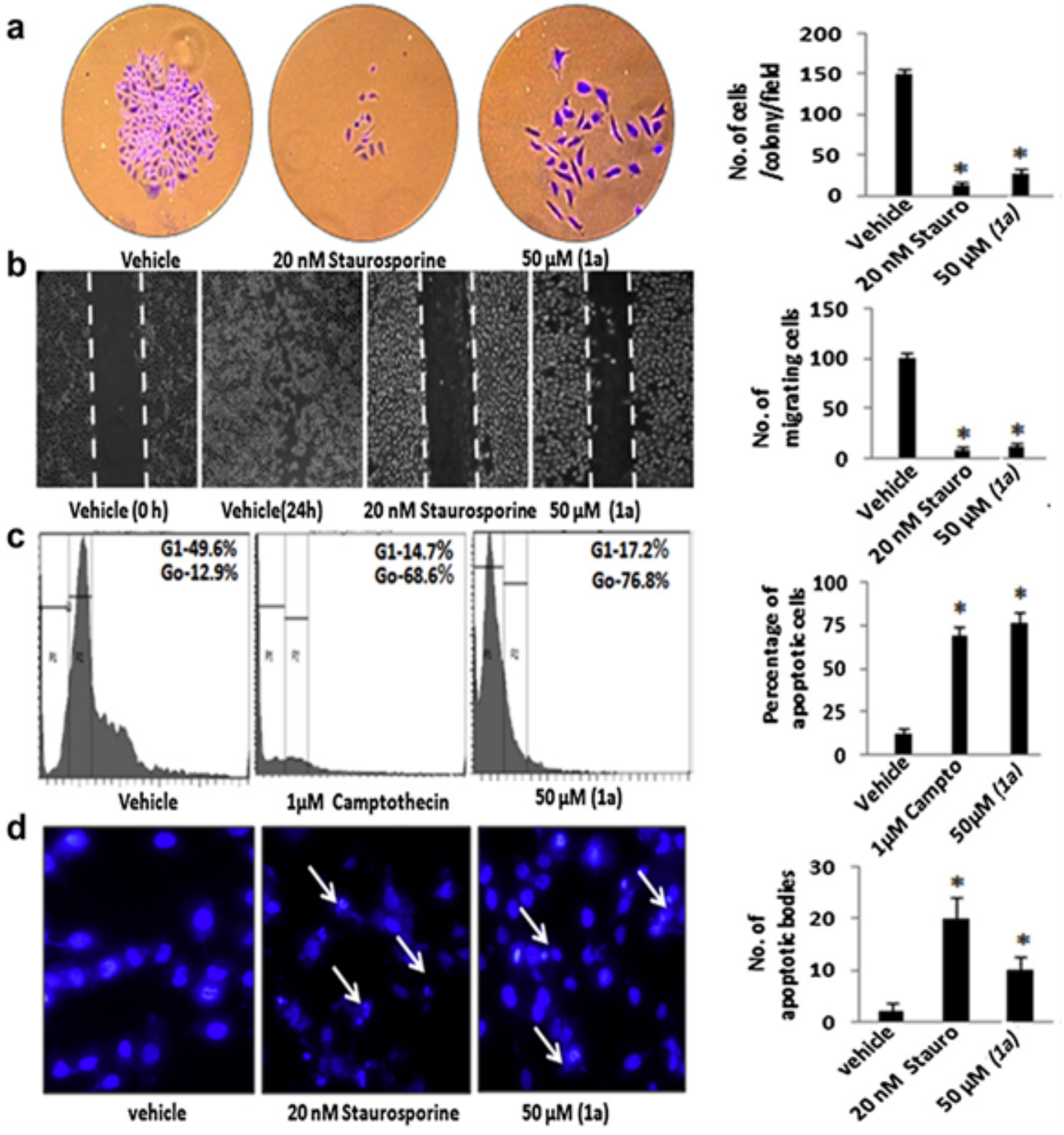

Figure 2: Assessment of cytotoxicity and cell motility of 1a at a concentration of 50 μM along with vehicle DMSO and positive control Staurosporine (25 nM) or Camptothecin (1 μM) against HeLa cells. (a) Colony formation assay was performed with 1 x10^3 cells/well and the number of stained cells per colony was counted randomly and images were captured in100x magnifications under inverted microscope. (b) Wound healing assay (0.5 x10^5 cells/well) to assess the degree of wound healing. The scratched areas were quantified in three random fields in each treatment, and data were calculated from three independent experiments. *P < 0.05 compared with untreated control. (c) Cell cycle analysis to determine cell cycle distribution. Data were calculated from three independent experiments. (d) HeLa cells (5 x 10^4) after fixation were stained with nuclear stain DAPI reagent and were photographed under fluorescence microscope (100x magnification) and data were calculated from three independent experiments. Columns mean; bars SD of three independent experiments. *P < 0.05 compared with untreated control.

3.13 CIA-A new model established/standardized for rheumatoid arthritis in DBA/1mice

Surjeet Singh, G. D. Singh, Anamika Khajuria, V.K. Gupta and R. A. Vishvakarma

Rheumatoid arthritis (RA) is a chronic inflammatory disease that is inadequately treated with currently available drugs. The existing drugs are tested against several mouse models of arthritis which have one or the other advantages or disadvantages. Collagen induced arthritis (CIA) is an autoimmune arthritis model having proven value as a research tool for the study of pathogenic mechanisms and testing new therapies. It is a widely used assay model to address questions of disease pathogenesis and to validate therapeutic targets. It shares several immunological, pathological and genetic features with human RA. In recent years, the CIA model has been instrumental in the testing and development of the new biologically based therapeutics e. g., TNF-α inhibitors. Arthritis is normally induced in mice or rats by immunization with autologous or heterologous type II collagen in adjuvant. Susceptibility to collagen-induced arthritis is strongly associated with major histocompatibility complex class II genes, and the development of arthritis is accompanied by a robust T- and B-cell response to type II collagen. The chief pathological features of CIA include a proliferative synovitis with infiltration of polymorphonuclear and mononuclear cells, pannus formation, cartilage degradation, erosion of bone, and fibrosis. As in RA, pro-inflammatory cytokines, such as tumor necrosis factor alpha (TNFα) , interleukin (IL) -6 and IL-1beta, are abundantly expressed in the arthritic joints of mice with CIA, and blockade of these molecules results in a reduction of disease severity.

DBA/1 mice of 6 to 8 weeks old were used for CIA experiments. All the animals were maintained in the animal house facility of IIIM in accordance to the institutional animal ethics committee. Animals were housed up to five per group per cage under standard conditions of light and temperature and fed with special laboratory feed with water ad libitum. Arthritis was induced by intradermal injection at the base of the tail with 50µL of the emulsion having 1mg/ml of chicken type -II collagen (CII). The emulsion for immunization was prepared by dissolving 2mg/ml of CII in 0.05M acetic acid in cold condition (below 4°C) for 12hr. and then emulsified in an equal volume of complete Freund's adjuvant (Sigma-Aldrich). Booster immunization containing 50µL of CII in incomplete Freund's adjuvant (Sigma-Aldrich) was done on 21 days after the primary immunization. The onset of arthritis appears around day 28 (Fig.1). All the mice were inspected every second or third day after booster and incidence of arthritis was scored as per the arbitrary scoring system i.e., 0 = no evidence of erythema and swelling, 1 = erythema and mild swelling confined to tarsals or ankle joint, 2 = erythema and mild swelling extending from the ankle to the tarsals, 3 = erythema and moderate swelling extending from ankle to metatarsal joint and 4 = erythema and severe swelling encompass the ankle, foot and digits, or ankylosis of the limb (Fig. 2). Drug treatment was given to the animals for four to twelve weeks and the animals were evaluated for their arthritic score twice in a week. The % change in the arthritic score was observed in comparison to the diseased control.

DBA/1 mice developed gradual onset of CIA after immunization with CII in CFA and booster with CII and IFA. For the evaluation of anti-arthritic effect three standard drugs viz., dexamethasone (10mg/kg p.o.) ibuprofen (100mg/kg p.o.) and rofecoxib (10mg/kg p.o.) were administered to the diseased animals from the day of the appearance of the signs of disease to eight weeks. The incidence of the arthritis was observed as per the arbitrary scoring system given in the methodology. All the animals were scored individually and mean ± SE was calculated of the individual group. Percent change was calculated in comparison to the control group.

The objective of the study was to establish and standardize the CIA model in the DBA/1 mice. As per our observations and the experimental data we have achieved the objective i.e., the establishment / standardization of the CIA model in the DBA/1 mice. The development of the disease in the animals indicates the establishment of the disease and the effect observed with the standard drugs (Fig. 3) signifies the standardization of the assay model for the screening of the identified molecules for this particular target.

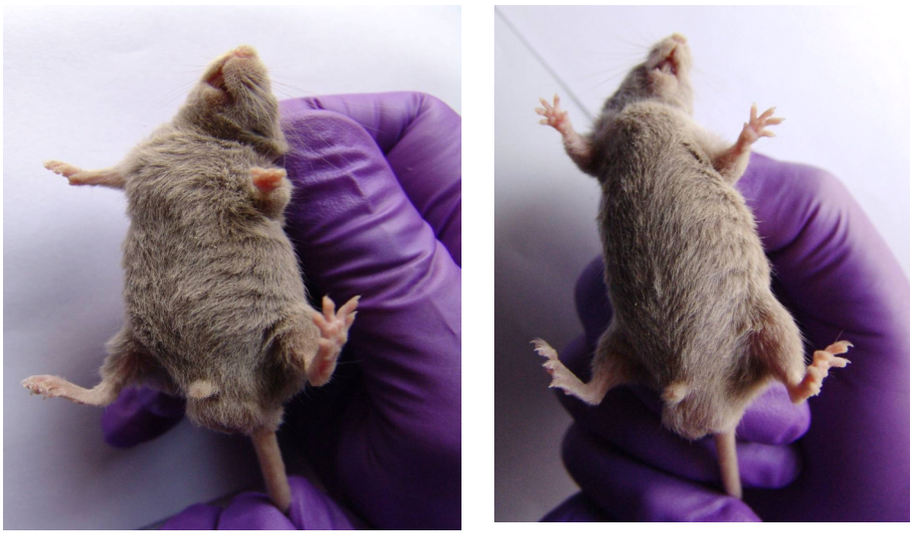

Diseased control

Normal Control

Figure 1: DBA/1 mice showing the collagen induced arthritis development in fore and hind limbs

Arthritic hind limb

Arthritic fore limb

Normal hind limb

Normal fore limb

Figure 2

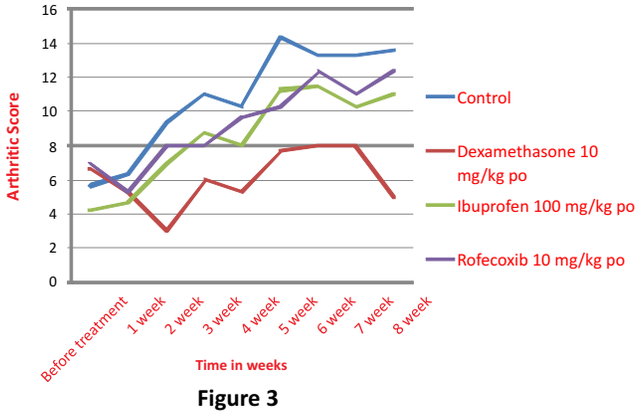

Figure 3

3.14 Screening of compounds on pro-inflammatory cytokine and immunomodulatory activities

Anpurna Kaul, Jasvinder singh, Amit Kumar, Shagun and A.K Saxsena

Thirty four plant extracts were screened on humoral and cell mediated immune response by haemmagglutinating antibody titre and delayed type hypersensitivity response to assess B-lymphocytes and T-lymphocytes in comparison to cyclosporine, cyclophosphamide and Levamisole (standards) in Balb/c mice .

Screened ninety two compounds by MTT Assay in spleenocytes of Balb/c mice to determine the cytotoxicity and cell viability in comparision with LPS and Con A.

Twenty five compounds were put for IL- 8 screening in THP-1 cell line (Tables 1 & 2). IL-8 interleukin is a member of a family of structurally -related low-molecular weight, It is produced by stimulated monocytes and is called as pro - inflammatory cytokine. It is an important mediator of the immune reaction in the immune response and an important chemoattractant for neutrophils respectively.

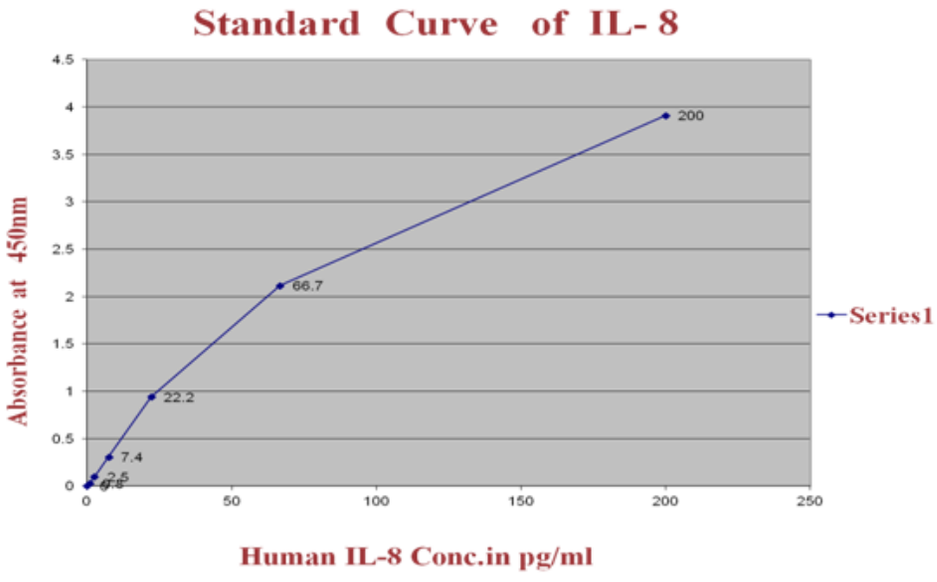

Test Compound	LPS	Dexa	Test Comd	Suppression
	ug/ml	nM	(uM)	(%)
Control				-
LPS	10			-
LPS + DEXA	10	50		90.22
KPK-83-AS-107	10		100	98.29
KPK-83-AS-109	10		100	97.07
KPK-83-AS-113	10		100	99.27
KPK-83-AS-116	10		100	96.33
KPK-83-AS-117	10		100	96.58
KPK-83-AS-105	10		100	90.22
KPK-83-AS-106	10		100	73.59
KPK-43-AVS-217	10		100	45.23
KPK-43-AVS-230	10		100	59.41
KPK-43-AVS-166	10		100	38.14
KPK-43-AVS-176	10		100	56.97
KPK-43-AVS- 47	10		100	79.22
KPK-43-AVS-157	10		100	87.53
KPK-43-AVS-218	10		100	97.56
KPK-27-VRK-204	10		100	91.69

Table 1: IL-8 secretion in LPS stimulated THP-1 cell line

Table 2: IL-8 secretion in LPS stimulated THP-1 cell line

Test Compound	LPS	Dexa	TestComd	Suppression
	ug/ml	nm	(uM)	**(%)**
LPS	10			-
LPS + DEXA	10	10		46.15
KPK/27/VRK/117	10		100	57.00
KPK/68/SSR/135	10		100	95.38
KPK/68/SSR/107	10		100	87.34
KPK/43/AVS/43	10		100	72.74
KPK/43/AVS/171	10		100	54.19
KPK/43/AVS/45	10		100	91.16
KPK/43/AVS/46	10		100	91.36
KPK/43/AVS/49	10		100	92.90
KPK/43/AVS/53	10		100	69.19
KPK/43/AVS/54	10		100	79.30

Twenty five (25) compounds were put for IL-8 screening. Four compounds have shown maximum suppression in LPS stimulated THP – 1 cell line .

4. DISCOVERY INFORMATICS

4.1 Computational studies on PI3K-α

Priya Mahajan, Amit Nargotra, Thanush Tatikonda, Parvinder Pal Singh and Ram Vishwakarma

There is a great deal of interest in PI3Ks as cancer targets, particularly for the p110α isoform which is mutated and/or over-expressed in more than 30% of tumours. Based on the availability of 3D crystal structure information of PI3Kα along with co-crystallized ligands/inhibitors, computational studies were carried out for this target in order to design novel PI3Kα inhibitors involving computer aided drug design approach. In order to validate the docking protocols in use at IIIM, several known inhibitors of PI3K-α were sketched and prepared for docking on to the 3D crystal structure of the target protein (i.e., PI3K-α). Several docking algorithm such as Standard Precision (SP)-alone, SP with expanded sampling, Extra Precision (XP)-alone, XP with expanded sampling etc. were used for docking. This was combined with different scoring functions and protein flexibility criteria. Finally, SP docking with expanded sampling and protein flexibility at 8Å was selected as the best, where in the actives were separated from the in-actives with minimum false positives.

Further, with the inputs from medicinal chemistry division, following class of compounds were taken for the docking studies on Pi3Kα :-

i. Imidazoquinoline analogs (NVP-BEZ235) - The parent compound being from Novartis, and the first PI3K inhibitor to enter the clinical trials.

ii. Liphagal analogs - Liphagal was first selective inhibitor of PI3Kα.

iii. Tetrazolyl Quinazolinone analogs (CAL-101) - The parent compound showed promising Phase I results and presently is in early Phase – II clinical trials.

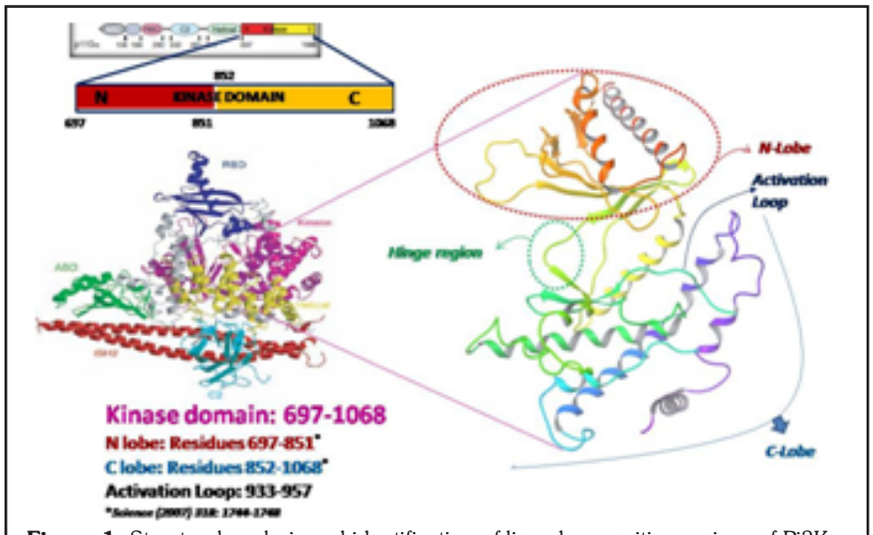

Figure 1: Structural analysis and identification of ligand recognition regions of Pi3K-α.

Docking studies on the above mentioned series were carried out in order to identify the better binders/inhibitors of PI3Kα. The interaction of the best analog of BEZ235 series showed the involvement of hinge region residue Val851 in H-bonding with the ligand, apart from Ser774 and Ser854. The extra stability to the ligand is proposed to be provided by the hydrophobic cleft formed by the residues Trp780, Leu807, Tyr836, Ile848,Val850, Val851, Met922, Phe930, Ile932 and Phe934 with Trp780 and Tyr836 also involved in π-π interaction with the ligand as shown in Figure 2a. For the other two series, it was observed that the introduction of boron helps in improving the binding affinity and hence the inhibitory activity of PI3Kα.

The overall inference based on the docking results could be summarized as under:

- The hinge region (Val851) plays a major role for the identification and binding of ATP competitor inhibitor.
- Besides this, Tyr836, Gln859 also plays an important role.
- The role of aldehyde moiety in liphagal was also identified from its interaction, where Gln859 is directly involved in H-bonding with the formyl group of liphagal.
- Allosteric site is proposed to be nearby the ATP binding site, but the effective residues are still not clear.

The interaction figures of the best binding compounds from the above mentioned series are shown in Figure 2.

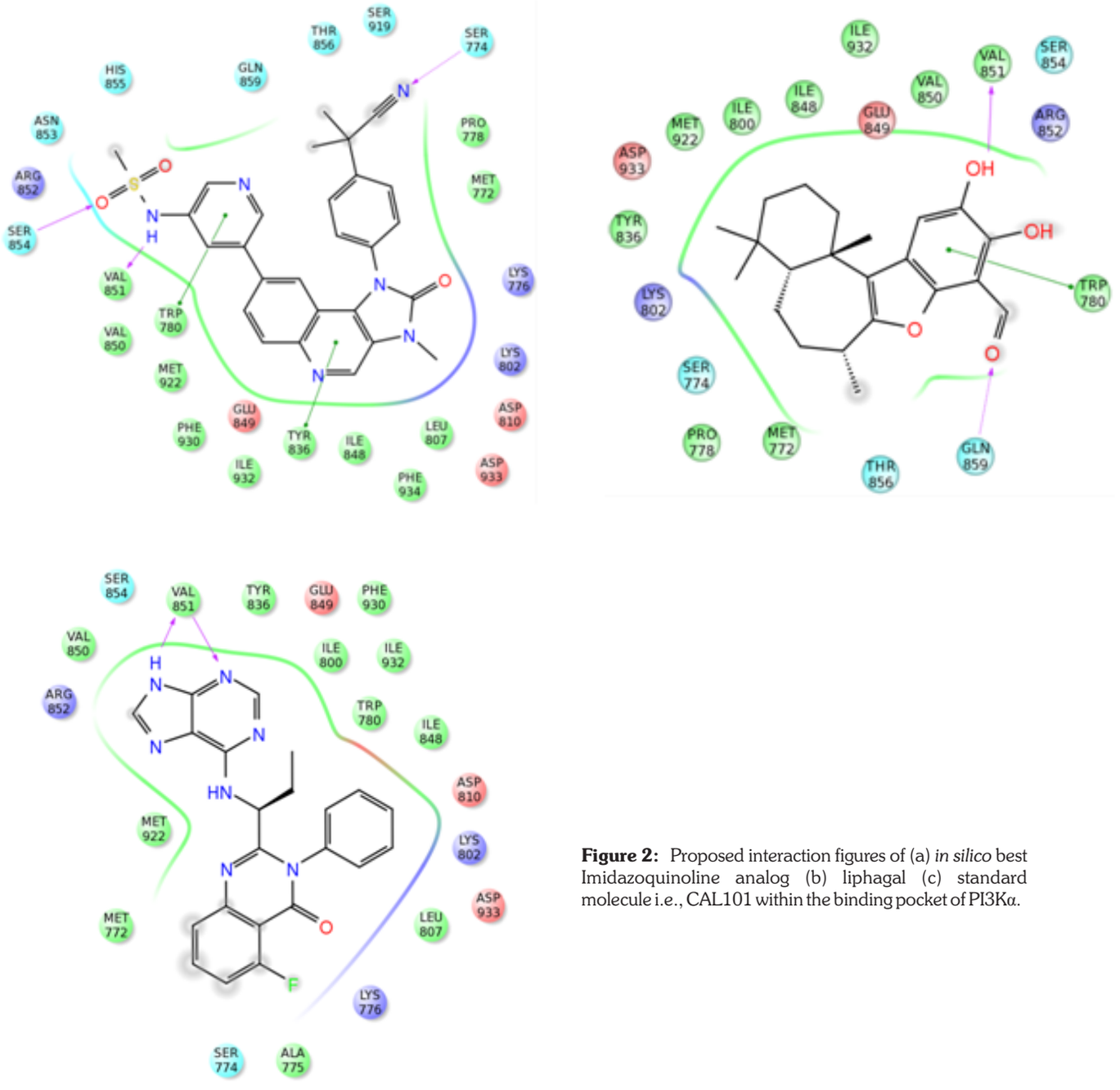

Figure 2: Proposed interaction figures of (a) *in silico* best Imidazoquinoline analog (b) liphagal (c) standard molecule i.e., CAL101 within the binding pocket of PI3Kα.

4.2 Development of theoretical Model for lead optimization of PI3K-α inhibitors

Priya Mahajan, Amit Nargotra and Ram Vishwakarma

In order to customize the generic software Schrodinger for the target Pi3K-α, a quantitative regression analysis was carried out between the experimental IC_{50} values of the known inhibitors (from literature) and the scoring functions used for their docking analyses with the selected target (PI3K-α). A data set of 65 molecules was taken for this study which was suitable divided into training set data and test set data. A highly statistical model was prepared for the theoretical evaluation of the inhibitory activity of a new molecule towards PI3K-α. The final model equation is as under:-

Activity = 11.06 -1.96 *r_glide_res:A836_dist + 1.45 *r_glide_XP_lipophilic Evd W- 1.22 * r_glide_res:A856_Vdw - 0.46 * r_glide_res: A854_Eint -0.13 * r_i_glide_ecoul +0.82 * r_glide_res: A932_dist -2.37 * r_glide_res:A 930_vdw+3.33 * r_glide_res:A 836_h bond

The model along with dock scores and interaction studies (of ligand with target) will also help in lead optimisation and would contribute towards the identification of a novel PI3K-α inhibitor.

4.3 Molecular docking studies of merioline analogs on CDK2

Priya Mahajan, Amit Nargotra, Umed Singh, Parvinder Pal Singh and Ram Vishwakarmaz

Meriolin is reported in literature as potent CDK inhibitor. Attempts have been made to prepare its more potent analogs by combining the common features of Variolin B and the meridianin family of natural products (known CDK inhibitors). These analogues, thus prepared, were docked on the 3D crystal structure of CDK2, and the binding region analyzed. The surface analysis of the binding site was also carried out in order to ascertain the space within the binding pocket for introduction of the functional moieties that can be substituted on the identified scaffolds (Fig. 3).

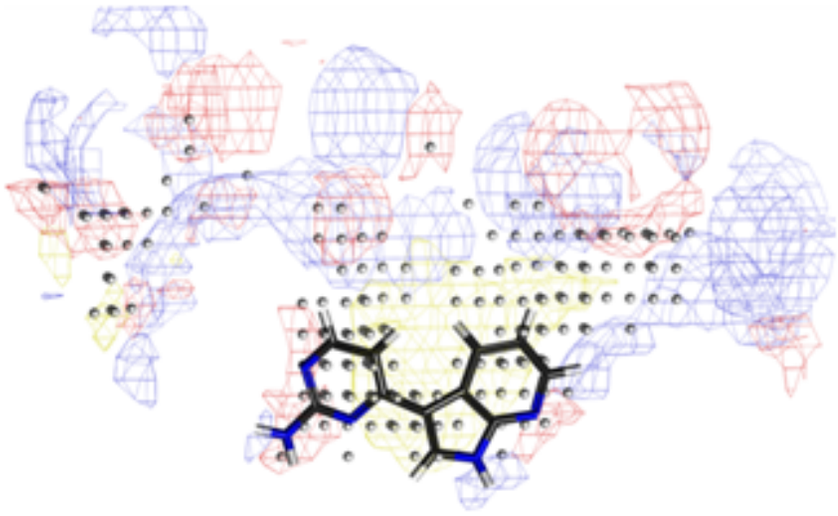

Figure 3: Binding site surface analysis of CKD2 w.r.t the molecule meriolin (seen docked) within the binding pocket. Yellow indicates hydrophobic group, blue indicates donor group and red indicates acceptor group.

Besides this, a virtual library around the selected scaffold was created by using the computational tools, which was also docked on CDK2. These compound libraries were rank ordered based on dock scores and binding energies. The top few scoring compounds thus identified, were submitted to the medicinal chemistry division for their synthesis and subsequent bio-evaluation studies.

4.4 Computational studies on *Mycobacterium tuberculosis* bacterial efflux pump Rv1258c (Linkage: OSDD project HCP001)

Rukmankesh, Amit Nargotra, Inshad Ali Khan and Surrinder Koul

Earlier we had predicted the 3D structure of Rv1258c and docked with piperine. The structure was further refined using multi-template modeling and docking studies of piperine, active compounds (synthesized by BOC and evaluated at Clinical Microbiology) and the known first line and second line anti-TB drugs was carried out on the proposed 3D structure. In order to get a reliable model, several online servers were used for modeling the structure of Rv1258c. A total of 48 models were built from the various selected servers. In order to filter out some poorly constructed model a filter criterion was set where the value for bad contacts was set at zero and RC core value was set more than 85%. Based on the set threshold value of 'bad contacts' and 'RC core', a total of 17 models were selected.

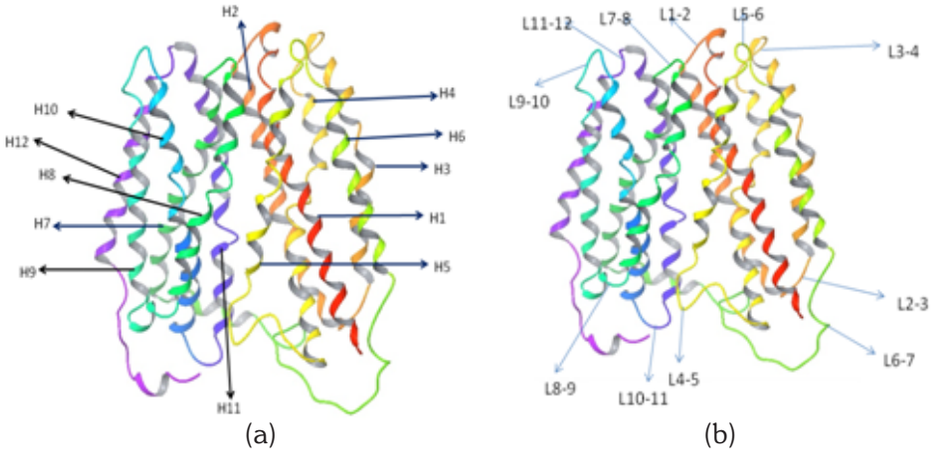

Figure 3: Predicted 3D structure model of Rv1258c. (a) the transmembrane helices numbered from 1 - 12 and (b) the loops interspersed by these helices.

The templates selected for modeling were 1PW4, 1PV6, 2GFP, 2CFQ, 2VCH, 2CFP, 307P, 2V8N, 1PV7. Out of these 1PW4, 1PV6, 2CFQ and 2GFP are the 3D structures of the transporters from the Multi Facilitator Superfamily (MFS), which gives more robustness to our predicted models based on the functional aspect. The final model consists of 12 transmembrane helices which is common in all MDR efflux pumps. The model alongwith the description of helices and loops is shown in fig.4.

Based upon the information from the template structures, it was observed that the binding location of the substrate lies within the centre of the main hydrophobic cavity at a similar distance from the central helices. Similarly, the binding site of the predicted structure was identified for molecular docking studies of Rv1258c. based on the docking studies, a specific orientation (central to the active site core) of the ligand within the binding pocket was observed for active molecules, which was not there in the inactive ones where the binding is towards the periphery (Fig. 5). Also, it was observed that among the first line and second line drugs, apart from rifampicin, amikacin also showed very good binding to the efflux pump. This observation has been passed on to the BOC and Clinical Microbiology for further evaluation and validation at their end.

The predicted structure was also used for docking studies of reserpine, a known inhibitor, and piperine. The figure showing the interaction of piperine with Rv1258c revealed that it is involved in H-bond interaction (2.06A°) with Arg141 to form a protein–ligand complex (Fig. 6a). Furthermore, the 1,3-dioxol ring of the piperine molecule is surrounded by Leu55, Leu56, Gln342 and His343 residues at a favourable distance (all ⩽ 3 A°) for H-bonding, thereby providing more stability to the ligand in the pocket (Fig. 6b). Additionally, piperine and the heterocyclic ring of His343 are seen to be favourably oriented to interact with a π-π interaction between the two.

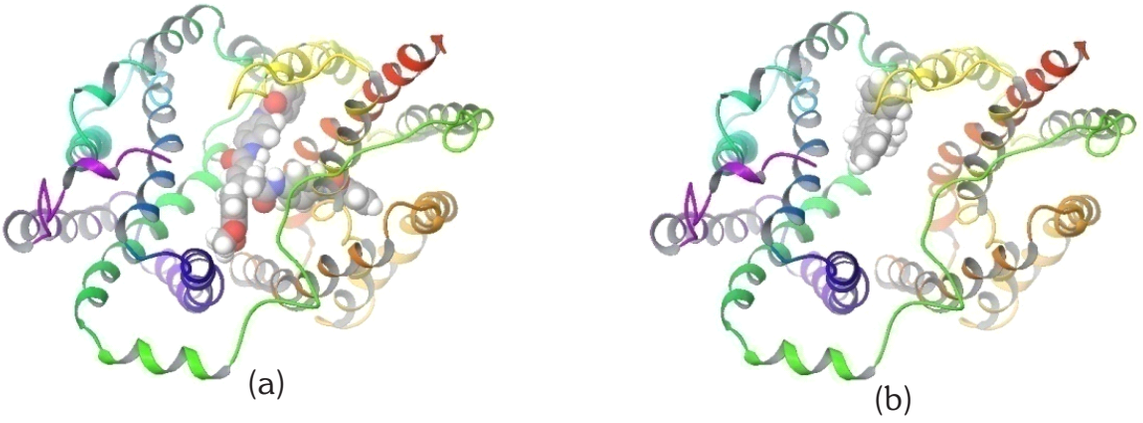

Figure 5: Binding location of an (a) active and an (b) in-active compound onto the predicted 3D structure of bacterial efflux pump Rv1258c. The active compound binds at the central cavity and completely blocks the passage, whereas the in-active one is bound towards the periphery.

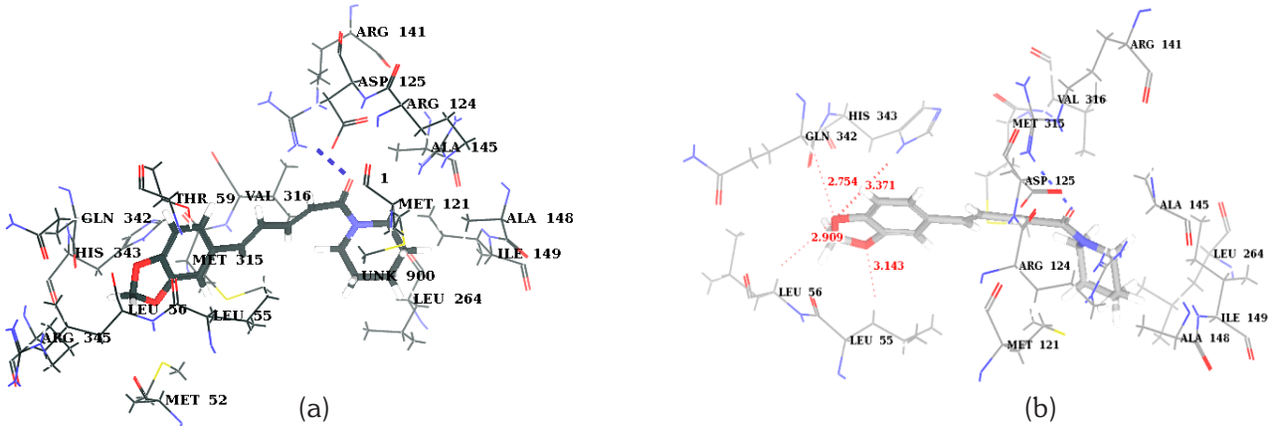

Figure 6: (a) Interaction of piperine within the identified binding pocket of Rv1258c. (b) The encircling of the 1,3-dioxol ring with Leu 55, Leu 56, Gln 342 and His 343.

4.5 Web-enabled database of Institutional compound repository

Monika Gupta, Amit Nargotra, Naresh Satti and Ram Vishwakarma

For any drug discovery programme, a repository of compounds is very essential. The IIIM compound repository comprise of the following:-

i. Natural product library of IIIM

ii. Synthetic compound library of IIIM

iii. Procured drug like compounds from external sources

A web-enabled database of all these libraries has been developed with sub-structural search facility for the user. The database contains the entire information about the compound such as name of depositor, purity profile, quantity available, HPLC data, date of submission etc. A coding system has been incorporated in order to distinguish the compound based on the type of library (internal or external, natural product or synthetic compound etc.). The external library comprising of 50,000 compounds, has been selected after applying several drug like filters on the large collection of Chembridge and Chemdiv Inc. The internal compound library at present contains more than 1000 compounds comprising of equal number of natural products and synthetic compounds. The number is growing at a considerable pace (Fig. 7).

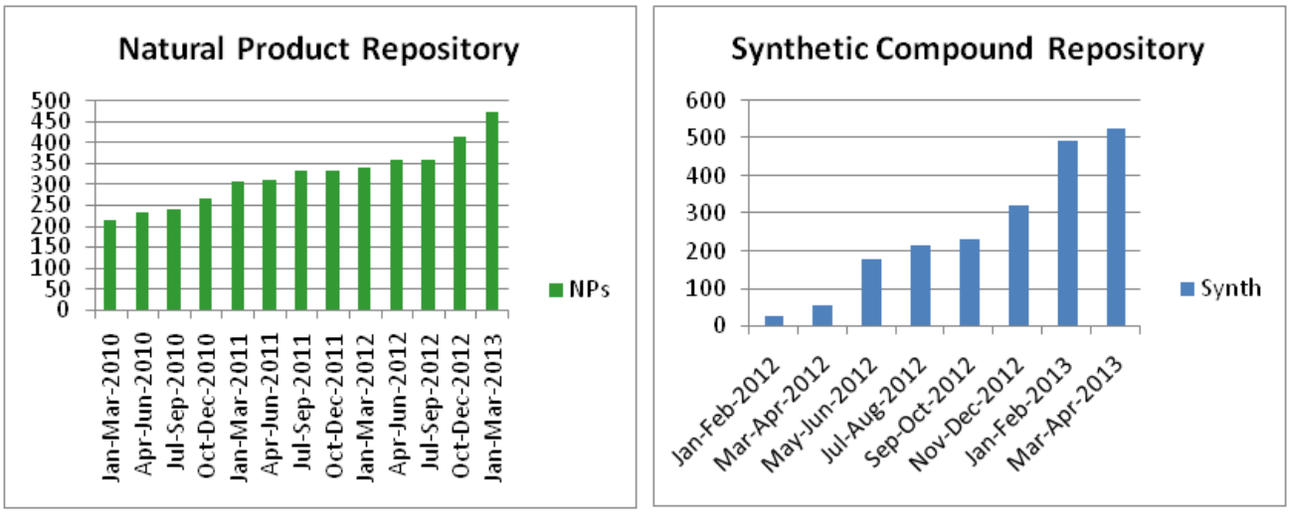

Figure 7: Institutional compound repository status (internal) of (a) natural product repository and (b) synthetic compound repository since its inception at IIIM.

5. NATURAL PRODUCT CHEMISTRY

5.1 Modulation of LPS induced inflammatory response by Lawsonyl monocyclic terpene from the marine derived *Streptomyces* sp.

Asif Ali, Anamika Khajuria, Tabasum Sidiq, Ashok Kumar, Narsinh L. Thakur, Deepak Naik and Ram A. Vishwakarma

Lawsonone (1), a novel Lawsonyl derivative isolated from marine-derived bacteria Streptomyces sp. was evaluated for its potent immunosuppressive activity on immune system. The effect of Lawsonone (1) was elucidated on the immune cells (splenocytes and macrophages) collected from BALB/c mice. Study was carried out to find the effect of Lawsonone (1) on Con-A and LPS stimulated splenocyte proliferation, LPS-induced NO, IL-1β, IL-6 and TNF-α production in macrophages. Furthermore, the effect of Lawsonone (1) on T-cell subsets (CD4 and CD8) and total B-cell (CD19) population was analysed by flow cytometry (Fig.1). Taken together, the present results suggest that Lawsonone (1) may act as a potent molecule for immunosuppression and anti-inflammation, supporting its immunopharmacologic application to modify the immune system.

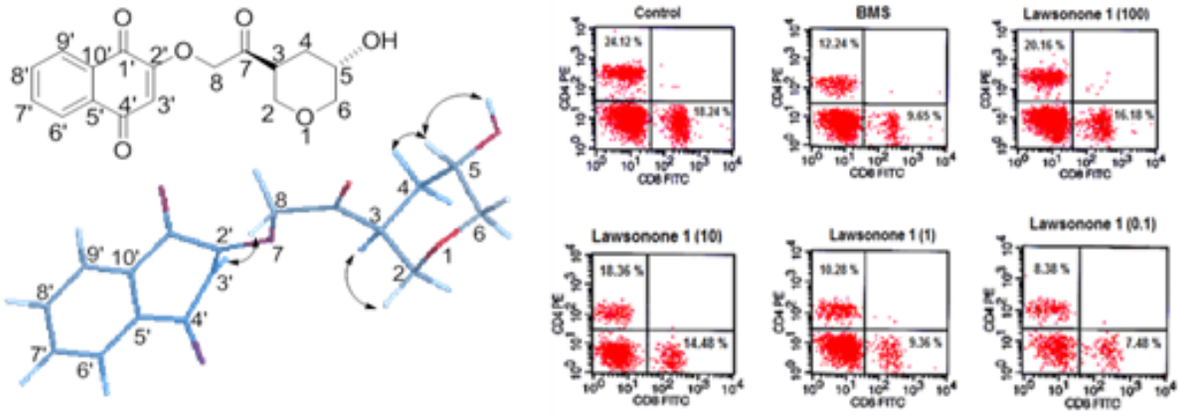

Figure 1: Key NOESY correlations and flow cytometric analysis of splenocytes from BALB/c mice treated with variable doses of Lawsonone **1**.

5.2 Bioactive metabolites from an endophytic *Cryptosporiopsis* sp. inhabiting *Clidemia hirta*

Mahesh K. Zilla, Masroor Qadri, Anup S. Pathania, Gary A. Strobel, Yedukondalu Nalli, Sunil Kumar, Santosh K. Guru, Shashi Bhushan, Sanjay K. Singh, Ram A. Vishwakarma, Syed Riyaz-Ul-Hassan and Asif Ali

An endophytic *Cryptosporiopsis* sp. was isolated from *Clidemia hirta* and analyzed for its secondary metabolites that lead to the isolation of three bioactive molecules. The compounds were purified from the culture broth of the fungus and their structures were determined by spectroscopic methods as *(R)-5*-hydroxy-2-methylchroman-4-one (1), 1-(2,6-dihydroxyphenyl) pentan-1-one (2) and (Z)-1-(2-(2-butyryl-3-hydroxyphenoxy)-6-hydroxyphenyl)-3-hydroxybut-2-en-1-one (3) Fig. 2. Compound 1 exhibited significant cytotoxic activity against the human leukemia cell line, HL-60 with an IC_{50} of 4 μg/ml. This compound induced G2 arrest of the HL-60 cell cycle significantly. In addition, out of these compounds, 2 and 3 were active against several bacterial pathogens. Compound 2 was active against *Bacillus cereus*, *Escherichia coli* and *Staphylococcus aureus* with IC_{50} values varying from 18-30 μg/ml, and compound 3 displayed activity against *Pseudomonas fluorescens* with an IC_{50} value of 6 μg/ml.

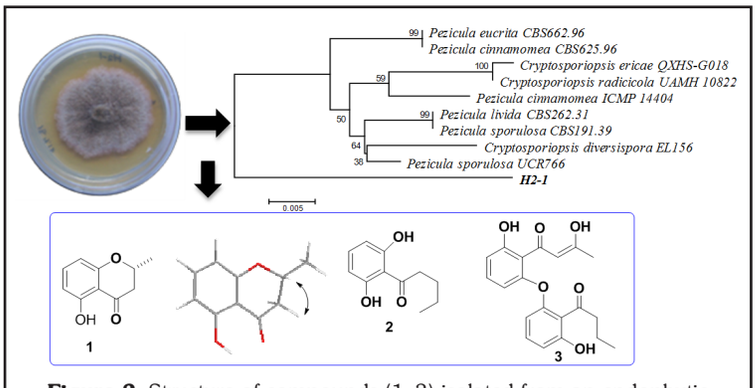

Figure 2: Structure of compounds (1–3) isolated from an endophytic *Cryptosporiopsis sp.* H2-1, inhabiting *Clidemia hirta*.

Compounds 2 and 3 are novel whereas compound 1 was reported earlier but the stereochemistry of its C-2 methyl is established for the first time.

5.3 Anticancer potential of flavonoids isolated from stem bark of *Erythrina suberosa* through induction of apoptosis and inhibition of STAT signaling pathway in human leukemia HL-60 cells

Sunil Kumar, Anup Singh Pathania, A.K. Saxena, Mohammad Arif, R.K. Thappa, R.A. Vishwakarma, Asif Ali and Shashi Bhushan

We have isolated four known distinct metabolites designated as α-Hydroxy erysotrine, 4'-Methoxy licoflavanone (MLF), Alpinumisoflavone (AIF) and Wighteone from *Erythrina suberosa*. Among four metabolites the two flavonoids, MLF and AIF were found to be the most potent cytotoxic activity with IC_{50} of ~20μM in Human leukemia HL-60 cells. Here we first time report the anticancer and apoptotic potential of MLF and AIF in HL-60 cells. Both MLF and AIF inhibited HL-60 cell proliferation and induce apoptosis as measured by several biological end points. MLF and AIF induce apoptotic bodies' formation, enhanced annexinV-FITC binding of the cells, increased sub-G0 cell fraction, loss of mitochondrial membrane potential ($\Delta\psi_m$), release of cytochrome c, Bax, activation of caspase-9, caspase-3 and PARP (poly ADP ribose polymerase), cleavage in HL-60 cells. MLF and AIF also increase the expression of apical death receptor, Fas, with inhibition of anti-apoptotic protein Bid. In spite of apoptosis these two flavonoids significantly inhibit nuclear transcription factor NF-κB and STAT (Signal Transducer and Activator of Transcription) signalling pathway, which are highly expressed in human leukemia. The present studies provide an insight of molecular mechanism of cell death induced by MLF and AIF in HL-60 cells which may find usefulness in managing and treating human leukemia.

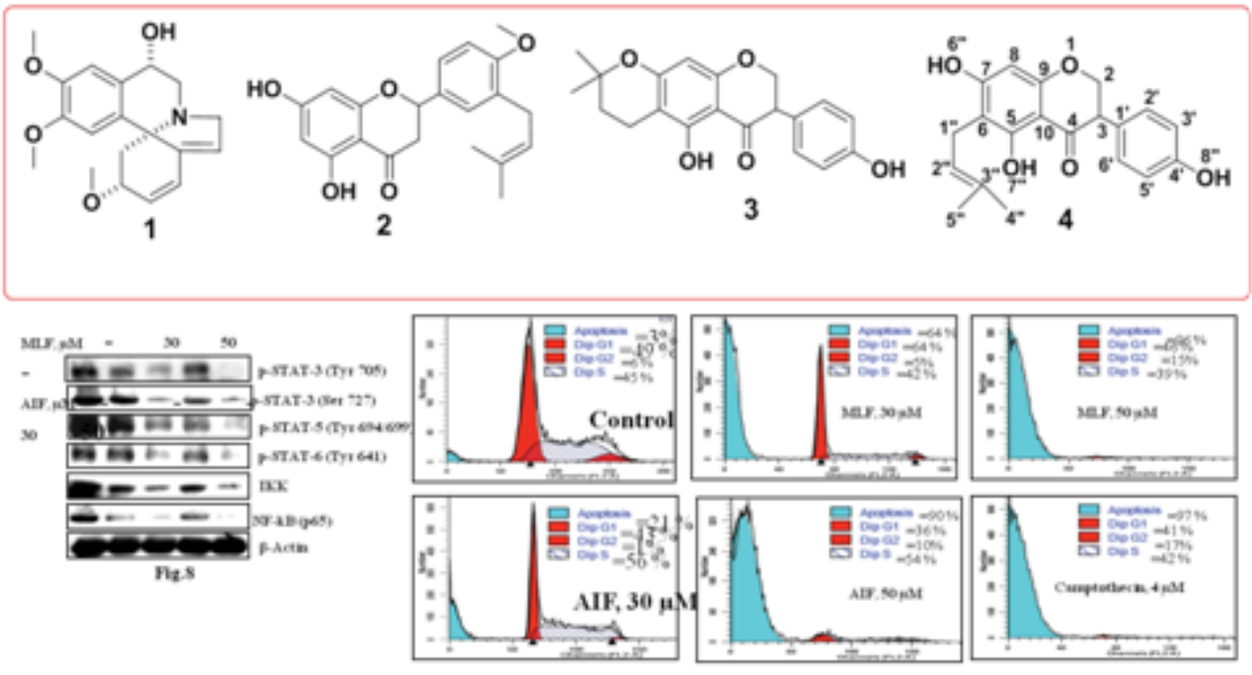

Fig.8

5.4 Extraction and isolation of chemical constituents of RJM/0010

N.K.Satti, Prabhu Dutt and Baldev Singh

The chemical investigation of the stem extract of RJM/0010 has resulted in the isolation of ecdysterone, tinosporoside, TC-1(2β,3β:15,16-Diepoxy-4α, 6β-dihydroxy-13(16),14-clerodadiene-17,12:18,1-diolide), Cordifolioside A (β-D-Glucopyranoside,4-(3-hydroxy-1-propenyl)- 2,6-dimethoxyphenyl 3-O-D-apio-β-D-furanosyl), -Sitosterol glucoside and 1-Octacosanol and chemical structures have been established by spectral analysis.

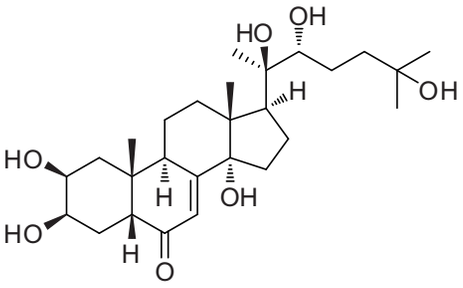

Ecdysterone

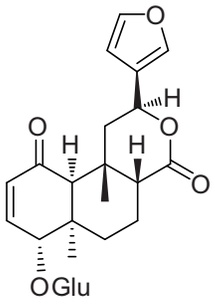

Tinosporoside

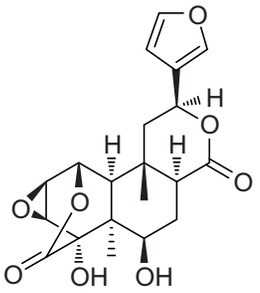

TC-1

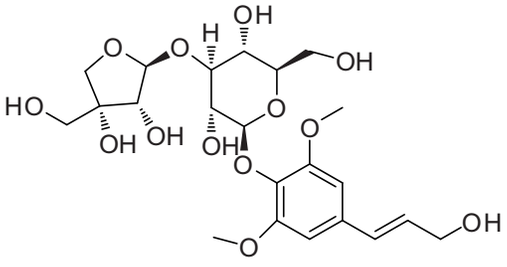

Cordifolioside A

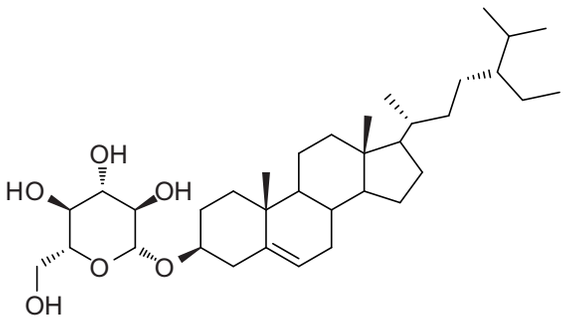

β-Sitosterol glucoside

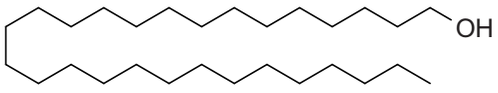

1-Octacosanol

5.5 Extraction and isolation of chemical constituents from *Prangos pabularia*

N.K.Satti, Prabhu Dutt and Baldev Singh

The chemical investigation of the ariel parts extract has resulted in the isolation of bergapten, isobergapten, imperatorin, isoimperatorin, xanthotoxin, osthol and behenic acid by column chromatography. Structures of the compounds have been established by spectral analysis.

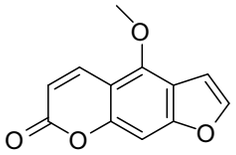

Bergapten

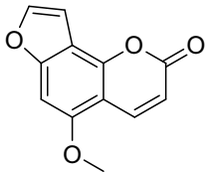

Isobergapten

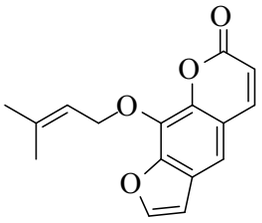

Imperatorin

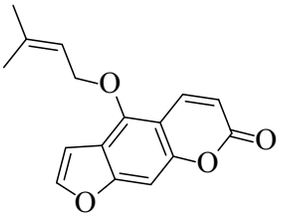

Isoimperatorin

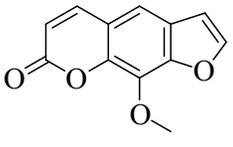

Xanthotoxin

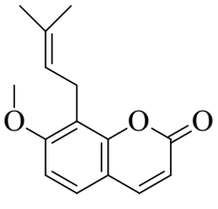

Osthol

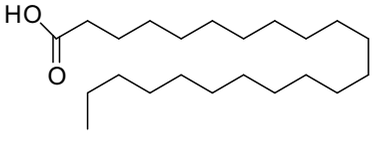

Behenic acid

5.6 Extraction and isolation of chemical constituents from *Pupalia lappacea*

N.K.Satti,, Prabhu Dutt and Baldev Singh

The chemical investigation of the aerial parts extract has resulted in the isolation of PL-1, PL-2, PL-3 and PL-4 by column chromatography. Structures of the compounds have been established by spectral analysis.

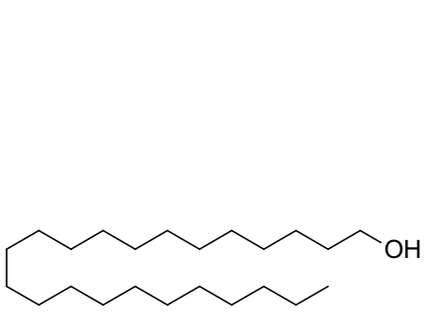

PL-1

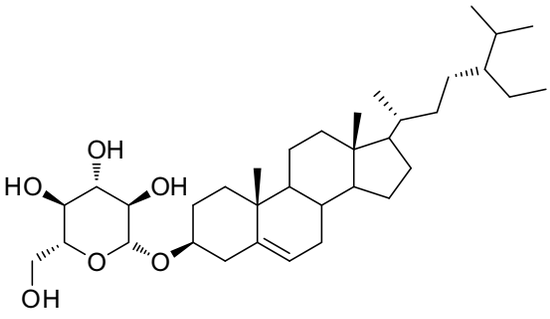

PL-2

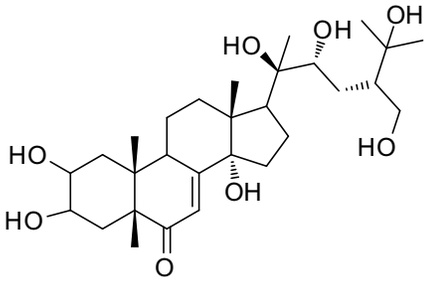

PL-3

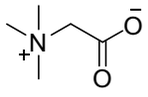

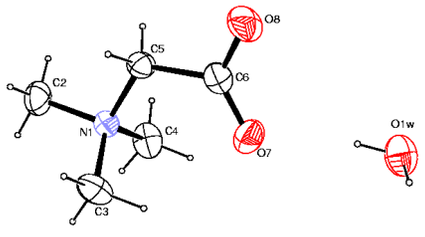

PL-4

5.7 Isolation, identification and quantification of prenylated flavonoids in *Epimedium elatum* by high performance liquid chromatography

Shahnawaz N Sofi, Shakeel-u-Rehman, Shabir H Lone, Haroon M Bhat and Khursheed A Bhat

A simple and reliable HPLC-UV-DAD method was developed for rapid resolution, identification and quantitation of prenylated flavonoids in *Epimedium elatum*, a plant endemic to Kashmir Himalayas. Three marker compounds Icariin, epimedoside A and epimedin C were isolated.

Five major prenylated flavonoids namely epimedoside A, epimedin A, epimedin B, epimedin C and icariin were quantified using HPLC in both underground and aerial parts of *E. elatum*.. All calibration curves showed good linearity ($r^2 > 0.998$) within test ranges and recoveries were 96.8 to 101.2%. The optimized method was successfully applied for the analysis of five major flavonoids in 18 samples of *E. elatum* collected from three different eco-geographical zones in three different harvesting seasons. The contents of five investigated compounds were greatly variant ranging from 8.73 to 10.96% in aerial parts and 2.52 to 5.06% in underground parts. The concentration of epimedin C was found to be the highest (6.42%) among the five quantified compounds in one of the accessions. The method established in this paper is simple and reliable and could be used for the quality control of *E. elatum*.

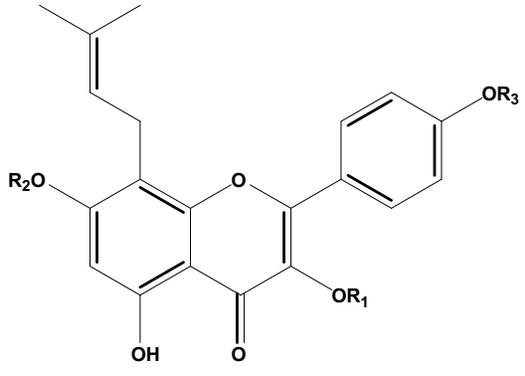

Compounds	R_1	R_2	R_3
Icariin	-rha	-glc	$-CH_3$
Epimedoside A	-rha	-glc	-H
Epimedin C	-rha(2-1)rha	-glc	$-CH_3$

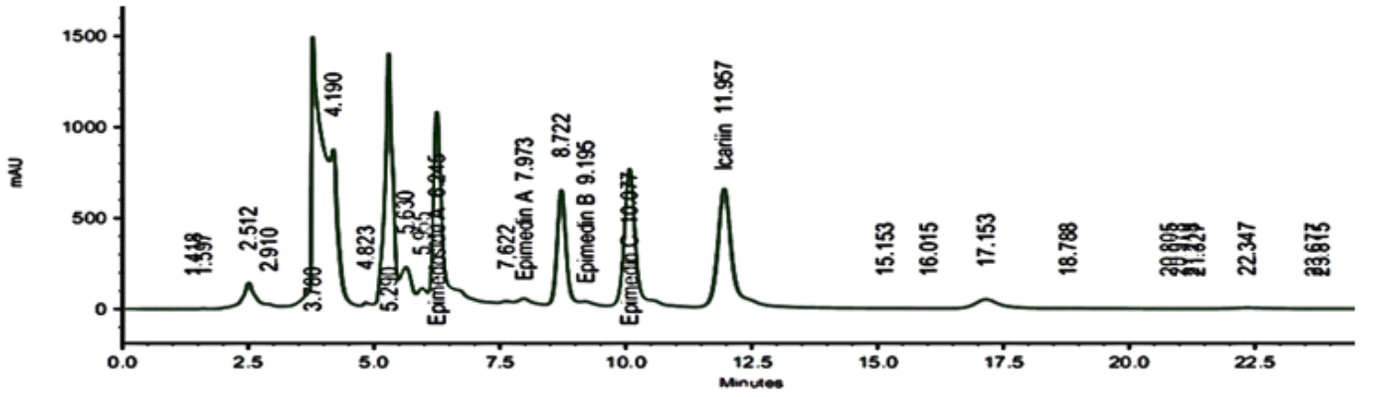

Figure 1: HPLC chromatogram of *Epimedium elatum* root extract

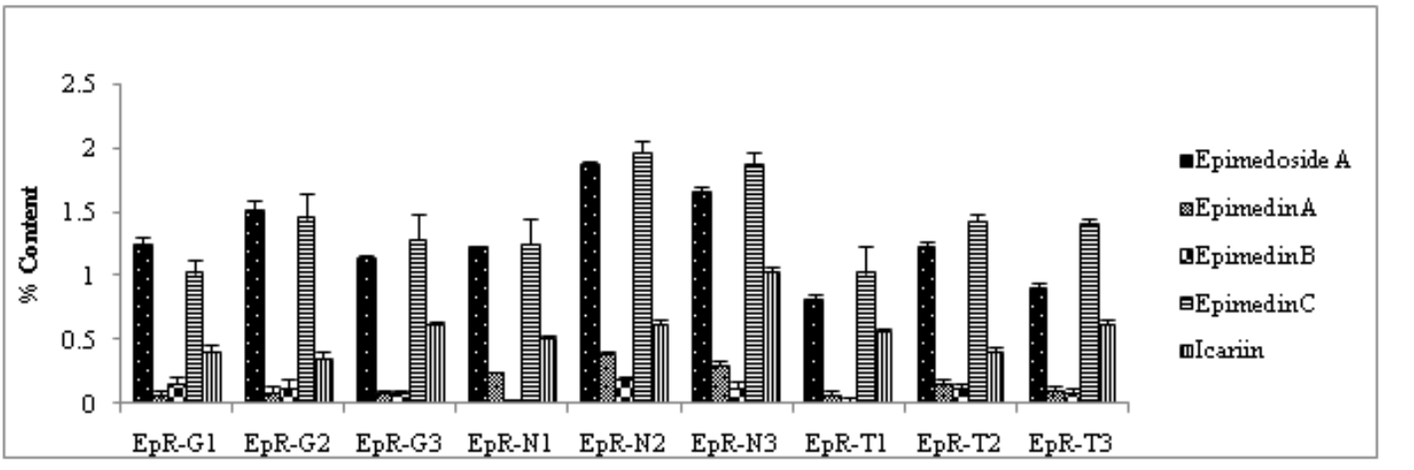

Figure 2: Content of five investigated compounds in underground parts of *E. elatum*

5.8 New natural compounds from *Rhododendron lepidotum*

Shakeel-u-Rehman and Khursheed Ahmad Bhat

Investigation of the aerial parts of *Rhododendron lepidotum* yielded three new compounds: 8-[2', 6'-dimethoxy-4'-(1", 2", 3"-trihydroxy propyl)-phenyl]-7-hydroxy benzopyranone (**1**), 3-*O*-*β*-D-glycopyranosyl betulinic amide (**2**) and 8-hydroxy-7, 7'-oxydicoumarin (**4**) and five known compounds. Among the known molecules, betulinic amide (**3**) was earlier reported as a semi synthetic product. The structures of new molecules **1**, **2** and **4** were elucidated on the basis of extensive spectroscopic investigations (1D, 2D NMR and mass spectrometry).

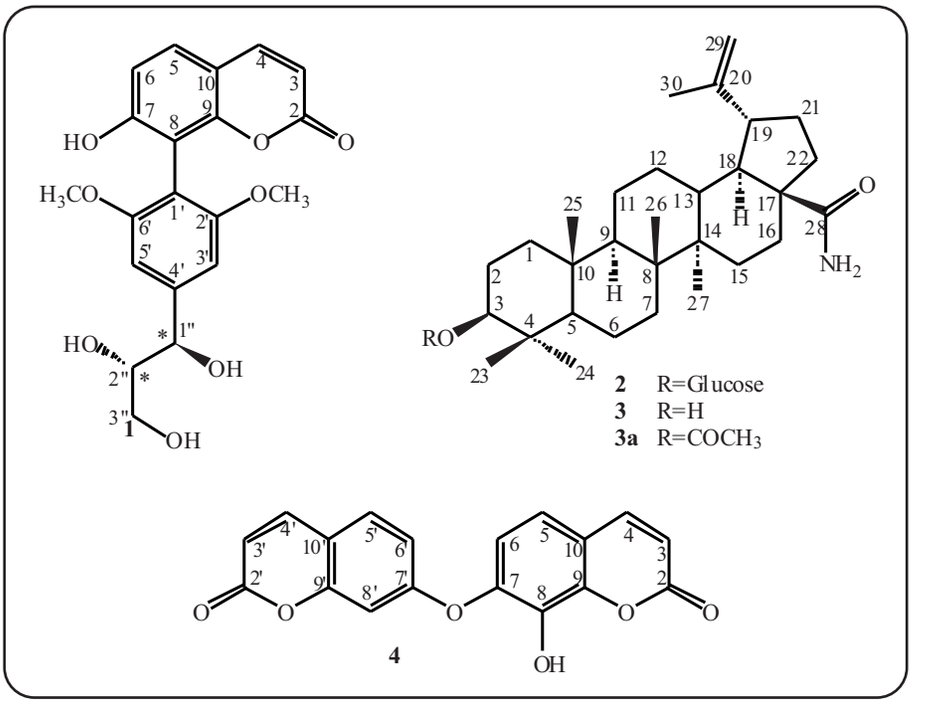

5.9 Tubulin inhibitors from an endophytic fungus isolated from *Cedrus deodara*

Manjeet Kumar, Masroor Qadri, Parduman Raj Sharma, Arvind Kumar, Samar S. Andotra, Tandeep Kaur, Kamini Kapoor, Vivek K. Gupta, Rajni Kant, Abid Hamid, Sarojini Johri, Subhash C. Taneja, Ram A. Vishwakarma, Syed Riyaz-Ul-Hassan and Bhahwal Ali Shah

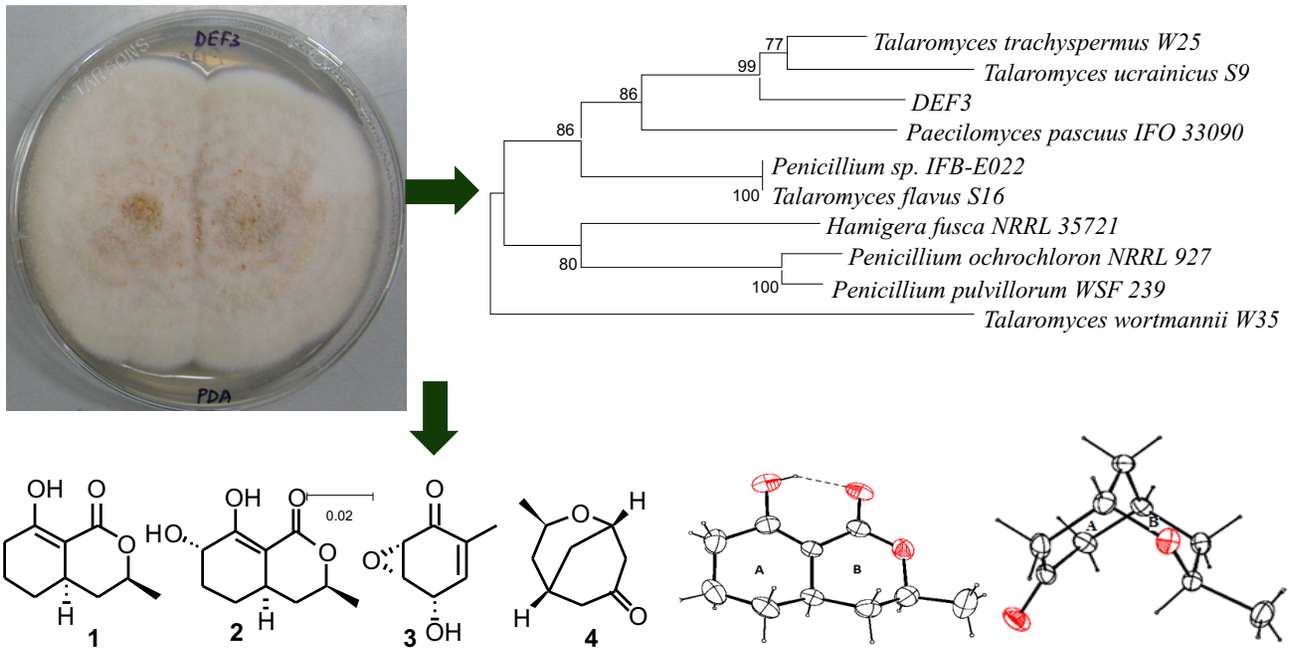

Endophytes have proved to be an excellent source of new bioactive molecules including antibiotics, antioxidants, anticancer, antiviral, immunosuppressive and antidiabetic agents. These endophytes also interfere with biosynthetic pathway of the host plants and sometimes produce the metabolites of the host plant, e.g., paclitaxel from *Taxomyces andreanae*, camptothecin from *Entrophospora infrequens*, podophyllototxin, vinblastine and vincristine from an *Alternaria sp.*, thus offering great promise for the isolation of new molecules. In this communication, we report the isolation and characterisation of two new **(2** and **4)** and two known metabolites, *i.e.*, (-)-ramulosin (**1**) and (-)-epoformin (**3**) from an endophytic fungus isolated from the plant *Cedrus deodara*. The structures of the metabolite **1** and **4** were defined by X-ray crystallography. The phylogentic analysis of the fungus showed that it is related to the *Talaromyces,* teleomorphic stage of *Penicillium* and *Paecilomyces*; the genus *Penicillium* has also proven to be a rich source of biologically active compounds such as antibiotics, isocoumarins and antifungals agents.

The isolated metabolites were screened for their *in vitro* cytotoxicity against different human cancer cell lines. Importantly, all the isolated metabolites induced cell death chiefly by apoptosis and displayed microtubule inhibition in human leukaemia (HL-60) cell lines.

The organism DEF3 (NFCCI -2857) in nature was found associated with *Cedrus deodara.* Fig. 1 shows the evolutionary history of the endophyte, inferred with the Neighbor-Joining method and based on the analysis of 18S- ITS1 ribosomal gene sequence (GenBank Acc. No. JQ769262). The sequence showed highest similarity (93%) with *Talaromyces trachyspermus,* followed by 90% similarity with *Talaromyces ucrainicus* and 86% with *Talaromyces flavus* and *Penicillium* sp. The sequence also displayed a similarity of 85% with *Paecilomyces pascuus,* however, with lower sequence coverage (87%). The data indicates that the endophyte is related to the *Talaromyces,* the teleomorphic stage of *Penicillium* and *Paecilomyces.* However, as the sequence similarity is only 93%, it cannot be assigned to a particular genus and species. Thus, this organism shows significant taxonomic novelty and was therefore

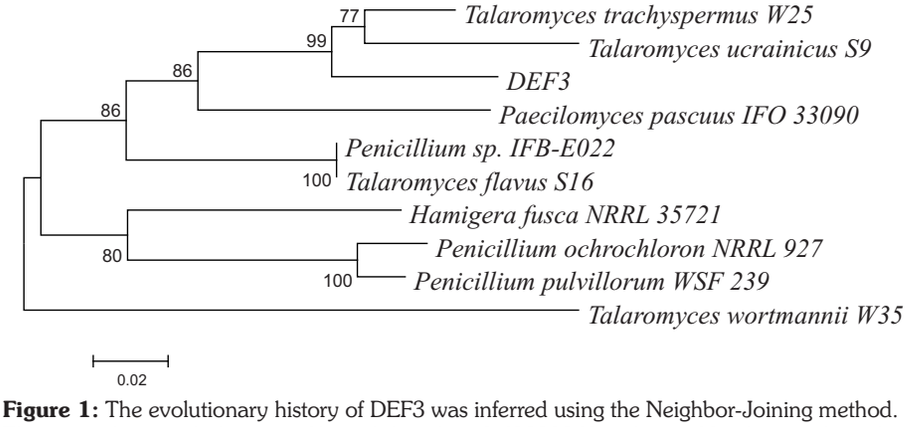

Figure 1: The evolutionary history of DEF3 was inferred using the Neighbor-Joining method. The optimal tree with the sum of branch length = 0.68880060 is shown. Numbers on branches represent the bootstrap values

selected for the potential isolation of novel bioactive molecules.

Fermentation and isolation of secondary metabolites: The fungus was cultured in potato dextrose broth (PDB) medium for 15 days with constant shaking containing 1L flasks. The fermentation broth was then extracted with dichloromethane following the National Cancer Institute's protocol. The extract was concentrated *in vacuo* and the crude mixture was subjected to column chromatography on silica gel using hexane-ethyl acetate leading to the isolation of pure compounds **1-4**. Two of the isolated compounds were identified as (-)-ramulosin (**1**) and (-)-epoformin (**3**), whereas compounds **2** and **4** were new. The structures of the compounds **1** and **4** were confirmed by X-ray crystallography.

Structure elucidation: The molecular formula of compound **2** was determined as $C_{10}H_{14}O_4$ by HRESIMS and NMR experiments. ^{1}H and ^{13}C-NMR spectra confirmed the presence of 10 carbons and 14 protons, including methyl and hydroxyl groups. The IR (KBr) spectrum showed absorption bands at 1643 and 3418 cm^{-1}, exhibiting the presence α,β-unsaturated ester group (1643 cm^{-1}) and hydroxyl (3418 cm^{-1}) respectively. The complete structural elucidation of **2** as well as assignment of all ^{1}H and ^{13}C NMR signals was based on 2D NMR experiments (HMBC, HSQC and COSY). ^{1}H NMR spectra revealed that methyl group is attached to C-3 having a doublet at δ_H 1.37 (J = 6.3 Hz), whereas the methine proton located as a multiplet at δ_H 4.48-4.50. The H-7 was assigned to a doublet (J = 4.4 Hz) at δ_H 4.26-4.27. Cross peak co-relations were clearly depicted in the HMBC spectrum between H-4a (δ_H 2.48) and C-8a (δ_C 96.40). Furthermore, the linkage from 3→7 was also confirmed by ^{1}H-^{1}H COSY co-relations between H-3 (δ_H 4.48-4.50, m) and H-4 (δ_H 1.97, 1.73), H4 (δ_H 1.97, 1.73) and H-4a (δ_H 2.48), H-4a (δ_H 2.48) and H-5 (δ_H 1.97, 1.37), H-5 (δ_H 1.97, 1.37) and H-6 (δ_H 1.73, 1.37), H-6 (δ_H 1.73, 1.37) and H-7 (δ_H 4.26-4.27). The NMR (^{1}H and ^{13}C) shifts of **2** at C-3 and C-4a were similar to **1**, suggesting that the stereochemistry at C-3 and C-4a were C-3*S* and C-4a*R*. The stereochemistry at C-7 was elucidated to be C-7*S*, as it didn't show any correlation with C-4a in NOESY. Thus, the structure of compound **2** was elucidated as (3*S*,4a*R*,7*S*)-7,8-dihydroxy-3-methyl-3,4,10,5,6,7-hexahydro-1H-isochromen-1-one.

The molecular formula of compound **4** was determined to be $C_9H_{14}O_2$ by HRESIMS and supported by NMR experiments. ^{1}H and ^{13}C-NMR spectra confirmed the presence of 9 carbon atoms and 14 proton signals, including a methyl group. The IR (KBr) spectrum showed absorption bands at 1073 and 1698 cm^{-1} indicating the presence of etheral C-O stretching (1073 cm^{-1}) and carbonyl function (1698 cm^{-1}) respectively. ^{1}H NMR reveals that the methyl group is attached to CH-3 showing a doublet at δ_H 1.11, which in turn shows an upfield signal at δ_H 3.67-3.71 due to direct linkage with an etheral O group. The proton signals for CH_2-8 splits in the spectra having two multiplets at δ_H 2.79 (1H) and δ_H 2.47-2.50 (1H) due to the CH-1. Also signals for CH_2-9 splits into two multiplets at δ_H 1.75 (1H) and δ_H 2.05 (1H) due to CH-1 and CH-5 stereo centres. Cross peak co-relations were shown in the HMBC spectrum between H-8 (δ_H 2.79, 2.48) and the carbonyl group C-7 (δ_C 208.4), H-1 (δ_H 4.42-4.43) and C-3 (δ_C 63.7), H-6 (δ_H 2.56-2.57) and C-7 (δ_C 208.4). Furthermore, H-1 and H-8 linkage has been confirmed by 1H-1H COSY co-relation between H-1 (δ_H 4.42-4.43) and H-8 (δ_H 2.48). Similarly the linkage from 3→6 has also been confirmed by 1H-1H COSY co-relations between H-3 (δ_H 3.67-3.71) and H-4 (δ_H 1.58-1.59), H-4 (δ_H 1.58-1.59) and H-5 (δ_H 2.46), H-5 (δ_H 2.46) and H-6 (δ_H 2.56-2.57). The stereochemistry was deduced as 1*S**, 3*R**, 5*R** through X-ray crystallography of compound **4**. Thus, the structure of compound **4** was elucidated as (1*S**,3*R**,5*R**)-3-methyl-2-oxa-bicyclo[3.3.1]nonan-7-one.

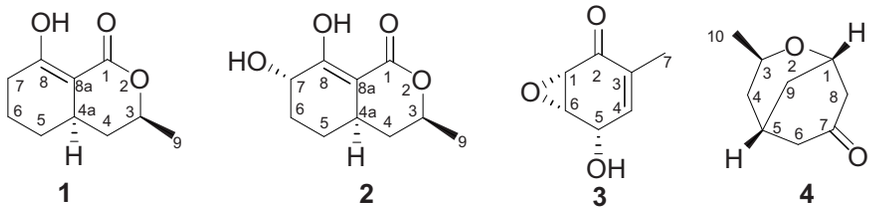

Figure 2: Structures of compounds **1-4**

An ORTEP view of the compounds **1** and **4** with their atomic labelings are shown in Fig.3. The data indicate that in the compound **1**, the cyclohexene ring (A) has a *distorted sofa* conformation, while heterocyclic ring (B) adopts a *sofa*

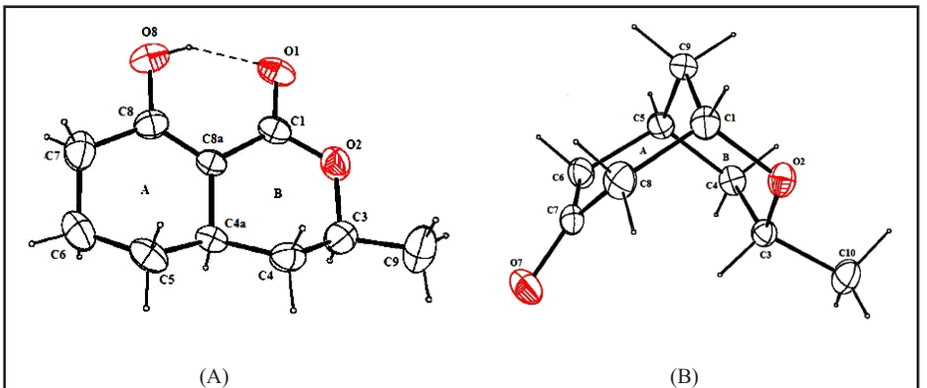

Figure 3: (A) ORTEP view of the compound **1**. (B) ORTEP view of the compound **4**

conformation. In compund **4**, the ring B adopts a normal chair conformation.

Biological activity: Sulforhodamine B cytotoxicity assay was performed using the four isolated compounds and the positive controls on a panel of human cancer cell lines of various origins (Table 1). The following cell lines were used; colon (HCT-116), lung (A-549), liver (HEP-1), leukemia (THP-1) and prostate (PC-3). The isolated molecules displayed a range of cytotoxicity as shown in Table 2. (-)-Epoformin was found to be the most active, followed by compounds **4**, **1** and **2** respectively. Further experiments were carried out to obtain mechanistic insights into their mode of action.

Fluorescence and scanning electron microscopy (SEM). In an attempt to decipher the insights of cell death, compounds **1-4** were evaluated for their ability to induce apoptosis. In the present study we used morphological analysis by scanning electron microscope (SEM) to identify the specific type of death of HL-60 cells both in control and treatment groups. It revealed that untreated HL-60 cells were spherical having microvilli on the entire surface and with a few surface projections (Fig. 4A-B). On incubation of the cells with 30 μM, **1-4** for 30 h condensation, smoothening of cell surface and blebbing of plasma membrane in a few cell was noted, which represents the morphological features of apoptotic cell (data not shown). However, after 30 h of treatment with the isolated compounds at 50 μM, the number of cells and features of apoptosis increased in all the treated cells to various degrees (Fig. 4C-H).

The results were further corroborated by nuclear morphological changes of HL-60 cells. The HL-60 cells were chosen since most of the isolated molecules were found to be active against this leukemia cell line. HL-60 cells were treated with 50 μM of each compound for 30 h and subsequently stained with DAPI. Cells were observed under fluorescence microscope (40x). The untreated cells have large intact nuclei (Fig. 5A). The treatment induced the condensation and fragmentation of nuclei (arrow) due to apoptosis (Fig. 5B-E), with the greatest number of apoptotic cells seen by treatment with the compound **2**.

Effect of compounds

Table 1: Cytotoxicity of the isolated molecules

Sample	Conc.	Lung	Liver	Leukemia	Prostate	Colon
		A-549 (%)	HEP-1 (%)	THP-1 (%)	PC-3 (%)	HCT (%)
1	50	15	23	54	23	44
2	50	35	3	40	34	35
3	50	98	100	50	22	56
4	50	71	26	0	23	59
Paclitaxel	1	82	-	71	-	72
Fluorouracil	20	22	-	84	-	55
Mytomycin C	1	-	-	-	59	-

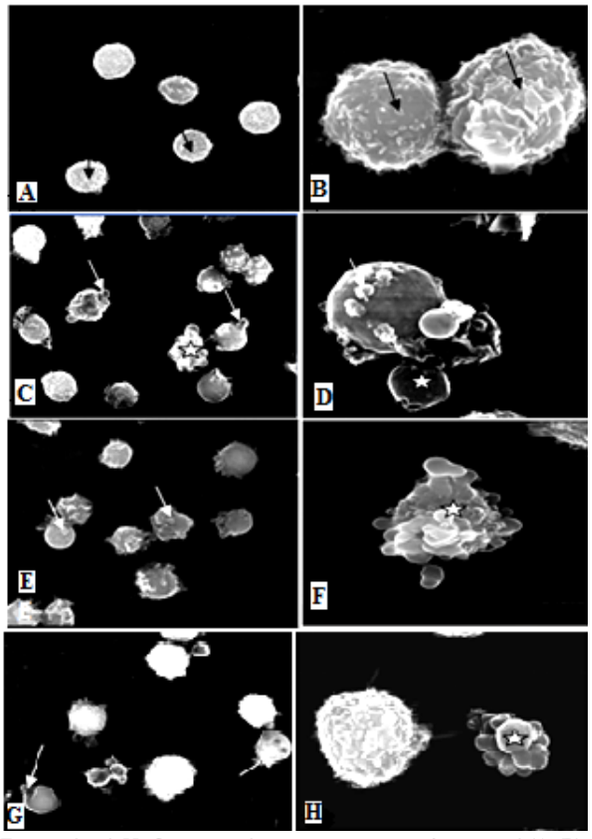

Figure 4: A-H. Scanning electron microscopy of untreated (A, B), **2** (C, D) and **3** (E, F) and **4** (G, H) treated HL-60 cells showing surface ultrastructure. The untreated cells show microvilli on cell surface (A, B, arrow). The treatment of 50 μM of **2** (C, D) and **3** (E, F) and **4** (G, H) respectively, after 30 h causes condensation, smoothening of cell surface and blebbing of plasma membrane (C, D, E, F, G, H- white arrows) and the formation of apoptotic bodies (C-H, asterisk). (Magnification A, C, E, G- 2000X; B, D, F, G- 5000X).

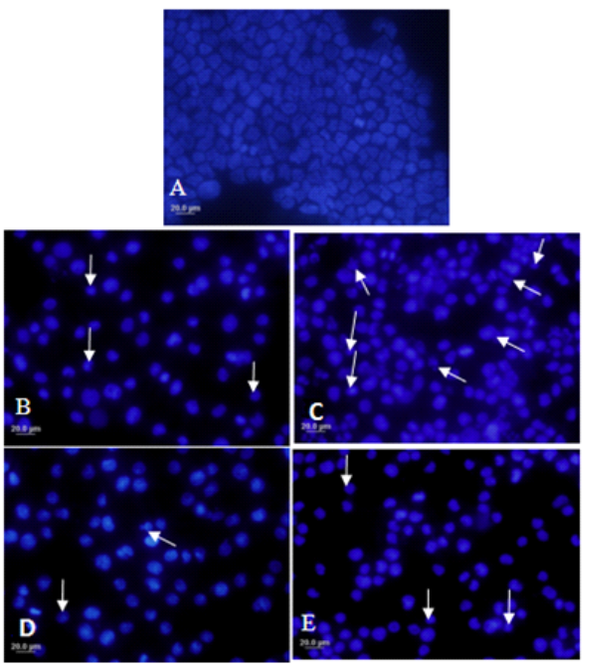

Figure 5: Effect of the compounds **1** to **4** on nuclear morphology of HL-60 cells. The cells were treated with 50 μM of different compounds for 30 h and subsequently stained with DAPI as described in materials and methods. Cells were observed under fluorescence microscope (40x). The untreated cells (A) have large sized intact nuclei. All the four compounds, **1** (B), **2** (C), **3** (D) and **4** (E) induced the condensation and fragmentation of nuclei (white arrows) due to apoptosis. The more number of apoptotic cells were seen in treatment with the compound **2** (D).

1-4 on microtubules by immunoflouroscense microscopic studies: Microtubules are attractive targets for chemotherapeutic agents. Since these play an important role in the regulation of the mitotic progression, disrupting the assembly of microtubules can induce cell cycle arrest in the M phase and trigger apoptosis. The microtubule inhibitors such as vinca alkaloids, colchicinoids and combretastatin inhibit tubulin polymerization, and the microtubule promoters, such as taxanes and epothilones, promote or stabilize the tubulin polymer form. We investigated the effect of compounds **1-4** on the microtubules structure in leukemia cells using confocal microscopy. As shown in Fig. 6 the treatment of THP-1 cells for 48 h with 50 μM, **1-4** showed a remarkable disruption and loss of microtubule organization compared to the untreated cells. Paclitaxel® treatment at 1μM for 24 h caused the stabilization of tubulin in the polymer form (data not shown). Although, all the tested compounds showed significant influence on microtubules in THP-1 treated cells, compound **2** was observed to be the most potent in disintegrating microtubule organization which eventually resulted in apoptotic cell death as observed in this study.

Further studies are underway to isolate additional metabolites from this fungus. Additional studies on the compounds **1-4** are aimed at elucidating more details of their molecular mode of action.

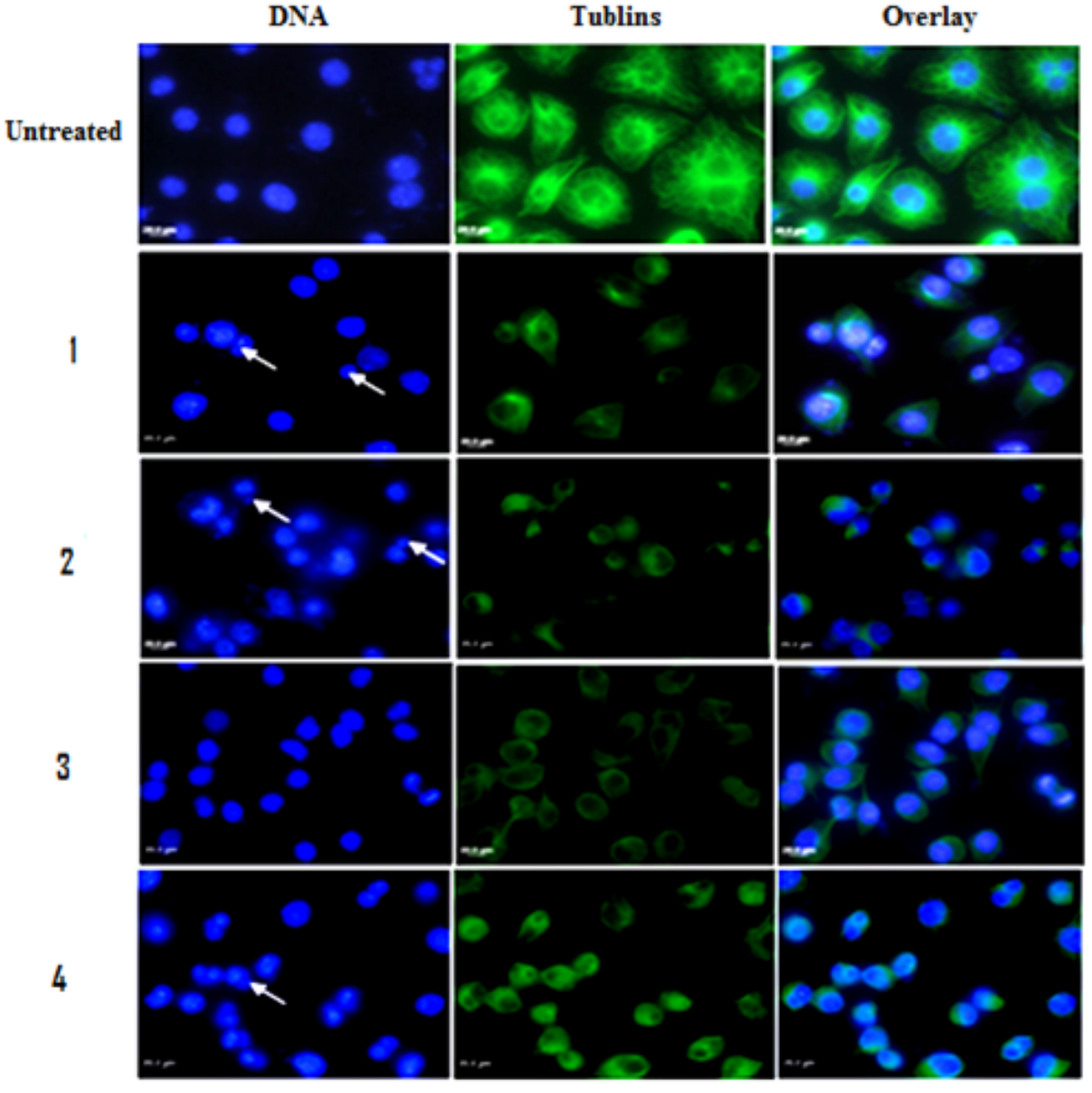

Figure 6: Effect of the compounds **1-4** on microtubules in THP-1 cells. Cells were plated on cover slips. After 24 h, the cells were treated with **1-4** for 48 h, at 50 μM for 48 h. Immunocytochemical staining was conducted using anti-α-tubulin antibody and Alexa Flour-488-labeled secondary antibody. Nuclei were stained with DAPI (left panel indicated by arrows). The data is representative of three separate set of experiments. Compounds **1**, **2** and **4** cause the fragmentation of nuclei (white arrows) due to apoptosis.

5.10 Acyl derivatives of boswellic acids as inhibitors of NF-κB and STATs

Ajay Kumar, Bhahwal A. Shah, Abid Hamid, Shashank K. Singh, Samar S. Andotra, Vijay K. Sethi, Ajit K. Saxena, Jaswant Singh and Subhash C. Taneja

The gum exudate of *Boswellia serrata* comprises of four boswellic acids (BAs) viz., -boswellic acid (BA) as the main triterpenic acid along with 3-*O*-α-acetyl-β-boswellic acid (ABA), 11-keto--boswellic acid (KBA) and 3-*O*-α-acetyl-11-keto-β-boswellic acid (AKBA). The gum resin of *Boswellia serrata* is traditionally used in Ayurvedic system of medicine for the treatment of various ailments. In the recent past many studies have reported their activities against inflammation, arthritis, ulcerative colitis, chronic colitis, asthma and hepatitis. However, it is their anticancer activity, that has attracted the most attention in the recent past due to their ability to induce apoptosis. They have been reported to inhibit growth and induce apoptosis in brain tumors, malignant glioma cells, colon cancer cells and leukemic cells. They have also been found to be more potent inhibitors of topoisomerase I and II in comparison to camptothecin, amsacrine or etopside respectively, using pure topoisomerase assay. Thus impelled by the potential of BAs and our interest in the identification and development of potent anticancer leads based on the natural products including BAs, we present our work related to acyl derivatives of BAs to study their potential as inducers of apoptosis. We further envisaged exploring the effect of the most active molecule/s on NF-κB (Nuclear Factor-kappa B) and some members of STAT (signal transducer and activator of transcription protein) family.

The idea behind the preparation of the alkyl acyl analogs was to study the effect of acyl groups of varying carbon length on 3-hydroxyl functionality including its stereochemistry on the bioactivity of BAs, which consequently may help in the establishment of the SAR and would offer direction to the future course of work. Thus, various acyl analogs of boswellic acids and their epimers were prepared using acylating agents. In order to prepare particularly 3-*O*-α-formyl-β-boswellic acid (**5**), BA was added slowly to the formylating reagent (prepared by adding formic acid to acetic anhydride) with constant stirring at room temperature. Other acyl analogs of BA were prepared by using corresponding anhydrides *i.e.*, acetic, propanoic and butyric anhydrides in presence of dimethyl amino pyridine (DMAP) as a catalyst in dry DCM to produce 3-*O*-α-acetyl-β-boswellic acid (**3**), 3-*O*-α-propionyl-β-boswellic acid (**6**) and 3-*O*-α-butyryl-β-boswellic acid (**7**) respectively in almost quantitative yields. Likewise, 3-*O*-α-formyl-11-keto-β-boswellic acid (**9**), 3-*O*-α-acetyl-11-keto-β-boswellic acid (**4**), 3-*O*-α-propionyl-11-keto-β-boswellic acid (**10**) and 3-*O*-α-butyryl-11-keto-β-boswellic acid (**11**) were also prepared in similar yields. It was also envisaged to improve hydrophilicity by suitably changing the functionality. Therefore, additional carboxylic acid functionality at C-3 was introduced through the formation of hemisuccinates. The reaction was accomplished by reacting succinic anhydride with **1** in the presence of pyridine to afford 3-*O*-α-hemisuccinyl-β-boswellic acid (**8**) and 3-*O*-α-hemisuccinyl-11-keto-β-boswellic acid (**12**) respectively in 85% yield (Scheme-1).

The configuration of hydroxyl function in the naturally occurring BAs at C-3 is α. Therefore to study the effect of change of configuration at C-3 on cytotoxicity, we envisaged the preparation of 3-*epi* BAs. To achieve it, BA/KBA in diethyl ether was treated with diazomethane (CH_2N_2) to afford methyl-3-α-hydroxyurs-12-en-24-oate (**13**) and methyl-3-α-hydroxy-11-oxours-12-en-24-oate (**14**) respectively in 95% yield. These esters were followed by their oxidation with PCC in DCM to convert them to corresponding 3-keto derivatives *i.e.*, methyl-3-oxours-12-en-24-oate (**15**) and methyl-3,11-dioxours-12-en-24-oate (**16**) in 85% yield. The 3-keto derivatives were then quantitatively reduced by $NaBH_4$ in methanol to produce methyl-3-β-hydroxyurs-12-en-24-oate (**17**) and methyl-3-β-hydroxy-11-oxours-12-en-24-oate (**18**) having (*S*) or β-configuration at C-3, because the steric hindrance caused by the -substituent groups mainly in the A/B ring of triterpenoid (e.g. 25-Me, 24-COOMe) facilitated the approach of hydride from α side. The methyl esters thus obtained were hydrolyzed using KOH/MeOH in a

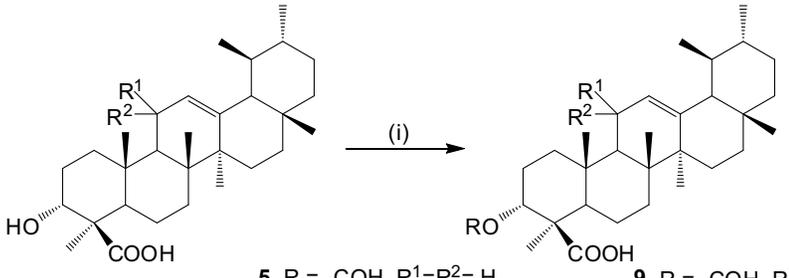

1 / 2

5. R = -COH, R^1=R^2= H
3. R = -$COCH_3$, R^1=R^2= H
6. R = -COC_2H_5, R^1=R^2= H
7. R = -COC_3H_7, R^1=R^2= H
8. R = -$COCH_2CH_2COOH$, R^1=R^2= H

9. R = -COH, R^1+R^2 = O
4. R = -$COCH_3$, R^1+R^2 = O
10. R = -COC_2H_5,R^1+R^2 = O
11. R = -COC_3H_7, R^1+R^2 = O
12. R = -$COCH_2CH_2COOH$, R^1+R^2 = O

Scheme-1: Reagents and conditions: (i) R_2O, DMAP, DCM (95%).

high pressure reaction vessel at 98-100 °C to afford 3-*epi*-β-boswellic acid (**19**) and 3-*epi*-11-keto-β-boswellic acid (**20**) respectively in 90% yields (Scheme 2).

Scheme 2: Reagents and conditions: (i) CH_2N_2, ether (95%) (ii) PCC, DCM, rt (80%) (iii) $NaBH_4$, MeOH, rt (90%) (iv) KOH, MeOH (88%) (v) R_2O, DMAP, DCM (95%)

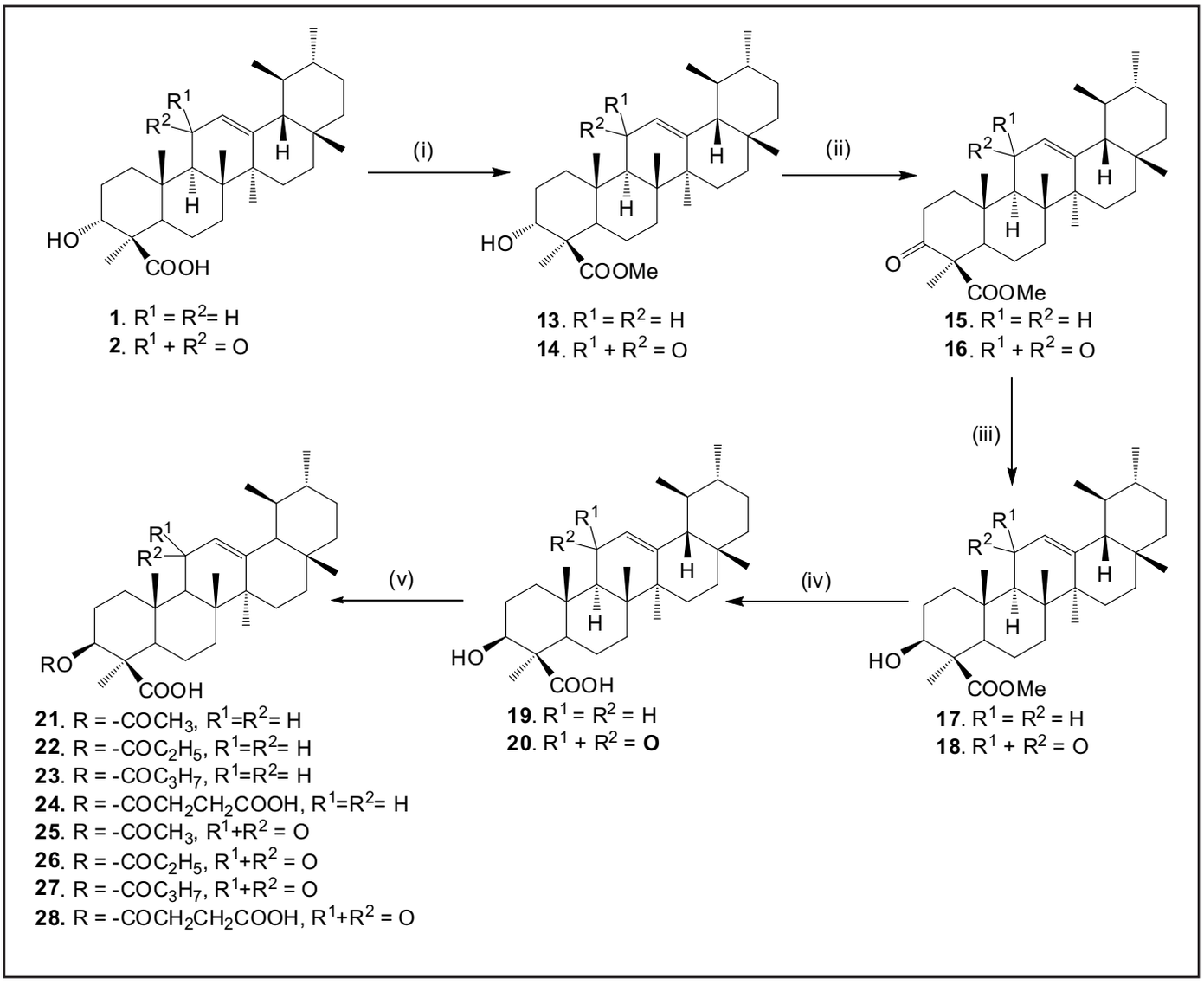

The 3-*O*-acyl analogs of 3-β-hydroxy-β-boswellic acid were similarly prepared using alkyl anhydrides in dry DCM using DMAP as a catalyst to obtain 3-*O*-β-acetyl-boswellic acid (**21**), 3-*O*-β-propionyl-β-boswellic acid (**22**) and 3-*O*-butyryl-β-boswellic acid (**23**) respectively. Similarly, 3-*O*-β-acetyl-11-keto-β-boswellic acid (**25**), 3-*O*-β-propionyl-11-keto-β-boswellic acid (**26**) and 3-*O*-butyryl-11-β-keto-boswellic acid (**27**) were prepared. The 3-*epi* BAs were also subjected to hemi succinate formation using succinic anhydride and pyridine to produce 3-*O*-β-hemisuccinyl-β-boswellic acid (**24**) and 3-*O*-β-hemisuccinyl-11-keto-β-boswellic acid (**28**) in almost quantitative yields (Scheme-2).

The preliminary screening results of BAs analogs at 50 μM concentrations showed that the propionate **6**, 11-keto butyrate **11** and 3-epi propionate **22** derivatives potently inhibited the growth (86-90%) in all the cell lines used [HT-29 (colon), SW-620 (colon), Colo-205 (colon), Hep-2 (larynx), DU-145 (prostate), PC-3 (prostate)], whereas, the parent compound **1** effectively inhibited the cell growth (95-100%) in prostate cancer cell lines DU-145 and PC-3 (Table 1). The butyrate **7** also showed high cytotoxic activity (>90%) in all the cancer cell lines except in PC-3 where it showed 75% growth inhibition (Table 1). The 11-keto propionate **10** as well was found to exhibit significantly enhanced cytotoxicity when compared to **1**, displaying >90% growth inhibition in HT-29, SW-620 and Colo-205 cell lines. Its growth inhibitory activity was improved against larynx Hep-2 cancer cell line; however, it was less effective in DU-145 and PC-3 as compared to **1**.

Table 1: *In vitro* cytotoxicity of natural BAs and their analogs against different human cancer cell lines

Compound	Conc.	HT-29	SW-620	Colo-205	Hep-2	DU-145	PC-3
		Colon			Larynx	Prostate	
		Growth inhibition %					
1	50	69	61	86	45	95	100
2	50	38	28	50	34	99	100
3	50	96	97	95	88	0	45
4	50	91	91	89	62	88	79
5	50	79	92	93	75	94	99
6	50	97	99	87	90	96	96
7	50	98	99	91	99	92	75
8	50	71	71	92	58	96	87
9	50	62	70	76	56	87	99
10	50	92	90	92	72	26	61
11	50	98	99	94	99	93	98
12	50	3	0	1	7	50	38
13	50	33	49	40	26	88	57
14	50	70	70	73	52	68	85
15	50	32	34	32	8	53	41
16	50	15	11	28	11	23	3
17	50	4	9	20	0	2	4
18	50	7	11	20	0	2	4
19	50	73	65	85	66	92	69
20	50	46	49	52	53	86	68
21	50	34	38	34	41	89	54
22	50	94	94	86	86	86	98
23	50	54	83	71	65	85	80
24	50	11	1	20	10	50	38
25	50	45	48	56	50	85	60
26	50	67	75	80	65	93	99
27	50	60	83	94	68	95	100
28	50	16	2	29	17	87	60
5FU	10	40	0	43	14	0	37
	100	21	7	39	5	20	52
Mitomycin C	1	33	57	28	46	29	24

Dysregulation of apoptosis is the hallmark of all cancer cells and the compounds that are capable of inducing apoptosis in cancer cells are considered to be important in anticancer therapeutics. On the basis of preliminary screening of toxicity in different cancer cell lines derivatives **6**, **7**, **10**, **11** and **22** were selected to study their apoptotic functioning. We used a p53 'null' human myeloid leukemia HL-60 cell line for apoptotic screening because of the fact that p53 is a tumour suppressor gene that provides a vital genetic defence against development of cancer and is reported to be mutated in about half of the cancers. Apoptosis is a complex phenomenon, which is regulated by genetic mechanisms and is principally characterized by morphological and

biochemical changes in the nucleus, including internucleosomal DNA fragmentation. The most active compounds were thus analyzed for their potential to induce DNA fragmentation in HL-60 cells. All the selected compounds caused DNA fragmentation at 50 μM concentration in HL-60 cells, which was visible in the form of a ladder of 180-200 bp fragments or multiples of it (Fig. 1A). In order to identify the most active molecule, MTT assay was used to calculate the IC50 values and relative cytotoxicity of selected analogs in HL-60 cells. The results showed IC50 value of **11** is lowest at 10 μM (Fig. 1B), whereas, the IC50 values of other analogs were found to be significantly higher (Fig. 1B). Normal cell line hGF was also treated with **11** for comparative studies on toxicity. The results showed IC50 value of **11** in hGF is 80μM (Fig.1C). Comparatively low toxicity in normal cell line hGF further strengthened the candidature of **11** for detailed studies.

Further to understand whether the toxicity caused by these derivatives is purely due to apoptosis as other types of cell death (necrosis and autophagy) also plays some role, flow cytometer based analysis was employed after staining the HL-60 cells with annexin-v-FITC/propidim iodide (to analyze apoptosis and necrosis) and acridine orange (to analyze autophagy). At 50 μM concentrations, all the derivatives induced cell death, predominantly by apoptosis, whereas the number of cells undergoing necrosis was relatively insignificant after 6 h exposure. None of the compounds produced autophagic death in HL-60 cells (data not shown). However, as expected, propionate **11** was found to be the most effective of all analogues producing approximately 80% of apoptotic cell population at the end of 6 h treatment, suggesting that **11** is probably a potential candidate that can be developed into an anti-cancer therapeutic lead. It exhibited relatively lower IC50 values and showed greater potential for inducing apoptosis, therefore, it warranted more studies to understand its molecular mechanism of action.

For the validation of the effectiveness of **11** against some of many putative molecular targets in cancer cells, the expressions of NF-κB against anti-apoptotic members of STAT family in HL-60 cells were analyzed. The transcription factors NF-κB and Stat3 are persistently active in most of the cancers and are involved in the regulation of genes required for cancer cell proliferation, survival, angiogenesis and invasion. Both these proteins work in conjunction with each other for the growth of cancer cells and require each other for their constitutive activity. Error! Bookmark not defined. In view of the importance of NF-κB and Stat3 and other procancerous members of STAT family, we analyzed effect of **11** on the expression of these proteins in HL-60 cells. The control cells showed a high level of NF-κB (p65) and NF-κB (p50) in the whole cell fraction whereas the 6 h treatment with **11** reduced the expression of NF-κB (p65) by about 90%, irrespective of the concentration (20 and 50 μM), while the expression of NF-κB (p50) was more potently inhibited at 50 κM concentration of **11** (Fig. 3A).

The anti-apoptotic members of STAT family contribute to the cancer cell growth by employing different mechanisms. Both the unphosphorylated and phosphorylated forms of STAT proteins work together for cancer cell survival. The analysis of anti-apoptotic members of Stat family (Stat3, Stat5 and Stat6) revealed differential expression of these proteins in HL-60 cells. The unphosphorylated Stat3κ, Stat3κ, Stat5 and Stat6 were

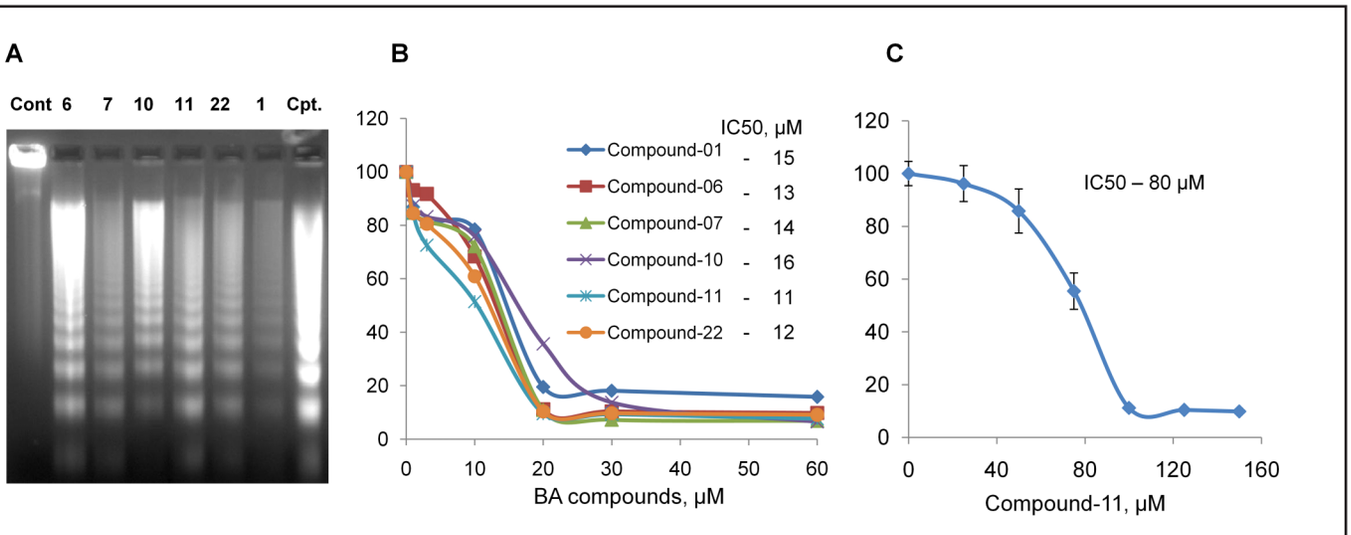

Figure 1: (**A) DNA fragmentation induced by selected dervatives of boswellic acids.** Apoptotic DNA ladder was observed when 2 x 10^6 HL-60 cells were treated with various derivatives of BAs at 50μM concentration for 6 h. The cells treated for 6 h with 4 μM camptothecin were used as positive control. (B) Inhibition of cell proliferation by selected dervatives of BAs in HL-60 cells and (C) in hGF cells. The cell proliferation analysis was performed in HL-60 cells by using MTT. The cells were incubated with each analog for 48 h at indicated concentrations and thereafter mitochondrial competence of MTT reduction as an index of cell viability determined. OD of untreated control was taken as 100% viability. IC50 values of all the compounds are depicted in the figure 1B-C.

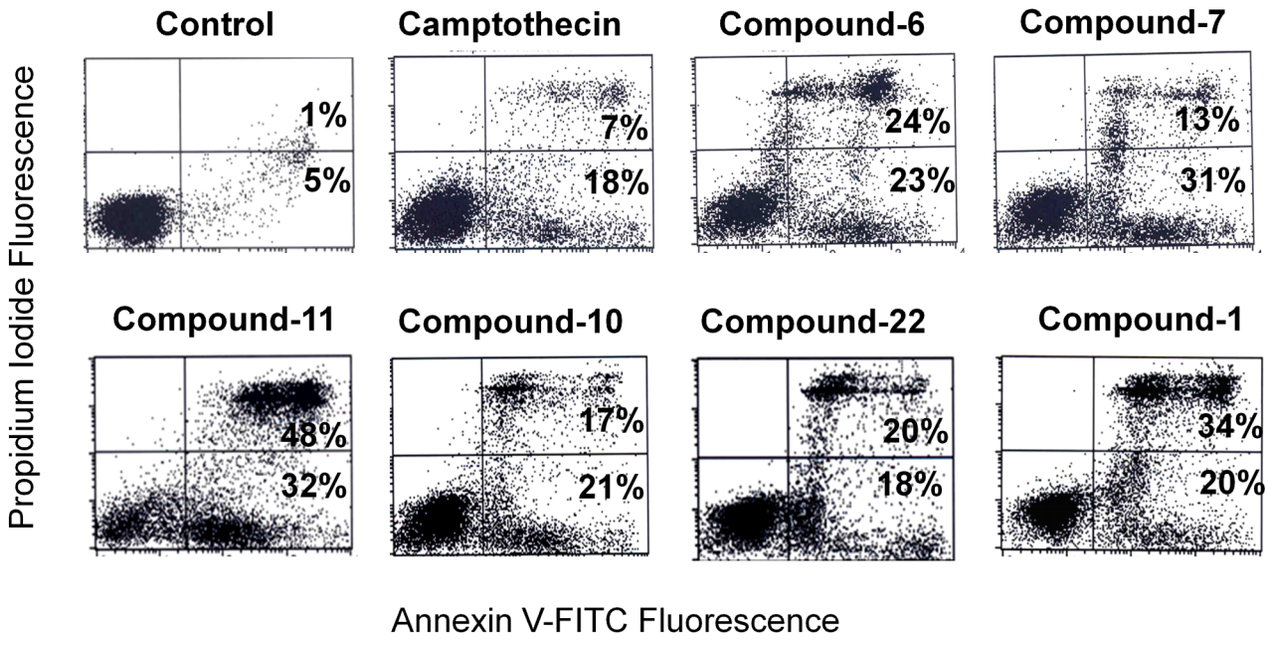

Figure 2: Effect of selected boswellic acid analogs on the relative efficiency of induction of apoptosis and necrosis in HL-60 cells. The cells were incubated with each analog at 50 μM concentration for 6 h and stained with annexin v-FITC/PI. The dot plots are the representative of one of the three experiments. Values in the lower right quadrant represent the apoptotic population, in the upper right as post apoptotic and in the upper left as necrotic. Other conditions are the same as described in the methods. The data shown are representative of one of the three similar experiments.

highly expressed in control HL-60 cells (Figs. 3B and 3C). However, treatment of HL-60 cells with **11** for 6 h strongly reduced the expression of all the unphosphorylated Stat proteins. The expression analysis of phosphorylated STAT proteins revealed that HL-60 cells show very high level of pStat3 (Ser 727) (Fig. 3B), which signifies the importance of pStat3 in the proliferation of HL-60 cells. Other STAT proteins showed varied expression in the control cells, where pStat3 (Ser 727) and pStat3 (Thr 705) had significantly high expression. pStat5 (Tyr 694/699) and pStat6 (Tyr 641) showed significantly low level of proteins (Fig. 3C). However, the treatment with **11** strongly reduced the expression of phosphorylated forms of all the members of STAT family studied. The data clearly suggests that cytotoxic effect of **11** is mediated by the inhibition of NF-κB-Stat3 tango along with other anti-apoptotic members of STAT family.

In conclusion, alkyl acyl derivatives of BAs were synthesized and screened for cytotoxicity against a panel of human cancer cell lines. The analogues exhibited a range of activities thereby, establishing a partial SAR as follows (i) in general the alkyl acyl derivatives displayed improved activity than parent BAs i.e., higher acyl homologues (**3-7** and **9-11**) displayed better cytotoxicity indicating free hydroxyl is not important for activity.

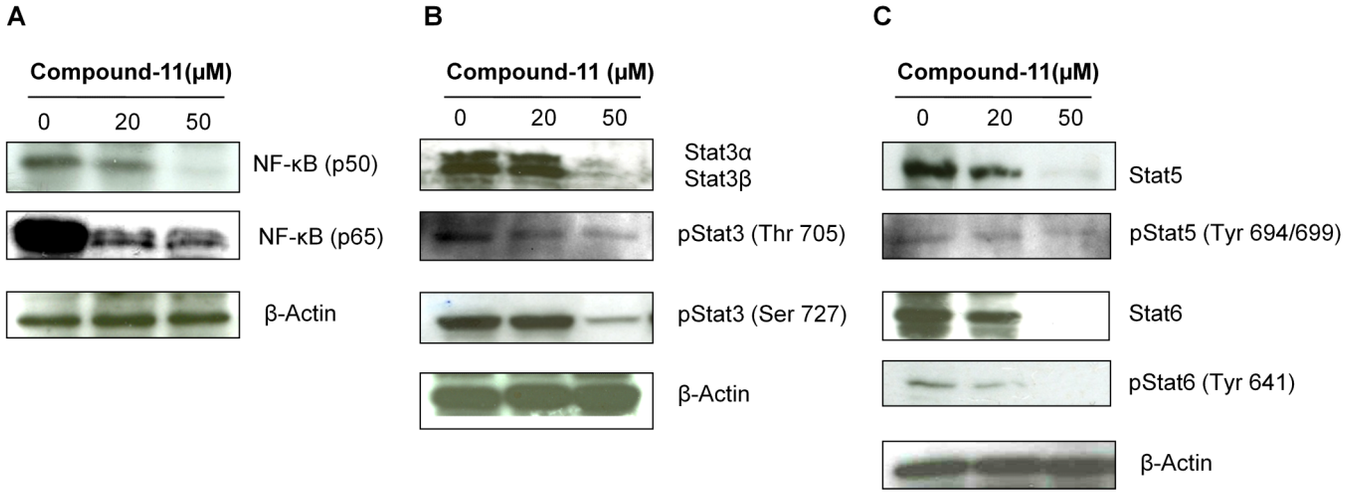

Figure 3: Effect of 11 on the expression of NF-κB and procancerous STAT proteins in HL-60 cells. **(A)** The cells were treated with or without **11** (20 and 50 μM) for 6 h. Total cell lysates were prepared for immunoblot analysis of NF-κB (p50 and p65). Protein samples (70 μg) were loaded on 10 % SDS-PAGE gel for western blot analysis. β-Actin was used as internal control to represent the same amount of protein applied for SDS-PAGE. Data are representative of one of three similar experiments. **(Figs. 3B and 3C)** Western blot analysis for STAT proteins as indicated in the figure. 8 % SDS-PAGE was used to resolve the STAT proteins; other conditions are same as in Fig 3A.

The attempts to increase hydrophilicity by way of C-3 hemi-succinate formation (**8**, **12**, **24** and **28**) did not improve cytotoxicity (ii) The esterification of acid group (**13-18**) led to the reduction/ loss of activity, implying that C-24 acid moiety is important for activity (iv) The 3-*epi* BAs (**19-28**) didn't display any significant improvement in activity indicating that κ-configuration at C-3 is more important for cytotoxicity. Besides, the propionate derivative **11** has been identified as a lead molecule that exhibited promising anti-cancer activity by inhibiting the NF-κB and STAT proteins and can further be developed into a potential anti-cancer therapeutic.

5.11 Development of a validated UPLC–qTOF-MS/MS method for determination of bioactive constituent from *Glycyrrhiza glabra*

D.K. Gupta, M. K. Verma, R. Anand and R. K. Khajuria

An ultra-performance liquid chromatography quadrupole time of flight mass spectrometry (UPLC–qTOF-MS/MS) method was developed and validated for the simultaneous determination ofglycyrrhizin and glycyrrhetic acid (Figs. 1 & 2). These analytes were separated () on a reverse phase C18column using a mobile phase of acetonitrile : 2%acetic acid in water (75:25,v/v) with a flow rateof200 mL/min. The qTOF-MS was operated under multiple reaction monitoring (MRM) mode using the electro spray ionization (ESI) technique with positive ion polarity. The multiple reaction monitoring (MRM) mode was used to monitor the transitions (845-823-453 and 493-471-177) of glycyrrhizin and glycyrrhetic acid respectively (Figs. 3 & 4). A typical UPLC–qTOF-MS/MS chromatograms were shown in Fig. 5. A comparison of three differen textraction techniques i.e. accelerated solvent extraction (ASE), extraction under ultrasonic waves (USW) and the classical extraction by percolation (CE) method were done and quantification of these extracts was also carried out by the proposed method.

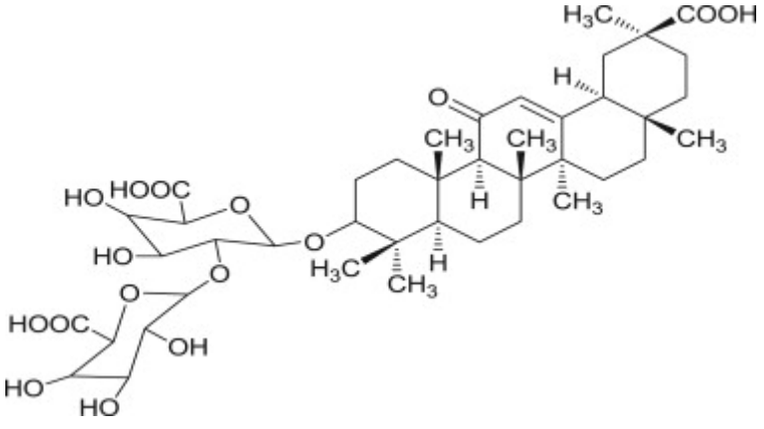

Figure 1: Structure of glycyrrhizin

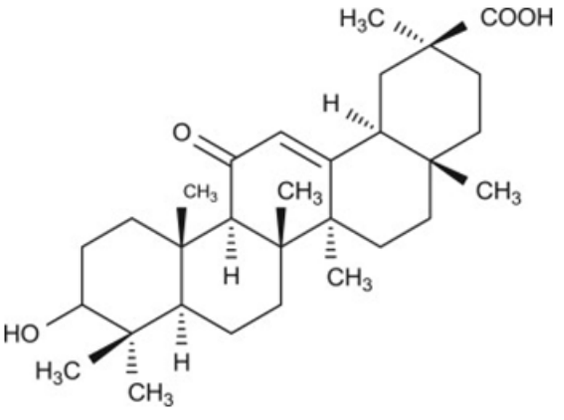

Figure 2: Structure of glycyrrhetic acid.

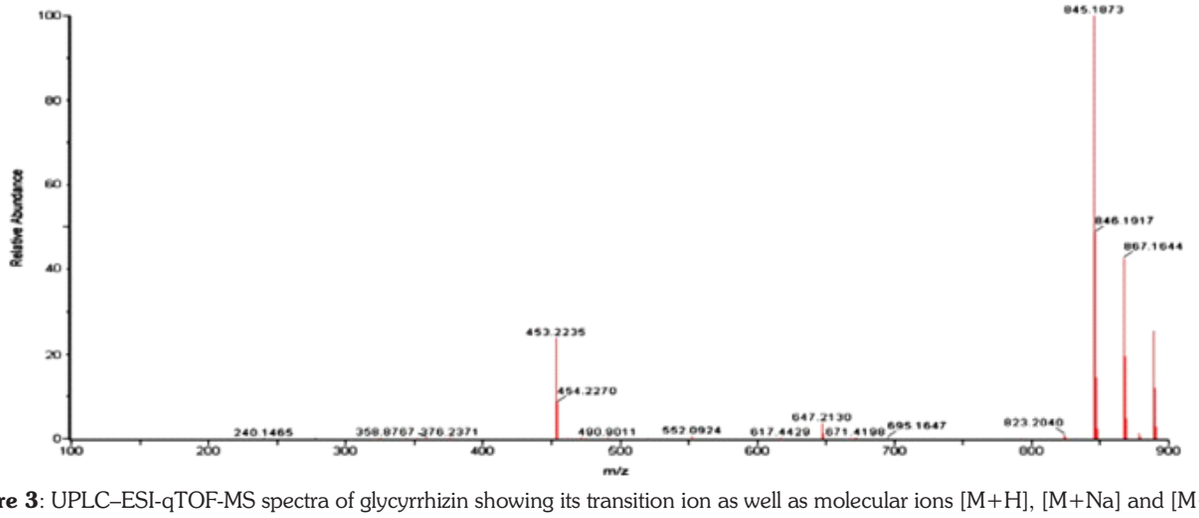

Figure 3: UPLC–ESI-qTOF-MS spectra of glycyrrhizin showing its transition ion as well as molecular ions [M+H], [M+Na] and [M+K].

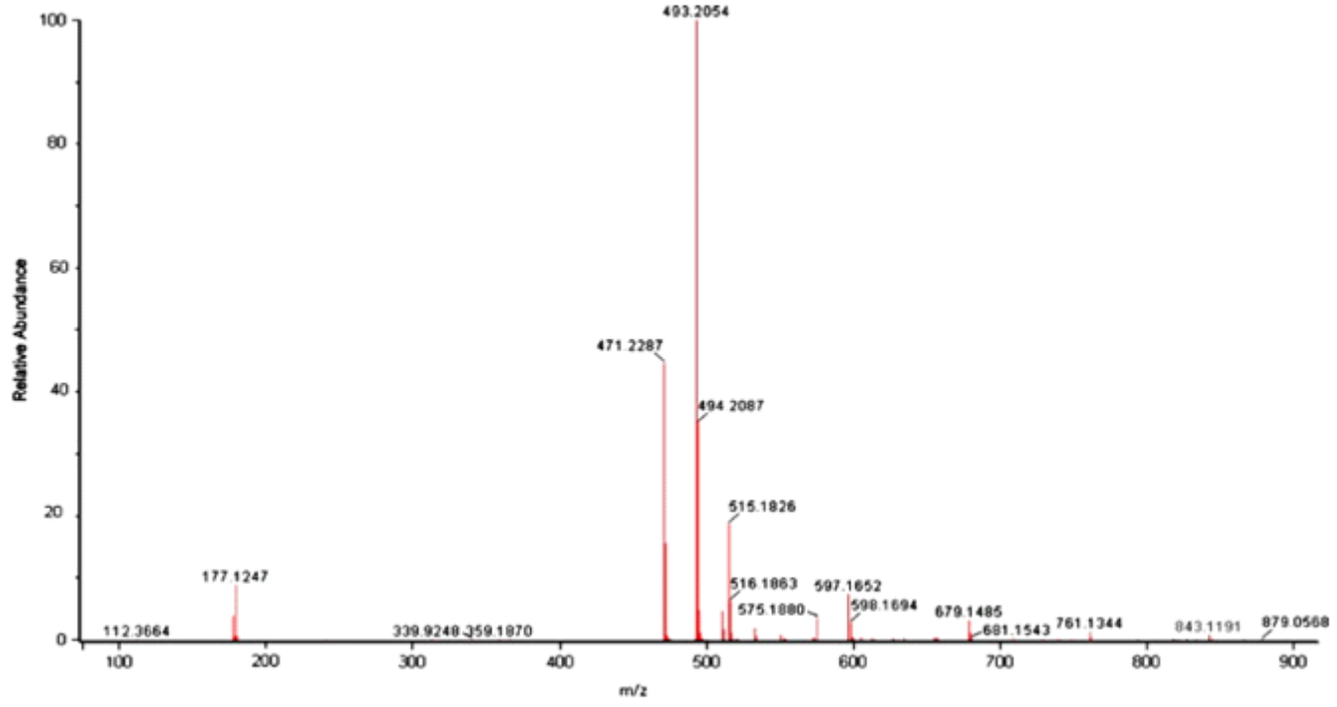

Figure 4: UPLC–ESI-qTOF-MS spectra of glycyrrhetic acid showing its transition ion as well as molecular ions [M+H] and [M+Na].

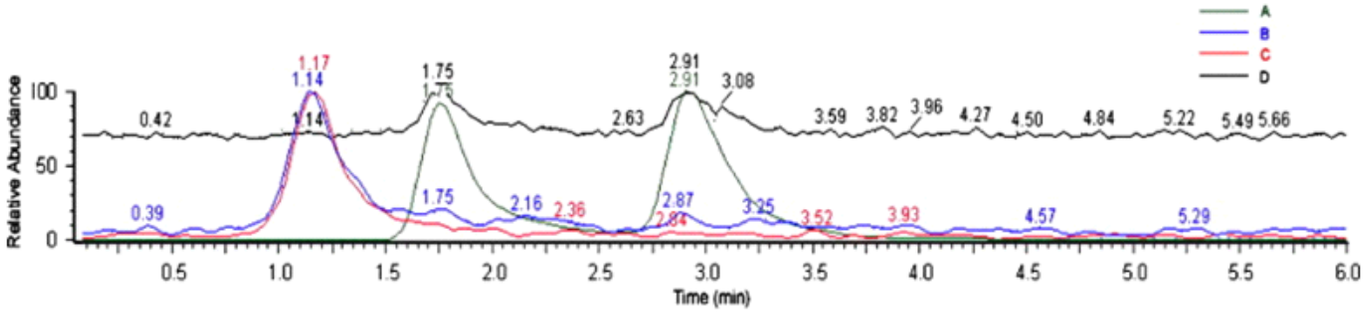

Figure 5: Typical chromatograms. (A) Extracted ion chromatograms of glycyrrhetic acid showing α and β isomers; (B) extracted ion chromatograms of transition ion of glycyrrhizin showing m/z 453.2235; (C) extracted ion chromatograms of glycyrrhizin showing m/z 845.1873 and (D) total ion chromatogram of both glycyrrhizin and glycyrrhetic acid.

5.12 Extraction efficiency studies of *Podophyllum hexandrum* using conventional and non conventional extraction methods by using HPLC –UV –DAD method

Devinder Gupta, Mahendra Verma, Shankar lal, Rajneesh Anand, Ravi Khajuria, Surinder Kitchlu and Surinder Koul

The composition of lignans extracted from *Podophyllum hexandrum* rhizomes was studied by sequential extraction with supercritical CO2, ethyl acetate modified CO2 and methanol modified CO2. The results were compared with the extracts obtained by Accelerated Solvent Extraction (ASE) and soxhlet's methods. The lignan contents comprising of Podophyllotoxin, deoxypodophyllotoxin, 4'-demethylpodophyllotoxin, Picropodophyllotoxin, Isopicropodophyllotoxin, Podophllotoxin-β-Dglucopyranoside and 4'-demethylpodophyllotoxin β-D-glucopyranoside (Figs. 1 a-g) in the extracts of *Podophyllum hexandrum* rhizomes obtained by different methods was studied. There was a variation in the concentration of lignan in the extracts obtained by different methods of extraction (Table. Podophyllotoxin formed the major component (36.55%) of the extract obtained by SFE and picropodophyllotoxin, isopicropodophyllotoxin, deoxypodophyllotoxin and 4'-demethylpodophyllotoxin were present in 6.82, 1.51, 1.46 and 0.85 % respectively whereas 4'-demethylpodophyllotoxin β-D-glucopyranoside was 1.89 % in the extract obtained by ASE which is

higher than SFE extracts. Soxhlet's derived extract contains better concentration of isopicropodophyllotoxin (24.49%) than SFE (Table 1 & Table 2). A simple, isocratic and reliable analytical HPLC-UV (DAD) method (Figs. 3 & 4) was developed for simultaneous identification and quantification of different seven lignans in the extracts of different extraction techniques.

Table 1: Concentrations of different lignans (1-7) obtained by various SFE methods

Extraction method	Extract Yield (%)	Concentration of different lignans (1-7) in extracts obtained by using different SFE conditions (%)						
		1	2	3	4	5	6	7
CO2 (S-1)	-	-	-	-	-	-	-	-
CO2 (S-2)	0.1	13.98	1.62	0.96	7.47	1.20	**5.51**	**7.73**
ethyl acetate modified CO2 (S-1)	0.61	**52.12**	0.76	**1.59**	**11.71**	**16.14**	0.72	0.09
ethyl acetate modified CO2 (S-2)	0.27	2.26	0.20	0.08	0.51	0.26	0.33	0.38
methanol modified CO2 (S-1)	0.20	44.33	**5.47**	0.65	5.47	9.51	0.08	0.24
methanol modified CO2 (S-2)	0.71	37.77	1.28	0.54	5.31	5.81	2.47	1.13

Table 2: Concentrations of different lignans (1-7) obtained by various extraction methods

Extraction process	Extract Yield (%)	Concentration of different lignans (1-7) in extracts obtained by different process (%)						
		1	2	3	4	5	6	7
SOX.	18.63	10.75	0.10	--	0.03	**24.49**	0.60	1.58
ASE 50^0	17.05	13.78	0.16	0.01	0.42	8.26	0.14	**1.89**
ASE 60^0	19.25	11.48	0.11	0.64	0.60	7.63	0.27	1.32
SFE	1.89	**36.55**	**1.46**	**0.85**	**6.82**	8.50	**1.51**	0.94

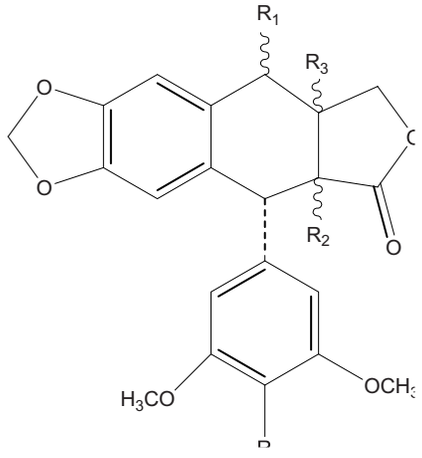

Name of Compounds	R	R_1	R_2	R_3
a. Podophyllotoxin	CH_3	α-OH	β H	α H
b. Deoxypodophyllotoxin	CH_3	H	β H	α H
c. 4'-Demethyl-deoxypodophylltoxin	H	H	β H	α H
d. Picropodophyllotoxin	CH_3	α-OH	α H	α H
e. Isopicropodophyllotoxin	CH_3	α-OH	β H	β H
f. Podophyllotoxin-β-D-glucoside	CH_3	β -D-glucoside	β H	α H
g. 4'-Demethyl podophyllotoxin-β-D-glucoside	H	β-D-glucoside	β H	α H

Figure 1: a-g Structure of different compounds

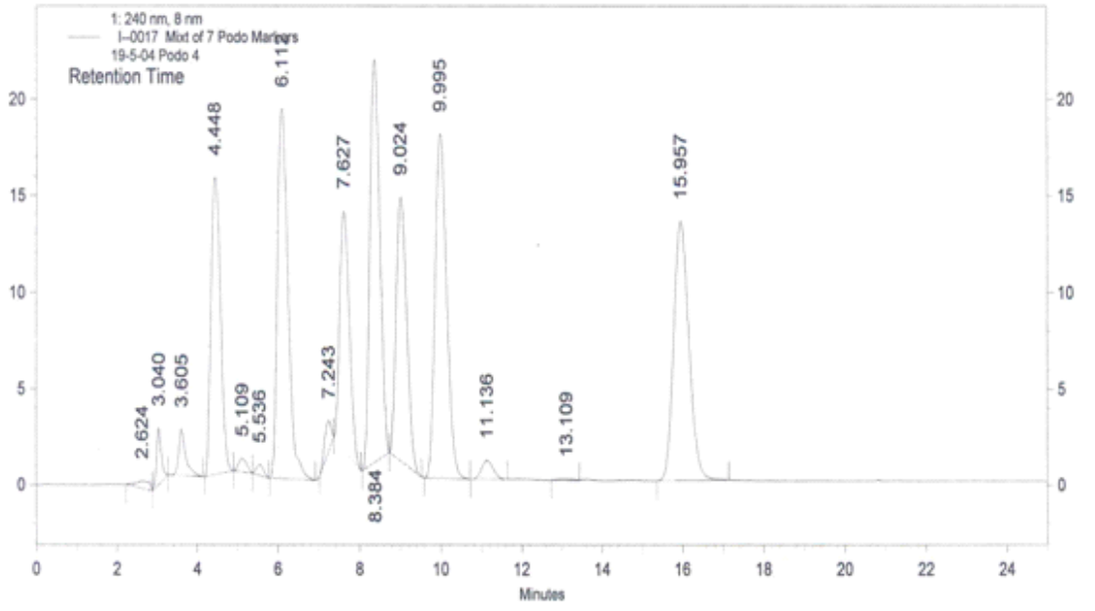

Figure 2: HPLC Chromatogram of standard markers of podophyllum

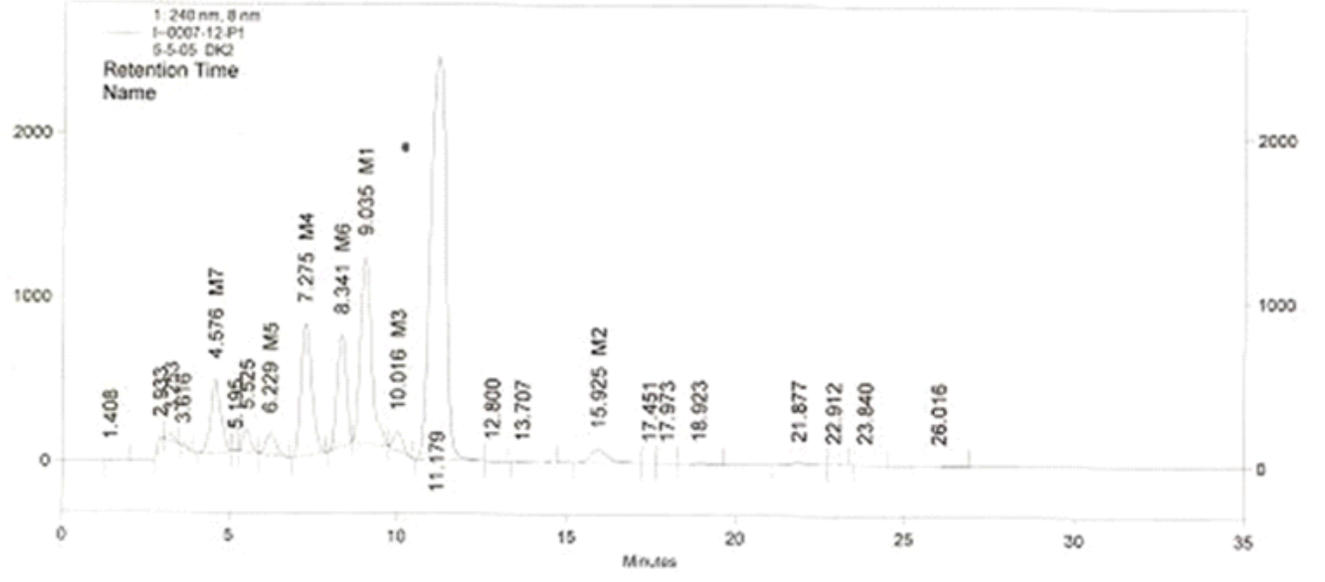

Figure 3: HPLC Chromatogram of extract obtained by SFE at 300 bars

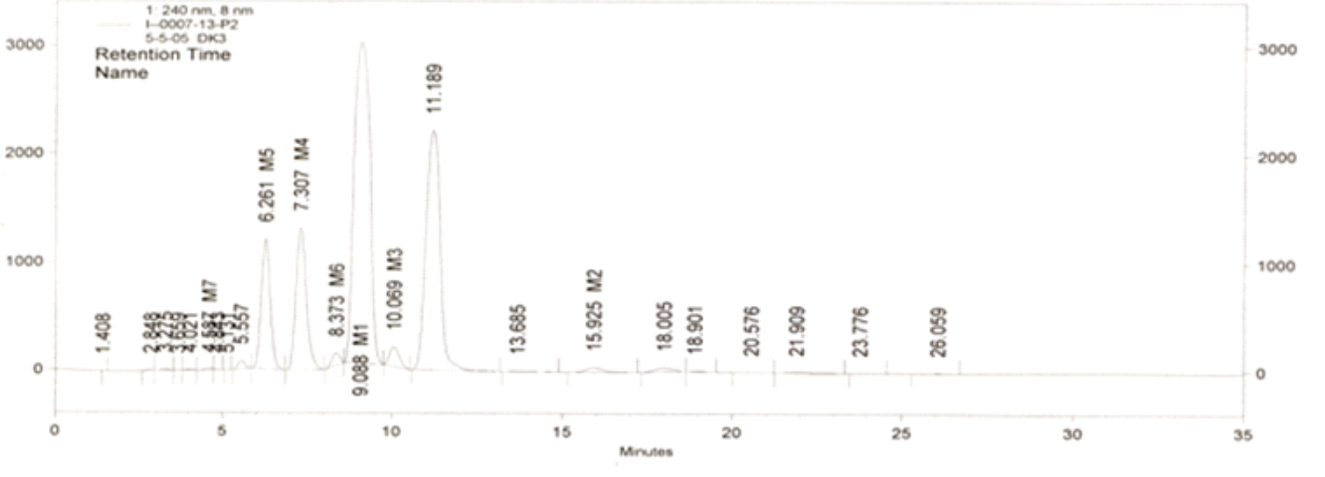

Figure 4: HPLC Chromatogram of SCFE extract obtained by EtoAc modified CO_2 300 Bars

5.13 Development of a validated UPLC-qTOF-MS method for the determination of curcuminoids and their pharmacokinetic study in mice

Mahendra K Verma, Ishtiyaq A Najar, Manoj K Tikoo, Gurdarshan Singh, Devinder K Gupta, Rajneesh Anand, Ravi K Khajuria, Subhash C Sharma and Rakesh K Johri

A specific and sensitive UPLC-qTOF-MS/MS method has been developed for the simultaneous determination of curcuminoids. These Curcuminoids comprises of curcumin, a principal curcuminoid and other two namely, demethoxycurcumin, and bisdemethoxycurcumin obtained from rhizomes of *Curcuma longa* an ancient Indian curry spice turmeric, family (*Zingiberaceae*). These analytes (Fig.1) were separated on a reverse phase C18 column by using a mobile phase of acetonitrile: 5% acetonitrile in water with 0.07% acetic acid (75:25 v/v), flow rate of 100 µL/min was maintained. The qTOF-MS was operated under multiple reaction monitoring (MRM) mode using electro-spray ionization (ESI) technique with positive ion polarity. The major product ions in the positive mode for curcuminoids were at m/z 369.1066, 339.1023 and 309.0214 respectively (Figs.2A, 2B & 2C). The recovery of the analytes from mouse plasma was optimized using solid phase extraction technique. The total run time was 5 min and the peaks of the compounds, bisdemethoxycurcumin, demethoxycurcumin and curcumin occurred at 2.06, 2.23 and 2.40 min respectively. The calibration curves of bisdemethoxycurcumin, demethoxycurcumin and curcumin were linear over the concentration range of 2–1000 ng/mL (r2, 0.9951), 2–1000 ng/mL (r2, 0.9970) and 2-1000 ng/mL (r2, 0.9906) respectively. Intra-assay and inter-assay accuracy (Table 1) in terms of % bias for curcumin was in between −7.95to +6.21, and −7.03 to + 6.34; for demethoxycurcumin was −6.72 to +6.34, and −7.86 to +6.74 and for bisdesmetoxycurcumin was −8.23 to +6.37 and −8.47 to +7.81. The values of Intra-assay and inter-assay precision are presented in Table 2. The lower limit of quantitation for curcumin, demethoxycurcumin and bisdemethoxycurcumin was 2.0 ng/mL. Analytes were stable under various conditions (in autosampler, during freeze-thaw, at room temperature, and under deep-freeze conditions) (Table 3). This validated method was used during pharmacokinetic studies of curcumin in the mouse plasma. A specific, accurate and precise UPLC-qTOF-MS/MS method for the determination of curcumin, demethoxycurcumin and bisdemethoxycurcumin both individually and simultaneously was optimized (Fig. 5).

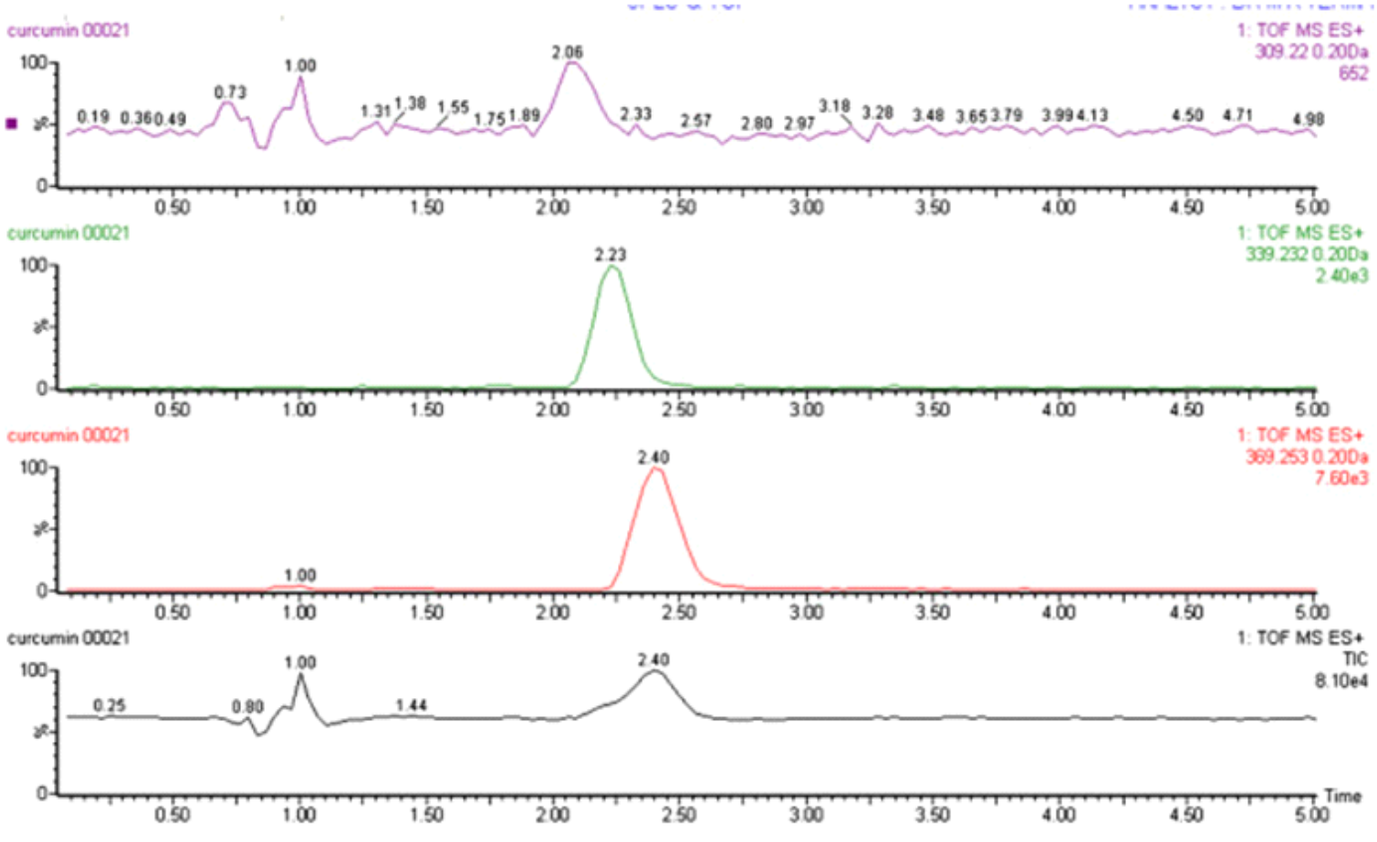

Figure 1: Typical UPLC-qTOF-MS/MS chromatograms showing Curcuminoids. 1 **A**. Extracted ion chromatogram (EIC) of bisdemethoxycurcumin. 1 **B**. Extracted ion chromatogram (EIC) of demethoxycurcumin. 1 **C**. Extracted ion chromatogram (EIC) of curcumin. 1 **D**. Total ion chromatogram (TIC) of Curcuminoids.

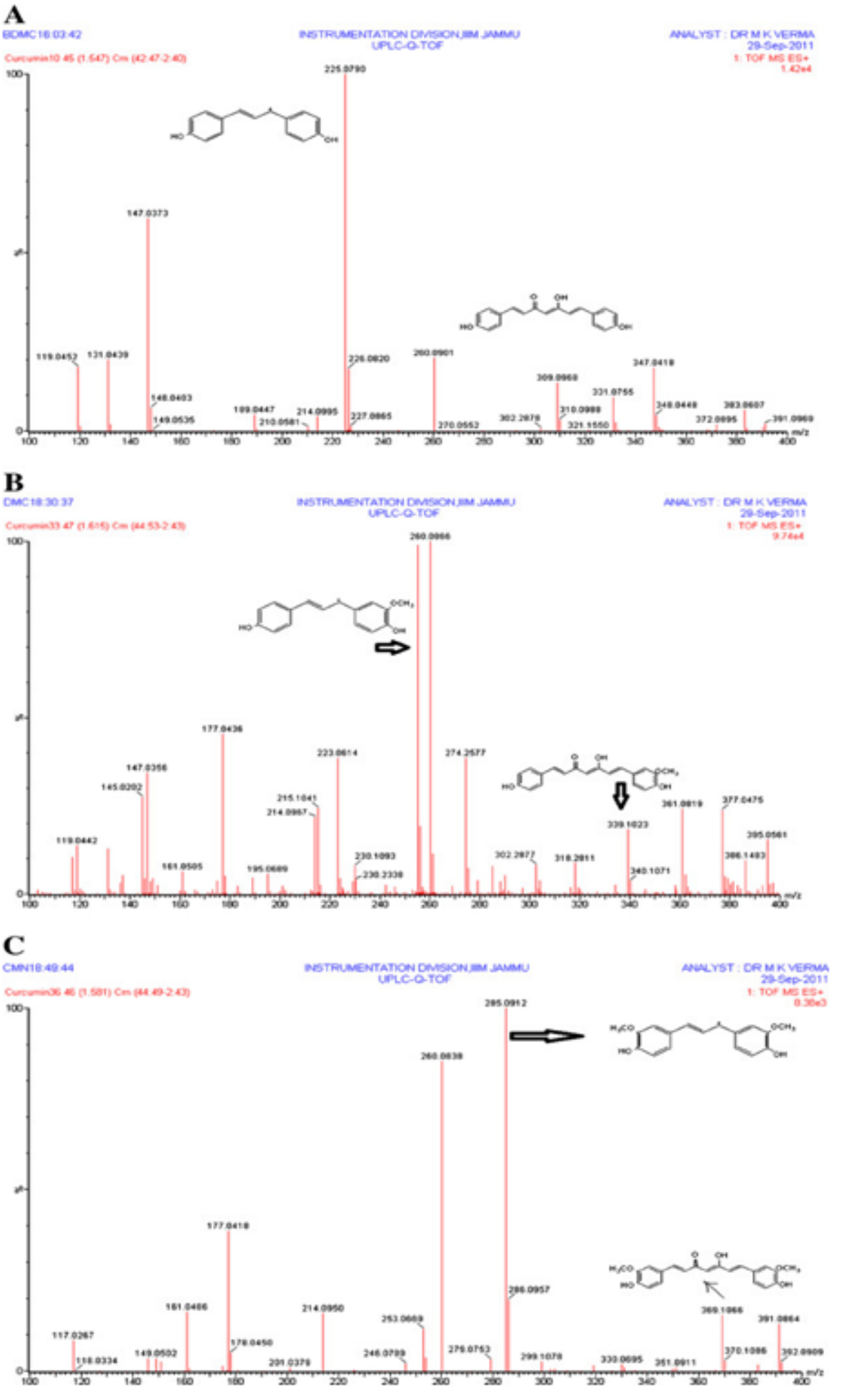

Figure 2: 2 A - Product ion spectra of bisdemethoxrcurcumin showing fragmentation transitions. 2 **B** - Product ion spectra of demethoxrcurcumin showing fragmentation transitions. 2 **C** - Product ion spectra of curcumin showing fragmentation transitions.

Table 1:

Accuracy (% bias) data

Compound	Nominal conc. (ng/mL)	Intra -assay			Inter-assay		
		Set 1	Set 2	Set 3	Set 1	Set 2	Set 3
Curcumin	**2**	+5.81		−7.02	+6.34	+5.38	−5.86
	6	+5.98	−6.29	+6.21	−7.03	+4.39	+5.39
	450	−4.23	+5.09	− 3.86	−5.61	+5.94	4.79
	900	+3.84	−4.72	−5.37	+4.67	−5.38	−5.01
DMC	**2**	+6.34	−5.81	−6.62	+6.74	+5.89	−5.06
	6	+5.68	−6.72	+6.04	−7.86	+4.95	+6.21
	450	−4.73	+5.89	− 5.31	−5.88	+5.04	−5.86
	900	+5.09	−4.38	−5.66	+5.17	−6.72	−4.71
BDMC	**2**	+6.37	−8.23	−7.91	+6.73	+7.81	−6.54
	6	+ 5.28	−6.98	+7.41	−8.47	+6.39	+5.86
	450	−6.29	+5.73	− 6.06	−6.80	+5.68	− 6.89
	900	+5.87	−6.32	−6.98	+5.69	−4.63	− 7.08

Table 2:

Precision (% RSD) data

Compound	Nominal conc. (ng/mL)	Intra-assay			Inter-assay		
		Set 1	Set 2	Set 3	Set 1	Set 2	Set 3
Curcumin	**2**	8.31	7.34	7.93	8.59	6.57	7.81
	6	6.38	7.51	8.76	7.77	8.32	6.68
	450	4.68	6.39	5.51	5.31	6.07	5.85
	900	2.94	3.89	4.79	5.28	4.79	5.53
DMC	**2**	9.27	8.86	9.65	9.85	8.89	9.41
	6	7.41	6.09	7.38	7.05	6.59	9.77
	450	5.24	4.84	6.07	6.18	7.04	6.17
	900	4.41	4.79	6.06	4.69	5.31	4.99
BDMC	**2**	11.37	9.98	10.57	9.23	10.88	10.54
	6	8.68	7.98	9.07	9.35	8.47	9.86
	450	5.86	7.79	8.95	6.32	5.89	5.49
	900	4.46	5.32	5.48	3.69	4.79	6.24

Table 3: Stability Data

Condition	CMN		DMC		BDMC	
	LQC	**HQC**	**LQC**	**HQC**	**LQC**	**HQC**
Recovery (ng) after storage (−80°C)		888.974 ± 1.876	5.90 ±0.161	885±1.948	5.71±0.209	874 ±2.375
0 month						
1 month	5.81±0.165 (98.14%)	853.41 ± 1.451 (95.99%)	5.78±0.178 (97.97%)	861±1.381 (97.29%)	5.57±0.393 (97.55%)	845 ±3.058 (96.68%)
Recovery (ng) after freeze thaw cycles	5.92 ± 0.141	888.974 ± 1.876	5.90± 0.161	885±1.948	5.71±0.209	874 ±2.375
Cycle 0	5.82±0.186	878.413±	5.84±0.181	869±1.768	5.65±0.219	870 ±2.435
Cycle 1	(98.31%)	1.381 (98.81%)	(98.98%)	(98.19%)	(98.94%)	(99.54%)
	5.76±0.314	871.274±	5.81± 0.173	865±1.549	5.63±0.179	864 ±2.021
Cycle 2	(97.29%)	1.576 (98.00%)	(98.47%)	(97.74%)	(98.59%)	(98.85%)
	5.62 ±0.372	852.560± 1.732	5.78± 0.196	861±1.598	5.60±0.247	859 ±2.564
Cycle 3	(94.93%)	(95.90%)	(97.96%)	(97.28%)	(98.07%)	(98.28%)
Recovery (ng) after storage at room temp.	5.92 ± 0.141	888.974 ± 1.876	5.90± 0.161	885±1.948	5.71±0.209	874 ±2.375
0 h	5.62± 0.198	832.231 ±	5.77± 0.293	829±1.321	5.37±0.901	821 ±1.967
24 h	(94.93%)	1.451 (93.61%)	(97.79%)	(93.67%)	(94.04%)	(93.93%)
Recovery (ng) after storage in auto sampler	5.92 ± 0.141	888.974 ± 1.876	5.90± 0.161	885±1.948	5.71±0.209	874 ±2.375
0 h	5.80± 0.219	872.136 ±	5.77± 0.293	858±1.973	5.56±0.214	854 ±3.057
24 h	(97.97%)	2.151 (98.10%)	(97.79%)	(96.95%)	(97.37%)	(97.71%)

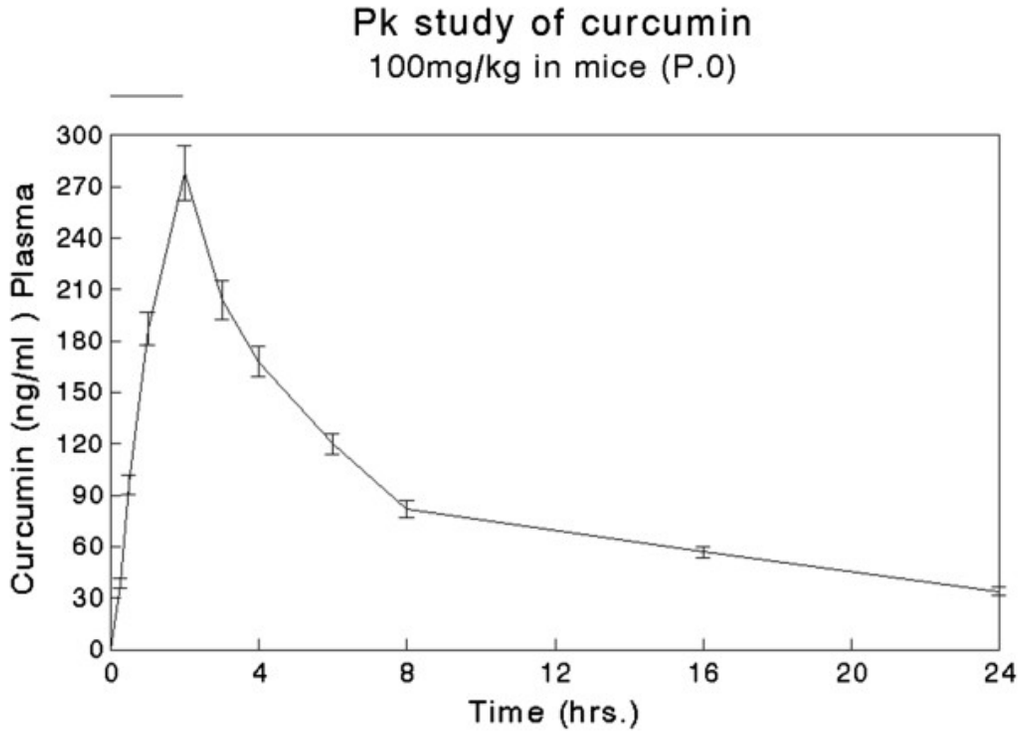

Figure 3: Plasma concn. vs. time curves of curcumin (100 mg/kg, p.o).

Table 4: Pharmacokinetic parameters (curcumin)

AUC $_{0-\infty}$ (ng*hr/ml)	
C $_{max}$ (ng/ml)	278.0± 18.6
T $_{max}$ (hr)	2.0
Half Life (hr.)	10.1±0.96
Clearance (L/hr)	46.125±2.39
Vd (L/kg)	502.06±23.2
MRT (hr.)	18.3±1.21

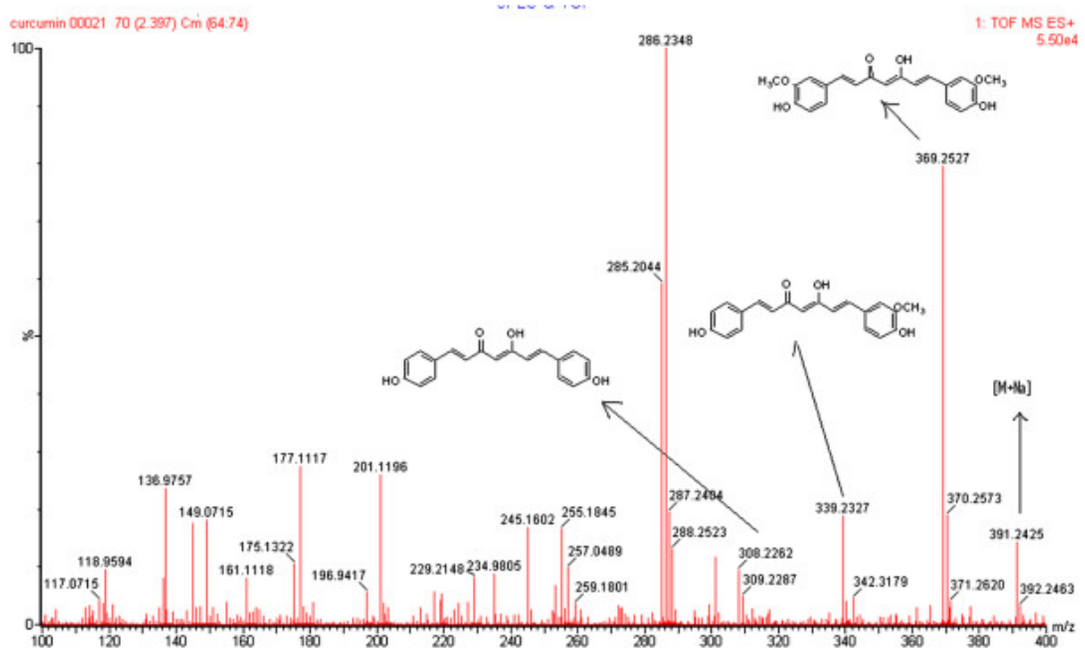

Figure 4: The mass spectrum of curcuminoids in combination showing the molecular ion peaks, chemical structures and molecular weights

5.14 Intramolecular base free reaction for the synthesis of benzannulated chiral macrocycles embedded in carbohydrate templates sonogashira

Altaf Hussain, Syed Khalid Yousuf, Deepak Kumar, Malikharjunarao Lambu, Baldev Singh, Sudip Maity and Debaraj Mukherjee

A base free intramolecular Sonogashira reaction based general approach has been established for the DOS of fused bi- and tri-cyclic systems containing benzannulated 10-13 membered chiral macrocycles embedded in carbohydrate templates. Macrocycles with different ring sizes have been prepared by pre-designing the chiral building blocks. Base sensitive groups like acetyl and TBDPS survived the reaction conditions (Fig. 1).

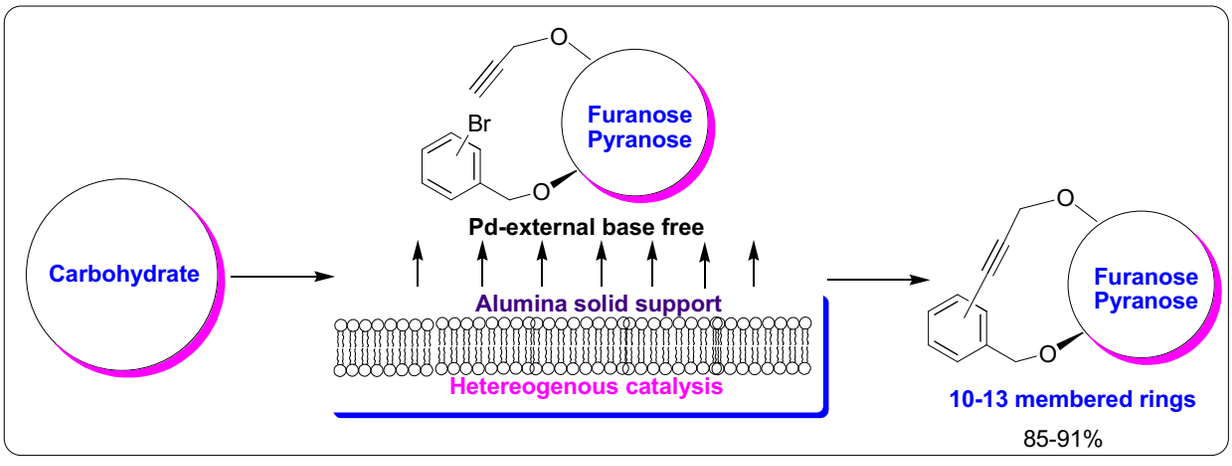

Figure 1: Synthesis of benzannulated 10-13 membered sugar derived macrocycles.

5.15 Regioselective azidotrimethylsilylation of carbohydrates and applications thereof

Mallikharjuna Rao L, Syed Khalid Yousuf, Debaraj Mukherjee and Subhash Chandra Taneja

Azidotrimethylsilylation of carbohydrates (monosaccharides and disaccharides) has been achieved in high yields under Mitsunobu conditions. The azidation of carbohydrates is effected at 0 °C essentially only at the primary alcoholic position in mono, di- and triols in protected/unprotected glycosides, whereas the remaining secondary hydroxyl groups got silylated. Surprisingly, no azidation of the secondary hydroxyls was observed in all the carbohydrate substrates. Applications of the methodology for the synthesis of amino sugars, triazoles and azasugars have achieved (Fig. 1).

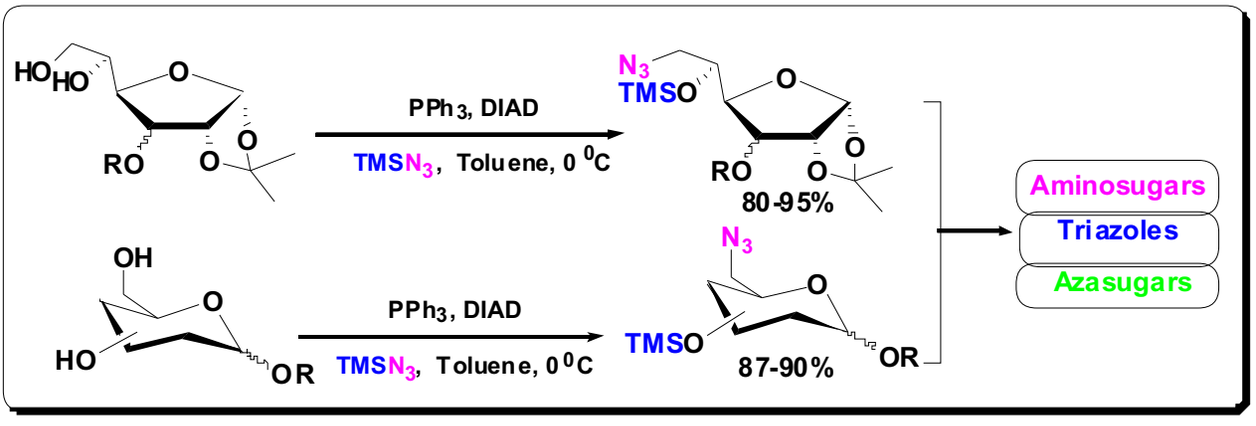

Figure 1: Tandem azidotrimethylsilylation of furanose and pyranose derivatives.

5.16 Design and synthesis of novel N,N'-glycoside derivatives of 3,3'-diindolylmethanes as potential antiproliferative agents

Deepak K. Sharma, Bilal Rah, Mallikharjuna R. Lambu, Altaf Hussain, Syed K. Yousuf, Anil K. Tripathi, Baldev Singh, Gayatri Jamwal, Zabeer Ahmed, Nayan Chanauria, Amit Nargotra, Anindya Goswami and Debaraj Mukherjee

A library of 34 compounds containing the DIM core have been synthesized and tested for their anticancer efficacy by measuring their cytotoxicity to cancer cell lines A549, HeLa and MCF-7. Some of the selected derivatives were N-glycosylated to increase their efficacy. Compound 7d, an N-glycosylated DIM derivative, was found to be effective at 1.3, 0.3 and 0.9 mmol concentrations against A549, HeLa and MCF-7, respectively. Immunochemistry studies revealed that it could induce apoptosis by upregulating a pro-apoptotic protein Par-4 and concomitantly diminishing the expression of prosurvival proteins Bcl-2 and GRP78. Flow cytometry studies showed that the compound arrested cells in the G1 phase of the cell cycle and significantly abrogated the motility of HeLa cells. Computer docking simulations of 7d with GRP78 suggested its involvement in two H-bonds with Asp78, two H-bonds with Arg290, one with Arg367, and one water mediated H-bond interaction. The interaction patterns also demonstrated that the presence of bromide in the vicinity (within 3.5 A°) of Lys294 generates the possibility of a halogen bond, which may also contribute in providing some extra stability to the complex. Hence, compounds of this class will be useful for the design of new anticancer agents (Fig. 1).

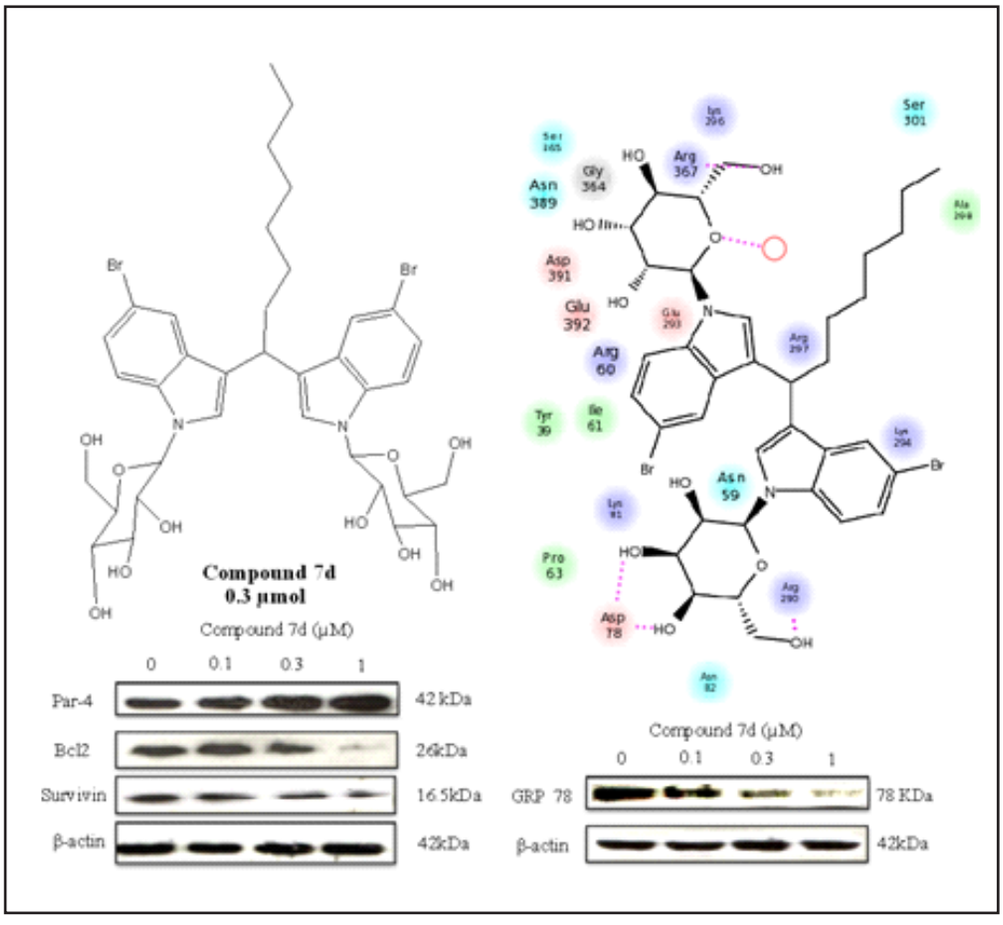

Fig.1: Anticancer activity of N,N' -glycoside derivatives of DIM toward Par-4 GRP78.

5.17 Fe/Al pillared clay catalyzed solvent-free synthesis of bisindolylmethanes using diversly substituted indoles and carbonyl compounds

Deepak Kumar Sharma, Altaf Hussain, Mallikharjuna Rao Lambu, Syed Khalid Yousuf, Sudip Maiety, Baldev Singh and Debaraj Mukherjee

Fe/Al pillard clay catalyzes solvent-free synthesis of bisindolylmethanes using diversly substituted indoles and carbonyl compounds. Reaction proceeds in the presence of 0.5 mol% of Fe/Al pillard clay-425°C for 10–30 min. Key features of the protocol include its efficiency for N substituted alkyl, benzyl, sulphonyl, glycosides and triazole derivatives of indoles. Products were obtained in excellent yields and the catalyst can be easily recycled several times without significant loss of activity (Fig. 1).

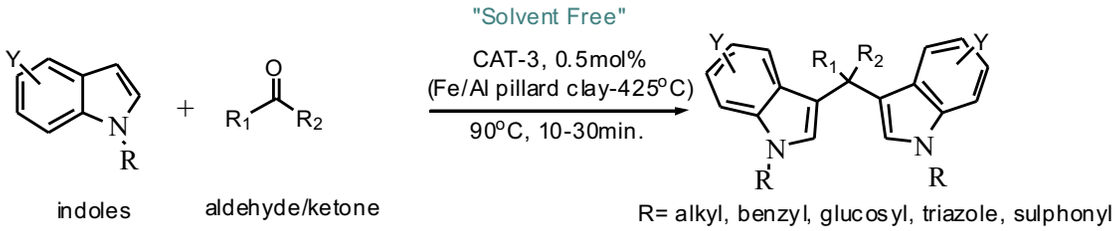

Fig.1: Synthesis of diindolylmethanes derivatives using Fe/Al pillard Clay-425°C

5.18 2,4,6-Trichloro-1,3,5-triazine (TCT) mediated one-pot sequential functionalisation of glycosides for the generation of orthogonally protected monosaccharide building blocks

Madhubabu Tatina, Syed Khalid Yousuf and Debaraj Mukherjee

Orthogonally protected monosaccharide building blocks have been prepared using TCT in a one-pot multicomponent transformation. The process involves successive steps of arylidene acetalation, esterification and regioselective reductive acetal cleavage. High regioselectivity, scope for using a broad range of substrates, functional group tolerance, mild reaction conditions, easy handling process and wide application range are a few advantages of the current process (Fig. 1).

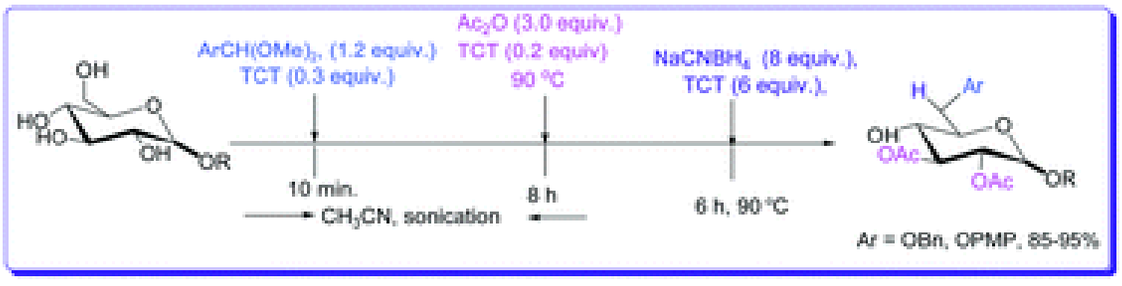

Fig.1: Genereation of orthogonally protected monosaccharide under TCT condition.

5.19 Catalyst and solvent-free, ultrasound promoted rapid protocol for the one-pot synthesis of α-aminophosphonates at room temperature

Bashir Dar, Amrinder Singh, Akshya Sahu, Praveen Patidar, Arup Chakraborty, Meena Sharma and Baldev Singh

An ultrasound promoted easy, efficient, and environment friendly process has been devised for the synthesis of α-aminophosphonates within seconds through a one-pot three-component condensation of the aldehydes, amines, and triethylphosphite (Scheme 1). The desired products were obtained in excellent yields and in high purity under solvent-free and catalyst-free conditions. Study with various aldehydes and amines reveals that ultrasound radiation plays a key role in the direct synthesis of α-aminophosphonates. α-Aminophosphonates are among the most studied bioactive compounds which are reported to possess antitumor,anti-inflammatory,and antibiotic activities. Their potential as good enzyme inhibitors, herbicides , peptide mimetics, fungicides, insecticides plant growth regulators etc. is also well documented.

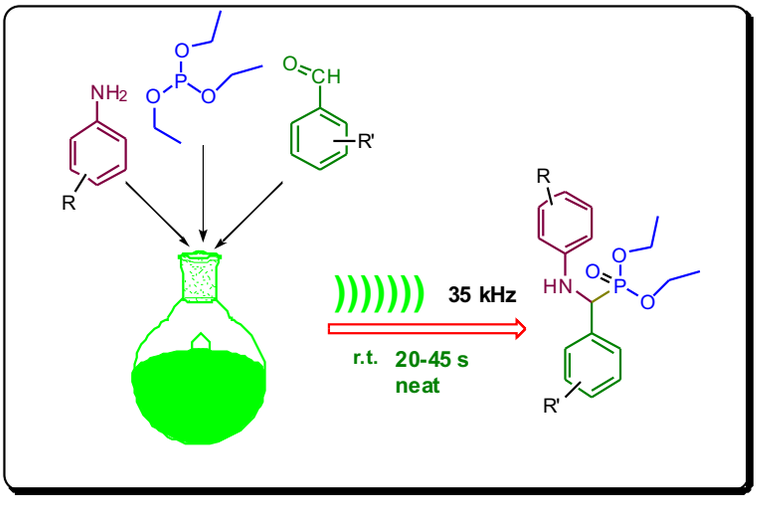

Scheme 1: Ultrasound promoted one-pot synthesis of α-aminophosphonates

The sonochemical effect might be the key factor to the high efficiency of the one-pot and solvent-free reactions. Various aromatic aldehydes containing electron donating or electron withdrawing functional groups were treated with various amines and did not show any remarkable difference in the yield of the desired products.

5.20 Heteropolyacid-clay nano-composite as a novel heterogeneous catalyst for the synthesis of 2,3-dihydroquinazolinones

Bashir A. Dar, Akshya K. Sahu, Praveen Patidar, Parduman R. Sharma, Nagaraju Mupparapu, Dushyant Vyas, Sudip Maity, Meena Sharma and Baldev Singh

A tremendous upsurge of interest in heterogeneous catalysis for various organic transformations has occurred because the heterogeneous catalysts possess the advantages such as operational simplicity, environmental compatibility, non-toxicity, reusability, low cost, and ease of isolation. Heterogenization of heteropolyacids by supporting them on solid supports such as zeolites and clays, has reached great development in different areas of organic synthesis. The Keggin-type heteropolyacids (HPAs), typically represented by the formula H_{8-x} $[XM_{12}O_{40}]$, (X = heteroatom, x is its oxidation state and M = addenda atom) have been extensively used in acidcatalyzed reactions because of their strong Brønsted acidity. $H_3[PW_{12}O_{40}]$ (TPA), is considered among the strongest acids and hasfairly high thermal stability decomposing at 465 °C. Vanadium substitution in the Keggin structure is reported to enhance the catalytic activity of the HPAs. Though the pure HPAs (homogeneous liquid phase) as catalysts are advantageous due to their low volatility, low corrosiveness, high acidity, activity and flexibility, the drawback lies in their low surface area (1–10 m^2/g) and the problem of separation from the reaction mixture. To overcome the above mentioned problems to be more effective for catalytic reactions, HPAs are usually impregnated on different porous materials. The type of carrier, its textural and structural properties influence the thermal stability and the catalytic activity of Keggin-type heteropolyacids. Clays have been reported to act as catalysts or catalyst supports because of their layer structure, high surface area, pore volume, pore diameter and higher surface acidity. Thus clays can be used as an efficient support for HPAs and it is believed that uniform dispersion of HPAs on porous clay support with high surface area increases the overall acidity and catalytic activity of the composites. High activity of vanadium-containing HPAs and the property of clays as catalyst support prompted us to explore the activity of vanadium substituted TPA supported on clay as a heterogeneous catalyst for the synthesis of 2,3-dihydroquinazolinones (Scheme 1).

We tried vanadium substituted Heteropolyacids-clay nano-composites of different HPA: Clay ratios. Out of which heteropolyacids HCNC-4 was found to be most active in terms of product yield, selectivity, ease of isolation and recyclability of the catalyst. To the best of our knowledge this catalyst has not been reported till date for the synthesis of 2,3-dihydroquinazolinones. This catalyst afforded excellent yields in very short reaction times that show high selectivity without affecting other functional groups, such as carbon–carbon double bond and heterocyclic moieties. The catalyst could be recycled at least six times and reused. The synthesis involves cyclo-condensation of anthranilamide with an aldehyde at room temperature in the presence of small amount of the catalyst. XRD and SEM of the catalyst are shown in figure 1 and figure 2 respectively.

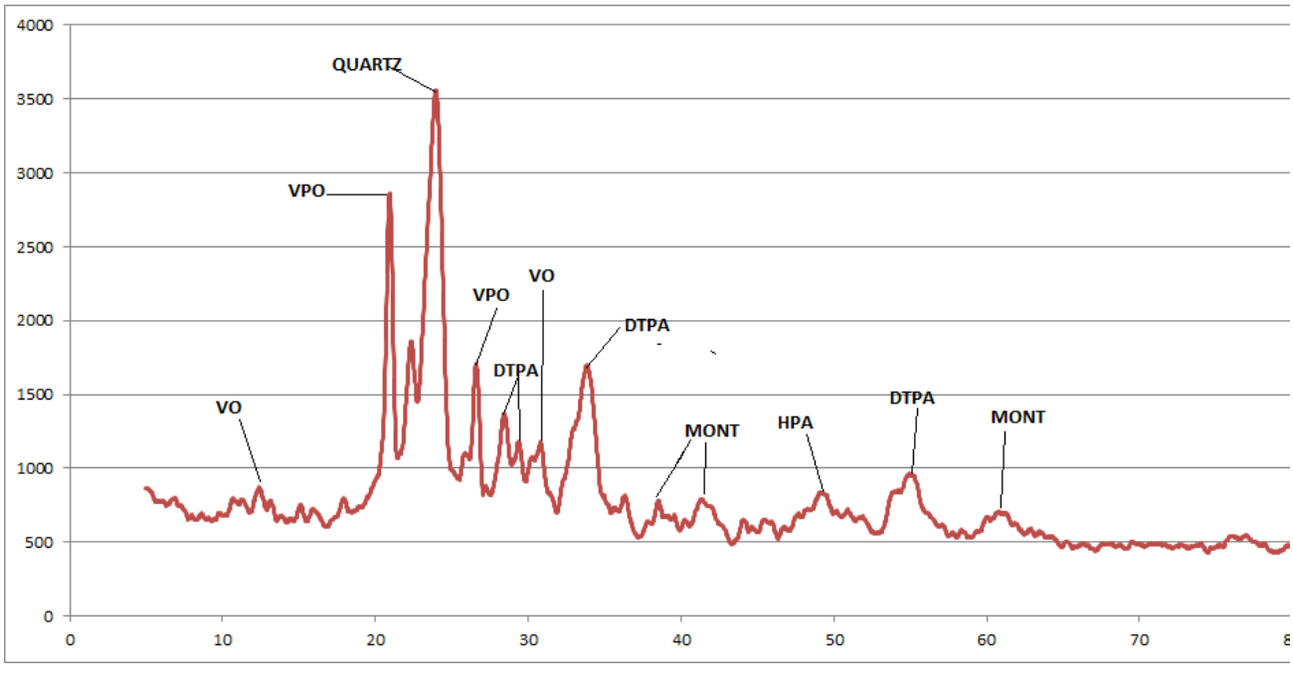

Figure 1: Powder X-ray diffraction for heteropolyacid supported on montmorillonite.

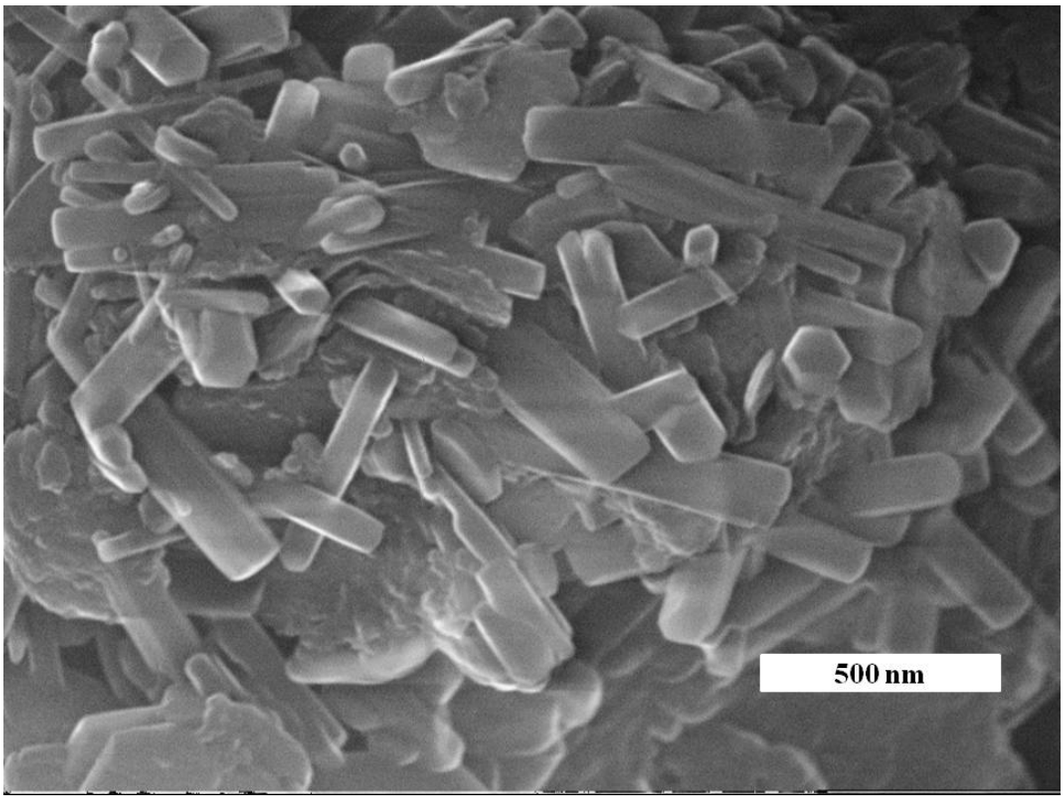

Figure 2: SEM image of Heteropolyacid clay nano-composite.

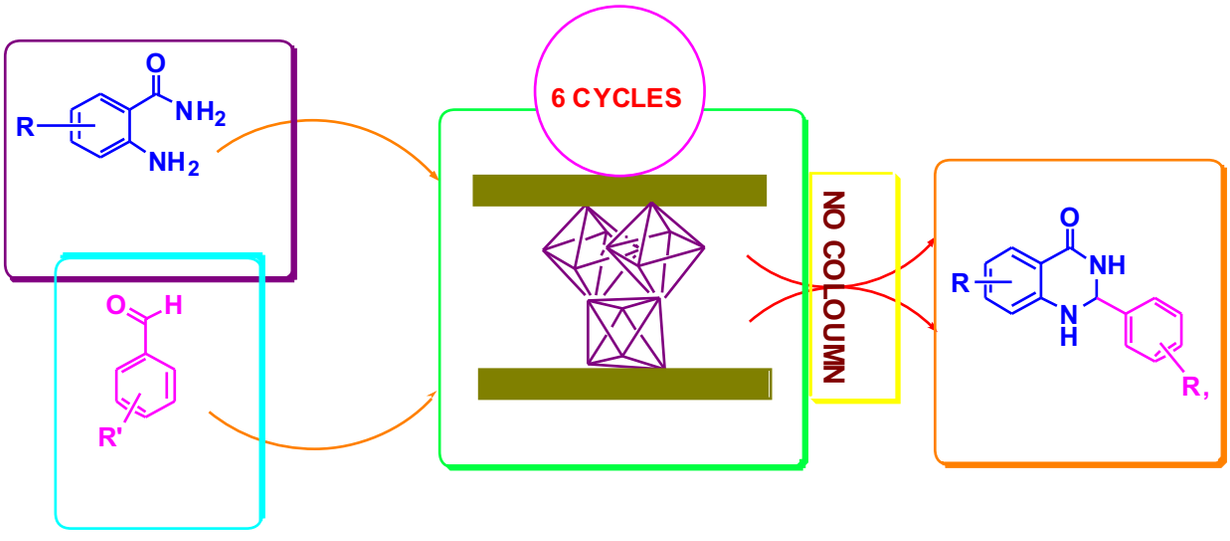

Scheme 1: HPA -Clay catalysed synthesis of 2,3-dihydroquinazolinones

5.21 Grinding-induced rapid, convenient and solvent free approach for the one pot synthesis of α-aminophosphonates using aluminium pillared interlayered clay catalyst

Bashir Ahmad Dar , Arup Chakraborty , Parduman R. Sharma , Varsha Shrivastava, Amrita Bhowmik , Dushyant Vyas, Prince Bhatti, Meena Sharma and Baldev Singh

An easy to prepare aluminium pillared interlayered clay (PILC) has been developed as a stable, recyclable and heterogeneous catalyst to promote the one-pot three component synthesis of α-aminophosphonates under solvent-free conditions using grindstone chemistry (Scheme 1). Utilization of mild reaction conditions, clean conversion and greater selectivity under grinding conditions along with effortless separation, and purification of reaction products make this process extra attractive. XRD and SEM of AlPILC are given in figure 1 and figure 2.

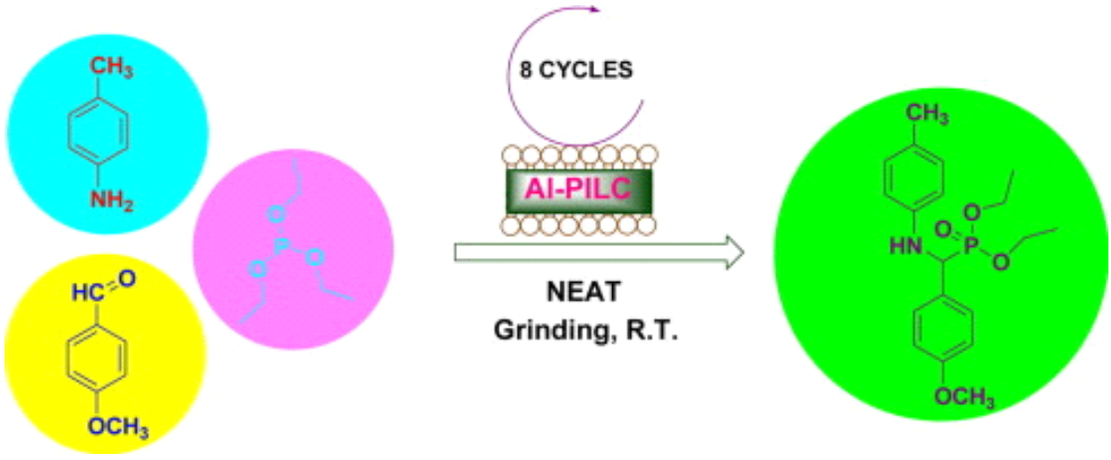

Scheme 1. Aluminium pillared interlayered clay catalysed one-pot three component synthesis of α-aminophosphonates using grindstone chemistry

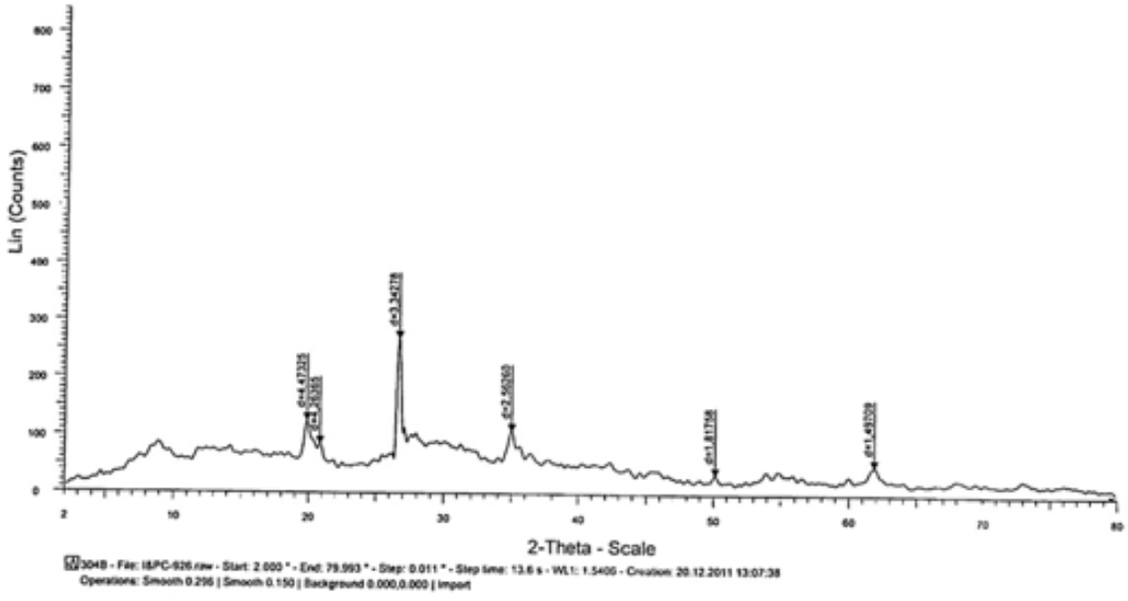

Figure 1 XRD of Al-PILC

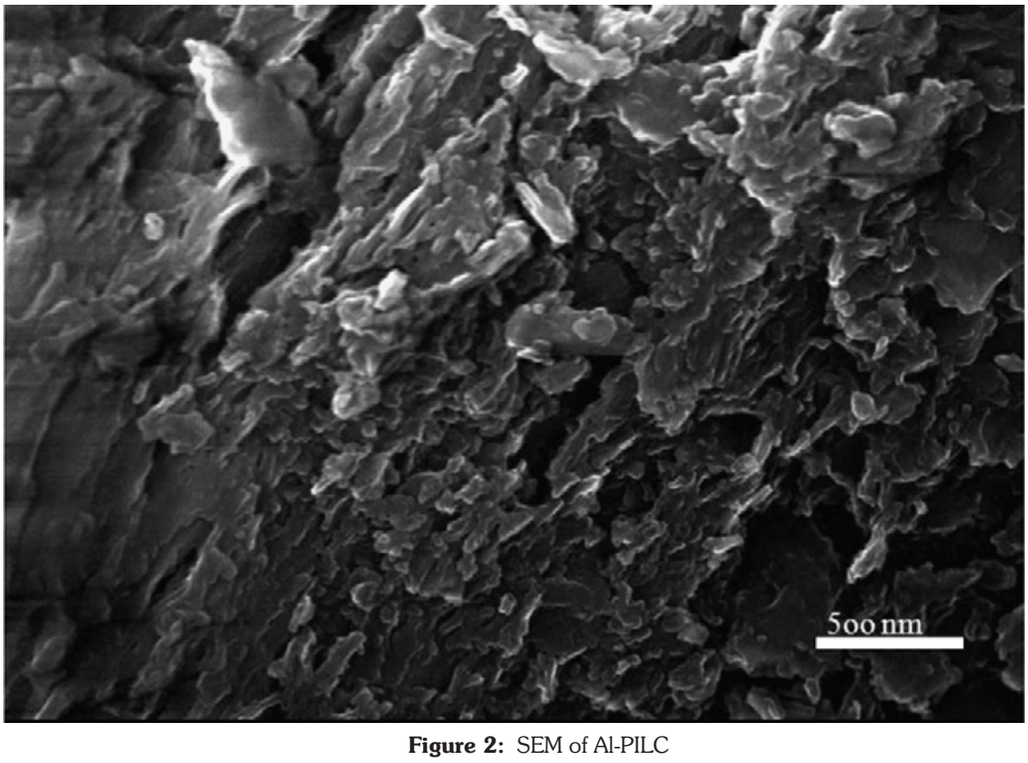

Figure 2: SEM of Al-PILC

5.22 Ultrasound promoted efficient and green protocol for the expeditious synthesis of 1, 4 disubstituted 1, 2, 3-triazoles using Cu(II) doped clay as catalyst

Bashir Ahmad Dar, Amrita Bhowmik, Amit Sharma, Pardhuman R. Sharma, Anish Lazar, A. P. Singh, Meena Sharma and Baldev Singh

We herein report Cu(II) doped Clay as a novel, environmentally benign, recyclable, efficient, and heterogeneous catalyst for the one pot synthesis of 1,2,3-triazoles via a three-component reaction of benzyl or alkyl halides, sodium azide and terminal alkynes, without using sacrificial reducing agents or ligands (using H_2O:EtOH (1:1) mixture as solvent) under ultrasonic conditions at room temperature (Scheme 1). Application of ultrasound irradiation along with heterogeneous Cu(II) catalyst makes this protocol far more advantageous than the earlier reported methods, which usually suffer from long reaction times even at elevated temperature. Ultrasound irradiation has been well established energy source to promote chemical reactions. Many homogeneous and heterogeneous reactions can be conducted smoothly by sonication under milder conditions and shorter reaction times to afford improved yields and increased selectivities. Ultrasound irradiation has some potential effects on a heterogeneous catalytic system, like increase of active catalyst surface area, promotion of cavitation bubble formation and removal of impurities deposited on the catalyst. The cavitational energy induced by ultrasonication, augments both mass transfer and electron transfer from the catalyst surface to the organic substrate and facilitates the catalyst reactant interaction. Clays and modified clays have received substantial consideration as heterogeneous catalysts in organic synthesis because of their high catalytic activity, environmental compatibility and reusability. Due to their typical layer structure and the excellent intercalation properties Clays have a great potential to host metals and metal oxides. Inspired by these properties of clays we prepared the Cu(II) doped clay catalyst(CDC) using commercially available Montmorillonite KSF and studied its catalytic activity for ultrasound promoted one pot synthesis of triazoles.

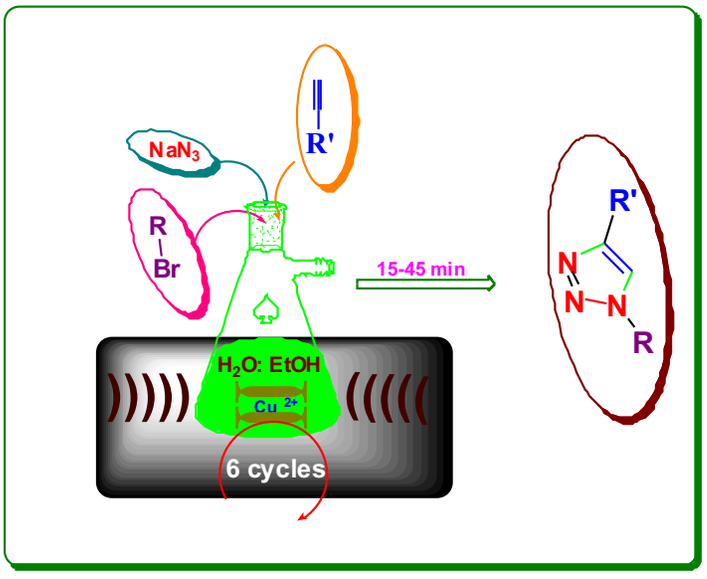

Scheme 1: Cu(II) doped Clay catalyzed one pot synthesis of 1,2,3-triazoles under ultrasonic conditions at room temperature

The H_2 TPR curves of the catalyst (fig.1) show three reduction peaks, a major peak centered at 225°C, small broad shoulder at 370°C and a small broad peak at 540°C which indicates stepwise reduction of Cu^{2+}. The large signal peak at 225°C can be attributed to the reduction of highly dispersed small CuO particles to Cu^{1+} and the small peak at 370°C is assigned to the reduction of bulk Cu^{1+} to Cu^{0+}. The small broad peak at and 540°C is attributed to reduction of iron impurities present in the clay.

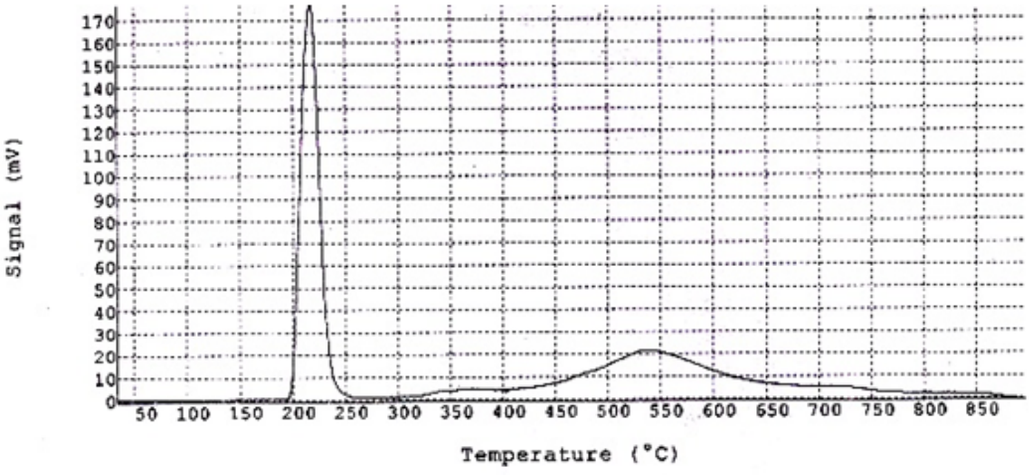

Figure 1: TPR curves of the catalyst

Fig. 2 shows the presence of very low intensity diffraction peaks at 2θ =36.1, 37.7, 38.9, 48.8, 53.60 and 58.7 attributing to (110), (002), (111), (202) of CuO indicates that there are no sharp crystalline phases, indicating that CuO is supported on MKSF in the form highly dispersed fine particles. These results are also supported by the SEM results (fig. 3)

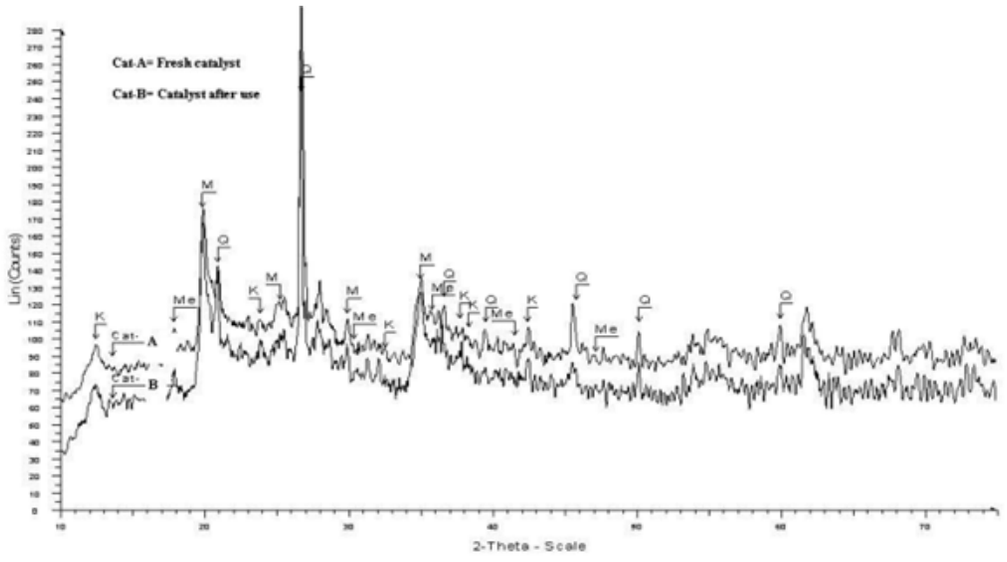

Me: Melanothallite [Cu_2OCl_2]; K: Kaolinite-1A, [$Al_2Si_2O_5(OH)_4$]; M: Montmorillonite-18A [$Na_{0.3}(AlMg)_2Si_4O_{10}OH_2\,6H_2O$]; Q: Quartz [$SiO_2$]

Figure 2: XRD of Cu-Clay catalyst

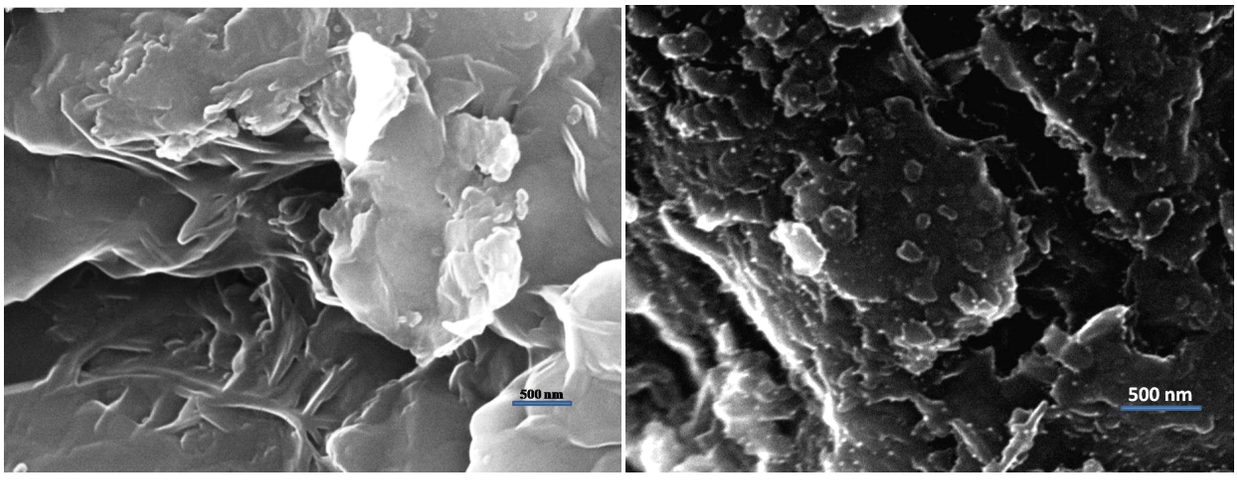

Figure 3: SEM of Clay SEM of Cu-Clay

5.23 Ultrasound promoted expeditious, catalyst free and solvent free approach for the synthesis of N,N'-diarylsubstituted formamidines at room temperature

Bashir Ahmad Dar, Syed Naseer Ahmad, Mohammad Arif Wagay, Altaf Hussain, Nisar Ahmad , Khursheed Ahmad Bhat, Mohammad Akbar Khuroo, Meena Sharma and Baldev Singh

An effortless and efficient protocol was developed for the synthesis of N,N'-diarylsubstituted formamidines under environment friendly conditions. Ultrasonic energy was employed to obtain the desired products in excellent yields with high purity under solvent-free and catalyst-free conditions. Products were purified by crystallization technique to avoid excess utilization of organic solvents. Organic compounds containing formamidine scaffold have been studied extensively because of their significant applications as bioactive molecules, synthons for various chemical transformations, chelating or bridging modes, building blocks in polymer synthesis, ultraviolet light absorbers, bleaching agents for paper, ligands in transition metal catalysts for asymmetric synthesis, protecting groups for primary amines and support linkers in solid phase synthesis. Moreover, formamidines are useful to the physical chemists for

dynamic NMR study. Some cryoscopic molecular weight determination experiments have also been reported using the molecular association property of benzene solution of diarylformamidines.

Several methods have been reported for the synthesis of formamidines but most of these protocols have suffered from several problems such as the use of toxic organic solvents (either in conducting of reaction or working-up of product), high temperatures, low reaction rate, strong acidic conditions, low yields of the products, tedious work-up and application of excess amounts of reagents. Therefore, highly efficient and environmentally benign procedure to prepare N,N-diarylformamidines is still demanded.

Application of ultrasonic energy in chemical transformation is an attractive and effective approach to solve the problem of poor reaction rate. The main cause of low reaction rate is due to poor contact between the reactants and poor mass transfer. Subjecting reaction mixture to the ultrasound irradiation coerces the fluids to generate huge number of cavitation bubbles which grow rapidly and subsequently undergo violent collapse. These vigorous collapses result in the creation of micro-jets that can produce fine emulsion between the reactants. Moreover, these collapses also lead to the amplification in the local temperature within the reaction mixture. Many chemical reactions can be conducted smoothly by sonication to afford improved yields and increased selectivity. Thus, the ultrasound irradiation has been established as an important technique in organic synthesis.[29] In continuation of our interest in ultrasound assisted organic reactions, we herein describe the ultrasound promoted procedure for the synthesis of N,N'-diarylsubstituted formamidines with different species of aryl amines, in catalyst free and solvent-free conditions (Scheme 1). The rapid kinetics under mild conditions, simple work-up and easy purification are added advantages of this protocol.

In the present study one of the reactants trethylorthoformate is a low molecular weight liquid so each reaction mixture is a liquid suspension. Sonochemical reactions occur due to acoustic cavitation in liquids. Cavitational collapse produces intense local heating (~5000 K), high pressures (~1000 atm), and enormous heating and cooling rates (>10 9 K/sec). Acoustic cavitation provides a unique interaction of energy and matter, and ultrasonic irradiation of liquids causes high energy chemical reactions to occur. When liquids containing solids are irradiated with ultrasound, cavity formed near a solid surface collapse is non-spherical manner and drives high-speed jets of liquid into the surface. Ultrasonic irradiation of liquid-powder suspensions produces high velocity inter-particle collisions as a result of acceleration of solid particles to high velocities caused by cavitation and the shockwaves it creates in slurry. Based on the results of this study, it seems that the ultrasound radiations are sufficient to drive this reaction in the absence of any catalyst with decreased reaction times and improved yields of desired products.

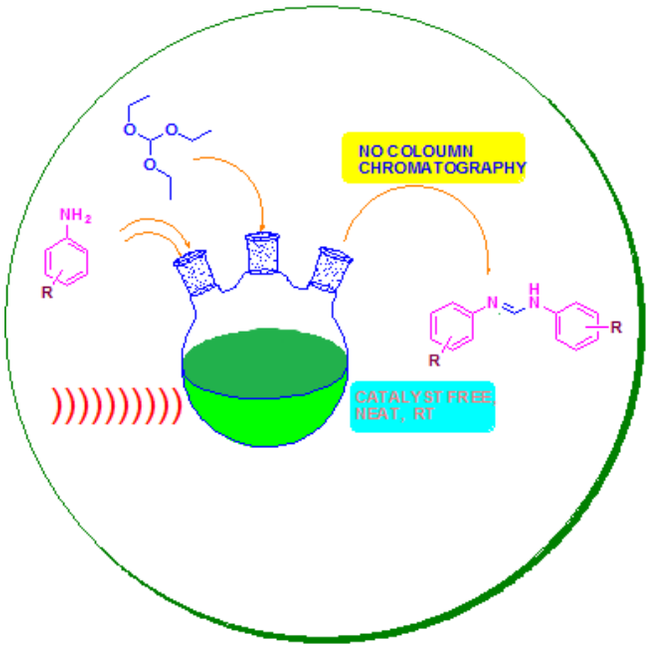

Scheme 1: Ultrasound promoted procedure for the synthesis of N,N'-diarylsubstituted formamidines.

6. MEDICINAL CHEMISTRY

6.1 Iron catalyzed cross coupling of electron-deficient heterocycles and quinone with organoboron species *via* innate C-H functionalization: Application in total synthesis of pyrazine alkaloid Botryllazine A

Parvinder Pal Singh, Sravan Kumar Aithagani, Mahipal Yadav, Varun Pratap Singh and Ram A. Vishwakarma

Here, we have reported an environmentally friendly iron-catalyzed cross coupling reaction of electron-deficient heterocycles and quinone with organoboron species via innate C-H functionalization. Iron (II) acetylacetonate along with oxidant ($K_2S_2O_8$) and phase transfer catalyst (TBAB) under open flask condition efficiently catalyzed the cross-coupling of pyrazine with arylboronic acid and gave monoarylated products in good to excellent yield (Table 1 and 2 and 3). Optimized conditions also worked for other heterocylces such as quinoxalines, pyridines, quinoline, isoquinoline as well as quinones. In addition, we demonstrated as a first example its application for the synthesis of anticancer marine pyrazine alkaloid Botryllazine A (Fig 1 and Scheme 1).

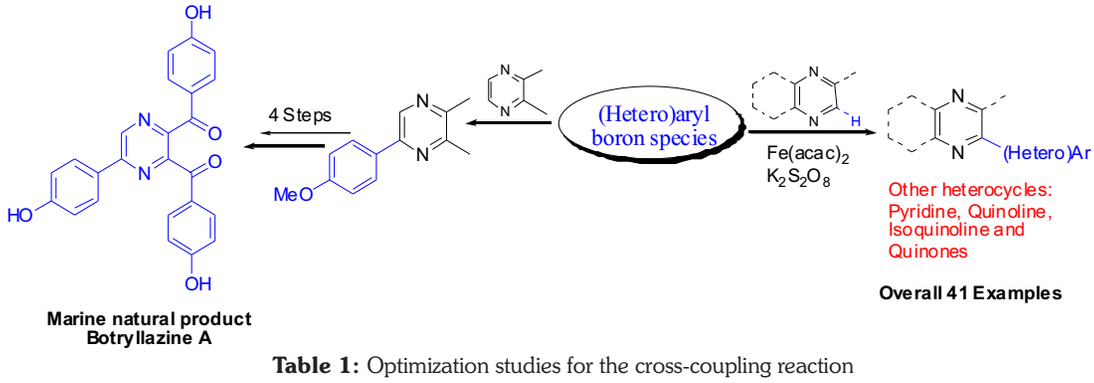

Table 1: Optimization studies for the cross-coupling reaction

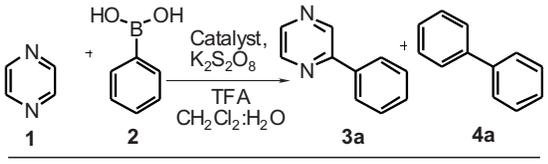

Entry	Catalyst	Qty (mol%)	Product composition[a]	
			3a	4a
a	$FeSO_4$	20	55	<10
b	FeO	20	50	12
c	Fe_2O_3	20	38	N.D.
d	$FeCl_3$	20	trace	N.D.
e	$FeBr_3$	20	trace	N.D.
f	FeF_2	20	trace	N.D.
g	$Fe(acac)_3$	20	65	7
h	**$Fe(acac)_2$**	**20**	**72**	**10**
i	$Fe(acac)_2$	10	65	5
j	$Fe(acac)_2$	30	70	<10
k	$Fe(acac)_2$	100	70	15
l	--	--	0	0

[a]Product composition was determined by HPLC
Reaction conditions (unless otherwise stated): Pyrazine (1mmol), TFA (1 mmol), **2** (1.1 mmol), $K_2S_2O_8$ (3.0 equiv.), rt, 12 h, air.
N.D. denotes Not detected

Table 2: Optimization studies for the cross-coupling reaction of pyrazine with phenylboronic acid

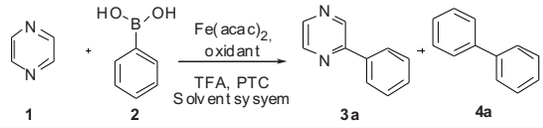

Entry	Solvent	Oxidant	Atm	Temp (°C)	PTC	Product composition[a]	
						3a	4a
a	DCM:H_2O	TBHP (3 eq.)	Air	rt	--	20	N.D.
b	DCM:H_2O	DTBP (3 eq.)	Air	rt	--	--	--
c	DCM:H_2O	Oxone (3 eq.)	Air	rt	--	--	--
d	DCM	$K_2S_2O_8$ (3 eq.)	Air	rt	--	--	--
e	H_2O	$K_2S_2O_8$ (3 eq.)	Air	rt	--	40	5
f	DMSO:H_2O	$K_2S_2O_8$ (3 eq.)	Air	rt	--	trace	N.D.
g	ACN:H_2O	$K_2S_2O_8$ (3 eq.)	Air	rt	--	trace	N.D.
h	Toluene:H_2O	$K_2S_2O_8$ (3 eq.)	Air	rt	--	45	8
i	**DCM:H_2O**	**$K_2S_2O_8$ (3 eq.)**	**Air**	**rt**	**TBAB**	**84**	**<10**
j[b]	**DCM:H_2O**	**$K_2S_2O_8$ (3 eq.)**	**Air**	**rt**	**TBAB**	**75**	**<10**
k	Toluene:H_2O	$K_2S_2O_8$ (3 eq.)	Air	rt	TBAB	50	8
l	DCM:H_2O	$K_2S_2O_8$ (2 eq.)	Air	rt	TBAB	70	6
m	DCM:H_2O	$K_2S_2O_8$ (1 eq.)	Air	rt	TBAB	65	N.D.
n	DCM:H_2O	--	Air	rt	TBAB	--	--
o	DCM:H_2O	$K_2S_2O_8$ (3 eq.)	O_2	rt	TBAB	80	N.D.
p	DCM:H_2O	$K_2S_2O_8$ (3 eq.)	Air	50	TBAB	82	10

Reaction conditions (unless otherwise stated): Pyrazine **1** (1 mmol), **2** (1.1 mmol), TFA (1 mmol), $Fe(acac)_2$ (20 mol%), 12 h.
[a]Yields were determined by HPLC
[b]Reaction was done with 20 mol% of $Fe(acac)_3$.

Table 3: Cross-coupling reaction of pyrazines with organoboronic acids

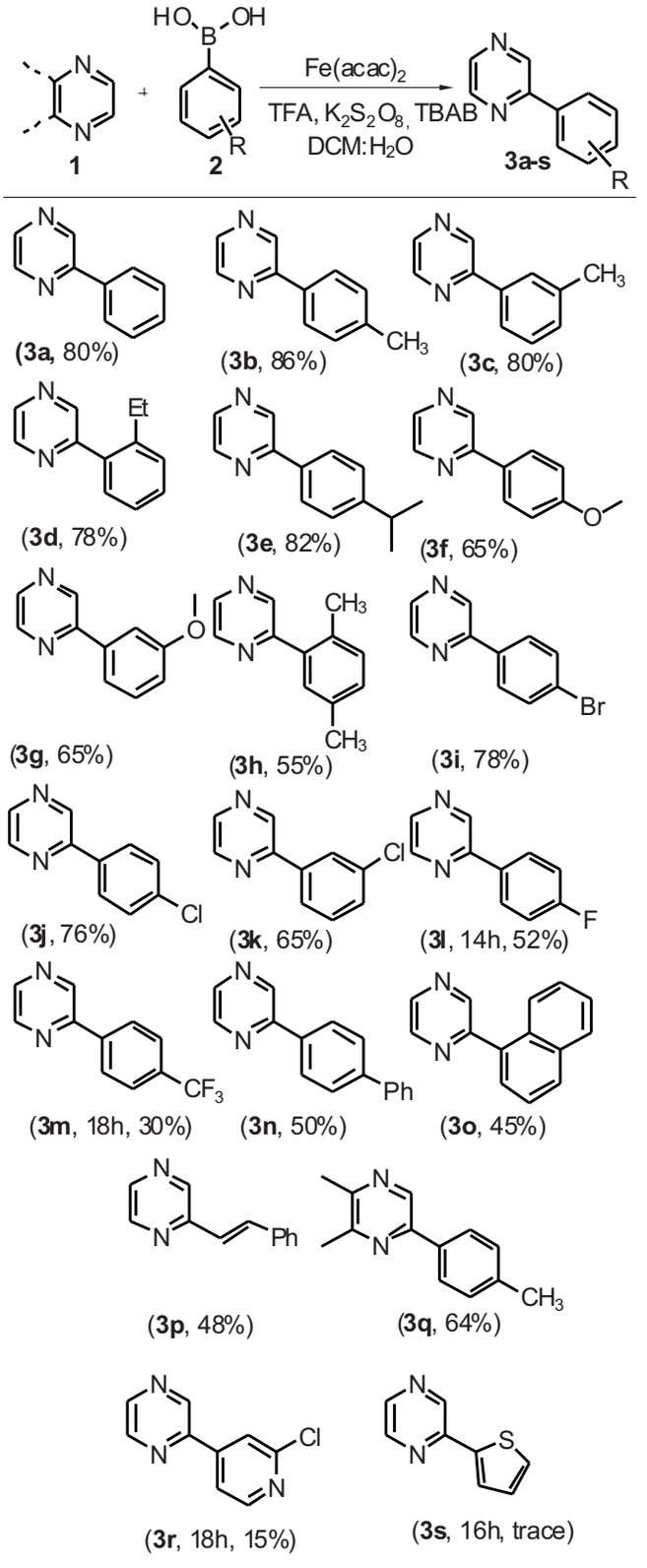

Reaction conditions (unless otherwise stated): Pyrazine **1** (1 mmol), **2** (1.1 mmol), TFA (1 mmol), $Fe(acac)_2$ (20 mol%), $K_2S_2O_8$ (3 mmol), TBAB (5mol%), CH_2Cl_2:H_2O, 12h, under air at rt. Yields represent isolated yields

Fig 1: Retro-synthetic strategies for the synthesis of pyrazine alkaloid-Botryllazine A

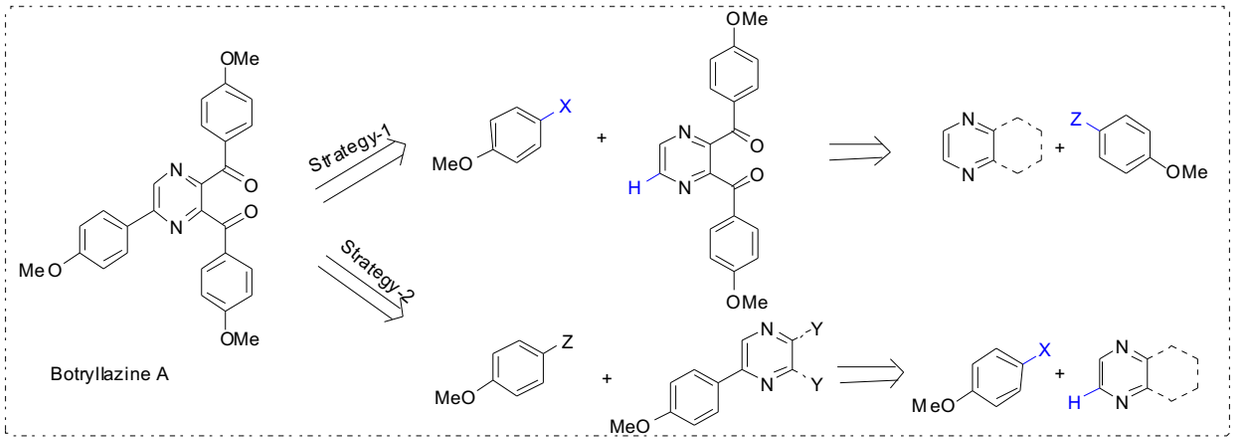

Scheme 1: Studies towards the synthesis of pyrazine alkaloid-Botryllazine A

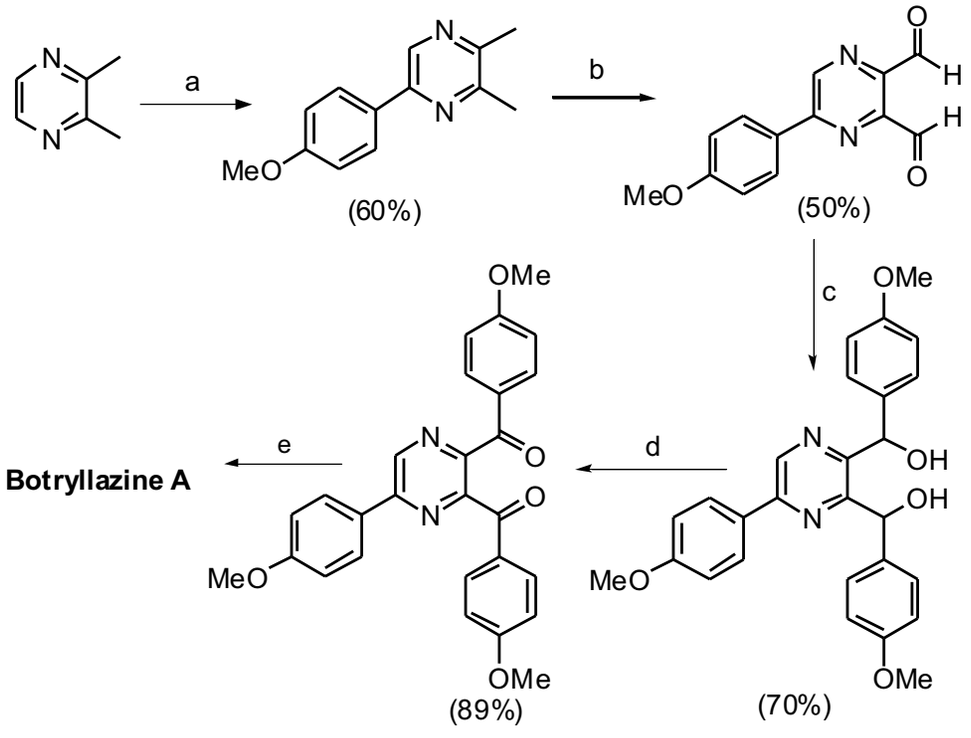

Reagents and conditions: **a**) 4-anisyl-$B(OH)_2$, TFA, $Fe(acac)_2$, $K_2S_2O_8$, TBAB, CH_2Cl_2:H_2O, 12h; **b**) SeO_2, dioxane, reflux, 24h; **c**) 4-anisyl-MgBr, Dry THF, -70^{0}C; **d**) PCC, DCM, rt; **e**) pyridinehydrochloride, 220 ^{o} C, 1h.

In summary, an environmentally friendly iron catalyzed cross coupling reaction for the electron-deficient heterocycles and quinone with organoboron species via innate C-H functionalization has been developed. Iron (II) acetylacetonate along with oxidant ($K_2S_2O_8$) and phase transfer catalyst (TBAB) in dichloromethane:water under open flask condition efficiently catalyzed the cross-coupling reaction of pyrazine with aryl boronic acid and gave monoarylated products in good to excellent yield. This optimized conditions worked with other N-heterocylces such as quinoxaline, pyridine, quinoline, isoquinoline as well as quinones. The present methodology was successfully utilized for the synthesis of Botryllazine A- a marine derived natural product. Moreover, heteroarylboronic acids also worked under optimized condition but gave less yield of coupled product. Further efforts towards its extension to other (hetero)arenes as well as bio-active natural product and studies towards yield improvement/regio-selectivity wherever noted is underway.

7. BIO ORGANIC CHEMISTRY

7.1 Diminutive effect on T and B - cell proliferation of non cytotoxic α-santonin derived 1,2,3-triazoles: A report

P. K. Chinthakindi, P. L. Sangwan, S. Farooq, R. R. Aleti, A. Kaul, A. K. Saxena, S. Koul

Immunosuppressant is an imperative class of clinical drugs for an array of medical processes, including transplant rejection and the treatment of autoimmune diseases such as systemic lupus erythematosus, rheumatoid arthritis, glomerulonephritis, and psoriasis. The FDA approval of Cyclosporine (CsA) in 1983 was a milestone in organ transplantation. T-lymphocytes play an integral role in transplant rejection and autoimmune diseases. Several natural products from plants and microorganisms are reported with clinically important therapeutic immunosuppressant activity. Although immunosuppressive drugs have been used in clinic for organ transplantation and treatment of autoimmune diseases, their side effects including liver toxicity, renal toxicity, infection, malignancy, and others cannot be neglected. Thus, there is a pressing need for novel potential immunosuppressive agents with high efficacy and low toxicity.

α-Santonin (1), from *Artemisia* species known for its activity against various human cancer cell lines, and has also been reported to possess antipyretic activity. Its derivatives such as cyclic peroxide and BIOS-based libraries are reported to possess antimalarial activity (ED_{50}=728.59 ng/mL) and 5-lipoxygenase inhibitory activity (IC_{50}=0.8 μM).

The unexplored immunosuppressant property of α-santonin derived α-desmotroposantonin 1,2,3-triazole analogues carrying diverse chemical features at N-1 position has been investigated. Huisgen 1,3-dipolar cycloaddition reaction has gained interest due to interesting biological activity of 1,2,3-triazoles. α-santonin 1 isolated from the aerial part of *Artemisia laciniata* was used as the starting material. The NP was subjected to rearrangement with Ac_2O/H_2SO_4 to get acetyl α-desmotroposantonin (2) which on deacetylation afforded α-desmotroposantonin (3). Propargylated α-desmotroposantonin (4) obtained by propargylation of 3 was subjected to Copper(I)-catalyzed one pot cycloaddition reaction (click chemistry strategy) with various substituted aromatic azides generated in situ by aryl boronic acids in methanol and water (1:1) in the presence of sodium ascorbate (reducing agent) to give 1,2,3-triazol-1-yl desmotroposantonin derivatives (5-31) in excellent yields (Scheme 1). All the synthesized compounds (2-31) were characterized by ^{1}H NMR, ^{13}C NMR, IR, and HRMS spectroscopic analysis.

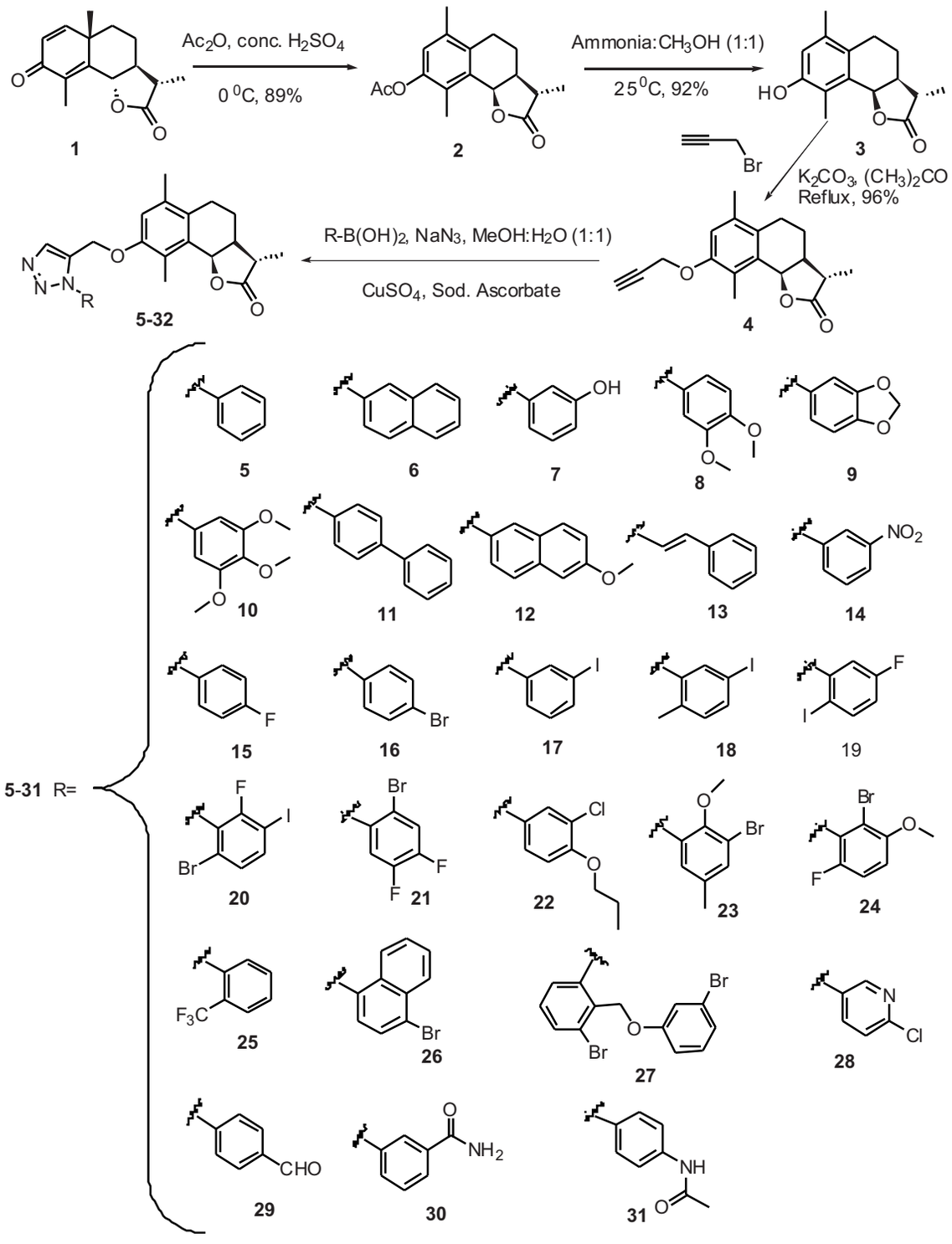

Scheme 1. Synthesis of 1N-substituted aryl-1,2,3-triazole α-desmotroposantonin chemical entities.

All the synthesised molecules along with the parent compound were tested for cell proliferation against ConA induced T-cell and LPS induced B-cells (Table 1). In comparison to the parent compound **1**, several of them as can be seen from the table-1 were found far more potent than the parent.

In the present study, the inhibitory activity of a novel library of 1,2,3-triazole desmotroposantonin derivatives created through Azide-Alkyne Huisgen 1,3-dipolar cycloaddition reaction and characterized by spectral analysis against ConA induced T-cell and LPS induced B-cell proliferation has been demonstrated. Six (**9**, **10**, **17**, **18**, **29**, and **30)** out of a library of 31 compounds have been identified as potent immunosuppressant agents showing inhibition against induced T-cell and B-cell proliferation and the bioactives found without any cytotoxic effect. Further, selective diminutive effect against ConA induced T-cell proliferation for compounds **12** and **13** have also been demonstrated. In terms of SAR, no clear relationship could be established.

Table 1.

Effect at three different concentrations ($1x10^{-4}$, $1x10^{-5}$ and $1x10^{-6}$ M) of compounds **1-31** on ConA and LPS induced Murine Lymphocyte Proliferation (10 μg/mL)

Entry	Conc. (M)	Cytotoxicity	ConA Mean+SE	ConA-induced T cell proliferation rate (%)	LPS Mean+SE	LPS-induced B cell proliferation rate (%)
	10^{-4}	-	0.77±0.05	-6.09	0.74±0.01	-36.75
1	10^{-5}	-	0.85±0.10	+3.65	0.78±0.03	-25.64
	10^{-6}	-	0.49±0.04	-40.24	0.90±0.05	-23.07
	10^{-4}	-	1.21±0.12	+47.56	0.56±0.05	-52.13
2	10^{-5}	-	1.04±0.10	+26.82	0.87±0.01	-25.64
	10^{-6}	-	0.97±0.16	+18.29	0.89±0.01	-23.93
	10^{-4}	-	1.48±0.10	+80.48	1.39±0.94	+18.80
3	10^{-5}	-	0.62±0.07	-24.39	0.89±0.01	-23.93
	10^{-6}	-	0.65±0.02	-20.73	0.90±0.05	-23.07
	10^{-4}	-	0.72±0.01	-12.19	0.74±0.11	-36.75
4	10^{-5}	-	0.81±0.01	-1.21	0.91±0.04	-22.22
	10^{-6}	+	1.02±0.07	+24.39	0.82±0.09	-29.91
	10^{-4}	+	1.38±0.12	+97.14	0.71±0.16	+1.42
5	10^{-5}	+	0.70±0.09	0.00	0.76±0.32	+8.57
	10^{-6}	-	0.55±0.02	-21.42	0.91±0.15	+30.00
	10^{-4}	+	0.93±0.10	+13.41	1.15±0.12	-1.70
6	10^{-5}	-	0.84±0.06	+2.43	0.90±0.28	-23.07
	10^{-6}	-	0.92±0.03	+12.19	1.26±0.45	+7.69
	10^{-4}	-	1.08±0.04	-10.00	1.31±0.03	-9.16
7	10^{-5}	-	1.47±0.02	+22.50	1.11±0.04	-7.50
	10^{-6}	+	1.13±0.06	-5.83	0.97±0.01	-19.16
	10^{-4}	+	1.56±0.17	+90.24	1.32±0.18	+12.82
8	10^{-5}	-	0.95±0.03	+15.85	1.16±0.16	-0.85
	10^{-6}	-	1.44±0.18	+75.60	1.35±0.08	+15.38
	10^{-4}	**-**	0.67±0.08	**-29.47**	0.64±0.04	**-32.63**
9	**10^{-5}**	**-**	0.52±0.02	**-45.26**	0.47±0.03	**-50.52**
	10^{-6}	**-**	0.67±0.04	**-29.47**	0.81±0.08	**-14.73**
	10^{-4}	**-**	0.79±0.03	**-16.84**	0.81±0.08	**-14.73**
10	**10^{-5}**	**-**	0.81±0.04	**-14.73**	0.70±0.13	**-26.31**
	10^{-6}	**-**	0.76±0.06	**-20.00**	0.79±0.03	**-16.84**
	10^{-4}	+	0.84±0.06	+2.43	1.35±0.18	+15.38
11	10^{-5}	-	1.34±0.14	+63.41	1.13±0.35	-3.41
	10^{-6}	-	1.11±0.10	+35.36	1.38±0.31	+17.94
	10^{-4}	**-**	0.05±0.01	**-93.90**	0.84±0.09	-28.20
12	**10^{-5}**	**-**	0.05±0.01	**-95.12**	2.27±0.11	**-94.01**
	10^{-6}	**-**	0.05±0.01	**-93.90**	0.87±0.03	-25.64
	10^{-4}	**-**	0.04±0.01	**-95.12**	0.47±0.12	**-36.75**
13	**10^{-5}**	**-**	0.04±0.01	**-95.12**	1.74±0.16	+48.71
	10^{-6}	**-**	0.04±0.01	**-95.12**	1.08±0.13	-7.69
	10^{-4}	**+**	0.04±0.02	**-95.12**	1.60±0.16	+36.75
14	**10^{-5}**	+	0.05±0.01	**-93.90**	1.18±0.02	+0.85
	10^{-6}	-	0.05±0.03	**-93.90**	0.88±0.05	-24.78
	10^{-4}	-	1.19±0.09	+70.00	0.68±0.41	-2.85
15	10^{-5}	-	1.01±0.06	+44.28	0.77±0.34	+10.00
	10^{-6}	-	0.79±0.20	+12.85	0.78±0.19	+11.42
	10^{-4}	-	1.22±0.34	+48.78	0.99±0.30	-15.38
16	10^{-5}	-	0.84±0.07	+2.43	1.60±0.45	+36.75
	10^{-6}	-	0.81±0.05	-1.21	1.48±0.04	+26.49
	10^{-4}	**-**	0.92±0.18	**-3.15**	0.80±0.10	**-15.79**

Entry	Conc. (M)	Cytotoxicity	ConA Mean+SE	ConA-induced T cell proliferation rate (%)	LPS Mean+SE	LPS-induced B cell proliferation rate (%)
17	**10^{-5}**	**-**	0.76±0.08	**-20.00**	0.76±0.04	**-20.00**
	10^{-6}	**-**	0.80±0.15	**-15.79**	0.80±0.03	**-15.79**
	10^{-4}	**-**	0.73±0.13	**-23.15**	0.79±0.10	**-16.84**
18	**10^{-5}**	**-**	0.70±0.05	**-26.31**	0.81±0.11	**-14.73**
	10^{-6}	**-**	0.82±0.16	**-13.68**	0.62±0.08	**-34.73**
	10^{-4}	+	1.43±0.07	+19.16	1.03±0.06	-14.16
19	10^{-5}	-	1.33±0.06	+10.83	0.91±0.07	-24.16
	10^{-6}	+	0.99±0.09	-17.50	0.95±0.05	-20.83
	10^{-4}	-	0.89±0.01	+27.14	0.69±0.30	-11.42
20	10^{-5}	-	0.48±0.08	-31.42	0.56±0.08	-50.00
	10^{-6}	-	0.55±0.21	-21.42	0.63±0.17	-8.57
	10^{-4}	+	0.59±0.23	-15.74	0.65±0.10	-7.14
21	10^{-5}	+	0.56±0.18	-20.00	0.55±0.17	-21.42
	10^{-6}	+	0.85±0.06	+21.42	0.56±0.07	-20.00
	10^{-4}	-	0.75±0.29	+7.14	0.85±0.06	+21.42
22	10^{-5}	-	0.51±0.19	-27.14	0.79±0.32	+12.85
	10^{-6}	-	0.65±0.21	-7.14	0.99±0.03	+41.42
	10^{-4}	-	0.74±0.28	+5.71	0.81±0.37	+15.71
23	10^{-5}	-	0.75±0.25	+7.14	0.90±0.08	+28.57
	10^{-6}	-	0.74±0.28	+5.71	0.89±0.01	+27.14
	10^{-4}	+	0.38±0.12	-45.71	0.53±0.17	-24.28
24	10^{-5}	+	0.44±0.13	-37.14	0.71±0.14	+1.42
	10^{-6}	+	0.60±0.10	-14.28	0.69±0.28	-1.42
	10^{-4}	-	0.54±0.20	-22.85	0.62±0.24	-11.42
25	10^{-5}	-	0.49±0.11	-30.00	0.48±0.09	-31.42
	10^{-6}	-	0.65±0.15	-7.14	1.14±0.36	+62.85
	10^{-4}	+	0.63±0.28	-10.00	0.79±0.37	+12.85
26	10^{-5}	+	0.36±0.04	-48.57	0.58±0.17	-17.14
	10^{-6}	-	0.91±0.15	+30.00	0.89±0.14	+27.14
	10^{-4}	-	1.23±0.09	+2.50	0.99±0.02	-17.50
27	10^{-5}	-	1.20±0.05	0.00	1.00±0.01	-16.66
	10^{-6}	+	1.03±0.06	-14.16	0.91±0.02	-24.16
	10^{-4}	-	0.76±0.26	+8.57	1.23±0.22	+75.71
28	10^{-5}	-	0.79±0.20	+12.85	0.64±0.11	-8.57
	10^{-6}	+	0.50±0.14	-28.57	1.02±0.03	+45.71
	10^{-4}	**-**	0.95±0.05	**-20.83**	0.78±0.01	**-35.00**
29	**10^{-5}**	**-**	1.12±0.14	**-6.66**	0.93±0.01	**-22.50**
	10^{-6}	**-**	1.13±0.04	**-5.83**	0.91±0.04	**-24.16**
	10^{-4}	**-**	0.89±0.13	**-6.31**	0.87±0.11	**-8.42**
30	**10^{-5}**	**-**	0.67±0.08	**-29.47**	0.60±0.06	**-36.84**
	10^{-6}	**-**	0.68±0.05	**-28.42**	0.53±0.04	**-44.21**
	10^{-4}	+	1.53±0.05	+27.50	1.40±0.02	+16.66
31	10^{-5}	-	1.36±0.04	+13.33	1.02±0.01	-15.00
	10^{-6}	+	0.96±0.06	-20.00	0.90±0.01	-25.00

+ indicate immune stimulant agents while – indicate immunosuppressive agents.
Results are mean standard error (SE) of three separate experiments, conducted in triplicate at the concentrations1x10^{-4}, 1x10^{-5} and 1x10^{-6}M.

7.2 Synthesis of 3-O-propargylated betulinic acid and its 1,2,3-triazoles as potential apoptotic agents

P. K. Chinthakindi, I. Khan, R. Majeed, N. Thota, N. A. Dangaroo, P. L. Sangwan, A. Hamid, P. R. Sharma, A. K. Saxena, S. Koul

In continuation of our interest involving structural modification of natural products for better efficacy, lesser toxicity, betulinic acid was chosen for chemical modification. Betulinic acid (**1**) is reported as cytotoxic against several human cancer cell lines with IC_{50} > 40 baring one or two cell lines where single digit IC_{50} value is observed. The molecule offers several hot spots (e.g. C-3, C-20 and C-28) to provide enough space for chemical modification. We selected C-3 site as this center is shown to play a lesser role in anti-cancer activity compared to other two important sites. One of the goals of cancer chemotherapy is to explore and develop discovery leads that can selectively induce apoptosis in cancer cells. The strategy envisaged in the present study involved the prologue of nitrogen atom to generate molecules bearing heterocyclic moiety. To achieve this, preparation of 1,2,3-triazole derivatives was undertaken and click chemistry strategy was adopted on the 3-propargyloxy betulinic acid (**2**) (prepared as per Scheme 1) and made to react with appropriate azide (prepared as per Scheme 2). A library of 18 triazoles derivatives bearing structural diversity were thus prepared (Scheme 1) and their chemical identity established by spectral analysis. The overall chemical yields of the synthesized compounds ranged from 92 to 98%.

Compound **1** and its derivatives (**3-20**) were screened against a panel of nine human cancer cell lines namely A-549, PC-3, DU-145, SF-295, MCF-7, THP-1, HCT-15 and HL- 60 cells to assess their cytotoxic potential using sulpharhodamine B (SRB) assay. The active compounds from the first screening were then tested at two lower doses of 30 and 10 μM concentration(Table 1).

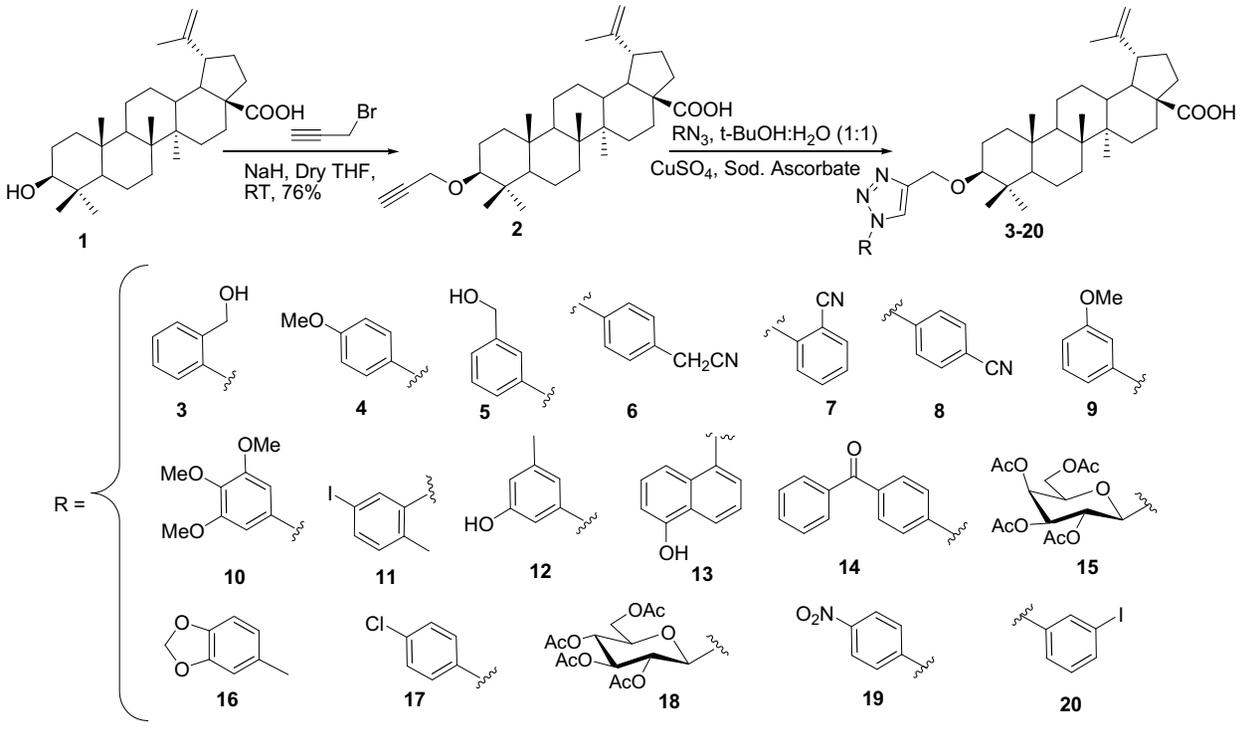

Scheme 1. Propargylation of betulinic acid **1** and preparation its 1,2,3-trizole derivatives.

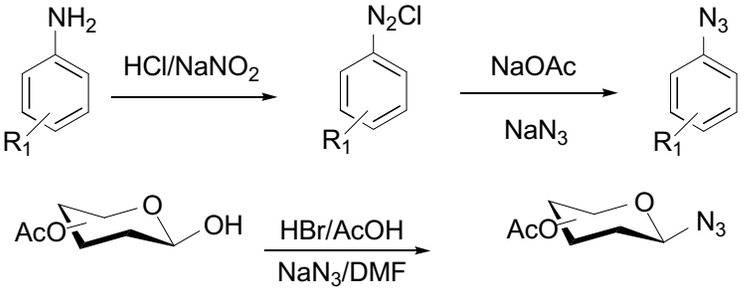

Scheme 2. Synthesis of substituted aryl azides and acetylated sugar azides.

Table-1

Cytotoxic activity[a] (%age growth inhibition) of betulinic acid and its derivatives against various human cancer cell lines at 50, 30 and 10 μM concentration.

Tissue		Liver	Lung	Prostate	Leukemia			Breast	CNS	Colon
Cell line types		HEP-2	A-549	DU-145	PC-3	THP-1	HL-60	MCF-7	SF-295	HCT-15
Compound	Conc. (μM)	% Growth Inhibition								
1	50	78	74	84	94	99	98	88	99	94
	30	66	48	70	29	69	73	36	88	80
	10	41	20	12	8	30	35	7	11	45
2	50	64	57	65	52	78	80	80	77	82
	30	61	55	55	28	65	69	72	72	80
	10	45	54	43	10	45	50	50	35	50
3	50	74	51	53	52	97	99	93	59	57
	30	54	40	37	8	77	82	62	46	55
	10	41	38	35	5	50	54	44	20	55
4	50	78	67	65	49	93	95	75	47	71
	30	74	45	52	29	91	93	71	37	70
	10	51	43	43	04	50	53	36	27	11
5	50	71	60	68	64	96	98	99	83	56
	30	69	57	61	48	95	96	98	81	27
	10	45	32	30	42	43	46	42	44	17
6	50	68	79	84	86	92	98	97	71	89
	30	59	74	65	71	89	90	81	66	61
	10	45	60	32	34	50	65	60	45	40
7	50	60	36	20	42	47	48	51	54	39
	30	49	28	15	5	44	40	32	18	30
	10	01	22	01	3	21	15	5	5	14
8	50	57	45	30	28	54	60	75	55	84
	30	56	38	18	10	41	45	59	48	53
	10	30	34	17	4	17	20	46	15	23
9	50	48	41	11	46	58	65	74	51	43
	30	38	26	10	30	44	51	71	51	35
	10	8	25	03	8	35	41	50	28	47
10	50	25	6	65	4	96	97	74	35	34
	30	14	53	41	22	56	60	54	20	25
	10	7	43	24	5	38	40	30	8	9
11	50	42	71	97	91	99	98	96	90	66
	30	25	59	51	74	85	90	96	75	56
	10	9	23	10	47	15	24	70	23	28
12	50	74	72	86	94	92	98	82	87	72
	30	63	60	69	61	82	95	63	61	64
	10	45	42	38	35	51	63	51	18	40
13	50	25	58	50	3	91	94	44	12	46
	30	26	37	09	4	24	30	25	19	41
	10	25	32	06	6	3	6	29	8	43
14	50	58	37	36	40	72	74	52	39	63
	30	41	10	20	32	61	66	44	20	51
	10	25	6	08	5	50	62	35	8	39
15	50	67	40	91	61	52	61	82	65	50
	30	56	40	50	32	46	50	68	55	36
	10	9	22	10	2	33	41	7	36	22
16	50	55	83	55	53	94	96	80	32	66
	30	43	59	43	40	69	74	63	20	53
	10	28	52	28	22	50	61	42	5	46
17	50	44	43	08	11	76	80	32	5	62
	30	39	20	04	7	58	63	15	5	54
	10	24	5	07	8	44	52	8	8	39
18	50	72	62	72	74	93	94	53	87	65
	30	54	49	54	59	68	78	44	72	52
	10	43	28	43	48	51	63	20	52	36
19	50	72	33	62	27	56	64	61	66	54
	30	74	27	62	24	41	45	58	27	45
	10	71	28	23	8	9	13	51	6	29
5-Flurouracil	20	-	75	72	64	83	89	-	73	72
Mitomycin-C	1	68		-	-	-	-	-	76	

[a]Results are mean value of three similar experiments, each carried out in quadruplicate at 50, 30 and 10 μM concentrations. The bold values are shown for those compounds which have proved to be active.

Many of compounds produced concentration dependent growth inhibition effect on several cancer cell lines. Triazole derivatives **5**, **7**, **13**, **15**, **17**, **18** (HL-60 only) and **19** at lowest concentration (10 μM), effected THP-1 and HL-60 the most among all the cell lines tested. Compounds **7**, **13**, **15**, **17**, and **19** were able to cause maximum inhibition (60-65%) of cell proliferation against HL-60 compared to THP-1 where the effect was only 50-55%. For liver (HEP-2) cancer cell line, only two compounds **5** and **20** were able to sensitize the liver cell line at 10 μM, and maximum inhibition of 71% was observed for compound **20**. For lung (A-549) cell line, only three compounds (**5**, **7**, and **17**) showed cytotoxic effects with maximum effect displayed by **7** (60% inhibition). Among prostate (DU-145) and breast (MCF-7) cancer cell lines, baring compound **12** which showed inhibition (70%) against MCF-7, the rest of the compounds failed to exhibit any significant inhibitory effect. In case of CNS cell line, only compound **19** showed cytotoxic effect displaying 52% inhibition (at 10 μM concentration). For colon cancer cell line, only compounds **3** and **4** exhibited cytotoxic effect (10 μM conc.) with latter displaying marginally better activity profile.

With the advantage of having more potent compounds than betulinic acid, their IC_{50} values were determined along with betulinic acid (**1**) against cancer cells of different tissue origin (50% growth inhibition) by plotting the graph between concentration *vs* growth inhibition (Table 2).

Though no clear cut structure activity relationship (SAR) could be established, some inferences could still be drawn. Monoalkyloxy (**9**) and hydroxymethyl (**3** and **5**) analogs in general showed better cytotoxic effect than the parent and di- as well as trialkyloxy compounds (**16** and **10**). Among *ortho*- and *para*-cyano (**7** and **8**) isomers, better inhibitory effect was observed for compound **7**. Similar type of effect was also observed for the derivatives bearing phenolic group in the aryl part of the molecules with compound **13** showing maximum inhibitory effects. Halogen bearing aryl moiety also showed significant inhibitory effect similar to that of compound **7**.

Among all the cell lines, leukemia cells (HL-60 and THP-1) proved most sensitive towards the semi-synthetic analogues in particular compounds **7** and **13** showed maximum cytotoxic effect and were chosen for further detailed study. To verify whether the cancer cell death induced by **7** and **13** was apoptotic, both the compounds were found potent apoptosis inducers, as proved by the measurement of DNA fragmentation.

The overall results showed high potency of two semi-synthetic derivatives **7** and **13** along with substantial evidence for their apoptotic mode of action against HL-60 and THP-1 cancer cell lines. In addition, the induction of apoptosis by these molecules is evidenced by the loss in mitochondrial membrane potential and appreciable DNA fragmentation. Inhibition of cell migration and inhibitory effect on the ability of the cells to reproduce and form large colonies further substantiated our findings. These studies provide sufficient evidences to advance the compounds (**7** and **13**) for *in vivo* testing in models of human leukemia.

Table 2.
Ic_{50} values in μM of Betulinic acid and its analogs on the panel of human cancer cell lines.

Compound	Leukemia		Prostate		Liver	Breast	Lung	CNS	Colon
	THP-1	HL-60	DU-145	PC-3	HEP-2	MCF-7	A-549	SF-295	HCT-15
1	20	17	22	37	16	37	31	22	12
3	15	10	16	49	14	10	14	17	10
4	10	**8**	48	49	23	14	50	44	**8**
5	10	**7**	23	50	**8**	17	32	53	25
6	12	11	23	32	13	12	25	13	46
7	**4.5**	**2.5**	18	14	12	**4.8**	**5**	15	20
8	>50	32	>50	>50	32	49	>50	48	>50
9	47	37	>50	>50	29	12	>50	32	26
10	39	37	>50	>50	>50	10	>50	27	>50
11	22	18	39	>50	>50	27	23	>50	>50
12	18	14	28	13	>50	**3.8**	26	19	26
13	**8**	**3.5**	14	16	13	**9**	16	25	15
14	44	40	50	>50	>50	>50	36	>50	>50
15	50	**5.5**	>50	>50	40	45	>50	>50	28
16	34	30	30	43	26	13	>50	18	50
17	10	**5.5**	34	43	44	15	**8**	>50	13
18	20	**8**	>50	>50	>50	>50	>50	>50	27
19	**9**	**4.5**	24	13	15	38	15	**8**	28
20	46	43	25	39	**3.8**	**8**	>50	44	39

Bold values are shown for those compounds bearing single digit IC_{50} value.

7.3 A validated high-performance thin-layer chromatography method for identification and simultaneous quantification of six markers from Platanus orientalis: Their cytotoxic profiles against skin cancer cell lines

Imran Khan, P. L. Sangwan, A. A. Dar, R. A. Rafiq, M. R. Farrukh, J. K. Dhar, S. A. Tasduq, S. Koul

From *Platanus orientalis,* betulinic acid (**1**), betulinic acid-3-acetate (**2**), 3-acetyl betulinaldehyde (**3**), oleanolic acid-3-acetate (**4**), 3-β-hydroxy-28,19β-olenolide (**5**) and β-sitosterol (**6**), were isolated and a HPTLC method developed for their simultaneous quantification. The markers were first derivatized on the chromatogram with cerric ammonium sulfate reagent and then HPTLC densitometry carried out. Chromatographic separation of these markers was carried out on silica-gel 60 plate, using ternary solvent system n-hexane: toluene: acetone (6:3.5:1 v/v/v) as mobile phase. The method was validated for accuracy, precision, LOD and LOQ. All calibration curves showed a good linear relationship ($r>0.9919$) in test range. Precision was evaluated by intra- and inter-day study showed RSDs <2.51% and accuracy validation recovery between 95.54 to 99.33% with RSDs below 1.55%. The successful application of the validated method showed betulinic acid as most abundant component (4.63%) and 3-β-hydroxy-28,19β-olenolide (0.017%) the least. The markers displayed significant cytotoxic effect against human keratinocyte, mouse melanoma and human skin epithelial carcinoma cancer cells using 3-(4,5-dimetylthiazol-yl)-diphenyl-tetrazolium-bromide assay.

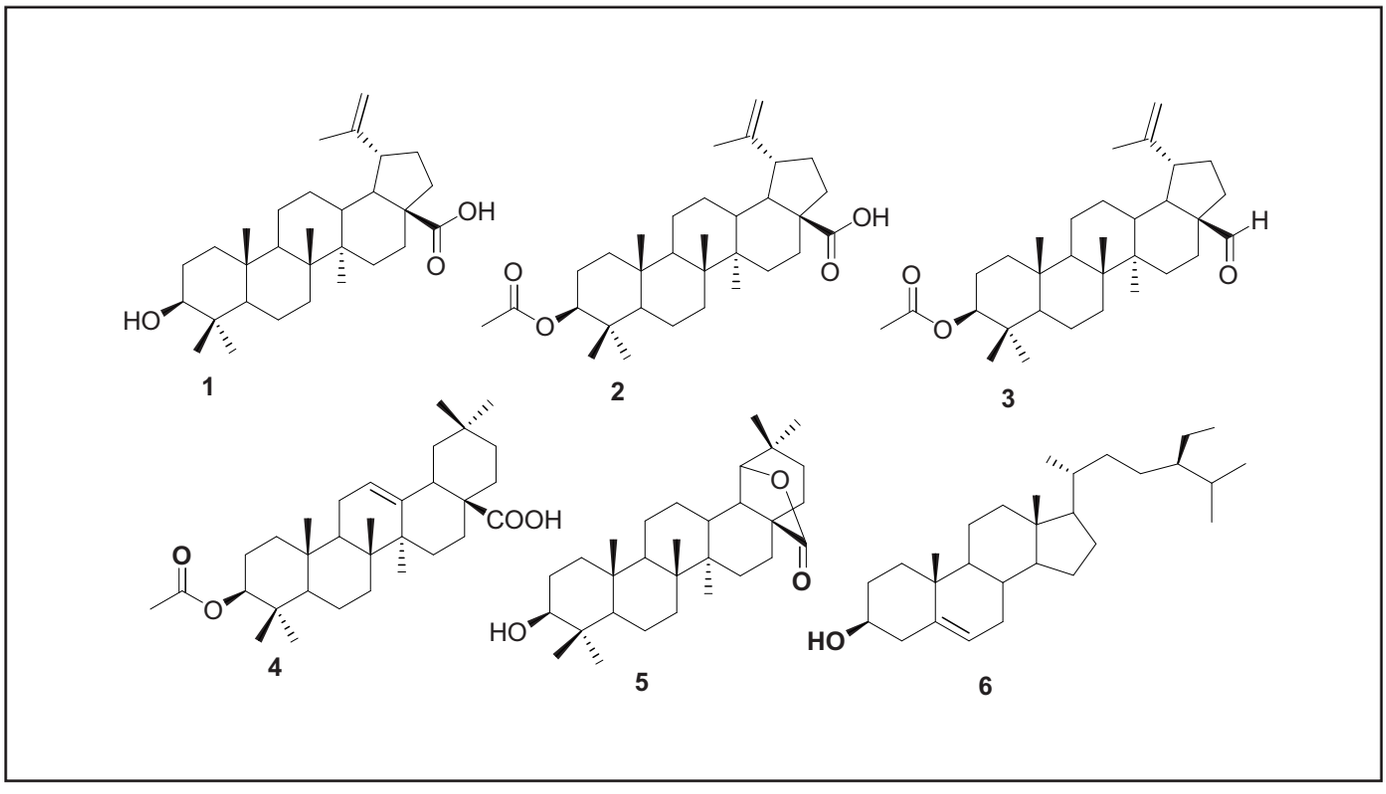

Figure 1. Chemical **s**tructure of markers betulinic acid **(1)**, betulinic acid-3-acetate (**2**), 3-acetylbetulinaldehyde (**3**), oleanolic acid-3-acetate (**4**), 3β-hydroxy-28,19β-olenolide (**5**), β-sitosterol (**6**).

n-hexane: toluene: acetone (6:3.5:1 v/v/v) system afforded the best separation with distinct R_f difference and a successful base line separation of the marker compounds **1-6** (Fig. 2. Segment A) was achieved. The mean R_f determined for the standards for marker compounds was as follows: betulinic acid 0.16±0.02, betulinic acid-3-acetate 0.42±0.01, 3-acetylbetulinaldehyde 0.85±0.01, oleanolic acid-3-acetate 0.37±0.02, 3-β-hydroxy-28,19β-olenolide 0.25±0.01 and β-sitosterol 0.29±0.02 respectively. Matching the R_f of marker compounds in the sample with those of reference standards and identification of these six compounds were further confirmed by *in situ* UV spectra of the above bands of the densitogram as shown in Fig. 3. The developed chromatograms produced compact, flat and dark bands of reference standards when viewed under UV 366 nm after the post chromatographic derivatization. The relationship between the peak areas and the amount of standard applied showed good calibration. For routine analysis 6-point polynomial calibration curve was used.

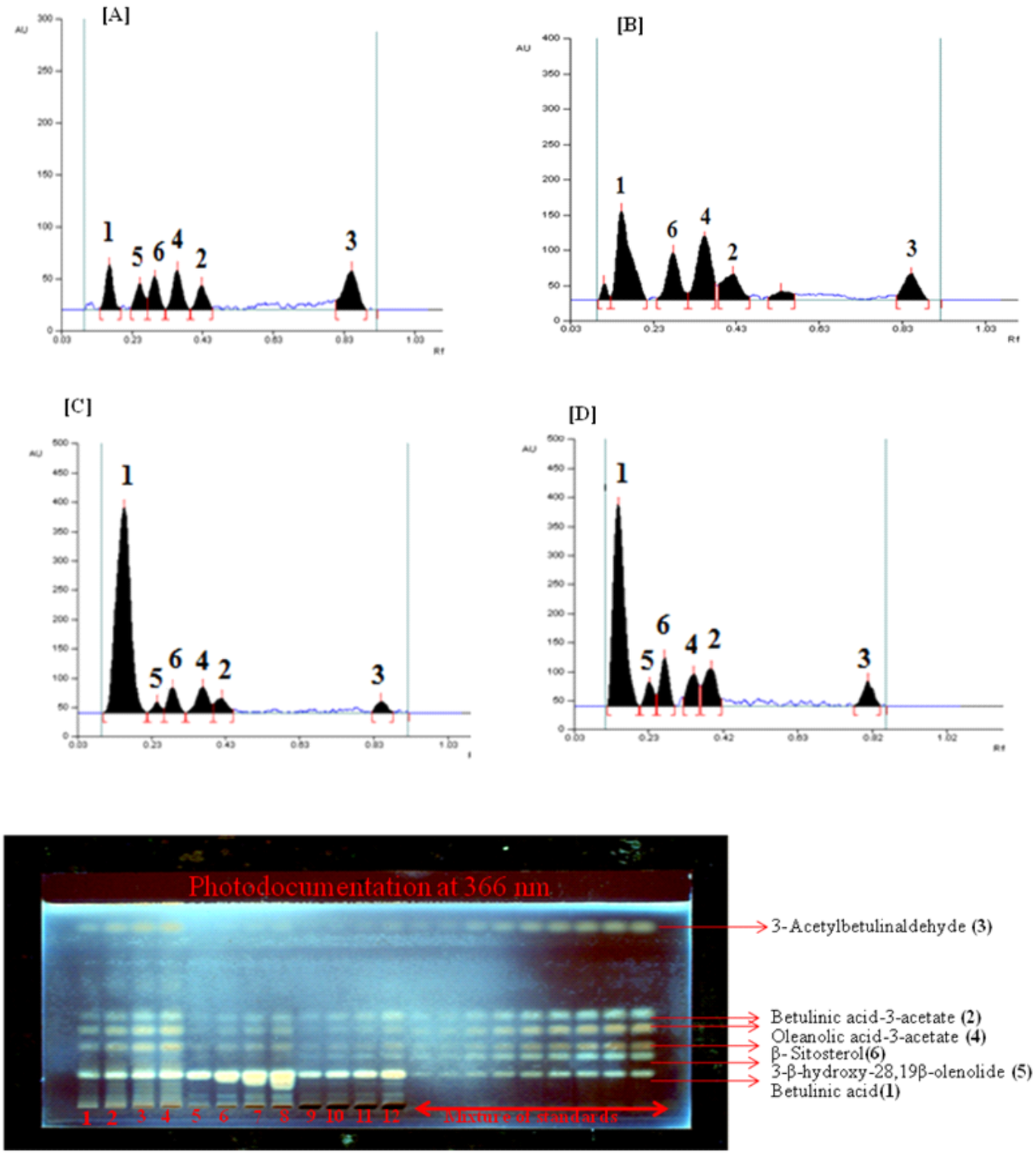

Figure 2. Segment A: HPTLC chromatograms of mixture of standards (**1-6**), **Segment B-D:** DCM, DCM: MeOH (1:1) and MeOH extracts of *P. orientalis* stem bark. **Segment E: Track assignment for HPTLC plate** 1-4: *P. orientalis* DCM extract, 5-8: *P. orientalis* DCM: MeOH (1:1) extract, 9-12: *P. orientalis* MeOH extract. **Standard track:** Mixture of betulinic acid **(1)**, betulinic acid-3-acetate (**2**), 3-acetylbetulinaldehyde (**3**), oleanolic acid-3-acetate (**4**), 3β-hydroxy-28,19β-olenolide (**5**) and β-sitosterol (**6**).

The method was validated with respect to linearity LOD, LOQ, recovery, precision and accuracy in accordance with the guidelines of ICH by analyzing reference compounds and the analytes. The absence of any interfering peak indicated that the method is specific. The calibration curves for all the six marker compounds, six point calibration point were used in the range of 100-600 ng which showed goodness fit within the test range of 0.99193–0.99951. For validation and linearity, the polynomial calibration curves were plotted for the compounds (**1-6**) at the five levels of calibration standards by applying at the lowest and highest concentration five times each and for all other levels in duplicate. Linearity curves of **1-6** obtained on the basis of polynomial regression mode. The results obtained for compounds **1-6** in different

extracts by the set-I was statically compared with set-II by applying the *t*-test for accuracy and *F*-test for precision. Calculated t- and *F*- values did not exceed the tabulated values at the 95% confidence level for four degree of freedom as shown in Table S1a-c, suggesting thereby that the proposed method does not differ significantly with respect to accuracy and precision. These results allowed inferring that the present method is precise, accurate and sensitive enough for the simultaneous assay of six marker compounds in *P. orientalis* stem bark extracts.

The developed HPTLC method was applied to the simultaneous determination and quantification of six marker compounds **1**-**6**. Typical HPTLC chromatograms of reference compounds with samples are shown in Fig. 2. The content of the marker compounds in the three extracts of *P. orientalis* were calculated (% w/w) and shown in Table 1. On quantification, the sequence of abundance of the component **1-6** was as follows: Betulinic acid (**1**) was found as the major constituent (4.63%) followed by β-sitosterol (**6**) (0.105%), betulinic acid-3-acetate (**2**) (0.054%), 3-aetylbetulinaldehyde **(3)** (0.049%), oleanolic acid-3-acetate (**4**) (0.0202%) and 3-β-hydroxy-28,19β-olenolide **(5)** (0.017%) respectively. On the basis of the quantification study the rich abundance of betulinic acid is a very interesting and encouraging as this compound is known for diverse pharmacological activities including anti-HIV, anti-cancer and anti-inflammatory activities, and so is its derivative Bevirimat (3-O-(3',3'-dimethylsuccinyl)betulinic acid which is reported to exhibit remarkable anti-HIV-1 activity against primary and drug-resistant HIV-1 isolates, representing a unique first in a class of anti-HIV compounds termed maturation inhibitors (MIs). Bevirimat has recently succeeded in Phase II clinical trials.

Table 1. Content of marker compounds (**1-6**) (%w/w) in plant material of *P. orientalis* stem bark by HPTLC

Marker	DCM extract	DCM: MeOH (1:1) extract	MeOH extract	Total abundance in dry plant
Betulinic acid (**1**)		3.93±0.03	0.450±0.02	4.630
Betulinic acid-3-acetate (**2**)	0.030±0.02	0.008±0.01	0.016±0.03	0.054
3-Acetylbetulinaldehyde (**3**)	0.018±0.01	0.015±0.01	0.016±0.02	0.049
Oleanolic acid-3-acetate (**4**)	0.112±0.04	0.067±0.02	0.023±0.01	0.202
3-β-hydroxy-28,19β-olenolide (**5**)	N.D.	0.009±0.01	0.008±0.02	0.017
β-sitosterol (**6**)	0.041±0.03	0.038±0.02	0.026±0.02	0.105

N.D. = Not detected

7.4 Capsaicin, a novel inhibitor of NorA efflux pump reduces the intracellular invasion of *Staphylococcus aureus*

NP Kalia, P.Mahajan, Rukmankesh [2], A Nargotra, JP Sharma, S Koul, IA Khan

Bacterial multidrug efflux pumps are the major contributors of microbial resistance to several classes of antibiotics. The physiological role of efflux pumps appears to be far more complex than merely that of an antibiotic export system, and data are emerging to suggest their importance in the pathogenicity of the organism and/or survival in their ecological niche. Efflux of an antibiotic confers an environment of greater selection of resistant mutants having mutations in drug targets. As the inhibition of an efflux pump can potentially improve the clinical efficacy of an antibiotic and simultaneously decrease the selection of resistant mutants, pharmaceutical companies and research institutes are therefore focusing on identifying novel efflux pump inhibitors (EPIs), which may be clinically useful. To date, more than 10 efflux pumps (EPs) have been described for *S. aureus*. Most of these pumps belong to the major facilitator superfamily, namely the chromosomally encoded NorA, NorB, NorC, MdeA and SdrM as well as the plasmid-encoded QacA/B

pumps. *S. aureus* is less susceptible to hydrophilic quinolones due to their active expulsion from the cells by the NorA multidrug resistant (MDR) efflux pump. There has been a continuous search for EPIs that can restore the activity of hydrophilic quinolones by inhibiting the NorA MDR efflux pump. We have previously described the role of piperine, SK-20 and 2-(dihydronaphthalene)- propenoic acid amides as a putative bacterial EPIs. Further in our pursuit to identify natural molecules as novel EPIs we identified capsaicin (8-methyl-*N*-vanillyl-6-nonenamide), chemical component of hot chilli as novel EPI of NorA efflux pump of *S. aureus*. It has a wide range of other biological activities in humans, affecting the nervous, cardiovascular, and digestive systems as well as finding use as an analgesic.[29] Although possibly detrimental to the human gastric mucosa, capsaicin is also bactericidal to *Helicobacter pylori*.

Capsaicin showed an inhibitory effect on the function of P-glycoprotein which suggests that it can potentially give rise to P-glycoprotein mediated drug interactions. The potentiating effect of capsaicin with ciprofloxacin in *in vitro* combination studies against *S. aureus* and its suggestive role as an efflux pump inhibitor was observed for the first time. We further examined the influence of capsaicin on the invasiveness of NorA overproducing *S. aureus* strain SA 1199B, and *norA* knockout *S. aureus* SA-K1758.

Capsaicin significantly reduced the MIC of ciprofloxacin against *S. aureus* SA1199 and SA1199B. Furthermore, capsaicin also extended the post antibiotic effect of ciprofloxacin by 1.1 h at MIC concentration. There was decrease in mutation prevention concentration of ciprofloxacin when combined with capsaicin. Inhibition of ethidium bromide efflux by NorA overproducing *S. aureus* SA1199B confirmed the role of capsaicin as NorA efflux pump inhibitor. The most significant finding of this study was the ability of capsaicin to reduce the intracellular invasion of *S. aureus* SA1199B (NorA overproducing) in J774 macrophage cell lines by 2 $\log_{10}$.

From the docking studies of reserpine (known inhibitor) and capsaicin in the binding site of NorA, it was observed that Arg98 and Ile23 are involved in key interactions and hence play an important role in the ligand binding. Also, a hydrophobic cleft formed by Leu26, Val44 and Phe47 at one end and by Pro24, Phe140, Ile244, Gly248 and Phe303 at the other (particularly for capsaicin) provides some extra stability to the complex. H-bond formation between reserpine and Gln51 is further supposed to provide strength to the reserpine-NorA complex. A strong H-bond interaction at a distance of 1.89Å with Ile23 of the protein NorA is observed in case of capsaicin. The orientation of capsaicin within the binding site (as shown in figure 4B) allows its aliphatic chain to extend into the hydrophobic cleft involving residues Pro24, Phe143, Ile244, Gly248 and Phe303 which enables strong hydrophobic interactions due to the close proximity of the ligand with these residues (distance ranges between 1.7Å to 3.2Å). A weak H-bond between Arg98 and the hydroxyl group of the aryl moiety of capsaicin may be attributing extra stability to the capsaicin-NorA complex.

7.5 4-*epi*-Pimaric acid: A phytomolecule as a potent antibacterial and anti–biofilm agent for oral cavity pathogens

F.Ali, PL Sangwan, S.Koul, A.Pandey, S.Bani, ST Abdullah, PR Sharma, S.Kitchlu, IA Khan

Dental caries and periodontitis are the two most common human diseases associated with the oral cavity infections and there are recent reports that suggest potential role of periodontal infections in more serious systemic diseases including cardiovascular disease, respiratory infections, diabetes and low-birth weight complications. Oral biofilms formation is an important event associated with the initiation of most common infections in the oral cavity such as caries, gingivitis, and periodontal diseases. *Streptococcus mutans* has been implicated as one of the principal etiological agents in the pathogenesis of dental caries in human and are also involved in infective endocarditis, a serious disease with a mortality rate of up to 50 % despite antibiotic treatment. Colonization of enamel surfaces by the cariogenic bacteria such as *S. mutans* and *Actinomyces viscosus* is thought to be initiated by attachment to a saliva-derived conditioning film, the acquired enamel pellicle (AEP) and through series of actions the adhered bacteria decalcify the minerals in the enamel, leading to decavitation of the tooth. Therefore, inhibition of overgrowth and biofilm formation of *S. mutans* is one of the preventive strategies of dental caries.

A renewed interest in natural substances has focused attention on plants rich in bioactive compounds well known for their antimicrobial properties [11, 12]. There are many reports that show natural molecules as good antibacterial agents active against oral pathogens like-*Streptococcus mutans*, *Actinomyces viscosus*, *Streptococcus sanguis*, *Fusobacterium nucleatum, Prevotella intermedia*, *Haemophilus actinomycetemcomitans*, and *Porphyromonas gingivalis* [13-17].

The present work describes the

detailed antibacterial study of 4-*epi*-pimaric acid isolated from the aerial part of *A. cachemirica* against a panel of oral cavity pathogens.

The phytomolecule a colourless crystalline compound in MS spectrum (LCMS) showed molecular ion peak at m/z (M^+–1) 301 compatible with molecular formula $C_{20}H_{30}O_2$, it exhibited laevorotation $[\alpha]_D$ = –110° (C 0.75 $CHCl_3$) and in the IR spectrum, bands were observed at 3345, 2951, 2826, 1692,1451 and 918 cm^{-1}. In the ^1H NMR spectrum, the signals for H–14, H–15, H–16a and H–16b olefinic protons were observed at δ 5.15 (brs), 5.72 (1H, dd, *J*=16.80, 10.77 Hz), 4.92 (1H, dd, *J*=17.01, 1.82 Hz) and 4.94 (1H, dd, *J*=10.54, 1.79 Hz) respectively. Signals for H–17, H–18 and H–20 methyls were observed as singlets at δ 1.00, 1.26 and 0.65 respectively. In ^{13}C NMR, signals for carbons were observed at δ 39.19 (C–1), 19.56 (C–2), 38.56 (C–3), 44.02 (C–4), 56.07 (C–5), 24.09 (C–6), 36.40 (C–7), 137.94 (C–8), 50.50 (C–9), 39.19 (C–10), 19.21 (C–11), 35.77 (C–12), 37.94 (C–13), 127.96 (C–14), 147.17 (C–15), 112.67 (C–16), 29.33 (C–17), 29.10 (C–18) 184.13 (C–19) and 13.79 (C–20) respectively. On the basis of above data, the compound was identified as 4-*epi*-pimaric acid (Fig. 1) which is in full agreement with the spectral data reported in the literature for 4-*epi*-pimaric acid one of the four naturally occurring diastereoisomers of pimaric acid.

4-*epi*-Pimaric exhibited minimum inhibitory concentration (MIC) in the range 4 to 16 μg/ml and minimum bactericidal concentration (MBC) 2 to 4 folds higher than MIC. There was significant inhibition in the biofilm formation by *Streptococcus mutans* on saliva coated surface ($P < 0.05$) and confocal microscopy revealed that 4-*epi*-pimaric acid inhibited the clumping and attachment of *S. mutans*. At 8 × MIC concentration, it significantly prevented the pH drop and reduced *S. mutans* biofilms ($P < 0.05$). Increased propidium iodide staining and leakage of 260 and 280 nm absorbing material by 4-*epi*-pimaric acid treated cells of *S. mutans* suggested that it probably causes disruption of the cytoplasmic membrane structure. It also exhibited significant suppression of TNF–α expression in human neutrophils, suggestive of its anti-inflammatory activity. Further, the compound was found to be significantly safe (IC_{50} >100 μg/ml) in the MTT assay on AML-12 cell lines. In conclusion, 4-*epi*-pimaric acid showed promising antibacterial, anti-biofilm and anti-inflammatory potency and this compound can be exploited for therapeutic application in oral microbial infections.

8. FERMENTATION TECHNOLOGY

8.1 Optimization of Nitrilase Production from *Fusarium proliferatum*

Asha Chaubey, Farnaz Yusuf, Urmila Jamwal and Rajinder Parshad

The fungal isolate from *Fusarium proliferatum* strain AUF-2 has been found to have an efficient nitrilase activity. Optimization of growth conditions and production media has been carried out in order to achieve maximum nitrilase production. Our results have shown that the most effective carbon and nitrogen sources are glucose and sodium nitrate respectively. ε-caprolactam was found to be the best inducer for maximum nitrilase production with 80g/l biomass and 26U/g activity. Overall nitrilase activity of ⩾ 2000U/l culture was obtained in this study, which is one of the best activities reported so far in any *Fusarium* strain. The individual and interactive effects of three independent variables i.e. carbon source (glucose), nitrogen source (sodium nitrate) and inducer (ε-caprolactam) on nitrilase production from *Fusarium proliferatum* were also investigated using design of experiments (DOE) methodology. Response surface methodology (RSM) was followed to generate the process model and to obtain the optimal conditions for maximum nitrilase production. Based on central composite design (CCD) a quadratic model was found to fit the experimental data ($p<0.0001$) and maximum activity of 59.0U/g biomass was predicted at glucose concentration (53.22g/l), sodium nitrate (2.31g/l) and ε-caprolactam (3.58g/l). Validation experiments were carried out under the optimized conditions for verification of the model. The nitrilase activity of 58.3U/g biomass obtained experimentally correlated to the predicted activity which proves the authenticity of the model. Overall 2.24 fold increase in nitrilase activity was achieved as compared to the activity before optimization (26U/g biomass).

Three variables namely carbon source, nitrogen source and inducer are the most significant constituents responsible for nitrilase production. It was also found that our strain *Fusarium proliferatum* produces maximum nitrilase (26U/g biomass) with glucose as carbon source, sodium nitrate as nitrogen source and ε-caprolactam as inducer. We therefore, optimized the concentrations of these three independent variables using One-variable-at-a-time Approach. Optimization results revealed that 50g/l glucose, 2.5g/l sodium nitrate and 3.5g/l ε-caprolactam would result in maximum nitrilase enzyme production (56.8 U/g). These values were therefore selected as the zero coded values of glucose, sodium nitrate and ε-caprolactam respectively for further optimization using RSM.

The values of three variables i.e. glucose, sodium nitrate and ε-caprolactam with the actual and predicted nitrilase activity (U/g) in 20 random experimental runs. The second order polynomial model was used to correlate the independent variables with nitrilase activity. The best candidate to fit the data was the quadratic model after fit summary comparison ($p<0.0001$).

Table 1: Model fitting values

Model terms	Values
CV (%)[a]	7.35
R^2 [b]	0.91
Adjusted R^2 [c]	0.83
Adequate precision [d]	10.58
Standard deviation	3.57

[a] CV (%): coefficient of variance, is the standard deviation which is expressed as a percentage of the mean.

[b] R^2: is the measure of variation around the mean explained by the model.

[c] Adjusted R^2: is the measure of variation around the mean explained by the model, adjusted for the number of terms in the model. The adjusted R^2 decreases as the number of terms in the model increases provided those additional terms do not add value to the model.

[d] Adequate precision: compares the range of predicted value at the design points to the average prediction error.

The quadratic model was found to be the best fit model using sum of square analysis which compares the ratio of mean sqaure regression to the mean square residuals (Table 1). A low value (7.35 %) of the coefficient of variance (CV) indicates a very high degree of precision and good reliability of experimental values. Both the R^2 value (0.91) and the adjusted R^2 value (0.83) were high in this model indicating the fit of model. Adequate Precision for our model has a signal-to-noise ratio of 10.584 which indicates an adequate signal.

Table 2: Analysis of Variance (ANOVA) for Response Surface Quadratic Model

Source	Sum of squares	df	Mean square	F-value	p-value prob > F
Model	1355.14	9	150.57	11.79	0.0003
Lack of fit	94.33	5	18.87	2.83	0.1391
B- Sodium nitrate	30.36	1	30.36	2.38	0.1540
C- Caprolactam	8.86	1	8.86	0.69	0.4242
B^2	126.67	1	126.67	9.92	0.0103
C^2	1160.86	1	1160.86	90.93	<0.0001
Pure error	33.33	5	6.67		
Cor total	1482.80	19			

Table 2 shows the ANOVA of the best fitted quadratic model. It has three factors having nine significant variances (A, B, C, AB, AC, BC, A^2, B^2 and C^2). Each variance has been evaluated by ANOVA. The Model F-value of 11.79 implies that the model is significant. There is only a 0.03% chance that a "Model F-Value" could occur due to noise. The ANOVA table shows only the significant variances i.e. B (nitrogen source, $NaNO_3$), C (inducer, ε-caprolactam), B^2 (quadratic terms of $NaNO_3$, p value of 0.0103) and C^2 (quadratic terms of ε-caprolactam, p value of <0.0001).

The values of regression coefficients were calculated and the experimental results of CCD were fitted with second order polynomial equation. The predicted values of nitrilase production (Y) for 20 independent experiments were calculated by the following equation with actual values of glucose (A), sodium nitrate(B), and ε-caprolactam(C).

$Y = +58.17 + 0.78*A - 1.49*B + 0.81*C - 1.62*A*B - 0.62*A*C - 2.37*B*C - 2.08*A^2 - 2.96*B^2 - 8.98*C^2$

Based on the above equation, predicted value of nitrilase activity at any variable concentration can be calculated. Fig.1 represents three dimensional surface plots showing the combined effect of two independent variables for nitrilase production, while the third variable was kept at zero coded value. Based on the model, optimum medium composition was obtained at 53.22g/l glucose, 2.31g/l sodium nitrate and 3.58g/l ε-caprolactam concentration resulting in predicted nitrilase activity of 59.0 U/g biomass. Validation of the predicted results was done under optimized conditions in three independent experiments. The experimental nitrilase activity of 58.3U/g was obtained which correlated to the predicted activity (59.0U/g) confirming the rationality of the model. This is 2.24 fold higher than that obtained before optimization (26.0 U/g). Thus, overall 2.24 fold increase in nitrilase activity was observed after optimization using RSM.

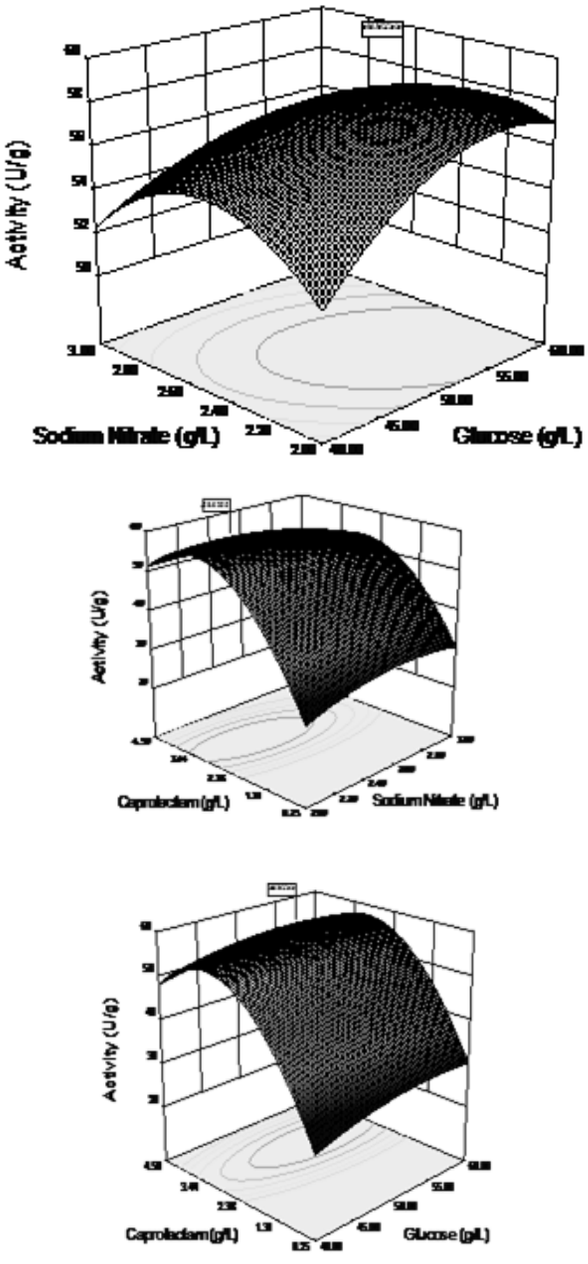

Figure 1: Three dimensional contour plots showing the effect of different variables on the nitrilase production by *Fusarium proliferatum*

Table 3: Chemoprofiling of newly isolated strain from *Fusarium proliferatum*. strain AUF-2

Substrate	Activity (U/g)
Benzylnitrile	2.5
Benzonitrile	26
3- Nitrobenzonitrile	13
4-Nitrobenzonitrile	nd
Malononitrile	nd
Acrylonitrile	25
Fumaronitrile	nd
2-cyanopyridine	nd
3-cyanopyridine	20
4-cyanopyridine	55
Propionitrile	35
Butyronitrile	43
Valeronitrile	37
2-Cholorobenzonitrile	nd
Cinnamonitrile	16
3-Aminobenzonitrile	16
4-Aminobenzonitrile	13
Trichloroacetonitrile	nd
2-Aminoacetonitrile	nd
Diphenylacetonitrile	nd

Table 3 demonstrates our results obtained for chemo - profiling of our strain. It can be seen that the strain is capable to hydrolyse a range of both aliphatic as well as aromatic nitriles. The strain also showed vast substrate specificity from aliphatic nitriles to aromatic nitriles, butyronitrile being the best aliphatic substrate and 4-cyanopyridine being the best aromatic substrate for our strain from *Fusarium proliferatum* strain AUF-2. Efforts are now being made to use the strain for biotransformation of pharmaceutical substrates.

In conclusion, second order quadratic model was found to fit the experimental data obtained from RSM using three key medium components glucose (carbon source), sodium nitrate (nitrogen source) and ε-caprolactam (inducer). It has been found that the inducer i.e. ε-caprolactam is the most significant variable for nitrilase production. Validation experiments of optimal conditions showed 2.24 fold increase in nitrilase production resulting in 58.3U/g nitrilase activity in *Fusarium proliferatum* strain.

8.2 Lipase Catalyzed Hydrolysis of (±)-Methyl 1,4-Benzodioxan -2-Carboxylate

Asha Chaubey, Abdul Rouf, R. Parshad and S.C. Taneja

Synthesis of both the enantiomers of 1,4-benzodioxan-2-carboxylic acid, a key intermediate in the synthesis of doxazosin mesylate, was achieved in good yields and excellent enantioselectivity (ee >99%, E >400) via ABL catalyzed kinetic resolution. Also the effect of co solvent and immobilization on kinetic resolution of (±)-1,4-benzodioxan-2-carboxylic acid is described.

Doxazosin mesylate belongs to quinazoline group of drugs; it is used in the treatment of hypertension and benign prostatic hyperplasia. Compounds containing 1,4-benzodioxin and 1,4 - benzodioxan structures have attracted considerable interest in recent years, mainly due to their interesting biological activities. For example, various 2-substituted 1,4-benzodioxans have shown interesting properties as α- or *β*-blocking agents and are used in antidepression or antihypertension therapy. Others exhibit antihyperglycemic properties or act as inhibitors of 5-lipoxygenase. Moreover, the 1,4-benzodioxan structure is found in a variety of biological active natural products. Finally, these compounds could also be used as intermediates for very useful synthetic transformations.

Enantiomerically pure 1,4-benzodioxan-2-carboxylic acid has attracted considerable interest due to its significant contribution in medicinal chemistry. Recently, it has been found that both the enantiomers of (±)-1,4-benzodioxan-2-carboxylic acid, used as an intermediate for the synthesis of doxazosin mesylate, have different biological activities e.g. (*S*)-1,4-benzodioxan-2-carboxylic acid offer both reduced side effects (viz asthenia and dizziness) and improved efficacy over the (±)-DXZN{(±)-1-(4-amino-6,7-dimethoxy-2-quinazolinyl)-4-[(2,3-dihydro-l,4-benzodioxin-2-yl)carbonyl]

piperazine monomethane sulfonate} for the treatment of benign prostatic hyperplasia (BPH) whereas its *R*-(-) enantiomer possessed higher selectivity for lower urinary tract between the cardiovascular system and the urinary system in the animal experiments in comparison with that of (±)-doxazosin and (+)-doxazosin. Moreover, it has been found that *R*-(+)-1,4-benzodioxan-2-carboxylic acid is the precursor of 2*S*-2-hydroxymethyl- and 2*S*-2-aminomethyl-1,4-benzodioxanes which are chiral fragments for an antidepressant in Phase II clinical trials, and a potent α-adrenergic antagonist. Also *R*-2-hydroxymethyl-1,4-benzodioxane derivative was reported to be one of a new class of potent, selective and orally active prostaglandin D2 (PGD2) receptor antagonists.

A kinetic resolution through hydrolysis of the ester (±)-methyl-1,4-benzodioxan-2-carboxylate with ABL (whole cells) was carried out in 0.1 M phosphate buffer; however good selectivity was not observed. Therefore, the reaction was carried out in a biphasic system containing different organic solvents. Between the methyl and ethyl derivatives of (±)methyl-1,4-benzodioxan-2-carboxylate, ABL showed both higher selectivity and conversion rate for the methyl ester. Therefore, the optimization of reaction conditions was carried out on the methyl ester with different co-solvents with variations in their concentrations, reaction temperatures, pH and substrate concentrations, immobilization, etc. to improve overall time-space yields. For the optimization study with methyl ester, a variety of polar and non-polar solvents ranging from 10 to 50% (v/v) in buffer were used and their effects on the rate of hydrolysis, as well as enantioselectivity, were measured. As shown in Table 1, addition of 20–30% of co-solvent markedly improved the enantioselectivity as well as the rate of hydrolysis.

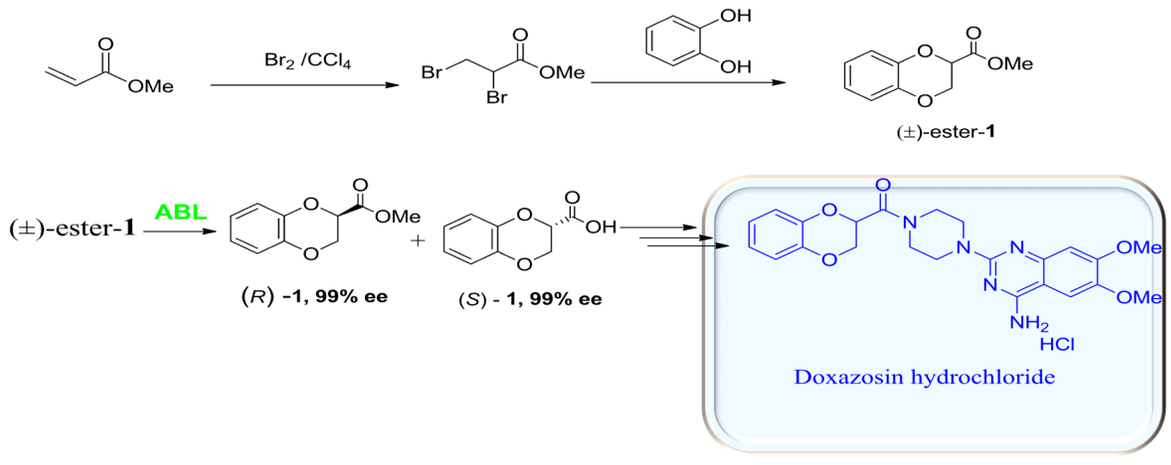

Table 1 : Effect of co solvents (20%) on hydrolysis of (±) **-6** at 20 g/L using *Arthrobacter* species lipase (ABL)

Entry	Enzyme	Cosolvent	Convn(%)	Time (h)	ee_p (%)	ee_s (%)	**E**
1	Cells	Nil	50	4	0	45	
2	Cells	n-butanol	47	7	93	88	79.6
3	**Cells**	**n-butanol**	**42**	**4**	**99**	**73**	**429.2**
4	**Immobilized Cells***	**n-butanol**	**46**	**24**	**99**	**87**	**535.6**
5	Free enzyme	n-butanol	37.3	18	67	40	7.3
6	**Immobilized enzyme**	**n-butanol**	**41**	**24**	**99**	**71**	**411.9**
7	Cells	Toluene	47	6	89	81	41
8	Cells	Dioxane	68	6	45	97	9.1
9	Cells	Isopropanol	65	12	41.5	79	5.27
10	Cells	Acetonitrile	44	12	91.5	73	48
11	Cells	DMSO	79	12	23	87	3.8
12	Cells	DIE	70	4	41	99	8.1
13	Cells	**DIE**	**55**	**2**	**79**	**99**	**33**
14	Cells	DIE	44	20 min	89	71	35.9
15	Cells	t-butanol	40	4	90	60	34.9
16	Cells[a]	n-butanol	52	5h	88	99	58.8
17	Cells[b]	n-butanol	42	5h	90	65	37.2

Experimental conditions: * cells entraped in sol-gel supports , [a] substrate adsorbed on celite, [b]substrate adsorbed on silica, substrate adsorbed on aluminaall the reactions were performed at 25 °C in a shaker at 320 rpm, *ee* (%) was measured by a chiral HPLC and conversion was calculated using formula c = (ee_s x 100)/(ee_p+ee_s)%, DIE – diisopropylether.
E= ln[1-c(1+*eep*)]/ln[1-c(1-*eep*)],[20] p= product.
The *ees* were determined by Chiral HPLC column OJ-H using triflouroacetic acid:isopropyl alcohol:hexane; (0.1:5:95) solvent system at 0.5 ml/min flow rate.

During the kinetic resolution studies, we observed that the enantiomeric excess was strongly dependent on the extent of hydrolysis and so it was important to carry out the reaction beyond 50% hydrolysis (~58%) in order to obtain the enantiopure ester (R)- (*ee* >99%) in good yields when diisopropyl ether was used as the co-solvent. In order to obtain its enantiomer, (S)-, the reaction was stopped at 42% for >99% enantioselectivity using n-butanol as the co-solvent.

Attempts were also made to observe the effect of immobilized substrates on hydrolysis, a methodology found to be highly useful in the kinetic resolution of spiro-b-lactams. The substrate was adsorbed on different supports such as *Celite*, silica, and neutral alumina. However, it was observed that adsorption of the substrate on *Celite* and silica had no significant advantage (*ee* ~88–90%), whereas in the alumina adsorbed substrate, the *ee*% decreased further. In order to assess the effect of the immobilized enzyme (ABL), hydrolytic reactions were performed using a sol–gel entrapped isolated enzyme as well as entrapped whole cells. It was observed that the selectivity as well as conversion increased by immobilizing whole cells (E = 535.6) whereas a very significant increase in enantioselectivity was recorded with immobilized enzyme compared to free enzyme. However, the whole cell immobilization displayed slight advantages over the immobilized isolated enzyme. It should be noted that the time of hydrolysis increased significantly (24 h) when using immobilized biocatalysts. Moreover, the immobilized whole cells/enzymes could be reused after washing with organic solvent/sodium bicarbonate/distilled water to remove any traces of the substrate/product. Upon varying the ratios of the substrate and whole cell mass, the best results were observed with a substrate/whole cell ratio of 1:3.

Keeping all other reaction parameters constant, the substrate concentration was also varied from 10 to 50 g/L (51–258 mmol) and we observed that the lipase remained quite active up to 50 g/L (258 mmol) with no effect on the enantiomeric excess.

In conclusion, immobilized whole cells of an indigenous microorganism *Arthrobacter* species (MTCC no. 5125) bearing lipase have been successfully used for the kinetic resolution of (±)-1,4–benzodioxan-2-carboxylic acid, which was then converted into enantiomerically enriched enantiomers of bioactive molecules such as piperoxan, prosympal, dibozane, and doxazosin.

9. CLINICIAL MICROBIOLOGY

9.1 Capsaicin, a novel inhibitor of NorA efflux pump reduces the intracellular invasion of *Staphylococcus aureus*

Nitin Pal Kalia , Priya Mahajan, Rukmankesh Mehra, Amit Nargotra, Jai Parkash Sharma, Surrinder Koul and Inshad Ali Khan

Capsaicin (8-methyl-*N*-vanillyl-6-nonenamide) is the main component of hot chilli, member of genus *Capsicum* (Fig. 1). Because of its interesting pharmacological and toxicological profiles, capsaicin has generated much research interest in the past decade. Capsaicin showed an inhibitory effect on the function of P-glycoprotein which suggests that it can potentially give rise to P-glycoprotein mediated drug interactions. It also, has a wide range of other biological activities in humans, affecting the nervous, cardiovascular, and digestive systems as well as finding use as an analgesic. Although possibly detrimental to the human gastric mucosa, capsaicin is also bactericidal to *Helicobacter pylori*. In this report, we describe for the first time the potentiating effect of capsaicin with ciprofloxacin in *in vitro* combination studies against *S. aureus* and its suggestive role as an efflux pump inhibitor. We further examined the influence of capsaicin on the invasiveness of NorA overproducing *S. aureus* strain SA 1199B, and *norA* knockout *S. aureus* SA-K1758.

Capsaicin was evaluated in *S. aureus* SA 1199B overproducing the target NorA efflux pump which is the initial contributor to the wild-type fluoroquinolone resistance resulting in the emergence of first-step mutants. These mutants decrease the intracellular drug concentrations and bacterial cells subsequently accumulate additional target mutations under treatment, leading to commonly encountered high-level fluoroquinolone-resistant clinical strains. Moreover, NorA is the prototype of other major facilitator super-family (MFS) pumps with 12 transmembrane segments, such as PmrA in *Streptococcus pneumonia*, and has generally served as the model for studying EPIs of MDR pumps in Gram-positive organisms.

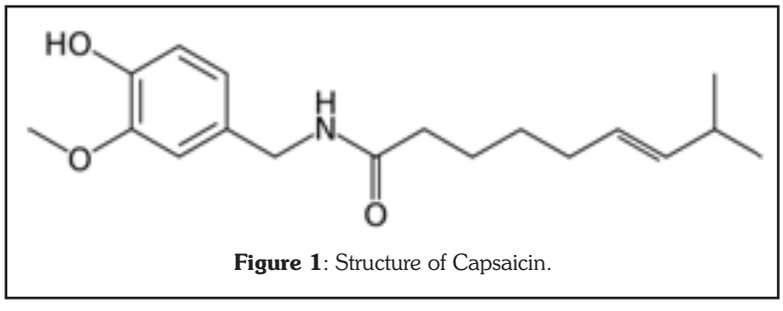

Figure 1: Structure of Capsaicin.

Capsaicin not only increased the intrinsic susceptibility of *S. aureus* to ciprofloxacin but also significantly reduced the emergence of ciprofloxacin-resistant mutants of *S. aureus*. A combination of ciprofloxacin (2 mg/L) and capsaicin (25 mg/L) exhibited bactericidal effect and > $3\log_{10}$ reduction in cfu was observed in 8 h, whereas ciprofloxacin alone exhibited the same effect at the higher concentration of 8 mg/L (Fig. 2).

Furthermore, capsaicin enhanced the PAE of ciprofloxacin in a concentration dependent manner. In terms of percentage increase in PAE of ciprofloxacin, 233% increase in PAE was observed at 2 mg/L (1/4 MIC) of ciprofloxacin in combination with capsaicin. However, the most extended PAE of 2.4 h was observed with ciprofloxacin at 8 mg/L when tested in combination with capsaicin at 25 mg/L (Table-1).

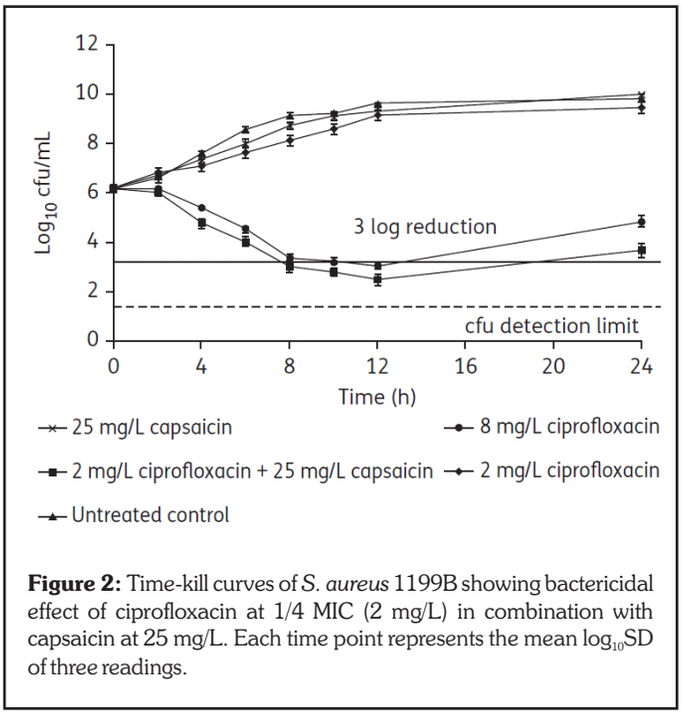

Figure 2: Time-kill curves of *S. aureus* 1199B showing bactericidal effect of ciprofloxacin at 1/4 MIC (2 mg/L) in combination with capsaicin at 25 mg/L. Each time point represents the mean $\log_{10}$SD of three readings.

Accumulation and efflux of ethidium bromide are good indicators of the involvement of efflux pumps in the resistance mechanism, particularly in Gram-positive bacteria such as *S. aureus*. The fluorescence based efflux studies of ethidium bromide preloaded NorA overproducing *S. aureus* cells in the presence and

Table 1: Post antibiotic effect (h) of ciprofloxacin alone and in combination with capsaicin against *S. aureus* SA1199B after exposure of 2 h.

Regimen	Mean PAE (h) ± SD		
	0.25× MIC (2 mg/L)	0.5× MIC (4 mg/L)	MIC (8 mg/L)
Ciprofloxacin	0.3 ± 0.1	1.0 ± 0.1	1.3 ± 0.17
Ciprofloxacin + capsaicin (25 mg/L)	1.0 ± 0.2	1.5 ± 0.17	2.4 ± 0.2

absence of capsaicin showed reduced efflux in presence of capsaicin, thus indicating the inhibition of the efflux mechanism and confirmed capsaicin, another P-glycoprotein inhibitor that inhibits ciprofloxacin efflux from bacterial cells (Fig.3).

Though *S. aureus* is not classically considered as an intracellular pathogen but gaining an intracellular niche, even briefly, might afford a window of opportunity to survive and promote disease. In this regard our studies confirmed the role of NorA overproduction in intracellular invasion of *S. aureus* in macrophage J774 cell lines and further the involvement of capsaicin as an efflux pump inhibitor, in reducing the invasion of NorA overproducing *S. aureus* (Fig. 4).

Docking results of capsaicin and *in silico* predicted 3D structure of NorA revealed the orientation of capsaicin within the binding site (as shown in figure 5B) which allows its aliphatic chain to extend into the hydrophobic cleft and a weak H-bond between Arg98 and the hydroxyl group of the aryl moiety of capsaicin contributing extra stability to the capsaicin-NorA complex. Apart from the other key interactive residues, it was found that Val44, Phe47, Gln51, Phe140, Ile244, Gly248 and Phe303 forms the residues of the conserved domain of the MFS transporter family (Supplementary Data). Since MFS transporter facilitate the transport of many different substrates; the residues involved in substrate binding may not be strictly conserved among superfamily members.

In conclusion, we have, for the first time, shown that capsaicin, a novel EPI which not only inhibits NorA efflux pump of *S. aureus* but also reduces the invasiveness of *S. aureus*, thereby reducing its virulence.

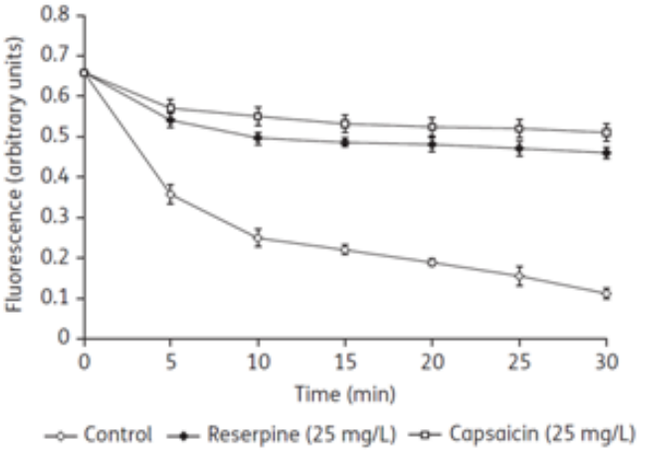

Figure 3: Fluorescence based determination of ethidium bromide efflux by *S. aureus* SA 1199B cells in the presence and absence (control) of capsaicin at 25 mg/L. Reserpine at 25 mg/L was used as known EPI control. Each time point represents the mean $\log_{10}$SD of three readings.

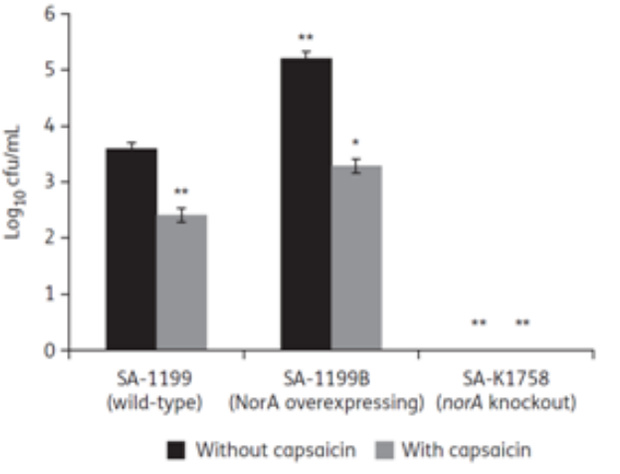

Figure 4: Influence of capsaicin (25 mg/L) on the invasive capacities of *S aureus* wild-type (SA1199) its NorA (SA1199B) overproducing mutants as well as *norA* knockout (SA-K1758) strain. The invasiveness of SA-1199 and 1199B was significantly reduced in the presence of 25 mg/L of capsaicin.

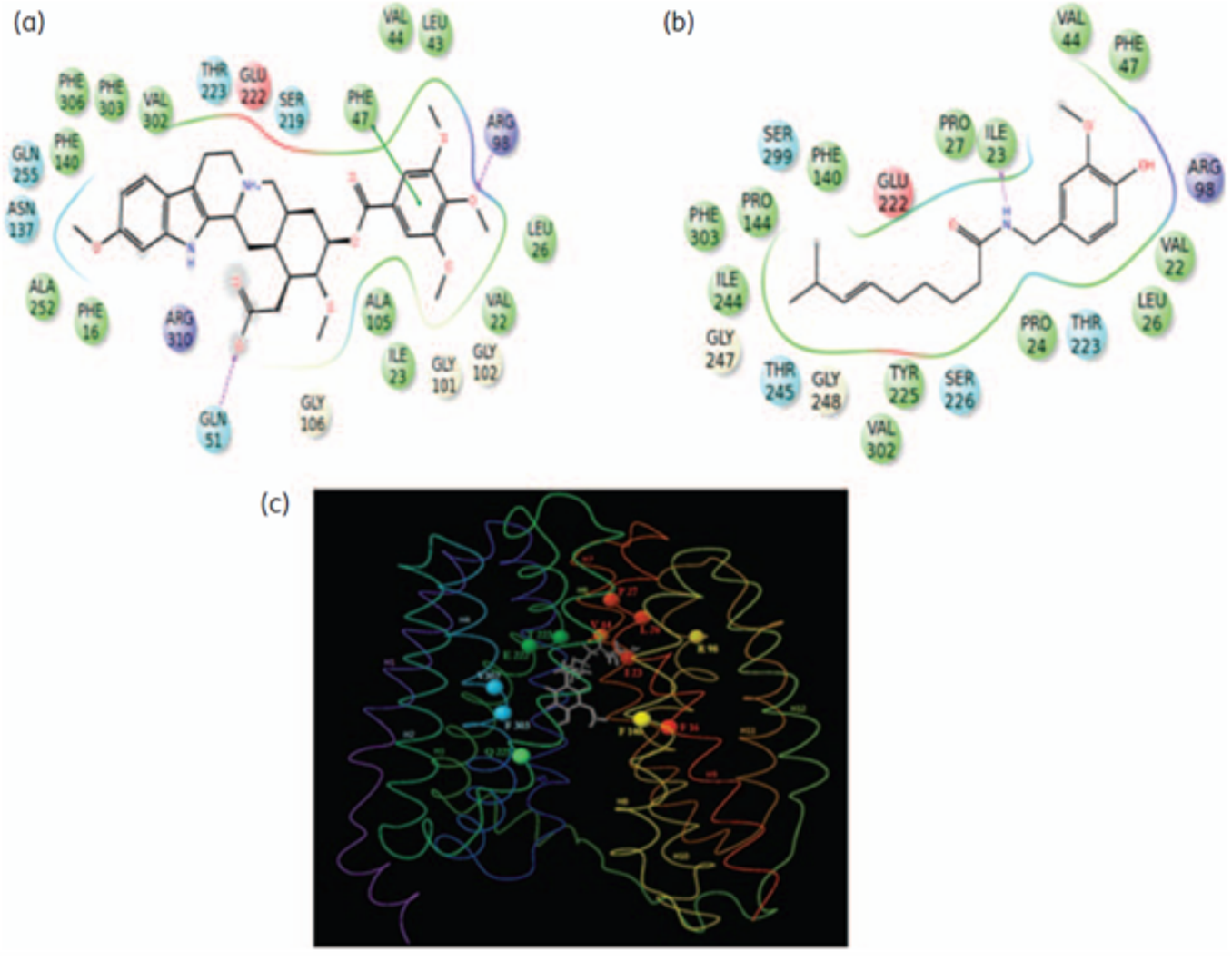

Figure 5: (A) Interaction of reserpine in the binding site of NorA. A H-bond formation between reserpine and Gln51, thereby providing stability to protein- ligand complex. (B) The orientation of capsaicin within the binding site allows its aliphatic chain to extend into the hydrophobic cleft involving residues Pro24, Phe143, Ile244, Gly248 and Phe303 which enables strong hydrophobic interactions due to the close proximity of the ligand with these residues. (C) The relative orientation of the binding site residues with respect to the trans-membrane helices of the predicted 3D structure of NorA. All the 12 trans-membrane helices of the protein are coloured differently and labelled. Capsaicin is also shown bound to the central cavity of the protein.

10. RURAL DEVELOPMENT AND SOCIETAL ACTIVITIES

10.1 Training programmes organized

1. A two days training programme organized for farmer of Gujarat state on 10th-11th April, 2012 to make them aware about the importance of medicinal and aromatic plants.

- Workshop-cum-Training programmes on Medicinal, aromatic and other economic crops organized by IIIM, Jammu on 5th and 6th September, 2012 for the progressive farmers of Rajasthan and Gujarat for making awareness about medicinal and aromatic plants and their agro-techniques. Quality planting material was provided to the farmers on trial basis for cultivation.



2. The fruit and vegetable mandi was inaugurated at Kathua on 2nd January, 2013 by the Hon'ble Health Minister of J & K, Mr. Sham Lal Sharma, Hon'ble Agriculture Minister Jenab Javed Ahmed Dar and Choudhary Lal Singh (Member Parliament) also participated in the inauguration function. We also participated in the event with our products and plants.

- Training programme conducted for farmers of Sarthal, Kishtwar, Batote for rural prosperity



3. A training programme was conducted in joint collaboration with KVK, SKAUST-J at PG College Bhaderwah on 26th July, 2012 for the cultivation of Medicinal and Aromatic plants for commercial purpose in which about 60 progressive farmers & 150 graduates & post graduates participated.



4. A training programme was conducted in Distt. Bhaderwah of J & K in collaboration with Department of Floriculture, Jammu on 4th December, 2012 for conducting awareness on cultivation of Medicinal & Aromatic Plants for commercial purpose.



5. A tour was conducted by Director, Chief Scientist and Experts from IIIM, Jammu on 16th & 17th November, 2012 for monitoring and evaluation of the trials fields of Rajasthan and Gujrat fields. Experts from IIIM, Jammu also interacting and facilitating the farmers for cultivation of MAPs



10.2 Variety released

A geraniol rich variety of *Cymbopogon khasianus* Bor [IIIM (J) CK-10] "Himrosa" released for commercial cultivation on the occasion of IIIM(J) Foundation day on 1st December, 2012.

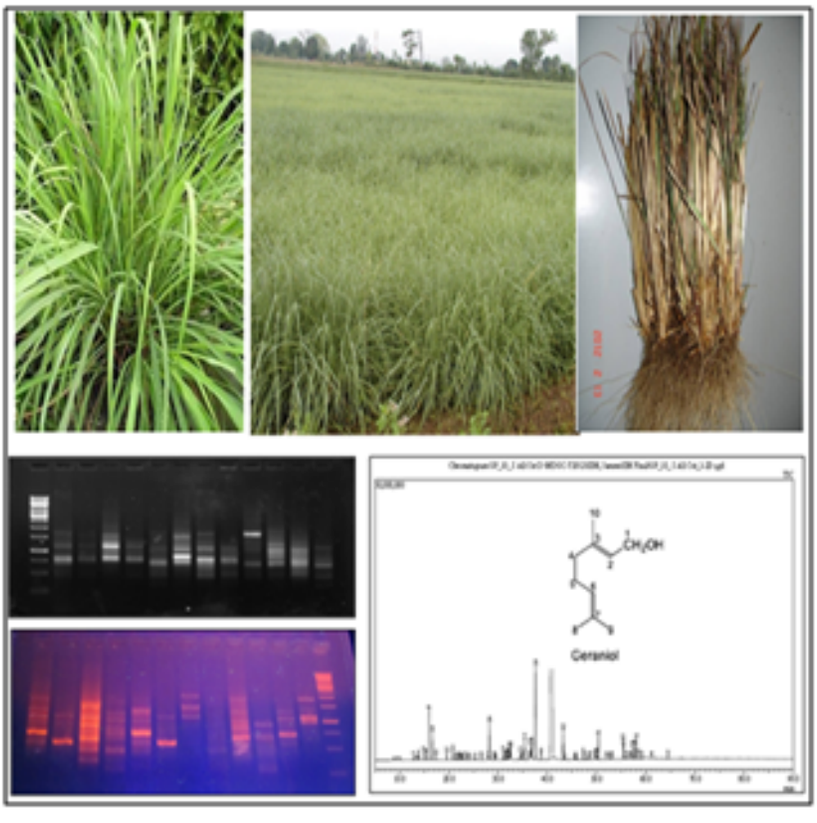


10.3 Painting competition

On the spot Painting/ Drawing competition for school children was organized by our Institute on 3rd March, 2013






10.4 Kissan mela and flower show organised

IIIM has a tradition of organizing Annual Flower Show in its campus since 1961. The prime purpose of this annual event has been to bring awareness among the general public about the culture of growing flowers and to infuse sense of environmental consciousness.

This year it was decided to expose the general public to the achievements of Indian science in addition to Flower show. Therefore, the event has been rechristened as "Kissan Mela and Flower Show" and is being organized on 17th March, 2013 at IIIM, Chatha Farm, Jammu.

The event was open to general public drawn from all quarters of society. Jenab Peerzada Mohammad Sayeed, Hon'ble Minister for Hajj, Aquaf, Floriculture and Public Enterprises were the Chief Guest Inaugural Ceremony of Kissan Mela. Nawang Rigzin Jora, Hon'ble Minister for Urban Development & Urban Local Bodies were the Chief Guest for Flower Show & Prize Distribution and Mr. Shaleen Kabra, Hon'ble Commissioner/Secretary, Agriculture Production Department, J & K Govt. were also present there to grace the occasion.





10.5 IIIM Sports Club Activities

Indian Institute of Integrative Medicine is a scientific organization having international recognition with state of art facilities. It is a multidisciplinary organization having a strength more than 400 employees. Apart from the scientific caliber it has a CSIR supported sports club having more than 300 members. The club is run by an elected body which is headed by the director of the institute as President of the club. General Secretary and the Sports Secretary are the other two main functionaries. Our club has the following sports activities viz., Cricket, Volleyball, Badminton, Table-tennis, Chess, Carom and Brig which are played regular throughout the year. Our teams participate in the tournaments which are organized by the CSIR and Central Govt. Co-ordination committee of Jammu. Under CSIR programme we have indoor and outdoor tournaments on the alternate years. In the year 2012-13 our teams participated in the outdoor (at Durgapur) and indoor tournaments (at Roorki) of CSIR and reached in the finals of Volley ball, Badminton, Table-tennis and Brig. Two of our players of Brig were given the title of Master pair of the tournament. For these sports activities we have the best facilities for Cricket, Volleyball, Badminton, Table-tennis, Chess, Carom and Brig. We in IIIM celebrate a week long sports week on the foundation day of the institute which falls on the last week of November. During this week we the employees of IIIM take part in different games viz., Cricket, Volleyball, Badminton, Table-tennis, Chess, Carom Brig, Tug-of-war and fun games. Around 200 participants took part in all these events in the year 2012. The biggest achievement of the year 2012-13 is the establishment of the GYM which is one of its own kinds with the best available equipments and environment (Figs. 1&2).

Figure 1 : Chief Guest Prof. Kumar Inaugurating the IIIM GYM

Figure 2 : Dr. Ram Vishwakarma, Director, IIIM Jammu showing the facilities created in IIIM JYM

Performance Parameters

Budget (Rs. in Lakh)

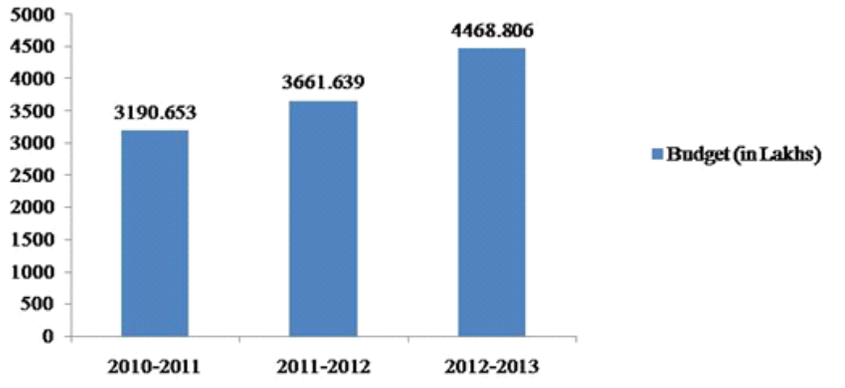

Institute's Reserve (Rs. In Lakhs)

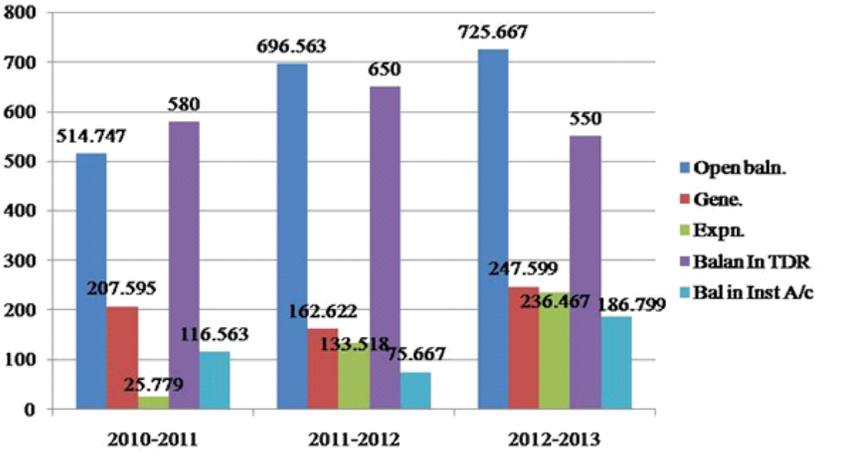

External Cash Flow(Rs. In lakhs)

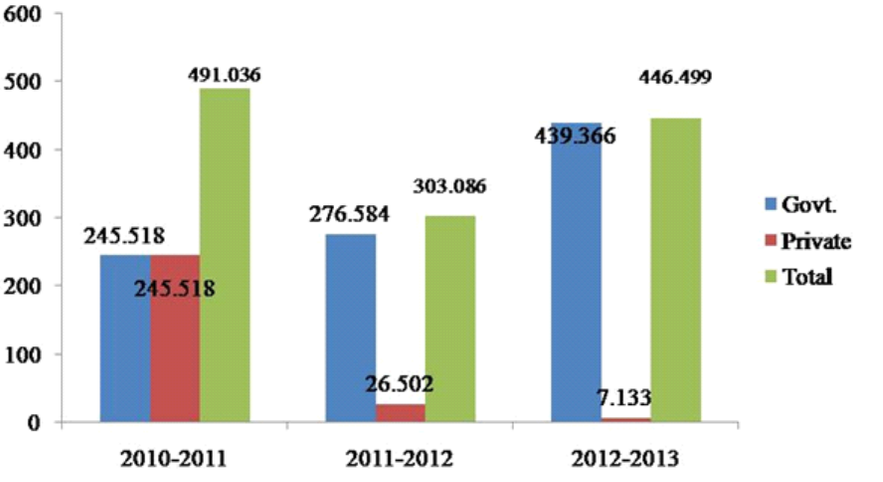

Publications

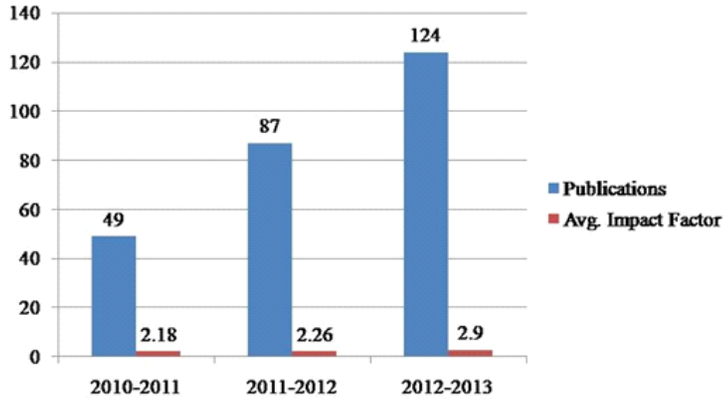

Patent filed

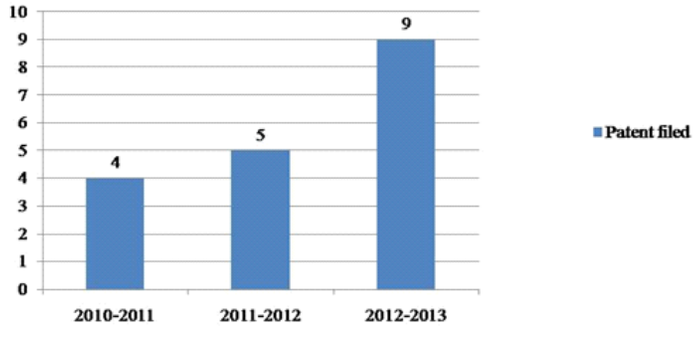

Fellows

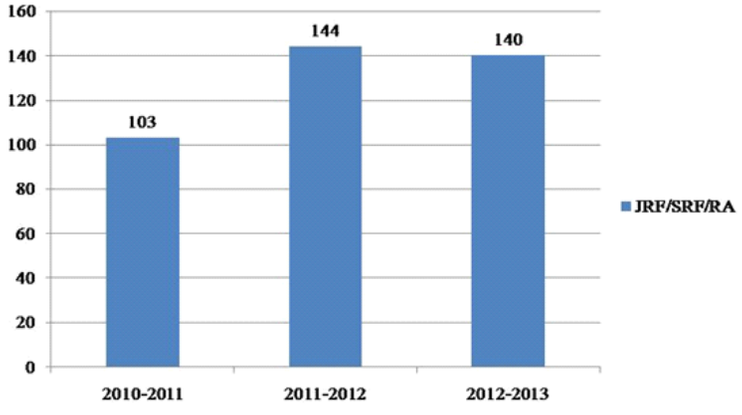

PUBLICATIONS (SCI JOURNALS)

1. Afnan, Q., Adil, M.D., Nissar-Ul, A., Rafiq, A.R., Amir, H.F., Kaiser, P., Gupta, V.K., Vishwakarma, R., and Tasduq, S.A. (**2012**). Glycyrrhizic acid (GA), a triterpenoid saponin glycoside alleviates ultraviolet-B irradiation-induced photoaging in human dermal fibroblasts. *Phytomedicine*, **19(7)**:658-64.

2. Ahmed, M., Hamid, A., Hussain, A., Majeed, R., Qurishi, Y., Bhat, J.A., Najar, R.A., Qazi, A.K., Zargar, M.A., Singh, S.K., and Saxena, A.K. (**2012**). Understanding histone deacetylases in the cancer development and treatment: An epigenetic perspective of cancer chemotherapy. *DNA and Cell Biol*., S62-71.

3. Ali Mohd Lone, Bilal Ahmad Bhat, and Goverdhan Mehta. A. **(2013).** general, flexible, ring closing metathesis (RCM) based strategy for accessing the fused furo[3,2-b]furanone moiety present in diverse bioactive natural product. *Tetrahedron Lett.*, **54**: 5619

4. Ali, A., Khajuria, A., Sidiq, T., Kumar, A,, Thakur, N. L., Naik, D., and Vishwakarma, R. A. **(2013).** lawsonone immunosuppressive lawsonyl monocyclic terpene from the marine-derived *Streptomyces* sp. *Immunology Lett.*, **150**: 79– 86.

5. Ali, F., Sangwan, P.L., Koul, S., Pandey, A., Bani, S., Abdullah, S.T., Sharma, P.R., Kitchlu, S., and Khan, I.A. (**2012**). 4-epi-Pimaric acid: A phytomolecule as a potent antibacterial and anti–biofilm agent for oral cavity pathogens. *Eur. J. Clin. Microbiol. Infect. Dis.*, **31**: 149-159.

6. Amna, T., Amina, M., Sharma, P. R., Puri, S. C., Al-Youssef, H. M., Al-Taweel, A. M. and Qazi, G. N. (**2012**). Effect of precursors feeding and media manipulation on production of novel anticancer prodrug camptothecin from endophytic fungus. *Braz. J. Micr*., 1476-1489.

7. Anjali Pandey, Sarang Bani, Naresh Kumar Satti, Bishan Datt Gupta and Krishan Avtar Suri.(2012).Anti-arthritic activity of agnuside mediated through the down-regulation of Inflammatory mediators and Cytokines. *Inflammation Research,* **61(4)**: 293-304.

8. Asif Ali, Anamika Khajuria, Tabasum Sidiq, Ashok Kumar, Narsinh L. Thakur, Deepak Naik, and Ram A. Vishwakarma. (**2012**). Modulation of LPS induced inflammatory response by Lawsonyl monocyclic terpene from the marine derived *Streptomyces* sp. *Immunol. Lett.*, **150**: 79–86.

9. Bharate, S. B., Bharate, J. B., Khan, S. I., Tekwani, B. L., Jacob, M. R., Mudududdla, R., Yadav, R. R., Singh, B., Sharma, P. R., Maity, S., Singh, B.;, Khan, I. A., and Vishwakarma, R. A.(**2013**). Discovery of 3,3'-diindolylmethanes as potent antileishmanial agents. *Eur. J. Med. Chem*., **63**: 435-443.

10. Bharate, S. B., Mudududdla, R., Sharma, R., and Vishwakarma, R. A. (**2013**). The first method for C-devinylation of aromatic systems. *Tetrahedron Lett.*, **54**: 2913-2915.

11. Bharate, S. B., Padala, A., Dar, B.A., Yadav, R.R., Singh, B., andVishwakarma, R.A.(2013). Montmorrillonite clay Cu(II) catalyzed domino one-pot multicomponent synthesis of 3,5-disubstituted isoxazoles. *Tetrahedron Lett.,* **54**: 3558-3561.

12. Bharate, S.B., Manda, S., Joshi, P., Singh, B., and Vishwakarma, R.A. (**2012**) Total synthesis and anti-cholinesterase activity of marine-derived bis-indole alkaloid fascaplysin. *Med. Chem. Commun.,* **3**, 1098-1103.

13. Bharate, S.B., Manda, S., Mupparapu, N., Battini, N., and Vishwakarma, R.A. (2012). Chemistry and biology of fascaplysin, a potent marine-derived CDK-4 inhibitor. *Mini-Rev. Med. Chem.*, **12(7)**: 650-664.

14. Bharate, S.B., Mudududdla, R., Bharate, J.B., Battini, N., Battula, S., Yadav, R.R., Singh, B., and Vishwakarma, R.A.(2012). Tandem one-pot synthesis of flavans by recyclable silica-HClO4 catalyzed knoevenagel condensation and [4+2]-Diel's-Alder cycloaddition. *Org. Biomol. Chem.*, **10**: 5143–5150.

15. Bharate, S.B., Sawant, S.D., Singh, P.P., and Vishwakarma, R.A. (**2013**). Kinase inhibitors of marine origin. *Chem. Rev*., DOI: 10.1021/cr300410v.

16. Bharate, S.B., Singh, B., and Vishwakarma, R.A. (**2012**). Modulation of k-Ras signaling

by natural products. *Curr. Med. Chem.,* **19(14)**: 2273-2291.

17. Bharate, S.B., Singh, B., Bharate, J.B., Jain, S.K., Meena, S., and Vishwakarma, R.A. (**2013**). QSAR and pharmacophore modeling of N-acetyl-2-aminobenzothiazole class of phosphoinositide-3-kinase-alpha inhibitors. *Med. Chem. Res*., **22**: 890-899.

18. Bharate, S.B., Yadav, R.R., and Vishwakarma, R.A. (**2013**). QSAR and pharmacophore study of Dyrk1A inhibitory meridianin analogs as potential agents for treatment of neurodegenerative diseases. *Med. Chem. (Bentham),* **9(1)**: 152-161.

19. Bharate, S.B., Yadav, R.R., Battula, S., and Vishwakarma, R.A. (**2012**). Meridianins: A potent marine derived kinase inhibitors. *Mini-Rev. Med. Chem.,* **12(7)**: 618-631.

20. Bharate, S.B., Yadav, R.R., Khan, S. I., Tekwani, B. L., Jacob, M. R., Khan, I.A., and Vishwakarma, R.A. (**2013**). Meridianin G and its analogs as antimalarial agents. *Med. Chem. Commun*., **4**: 1042-1048.

21. Bharate, S.S., and Bharate, S.B. (**2012**). Modulation of TRPM8 by cooling compounds. *ACS Chem. Neurosci.*, **3(4)**: 248–267.

22. Bharate, S.S., and Vishwakarma, R.A.(2013). Impact of preformulation on drug development. *Expert Opin Drug Deliv.,* 2013 [Epub ahead of print] PMID: 23534681.

23. Bhat, A., Riyaz-Ul-Hassan, S., Ahmad, N., and Johri, S. (**2013**). Isolation of cold-active, acidic endocellulase from Ladakh soil by functional metagenomics. *Extremophiles*, **17(2)**: 229-239.

24. Bilal Ahmad Mir, Jabeena Khazir, Nisar A. Mir, Tanvir-ul Hasan and Sushma Koul. (2012). Botanical, chemical and pharmacological review of *Withania somnifera* (Indian ginseng): an ayurvedic medicinal plant. *Indian Journal of Drugs and Diseases*. **1(6)**: 147-160.

25. Bilal Ahmad Mir, Sushma Koul and Amarjit S. Soodan (2013). Reproductive biology of *Withania ashwagandha* sp. novo (Solanaceae). *Industrial Crops and Products,* **45**:442-446.

26. Chaubey, A., Parshad, R., Taneja,S.C., Deokar,S., Rajan, C.R. and Ponrathnam, S. (**2012**). Immobilization of enantioselective lipase on soluble supports for kinetic resolution of drug intermediates. *J. Bioact. Compat. Polym*., **27**: 499-509.

27. Chaubey, A., Raina, C., Parshad, R., Rouf, A., Gupta, P., and Taneja, S.C (**2013**). Bioconversion of sucralose-6-acetate to sucralose using immobilized microbial enzymes. *J Mol Cat B*., **91**: 81-86.

28. Parveen K. Chinthakindi, Payare L. Sangwan, Saleem Farooq, Rajeshwar R. Aleti, Anupurna Kaul, Ajit K Saxena, Y.L.N. Murthy, Ram A. Vishwakarma, and Surrinder Koul. (**2013**). Diminutive effect on T and B - cell proliferation of non cytotoxic α-santonin derived 1,2,3-triazoles: A report. *Eur . J. Med. Chem*., **60**: 365-375.

29. Dar, B. A., Sahu, A. K., Patidar, P., Sharma, P. R., Mupparapua, N., Vyas, D., Maity, S., Sharma, M., and Singh, B. (**2012**). Heteropolyacid-clay nano-composite as a novel heterogeneous catalyst for the synthesis of 2,3-dihydroquinazolinones. *J. Indus. & Eng. Chem.,* **19:** 407-412.

30. Dar, B. A., Chakraborty, A., Sharma, P. R., Shrivastava, V., Bhowmik, A., Vyas, D., Bhatti, P., Sharma, M., and Singh, B. (**2012**). Grinding-induced rapid, convenient and solvent free approach for the one pot synthesis of a-aminophosphonates using aluminium pillared interlayered clay catalyst. *J. Indus. & Eng. Chem.,* **19**: 732-738.

31. Deepak K. Sharma, Altaf Hussain, Mallikharjuna Rao Lambu, Syed Khalid Yousuf, Sudip Maiety, Baldev Singh and Debaraj Mukherjee (**2013**). Fe/Al pillared clay catalyzed solvent-free synthesis of bisindolylmethanes using diversely substituted indoles and carbonyl compounds. *RSC Adv.,* **3**: 2211-2215.

32. Deepak K. Sharma, Bilal Rah, Mallikharjuna R. Lambu, Altaf Hussain, Syed K. Yousuf, Anil K. Tripathi, Baldev Singh, Gayatri Jamwal, Zabeer Ahmed, Nayan Chanauria, Amit Nargotra, Anindya Goswami and Debaraj Mukherjee (**2012**). Design and synthesis of novel N,N′-glycoside derivatives of 3,3′-diindolylmethanes as potential antiproliferative agents. *Med. Chem. Commun*., **3**: 1082-1091.

33. Devinder Gupta, Mahendra Verma, Sankar lal, Rajneesh Anand, Ravi Khajuria, Surinder Kitchlu and Surinder Koul (**2012**). Extraction efficiency studies of *Podophyllum hexandrum* using conventional & non conventional extraction

methods by using HPLC –UV –DAD Method. *Journal of Liquid Chromatography & Related Technologies*, DOI:10.1080/10826076.2012.745134.

34. Fayaz Malik, Hasan Korkaya, Shawn, G., Clouthier Max, and S. Wicha (**2012**). Breast Cancer Heterogeneity: Need to Review Current Treatment Strategies. *Curr Breast Cancer Rep.,* **4**: 225–231.

35. Felnagle E.A., Chaubey A., Noey E.L., Houk K.N. and Liao J.C.(**2012**). Engineering synthetic recursive pathways. *Nat. Chem. Biol*., **8**: 518-526.

36. Ganie, S.A., Amin, S., Hamid, R., Hamid, A., Majeed, R., Qurishi, Y., Zargar, B.A., Masood, A., and Zargar, M.A. (2012). *Podophyllum hexandrum* aqueous extract as a potential free radical scavenger. *Redox Rep*., **17(2)**: 54-62.

37. Gupta, D. K., Verma, M. K., Anand, R., and Khajuria, R. K. (**2013**). UPLC-qTOF-MS/MS method development and validation for extraction optimization of bioactive constituent of *Glycyrrhiza glabra* in different extracts. *J. Pharm. Anal*., **3(3)**: 205-210. DOI: 10.1016/j.jpha.2013.01.001.

38. Hitesh Kumar, Kiran Kaul, Suphla B Gupta, Vijay K Kaul and Sanjay Kumar. (2012). A Comprehensive Analysis of fifteen genes of steviol glycosides biosynthesis pathway in *Stevia rebaudiana* (Bertoni). *Gene*, **492(1)**: 276-284.

39. Hussain, A., Yousuf, S. K., Kumar, D. K., L, M., Singh, B., Maity, S., Debaraj Mukherjee. (**2012**). Synthesis of benzannulated chiral macrocycles embedded in a carbohydrate t emplate by intramolecular base free Sonogashira reaction on alumina support. *Advanced Synthesis and Catalysis.* **354**: 1933–1940.

40. Iram Saba, Parvaiz H. Qazi, Shabir A. Rather, Refaz A. Dar, Qurrat A. Qadri, Nasier Ahmad, Sarojini Johri, Subash C. Taneja and Sami Shawl (**2012**). Purification and characterization of a cold active alkaline protease from *Stenotrophomonas* sp., isolated from Kashmir, India. *World J Microbiol Biotechnol.,* **28**: 1071–1079.

41. Jain, S.K., Bharate, S.B., and Vishwakarma, R.A. (**2012**). Cyclin-dependent kinase inhibition by flavoalkaloids. *Mini-Rev. Med. Chem*., **12(7)**: 632-649.

42. Jain, S.K., Meena, S., Singh, B., Bharate, J.B., Joshi, P., Singh, V.P., Vishwakarma, R.A., and Bharate, S.B. (**2012**). KF/alumina catalyzed regioselective benzylation and benzoylation using solvent-free grind-stone chemistry. *RSC Adv.,* **2**: 8929-8933.

43. Katoch, M., Bhushan, S., Katoch, A., Kumar, R., and Kitchlu S. **(2013)**. *Streptomyces spiroverticillatus* from the rhizospheric soil of *Arnebia euchroma:* its antimicrobial and anticancer potential. *IJAPR.,* **4**: 1603-1607

44. Khan, S., Kaur, R., Shah, B.A., Malik, F., Kumar, A., Bhushan, S., Jain, S.K., Taneja, S.C., and Singh, J. **(2012)**. A novel cyano derivative of 11-keto-β-boswellic acid causes apoptotic death by disrupting PI3K/AKT/Hsp-90 cascade, mitochondrial integrity, and other cell survival signaling events in HL-60 cells. *Mol Carcinog*., **51(9)**: 679-95.

45. Kitchlu S, R Bhadauria, G Ram, K Bindu, RK. Khajuria, A Ahuja **(2013)**. Chemo-divergence in essential oil composition among thirty one core collections of *Ocimum sanctum* L. Grown under sub-tropical region of Jammu, India. *American Journal of Plant Sciences*, **4**: 302-308.

46. Korkaya, H., Kim, G.I., Davis, A., Malik, F., Henry, N.L., and Wicha, M.,S. (**2012**). Activation of an IL6 Inflammatory Loop Mediates Trastuzumab Resistance in HER2+ Breast Cancer by Expanding the Cancer Stem Cell Population. *Molecular Cell*, **47**: 570–584.

47. Kumar, A., Shah, B.A., Hamid, A., Singh, S.K., Andotra, S.S., Sethi, V.K., Saxena, A.K., Singh, J.,and Taneja, S.C. (**2012**). Acyl derivatives of Boswellic acids as inhibitors of NF-κB and STATs. *Bioorg Med Chem Lett*., **22**: 431–435.

48. Kumar, D., Kumar, L., Nagar, S., Raina, C., Parshad, R., and Gupta,V. K. (**2012**). Screening, isolation and production of lipase /esterase producing *Bacillus* sp. strain DVL2 and its potential evaluation in estrification and resolution. *Archives of Arch.Appl. Sci.Res.,* **4(4)**: 1763-1770.

49. Kumar, D., Kumar, Lalit, Nagar, S., Raina, C., Parshad, R., and Gupta,V.K . **(2012).** Isolation, production and application of lipase /estrase from *Bacillus* sp. strain DVL43. *J. Microbial. and Biotech. Res.,* **2(4)**: 521-525.

50. Kumar, D**.,** Nagar,S., Bhushan,I., Kumar, L., Parshad, R., Gupta,V.K. (**2013**). Covalent immobilization of organic solvent tolerant lipase on alumina oxide pellet for its potential esterification reaction. *J. Mol. Catalysis B:*

Enzymatic, **87**: 51-61.

51. Kumar, M., Qadri, M., Sharma, P.R., Kumar, A., Andotra, S.S., Kaur, T., Kapoor, K., Gupta, V.K., Kant, R., Hamid, A., Johri, S., Taneja, S.C., Vishwakarma, R.A., Riyaz-Ul-Hassan, S., and Shah, B.A. (**2013**). Tubulin Inhibitors from an endophytic fungus isolated from *Cedrus deodara*. *J. Nat. Prod*., **76(2)**: 194–199.

52. Kumar, S., Mehndiratta, S., Nepali, K., Gupta, M. K., Koul, S., Sharma, P.R., Saxena A.K., and Dhar, K. L. (**2013**). Novel indole-bearing combretastatin analogues as tublin polymerization inhibitors. *Org. Med. Chem. Lett.,* **3**: 3-16.

53. Kumar, S., Pathania, A. P., Saxena, A. K., Vishwakarma, R. A., Ali, A., and Bhushan, S. **(2013).** Anticancer potential of flavonoids isolated from stem bark of Erythrina suberosa through induction of apoptosis and inhibition of STAT signaling pathway in Human leukemia HL-60 cells. *Chem. Biol. Inter*., **205**: 128-137**.**

54. Madhubabu Tatina, Syed Khalid Yousuf and Debaraj Mukherjee (**2012**). 1.2,4,6-Trichloro-1,3,5-triazine (TCT) mediated one-pot sequential functionalisation of glycosides for the generation of orthogonally protected monosaccharide building blocks. *Org. Biomol. Chem.,* **10**: 5357-5360.

55. Mahendra K. Verma, Ishtiyaq A. Nazar, Manoj K. Tikoo, Gurdarshan Singh, Devinder K. Gupta, Rajneesh Anand, Ravi K. Khajuria, Subhash C. Sharma, Rakesh K. Johri (**2013**). Method validation and simultaneous determination of curcuminoids by UPLCqTOF-MS and pharmacokinetic study of curcumin in mice. *DARU-Journal of Pharmaceutical Sciences,***21**: 11. DOI: 10.1186/2008-2231-21-11.

56. Majeed, R., Reddy, M.V., Chinthakindi, P.K., Sangwan, P.L., Hamid, A., Chashoo, G., Saxena, A. K., and Koul, S. (**2012**). Bakuchiol derivatives as novel and potent cytotoxic agents: A report. *Eur. J. Med. Chem*., **49**: 55-67.

57. Majeed, R., Sangwan, P.L., Chinthakindi, P.K., Hamid, A., Saxena, A. K., and Koul, S. (**2013**). Synthesis of 3-O-Propargylated betulinic acid and its 1,2,3-triazoles as potential apoptotic agents. *Eur. J. Med. Chem.,* DOI: 10.1016/j.ejmech.2013.03.028.

58. Majeed, R., Hamid, A., Qurishi, Y., Qazi, A.K., Hussain, A., Ahmed, M., Najar, R.A., Bhat, J.A., Singh, S.K., and Saxena, A.K. (**2012**). Therapeutic targeting of cancer cell metabolism: role of metabolic enzymes, oncogenes and tumor suppressor genes. *J Cancer Sci and Ther.,* **4(9)**: 281-291.

59. Malik, F., Korkaya, H., Clouthier, S.G., and Wicha, M. S. (**2012**). Lin28 and HER2: two stem cell regulators conspire to drive aggressive breast cancer. *Cell Cycle*, **11**: 2780-2781.

60. Mallikharjuna Rao L., Syed Khalid Yousuf, Debaraj Mukherjee and Subhash Chandra Taneja (**2012**). Regioselective azidotrimethylsilylation of carbohydrates and applications thereof. *Org. Biomol. Chem.,* **10**: 9090-9098.

61. Marcheschi R.J., Zhang K., Noey E.L., Kim S., Li H., Chaubey A., Houk K.N. and Liao J.C. (**2012**). A Synthetic recursive "+1" pathway for carbon chain elongation. *ACS Chem Biol*., **7**: 689–697.

62. Mir, F., Rather, M.A.,Shawl, A.S., and Qurishi, M. A. (**2012**). Comparative GC-FID and GC-MS analysis of the leaf, stem and root essential oils of *Artemisia dracunculus*. L growing in Kashmir (India). *J Pharm Res*., **2**:1353-1356.

63. Mohammed, S., Padala, A.K., Dar, B.A., Singh, B., Sreedhar, B., Vishwakarma, R.A., and Bharate, S.B. (**2012**). Recyclable clay supported Cu (II) catalyzed tandem one-pot synthesis of 1-aryl-1,2,3-triazoles. *Tetrahedron,* **68**: 8156-8162.

64. Mudududdla, R., Jain, S.K., Bharate, J.B., Gupta, A.P., Singh, B., Vishwakarma, R.A., and Bharate (**2012**). Ortho-Amidoalkylation of phenols via tandem one-pot approach involving oxazine intermediate. *J. Org. Chem*., **77**: 8821-8827.

65. Nageswar Rao, D., Rasheed, S.K., Aravinda, S., Ram A. Vishwakarma and Parthasarathi Das (**2013**). Base and ligand free copper-catalyzed N-arylation of 2-amino-N-heterocycles with boronic acids in air. RSC Adv. 2013 **DOI:** 10.1039/C3RA40735G.

66. Nitin Pal Kalia, Priya Mahajan, Rukmankesh Mehra, Amit Nargotra, Jai Parkash Sharma,Surrinder Koul and Inshad Ali Khan (**2012**). Capsaicin, a novel inhibitor of the NorA efflux pump, reduces the intracellular invasion of *Staphylococcus aureus*. *J. Antimicrob. Chemother.*, **67**: 2401-2408.

67. P. Pandotra, A. P. Gupta, Gandhiram , Mohd K Husian,

and S. Gupta(2013). Genetic and Chemo-divergence in Eighteen Core Collection of *Zingiber officinale* from North-West Himalayas. *Scientia Horticulturae*, **160**: 283–291.

68. Pankaj Pandotra, Mohd Kashif Husain, Gandhi Ram, Suphla Gupta and Ajai Prakash Gupta. (**2013**). Evaluation of genetic diversity and chemical profile of ginger cultivar in North-Western Himalayas. *Biochemical Systematics and Ecology*, **48**: 281–287.

69. Pankaj Pandotra, Mohd Kashif Husain, Gandhi Ram, Suphla Gupta and Ajai Prakash Gupta. (**2013**). Retrotransposon based genetic status of North-West Himalayan *Zingiber officinale* revealed high heterogeneity. *Journal of Plant Biochemistry and Biotechnology* DOI 10.1007/s13562-013-0196-8.

70. Parvinder Pal Singh, Satish Gudup, Hariprasad Aruri, Umed Singh, Srinivas Ambala, Mahipal Yadav, Sanghapal D. Sawant and Ram A. Vishwakarma (**2012**). New method for C-H arylation/alkylation at α-position of cyclic aliphatic ethers by iron-oxide mediated reaction. *Org. Biomol. Chem.,* **10**: 1587-1597.

71. Parvinder Pal Singh, Sravan Kumar Aithagani, Mahipal Yadav, Varun Pratap Singh, and Ram A Vishwakarma (**2013**). Iron catalyzed cross coupling of electron-deficient heterocycles and quinone with organoboron species via innate C-H functionalization: Application in total synthesis of pyrazine alkaloid Botryllazine A. *J. Org. Chem.,* **78**: 2639−2648.

72. Parvinder Pal Singh, Thanusha Thatikonda, K. A. Aravinda Kumar, Sanghapal D. Sawant, Baldev Singh, Amit Kumar Sharma, P. R. Sharma, Deepika Singh and Ram A. Vishwakarma (**2012**). Cu-Mn spinel oxide catalyzed regio-selective halogenation of phenols and N-heteroarenes. *J. Org. Chem.,* **77**: 5823−5828.

73. Phalisteen, S., Arif Jan, Parvaiz Qazi, Naseer, A., and Atif, M. (**2012**). Quantitative estimation of iridoid glycosides in *Picrorhiza kurroa* Royle. *European Journal of Medicinal Plants,* (Accepted 2012).

74. Punita Sharma, Suresh Kumar, Furqan ali, sumati anthal, Vivek k gupta, Inshad A Khan, Surjeet singh, Payare L. Sangwan, Krishan A. Suri, Bishan D. Gupta, Devinder K. Gupta, Prabhu Dutt, Ram A. Vishwakarma, Naresh K. Satti (2013). Synthesis and biologic activities of some heterocyclic chalcone derivatives. *Med. Chem. Res.,***22(8)**: 3969-3983.

75. Qadri, M., Johri, S., Shah, B.A., Khajuria, A., Sidiq, T., Lattoo, S.K., Abdin, M.Z., and Riyaz-Ul-Hassan, S. (**2013**). Identification and bioactive potential of endophytic fungi isolated from selected plants of the Western Himalayas. *Springer Plus.,* **2**: 8.doi:10.1186/2193-1801-2-8.

76. Qurishi, Y., Hamid, A., Sharma, P.R., Wani, Z.A., Mondhe, D.M., Singh, S.K., Zargar, M.A., Andotra, S.S., Shah, B.A., Taneja, S.C., and Saxena, A.K. (**2013**). NFκB down-regulation and PARP cleavage by novel 3-α-butyryloxy-β-boswellic acid results in cancer cell specific apoptosis and *in vivo* tumor regression. *Anti-Cancer Agents Med Chem.,* **13(5)**:777-790.

77. Qurishi, Y., Hamid, A., Sharma, P.R., Wani, Z.A., Mondhe, D.M., Singh, S.K., Zargar, M.A., Andotra, S.S., Shah, B.A., Taneja, S.C., and Saxena, A.K. (2012). PARP cleavage and perturbance in mitochondrial membrane potential by 3-α-propionyloxy-β-boswellic acid results in cancer cell death and tumor regression in murine models. *Future Oncol.*, **8(7)**: 867-881.

78. Rah, B., Amin, H., Yousuf, K., Khan, S., Jamwal, G., Mukherjee, D., and Goswami, A. A. (**2012**). Novel MMP-2 inhibitor 3-azidowithaferin A (3-azidoWA) abrogates cancer cell invasion and angiogenesis by modulating extracellular Par-4. *PLoS ONE*, **7(9)**: *e*44039.

79. Rajeshwar R., Aleti, P. K., Chinthakindi, Saleem Farooq, Payare L. Sangwan, S. Koul (**2012**). N-Iodo succinamide catalysed iodo esterification. *Helvetica chimica acta.*, doi.10.1002/hlca.201200383 .

80. Rather, M. A., Hassan, T., Dar, B. A., Shawl, A. S., Qurishi M. A., and Ganai, B. A. (**2012**). Essential oil composition of *Nepeta raphanorhiza* Benth growing in Kashmir Valley. *Records of Natural Products*, **6(1)**: 67-70.

81. Rauf, A., Gupta, P., Aga, M. A., Kumar, B., Chubey, A., Parshad, R., and Taneja, S.C.(**2012**). Chemoenzymatic synthesis of piperoxan, prosympal, dibozane and doxazosin. *Tetrahedron Asymmetry*, **23**: 1615-1623.

82. Raut, A. A., Kumar, A., Kala, S. N., Chhokar, V., Rana, N., Beniwal, V., Jaglan, S., Samuchiwal, S. K., Singh, J. K., and Mishra, A. (**2012**). Identification of novel single nucleotide polymorphisms in

the DGAT1 gene of buffaloes by PCR-SSCP. *Gen. Mol. Biol.,* **35(3)**:610-613.

83. Rayees, S., Sharma, R., Singh, G., Najar, I.A., Singh, A., Ahamad, D.B., Sharma, S.C., Tikoo, M.K., Gupta, V.K., Sangwan, P.L., Singh, S., Koul, S., and Johri, R.K. (2013). Acute, sub-acute and general pharmacological evaluation of 5-(3,4-methylenedioxyphenyl)-4-ethyl-2E,4E-pentadienoic acid piperidide (SK-20): a novel drug bioavailability enhancer. Environ Toxicol Pharmacol., **35(2)**:347-359.

84. Rekha S. Dhar, Suphla Gupta, Parminder Singh,Sumeer Razdan,Wajid W. Bhat, Satinder Rana, Surrinder K Lattoo and Shabnam Khan (2012). Identification and characterization of protein composition in *Withania somnifera*-An Indian Ginsing. *Journal of Plant Biochemistry and Biotechnology*, **21(1)**: 77-87.

85. Riyaz-Ul-Hassan, S., Strobel, G., Geary, B., and Sears, J. (**2013**). An endophytic *Nodulisporium* sp. from Central America producing volatile organic compounds with both biological and fuel potential. *J.Microbiol. Biotechnol*., **23(1)**: 29–35.

86. Riyaz-Ul-Hassan, S., Verma, V., and Qazi, G.N. (**2013**). Real-time PCR based rapid and culture-independent detection of Salmonella in dairy milk- addressing some core issues. *Lett. Appl. Microbiol.,* **56**: 275–282.

87. Rouf, A., Gupta, P., Aga, M. A.,Kumar, B., Chaubey, A., Parshad,R., and Taneja, S.C. (**2012**). Chemoenzymatic synthesis of piperoxan, prosympal, dibozane and doxazosin. *Tetahedron: Asymmetry*, **23**: 1615-1623.

88. Rukmankesh Mehra, Amit Nargotra Bhahwal Ali Shah, Subhash C. Taneja, Ram Vishwakarma and Surrinder Koul. (2013). Pro-apoptotic properties of parthenin analogs: a quantitative structure–activity relationship study**.** *Medicinal Chemistry Research,* **22(5)**: 2303-2311.

89. Sajad, H. Wani, Asif amin, Shahnawaz, N. Sofi, Taseem A. Mokhdomi, 1.Shoiab Bukhari, Qazi Parvaiz Hassan and Raies A. Qadri (**2013**). RP- HPLC facilitated quantitative analysis of Tectorigenin in the different species of Iris plant and evaluation of its *in vitro* anticancer potential . *Int J Curr Res.,* **5**: 206-211.

90. Sajad, H. Wani, Asif Amin,1., Manzoor, A. Rather, Javid Ahmad Parray, Qazi Parvaiz, and Raies A Qadri. (2012). Antibacterial and phytochemical screening of different extracts of five Iris species growing in Kashmir. J.of Pharm Res., 5(6): 3376-3378.

91. Saleem Farooq, Payare L. Sangwan, Rajeshwar R. Aleti, P. K. Chinthakindi, Mushtaq A. Qurishi, and Surrinder Koul (**2012**). CuCN catalyzed one pot synthesis of γ-keto diesters: domino double Michael addition followed by Nef reaction. *Tetrahedron Lett*. **53**: 3305-3309.

92. Sanghapal D. Sawant, Mahesuni Srinivas, G. Lakshma Reddy, V. Venkateswar Rao, Parvinder Pal Singh, and Ram A. Vishwakarma (**2012**). One-pot multicomponent synthesis of medicinally important purine quinazolinone derivatives. *Tetrahedron Lett*., **53**: 6195-6198.

93. Sanghapal D. Sawant, M. Srinivas, K.A. Aravinda Kumar, G. L. Reddy, P. P. Singh, B. Singh, A. K. Sharma, P.R. Sharma, and R. A. Vishwakarma (2013). Ligand-free C–N bond formation in aqueous medium using a reusable Cu–Mn bimetallic catalyst; *Tet. Lett.*, **54(39)**: 5351-5354.

94. Satiander Rana, Niha Dhar, Wajid Waheed Bhat, Sumeer Razdan, Shabnam Khan, Rekha S. Dhar, Prabhu Dutt and Surrinder K. Lattoo. (**2012**). A 12-deoxywithastramonolide-rich somaclonal variant in *Withania somnifera* (L.) Dunal – molecular cytogenetic analysis and significance as a chemotypic resource. *In Vitro Cell. Dev. Biol. Plant,* **48**:546–554. *DOI: 10.1007/s11627-012-9458-8.*

95. Satiander Rana, Surrinder K. Lattoo, Niha Dhar, Sumeer Razdan, Wajid Waheed Bhat, Rekha S. Dhar and Ram Vishwakarma. (**2013**). NADPH-Cytochrome P450 reductase: Molecular cloning and functional characterization of two paralogs from *Withania somnifera* (L.) Dunal. *PLoS ONE,* **8(2)**: e57068. doi:10.1371/journal.pone.0057068.

96. Shairgojray, B. A., Dar, A. A., and Bhat, B. A. (**2013**). Micellar promiscuity: an expeditious approach to Morita-Baylis-Hillman reaction. *Tetrahedron Lett.,* **54**: 2391-2394.

97. Shawl, A. S., Rather, M.A., Rehman, S., Mir, F., and Qurishi, M. A. (**2012**). Chemical composition of essential oil of *Rhododendron lepidotum* wall. ex D. Don growing in Kashmir Himalayas. *Journal of Essential Oil Research*. **23(6)** : 25- 28.

98. Sheikh abid, Anamika

Khajuria, Qazi Parvaiz, Tabasum Sidiq, Aruna Bhatia, Surjeet Singh, Shabir Ahmad, M.K.Randhawa, N.K.Satti, Prabhu Dutt (**2012**). Immunomodulatory studies of a bioactive fraction from the fruit of *Prunus cerasus* in BALB/c mice. International *Immunopharmacology,* **12**: 626-634.

99. Showkat Rashid, Bilal Ahmad Dar, Rabiya Majeed, Abid Hamid, Bilal Ahmad Bhat. Synthesis and biological evaluation of ursolic acid-triazolyl derivatives as potential anti-cancer agents. *Eur. J. Med. Chem***.** 2013, *66*, 238.

100. Singh, B., Nadkarni, J.R., Vishwakarma, R.A., Bharate, S.B., Nivsarkar, M., and Anandjiwala, S. (**2012**). The hydroalcoholic extract of *Cassia alata* (Linn.) leaves and its major compound rhein exhibits antiallergic activity *via* mast cell stabilization and lipoxygenase inhibition. *J. Ethnopharmacol.,* **141**: 469-473.

101. Singh, I., Amin, H., Rah, B., and Goswami, A. (**2013**). Targeting EGFR and IGF 1R: A promising combination therapy for metastatic cancer. *Front Biosci (Schol Ed).,* **5**: 231-246.

102. Sinha, S., Mishra, P., Amin, H., Rah, B., Nayak, D., Goswami, A., Kumar, N., Vishwakarma. R., and Ghosal, S. (**2013**). A new cytotoxic quinolone alkaloid and a pentacyclic steroidal glycoside from the stem bark of *Crataeva nurvala*: Study of anti-proliferative and apoptosis inducing property. *Eur. J.Med.Chem.,* doi: 10.1016/j.ejmech.2012.12.017.

103. Srinivas, J., Reddy, D.M., Kumar, S., Malik, F., Sharma, A., Khan, I.A., Sampat H.M. Kumar (**2013**). Design and synthesis of novel magnolol derivatives as potential antimicrobial and antiproliferative compounds. *Eur. J. Med. Chem*., **51**: 35-41.

104. Sumati Anthal, Prabhu Dutt, N.K.Satti, Rajnikant, Vivek K.Gupta. (**2012**).Crystal structure of N-(4-Methyl-pyridine-2-yl)-3-oxo-butyramide. *X-ray Structure Online,* **19**: 73-74.

105. Sumeer Razdan, Wajid Waheed Bhat, Satiander Rana, Niha Dhar, Surrinder K Lattoo, Rekha S Dhar and Ram A Vishwakarma. (**2013**). Molecular characterization and promoter analysis of squalene epoxidase gene from Withania somnifera (L.) Dunal. *Mol Bio Rep.,* **40**:905–916. DOI: 10.1007/s11033-012-2131-9.

106. Suphla Gupta, Pankaj Pandotra , Ajai P Gupta, M.K. Verma, Ashok Ahuja and Ram A Vishwakarma **(2013)**. Direct rhizogenesis, *in vitro* stolon proliferation and high throughput regeneration of plantlets in *Glycyrrhiza glabra. Acta Physiologeae Plantarum,* **35 (9):** 2699-2705.

107. Suphla Gupta, Rajni Sharma, Pankaj Pandotra, Sundeep Jaglan and Ajai Prakash Gupta (2012). Chromolithic method development, validation and system suitability analysis of ultra-sound assisted extraction of glycyrrhizic acid and glycyrrhetinic acid from *Glycyrrhiza glabra*. *Natural Product Communications*, **7(8)**: 991 – 994.

108. Suresh Kumar, Ajay Kumar, Anup Singh Pathania, Santosh Kumar Guru, Srinivas Jada, H.M. Sampath Kumar, and Fayaz Malik (**2013**). Tiron and trolox potentiate the autophagic cell death induced by magnolol analog Ery5 by activation of Bax in HL-60 cells. *Apoptosis,* **18(5)**: 605-617.

109. Suthinee Ithimakin, Fayaz Malik, Kathleen C. Day, Dain Hayes, Hasan Korkaya, and Max S. Wicha (**2013**). HER2 drives luminal breast cancer stem cells in the absence of HER2 amplification: Implications for efficacy of adjuvant trastuzumab. *Cancer Research*, **73(5)**: 1635-46.

110. Tantry, M. A., Dar, J. A., Khuroo, M. A., and Shawl, A. S. (2012). Nor triterpenoids from the roots of *Paeonia emodi*. *Phytochem. Lett.,* **5(2)**: 253–257.

111. Tantry, M.A., Dar, J. A., Idris, A., Akber, S., and Shawl, A.S. (**2012**). Acylated flavonol glycosides from *Epimedium elatum*, a plant endemic to the Western Himalayas. *Fitoterapia*, **83**: 665-670.

112. Tarandeep Kaur, Hilal A. Bhat, Anuj Raina, Sushma Koul and Dhiraj Vyas (2013). Glutathione regulates enzymatic antioxidant defence with differential thiol content in perennial pepperweed and helps adapting to extreme environment. *Acta Physiol Plant*, **35**:2501–2511.

113. Tatina, M., Yousuf, S. K., Debaraj Mukherjee. (**2012**). TCT mediated one-pot multicomponent transformation for the generation of orthogonally protected monosaccharide building blocks *Organic & Biomolecular Chemistry,* **10**: 5357-5360.

114. Umer Farooq, Shahzad A. Pandith, Manjit InderS. Saggoo and Surrinder K. Lattoo (2013). Altitudinal

variability in anthraquinone constituents from novel cytotypes of *Rumex nepalensis* Spreng-a high value medicinal herb of North Western Himalayas. *Industrial Crops and Products*, **50**: 112– 117.

115. Verma , M.K., Anand, R., Shawl, A.S., Kitchlu, S., Shahi A.K., Chandra, S., Koul, S., and Khajuria, R.K.(**2012**). Variation in the composition of the essential oils of *Rosmarinus officinalis* L. grown in sub-tropical region of Jammu and temperate region of Kashmir, India. *Asian Journal of Chemistry*, **24(6)**:2799-2801.

116. Verma, V., Singh, K., Kumar, D., Klapötke, T. M., Stierstorfer, J., Narasimhan, B., Qazi, A. K., Hamid, A., and Jaglan, S. (**2012**). Synthesis, antimicrobial and cytotoxicity study of 1,3-disubstituted-1H-naphtho[1,2-e][1,3]oxazines. *Eur. J. Med. Chem.*, **56**:195-202.

117. Wajid Waheed Bhat, Niha Dhar, Sumeer Razdan, Satiander Rana, Rukmankesh Mehra, Amit Nargotra, A.Rekha S. Dhar, Nasheeman Ashraf, Ram Vishwakarma and Surrinder K. Lattoo (2013). Molecular characterization of UGT94F2 and UGT86C4, two glycosyltransferases from *Picrorhiza kurrooa*: Comparative structural insight and evaluation of substrate recognition. *PLoS ONE*, doi:10.1371/journal.pone.0073804

118. Wajid Waheed Bhat, Surrinder K. Lattoo, Satiander Rana, Sumeer Razdan, Niha Dhar, Rekha S. Dhar and Ram Vishwakarma (**2012**). An efficient plant regeneration *via* direct organogenesis and *Agrobacterium tumefaciens*-mediated genetic transformation of *Picrorhiza kurrooa* - an endangered medicinal herb of alpine Himalayas. *In Vitro Cell. Dev. Biol.-Plant*, **48(3)**: 295-303.

119. Wajid Waheed Bhat, Surrinder K. Lattoo, Sumeer Razdan, Niha Dhar, Satiander Rana, Rekha S. Dhar, Shabnam Khan and Ram Vishwakarma. (**2012**). Molecular cloning, bacterial expression and promoter analysis of squalene synthase from *Withania somnifera* (L.) Dunal. *Gene,* **499**: 25–36.

120. Wani, B.A., Ramamoorthy, D., Rather, M.A., Arumugam, N., Hamid, A., Ganie, S.A., Ganai, B.A., Anand, R., and Gupta, A.P. (**2013)**. Induction of apoptosis in human pancreatic MiaPaCa-2 cells through the loss of mitochondrial membrane potential (ΔΨm) by *Gentiana kurroo* root extract. *Phytomedicine*, 2013 Feb 28. doi:pii: S0944-7113(13)00042-1.

121. Wani, N.A., Hamid, A., and Kaur, J. (**2012**). Alcohol associated folate disturbances results in altered methylation of folate regulating genes. *Mol Cell Biochem.,* **363**:157–166.

122. Yadav, R.R., Battini, N., Mudududdla, R., Bharate, J.B., Muparappu, N., Bharate, S.B., and Vishwakarma, R. A. (**2012**). Deformylation of indole and azaindole-3-carboxaldehydes using anthranilamide and solid acid heterogeneous catalyst via quinazolinone intermediate. *Tetrahedron Lett.*, **53**: 2222-2225.

123. Yadav, R.R., Vishwakarma, R.A., and Bharate, S.B. (**2012**) Catalyst-free ipso-nitration of aryl boronic acids using bismuth nitrate. *Tetrahedron Lett.*, **53**: 5958-5960.

124. Yousuf, Deepak Kumar, Malikharjunarao Lambu, Baldev Singh, Sudip Maity, and Debaraj Mukherjee (**2012**). Sonogashira reaction for the synthesis of benzannulated chiral macrocycles embedded in carbohydrate templates. *Adv. Synth. Catal.*, **354**: 1933–1940.

Patents Applied/Filed

S. No.	Patent title	Inventors	NF Number
1	Synthesis and biological evaluation of Isoform selective analogs of tetrazolyl-Quinazolinone scaffold as anticancer agents :P13K-alpha/beta inhibitors	Vishwakarma Ram A. Sawant Sangapal Damodar, Singh Parvider Pal, Dar Abid Hamid, Nargotra Amit, Sharma Parduman Raj, DM Mondhe, Saxena Ajit Kumar, Mahesuni Srinivas, Hussain, Ashiq, Qazi Asif Khurshid, Mahajan Priya	150NF/2012
2	Tetrahydro-2H-Pyrano [3,2-C] Isochromene-6-Ones for the treatment of inflammatory Disorders.	Jain Shreyans kumar, Sidiq Tabasum, Meena Samdarshi, Khajuria Anamika R. A. Vishwakarma, Bharate Sandip , Bibishan	NF0063/2012
3	A novel formulation useful in Cancer chemotherapy	Dilip Manikrao Mondhe, S.C. Taneja, S.Koul, J.K. Dhar, A.K. Saxena, R.K. Johri, Z.A. Wani, S.A. Andotra, S.C. Sharma, Surjeet Singh, Prem Narayan gupta, R.A. Vishwakarma	NF-0088NF2012
4	Cyclin-Dependent Kinase Inhibition by 5,7-Dihydroxy-8-(3-Hydroxy-1-Methyl Piperidin-4-Yl)-2-Methyl-4H-Chromen-4-One Analogs)	Vishwakarma Ram Asrey, Bharate Sandip Bibishan, Bhushan Shashi, Jain Shreyans Kumar, Meena Samdarshi, Guru Santosh Kumar, Pathania Anup Singh, Suresh Kumar	0219NF2012
5	Boronic acid bearing liphagane compounds as	R.A.Vishwakarma, S.D.Sawant, P.P.SINGH, A.H. Dar, P.R. Sharma, A.K.Saxena, A. Nargotra, K.A.Arvind Kumar, M.Ramesh, A.K.Qazi, A. Hussain, N.Cahauria.	0794DEL2012
6	Design and Synthesis of novel Triazolyl, Tetrazolyl, Isoxazlyl, Urea and Sulponaminde analogs of 6-Nitro-2,3-Dihydroimidazo [2,1-b] oxazoles scaffold as antimycobacterial agents	Parvinder Pal Singh, Gurunadham Munagala, Kushalava Reddy Yempalla, Inshad Ali Khan, Nitin Pal Kalia, Vikrant Singh Rajput, Amit Nargotra, Sanghapal Damodhar Sawant, Ram Asrey Vishwakarma	0225NF2012 dt. 07 Dec. 1012
7	New Chromone alkaloid dysoline for the treatment of cancer and inflammatory disorders.	Vishwakarma Ram Asrey, Bharate Sandip Bibishan, Bhushan Shashi, Jain Shreyans Kumar, Meena Samdarshi,Khajuria Anamika,Bhola Sunil Kumar,Qazi Asif Khurdhid,Hussain Aashiq,Hussain Aashiq,Uma Shaanker Ramanan,Ravikanth Gudasalamani,Vasudeva Ramesh,Mohan Kumar Patel,Ganeshaiah Kotiganahalli Narayanagowda	0037NF2013 Dated 28.03.2013

8	Brachiatins D and process for their production there of	Deepika Singh, Jai Parkash Sharma, Sundeep Jaglan, Abid Hamid Dar, Varun Partap Singh, Ram Asrey Vishwakarma	0039NF2013
9	6-Aryl-3-phenylamino-quinazoline analogs as phosphoinositide-3-kinase inhibitors	Vishwakarma, R.A.; Bharate, S.B.; Bhushan, S.; Yadav, R.R.; Guru, S.K.; Joshi, P.	0117NF2013

BOOKS

1. Perspectives in Animal Ecology and Reproduction-Vol. 9, V.K.Gupta, Anil K. Verma, G.D.Singh (Eds.). Daya Publishing House, New Delhi. 547p (2013).
2. Animal Diversity, Natural History and Conservation-Vol. 2, V.K.Gupta, Anil K. Verma (Eds.). Daya Publishing House, New Delhi. 490p (2013).
3. Animal Diversity, Natural History and Conservation-Vol. 3, V.K.Gupta, Anil K. Verma (Eds.). Daya Publishing House, New Delhi. 458p (2013).
4. Some Aspects of Medicinal Plant Biotechnology- Mohd. Shahnawaz, Shishpaul Bambotra, Surrinder K. Lattoo, LAP LAMBERT Academic Publishing, Germany, 266p (2013)

Book Chapters Published

1. Ajai Prakash Gupta and Suphla Gupta (2012). Elemental Profiling: Its Role and Regulations, Atomic Absorption Spectroscopy, Dr. Muhammad Akhyar Farrukh (Ed.), ISBN: 978-953-307-817-5, InTech
2. Amit Gupta, A,. Khajuria, S. Singh and V.K.Gupta (2012). Effect of Natural Plant Based and Non-Steroidal Anti-Inflammatory Drugs on the Immune System. In "*Natural Products: Research Review-Vol. 1*" Ed. V.K.Gupta, Daya Publishing House, New Delhi, pp 439–460.
3. G.D.Singh, S.Singh, A.Koul, P.Kaul and V.K.Gupta (2012). *Labisia pumila* (Kacip Fatimah), a Malaysian Medicinal Herb: An Update. In "*Medicinal Plants: Phytochemistry, Pharmacology and Therapeutics-Vol.2*" Eds. V.K. Gupta, G.D. Singh, Surjeet Singh and A. Kaul, Daya Publishing House, New Delhi, pp 81–96.
4. Musarat Amina, V.K.Sharma, N.K.Satti, Prabhu Dutt, V.K.Gupta, B.D.Gupta and K.A.Suri (2012). Chemistry, Pharmacology and HPTLC Standardisation of *Asparagus recemosus* (Shatavari), an Important Ayurvevic Herb. In "*Traditional and Folk Herbal Medicine: Recent Researches-Vol.1*" Ed. V.K.Gupta, Daya Publishing House, New Delhi, pp 93–132.
5. P. Koul, G. D. Singh, R. Sharma, V. K. Gupta and S. Singh (2012). Limonene: A Systematic Overview for its Chemistry and Bioactivity. In "*Bioactive Phytochemicals: Perspectives for Modern Medicine -Vol. 1*" Ed. V.K.Gupta, Daya Publishing House, New Delhi, pp 107–126.
6. R.K.Khajuria and D.K.Gupta (2012). Quality Control, Standardization and Chemo Profiling of Herbal Drugs and ISM Preparations. In "*Traditional and Folk Herbal Medicine: Recent Researches-Vol.1*" Ed. V.K.Gupta, Daya Publishing House, New Delhi, pp 315–328.
7. S.Koul, D.K.Gupta,V.K.Gupta and S.C.Taneja (2012). Supercritical Fluid Extraction as a Tool for Value Addition of Natural Products. In "*Natural Products: Research Reviews - Vol. 1*" Ed. V.K.Gupta, Daya Publishing House, New Delhi, pp 161–220.

Seminars and Workshops Attended

1. Farnaz Yusuf, Asha Chaubey, Urmila Jamwal and Rajinder Parshad (2012). Isolation and characterization of Nitrilase from *Fusarium proliferatum*, 22-25 Nov 2012, 53rd Annual Conference of Association of Microbiologists of India (AMI)-2012: International Conference on Microbial world: Recent Innovations and future trends, KIIT University, Bhubaneshwar, Odisha, India
2. Wajid.W. Bhat, Rekha S. Dhar, Ram.A. Vishwakarma, and Surrinder K. Lattoo(2012). Metabolic profiling of *Picrorhiza kurroa* and molecular characterization of key regulatory genes of picroside biosynthesis. *The 4th EMBO Meeting, Advancing the Life Sciences, Nice, France*, 22-25, September, 2012, *EMBO Abstracts*, p 183.
3. Suphla Gupta, Ashok Ahuja and Ram A Vishwakarma (2012). *In-vitro* Organogenesis from Root Culture Systems of *Glycyrrhiza glabra* 33rd Annual Plant Tissue Culture Association Meet and Symposium on "Impact of Plant Tissue Culture on Advances in Plant Biology" on in Plant Tissue Culture Association Jan 12-13 2012 at Ahmadabad.

Invited Talks

1. **Dr. Abid Hamid Dar**

   "Cell: Impact of its discovery" at BGSBU, Rajouri, Jammu & Kashmir on 3rd August 2012.

2. **Dr. Sandip B. Bharate**

   "Tandem one-pot strategies for synthesis of medicinally important natural product scaffolds and their pharmacological exploration" at 3rd Biennial conference on new developments in drug discovery from natural products and traditional medicines (DDNPTM-2012) at NIPER, SAS Nagar, Punjab from November 22-24, 2012.

3. **Dr. Suphla Gupta**

   "Strange World of Plant", at International Event on Fascination of Plants Day, organized by the European Plant Science Organization at Sri Mata Vaishno Devi University in 2012.

   "Plant Barcoding" at Jammu University for Refresher course in Life science, jointly organized by Academy affairs and Jammu University on Feb. 22nd , 2012.

Fellowships Awarded

1. **Dr. Inshad Ali Khan**

   Awarded DHR fellowship by Indian Council of Medical Research, India in to work for six months (26th Dec 2012 to 25th June 2013) in NIAID, NIH, Maryland, USA.

MoUs and Agreements

S. No.	Name of the Organisation	Date of Agreement
1.	M/s Dabur Research Foundation 22, Site-IV, Sahibabad, Ghaziabad (UP)	8th June, 2012
2.	MOU between CMJ University Modrina Mansion, Laitumkhrah Shillong, Meghalaya-793003	18th October , 2012
3.	MOU between CRIA Care Pvt. Ltd., 15, Bachubai Building, J. Bhatankar Marg, Parel, Mumbai-400 012 India, Mumbai	29th October , 2012
4.	MOU between Unit for Research and Development of Information Products (URDIP), Jopasana Building, 85/1, Paud Road Kothrud, Pune-411 038	19th December, 2012
5.	Agreement between State Forest Research Institute Janipur Colony, Research Complex, Jammu	16th January , 2013
6.	MOU between Gujarat Ayurved university Chankaya Bhawan Jamnagar	11th Feb. 2013

RESEARCH COUNCIL

Prof. Goverdhan Mehta — **Chairman**
National Research Prof. and Lily- Jubilant Chair
School of Chemistry
University of Hyderabad
Hyderabad – 500046

Dr. Satyajit Rath — **External Member**
Staff Scientist, National Institute of Immunology
Aruna Asaf Ali Marg, JNU Complex, New Delhi -110 067

Prof. Sudhir K. Sopory — **External Member**
Vice Chancellor
Jawaharlal Nehru University
New Delhi 110067

Prof. Dipankar Chatterji — **External Member**
Molecular Biophysics Unit, Indian Institute of Science
Bengaluru -560012

Prof. Satyajit Mayor — **External Member**
Professor and Dean
National Centre for Biological Sciences,
(Tata Institute of Fundamental Research)
Bellary Road, GKVK Campus, Bengaluru -560065

Prof. Sushil Durani — **External Member**
Department of Chemistry, Indian Institute of Technology
Powai, Mumbai -400076

Dr. Raman Govindarajan — **External Member**
Sr. Vice President
Discovery Biology, Developmental & Translational Medicine
Jubilant Biosys and Jubilant Innovation,
96 Industrial Suburb, 2nd Stage Yeshwanthpur
Bengaluru -560022

Dr. R. Brakaspathy — **Agency Representative**
Scientist G
Department of Science & Technology,
Technology Bhawan, New Mehrauli Road
New Delhi -110016

Dr. P.K. Biswas — **DG Nominee**
Former Adviser (S&T), Planning Commission
MS-11/905, Kendriya Vihar,
Sector 56,Gurgaon, Haryana -122003

Dr. T.K. Chakraborty — **Sister Laboratory**
Director
Central Drug Research Institute,
Chatter Manzil Palace, P.B. No. 173
Lucknow -226001

Prof. Siddhartha Roy — **Cluster Director**
Director
Indian Institute of Chemical Biology (IICB)
4, Raja SC Mullick Road, Jadavpur,Kolkata -700032

Dr. Ram Vishwakarma — **Member**
Director
Indian Institute of Integrative Medicine,
Canal Road, Jammu-180 001

Head or his Nominee — **Permanent Invitee**
Planning & Performance Division
Council of Science & Industrial Research
Anusandhan Bhawan, 2, Rafi Marg,
New Delhi -110 001

Dr. Y.S. Bedi — **Secretary**
Chief Scientist Indian Institute of Integrative Medicine,
Canal Road, Jammu-180 001

MANAGEMENT COUNCIL

Dr. Ram Vishwakarma — **Chairman**
Director, Indian Institute of Integrative Medicine
Canal Road, Jammu

Dr. P.S. Ahuja — **Member**
Director, Institute of Bioresource Technology
Palampur

Dr. R.K. Raina — **Member**
Scientist G/Head, PME Division
Indian Institute of Integrative Medicine, Canal Road, Jammu

Dr. Sushma Kaul — **Member**
Scientist G
Indian Institute of Integrative Medicine, Canal Road, Jammu

Dr. S.K. Lattoo — **Member**
Technical Officer EI
Indian Institute of Integrative Medicine, Canal Road, Jammu

Sh. Amit Nargotra — **Member**
Scientist B
Indian Institute of Integrative Medicine, Canal Road, Jammu

Sh. Upendra Kumar — **Member**
F&AO
Indian Institute of Integrative Medicine, Canal Road, Jammu

Sh. Om Prakash — **Member**
AO
Indian Institute of Integrative Medicine, Canal Road, Jammu

सीएसआईआर–भारतीय समवेत औषध संस्थान, जम्मू में राजभाषा की प्रगति एवं विकास में हिन्दी के कार्यक्रम

नगर राजभाषा कार्यान्वयन समिति, जम्मू की छमाही बैठक दिनांक 12 जुलाई, 2012 को सायं 3.00 बजे भारतीय समवेत औषध संस्थान, जम्मू के कान्फ्रेंस हॉल में सम्पन्न।

अखिल भारतीय कवि सम्मेलन की स्मारिका का विमोचन करते हुए नराकास कार्यकारी अध्यक्ष डॉ. एस.सी.तनेजा ।

भारत सरकार, गृह मंत्रालय, राजभाषा विभाग के निर्देशानुसार नगर राजभाषा कार्यान्वयन समिति, जम्मू की छमाही बैठक दिनांक 12 जुलाई, 2012 (वृहस्पतिवार) को अपराह्न 3.00 बजे भारतीय समवेत औषध संस्थान, जम्मू के ऑडिटोरियम हॉल में आयोजित हुई। बैठक की अध्यक्षता संस्थान के वरिष्ठ वैज्ञानिक एवं नराकास के कार्यकारी अध्यक्ष डॉ. एस.सी.तनेजा ने की। इस अवसर पर मुख्य अतिथि श्री एस.के.मेहरा, अनुसंधान अधिकारी, भारत सरकार, गृह मंत्रालय, राजभाषा विभाग, उत्तर क्षेत्रीय कार्यान्वयन कार्यालय-1 (दिल्ली), श्री ए. के.तथई, आयुक्त आयकर, आयकर भवन, जम्मू/श्रीनगर, श्री ए.के.मोटा, मुख्य प्रबंधक, पंजाब नेशनल बैंक मंण्डल कार्यालय, जम्मू, श्री राजेन्द्र पाल, उपनियंत्रक, रक्षा लेखा प्रधान नियंत्रक, उत्तरी कमान, जम्मू तथा नगर जम्मू के केन्द्रीय कार्यालयों/बैंकों/उपक्रमों से आये सभी कार्यालय अध्यक्ष, हिन्दी अधिकारी/राजभाषा अधिकारी/नोडल अधिकारी/हिन्दी अनुवादक तथा प्रिन्ट एवं इलैक्ट्रॉनिक मीडिया के समस्त संवाददाता उपस्थित थे। इस अवसर पर अखिल भारतीय कवि सम्मेलन की स्मारिका का विमोचन संस्थान के वरिष्ठ वैज्ञानिक एवं कार्यकारी नराकास अध्यक्ष डॉ. एस. सी.तनेजा किया। इस अवसर पर अन्य गणमान्य व्यक्ति उपस्थित थे।

सर्वप्रथम बैठक में उपस्थित कार्यालय प्रमुखों एवं सज्जनों का स्वागत डॉ. अमर सिंह, वरि. हिन्दी अधिकारी एवं सचिव, नराकास, जम्मू ने किया। उन्होंने अपने स्वागत संबोधन में कहा, ''कि इस बैठक में प्रथम अक्टूबर, 2011 से 31 मार्च, 2012 के दौरान तिमाही प्रगति रिपोर्टों की समीक्षा की जाएगी तथा आपके कार्यालय में राजभाषा हिन्दी में किये गये कार्यों की समीक्षा व इससे संबंधित आपके कार्यालयों में उत्पन्न समस्याओं पर चर्चा की जाएगी। संघ के विभिन्न राजकीय प्रयोजनों में इसके प्रगामी प्रयोग को बढ़ावा देने के लिए राजभाषा विभाग प्रति वर्ष एक वार्षिक कार्यक्रम जारी करता है, जिसके अनुसार हम कार्यालयों में राजभाषा के कार्य सम्पन्न करते हैं। चूंकि सरकारी-कामकाज में मूल टिप्पण और प्रारूपण के लिए हिन्दी का ही प्रयोग किया जाए जिसके अन्तर्गत धारा 3(3) का हम सबको अनुपालन सुनिश्चित करना चाहिए। यही संविधान की मूलभावना के अनुरूप होगा। सभी भारतीय भाषाएं देश की एकता की प्रतीक हैं। भारतीय संविधान में जो प्रावधान किये गये हैं इसी के अनुसार हमें आदेशों/अनुदेशों का पालन करना चाहिए और राष्ट्रपति जी के संकल्पों का सम्मान करना चाहिए''।

तत्पश्चात् बैठक में उपस्थित सदस्यों के परिचय के साथ ही बैठक की कार्रवाई आरम्भ हुई। सचिव ने गत बैठक के कार्यवृत्त पर चर्चा के दौरान कहा कि सम्माननीय सदस्यों की कोई प्रतिक्रिया, सुझाव अथवा आपत्ति हो तो वे विचार रखें, लेकिन माननीय उपस्थित सदस्यों की ओर से कोई आपत्ति एवं प्रतिक्रिया न मिलने पर सचिव ने अध्यक्ष महोदय के अनुमोदन पर गत बैठक के कार्यवृत्त की पुष्टि की।

गत बैठक में लिए गये निर्णय और उन पर की गई अनुवर्ती कार्रवाई इस प्रकार हैं:-

गत बैठक में नगर राजभाषा कार्यान्वयन समिति मंच के माध्यम से दिनांक 29-30 मार्च, 2012 को यूनिकोड प्रशिक्षण कार्यक्रम आयुक्त आयकर, आयकर कार्यालय, जम्मू व श्रीनगर एवं सीमा शुल्क एवं केन्द्रीय उत्पाद शुल्क, आयुक्त जम्मू व श्रीनगर के सौजन्य से कम्प्यूटर पर यूनिकोड प्रशिक्षण कार्यक्रम का आयोजन किया गया साथ ही कार्यपालक निदेशक, पावर ग्रिड कारपोरेशन, पारेषण प्रणाली, उत्तरी क्षेत्र-।।, जम्मू/श्रीनगर व कार्यपालक निदेशक, एनएचपीसी क्षेत्र-।, के सौजन्य से 30 मार्च, 2012 को अखिल भारतीय कवि का सम्मेलन का आयोजन किया गया। इसी परिप्रेक्ष्य में एक ''स्मारिका'' का विमोचन किया गया और सभी केन्द्रीय कार्यालयों/बैंकों/ उपक्रमों के सदस्यों को

बैठक में उपस्थित नराकास जम्मू के सदस्यों का स्वागत करते हुए सदस्य-सचिव डॉ. अमर सिंह

प्रतियां वितरित की गयी।

नगर राजभाषा कार्यान्वयन समिति, भारतीय समवेत औषध संस्थान, जम्मू के कार्यालय से नगर के सभी सदस्य कार्यालयों की आई.डी. ई-मेल तैयार की गयी।

नराकास, जम्मू के सदस्य कार्यालयों की गृह पत्रिकाएं वर्ष 2011-2012 में प्रकाशित की गयी जो इस प्रकार हैं:-

नराकास, जम्मू कार्यालय की गृह पत्रिका ज्ञानवार्ता, पंजाब नेशनल बैंक, क्षेत्रीय कार्यालय, जम्मू की गृह पत्रिका त्रिकुटा, पावर ग्रिड कारपोरेशन, उत्तरी क्षेत्र-।।, जम्मू की गृह पत्रिका तवी प्रवाह, एनएचपीसी, क्षेत्र-।, जम्मू की गृह पत्रिका त्रिकुटा समाचार तथा प्रसार भारती, रेडियो कश्मीर, जम्मू की गृह पत्रिका तविषी तथा सीमा शुल्क एवं केन्द्रीय उत्पाद शुल्क ताज-ऐ-हिन्द राजभाषा गृह पत्रिका प्रकाशित हुई।

तदोपरान्त प्रथम अक्टूबर, 2011 से 31 मार्च, 2012 के दौरान प्राप्त दोनों प्रगति रिपोर्टों की समीक्षा का संक्षिप्त ब्यौरा सदस्य कार्यालयों के समक्ष प्रस्तुत किया।

बैठक में राजभाषा नीति कार्यान्वयन पर चर्चा एवं सदस्यों की प्रतिक्रियाएं उनके महत्वपूर्ण सुझाव जो इस प्रकार हैं:-

श्री एस.के.मेहरा, अनुसंधान अधिकारी, भारत सरकार, गृह मंत्रालय, राजभाषा विभाग, क्षेत्रीय कार्यान्वयन कार्यालय-1 (दिल्ली) ने अपने विचार व्यक्त करते हुए कहा, ''कि नरकास जम्मू की ओर से राजभाषा स्मारिका का प्रकाशन महत्वपूर्ण उपलब्धि है और राजभाषा नीति कार्यान्वयन की दिशा में उत्कृष्ट प्रयास हैं उन्होंने अध्यक्ष महोदय को इस प्रयास के लिए हार्दिक बधाई दी। उन्होंने कहा कि आज़ादी के बाद दिन प्रतिदिन राजभाषा हिन्दी की प्रगति हो रही है और नगर राजभाषा कार्यानवयन समितियों के माध्यम से राजभाषा कार्यान्वयन प्रगति की दिशा में आशा के अनुकूल प्रभावी हुआ है। भारत सरकार, गृह मंत्रालय की ओर से सभी संसाधन उपलब्ध कराने के प्रयास जारी हैं। सरकार का लक्ष्य है कि शतप्रतिशत कार्य हिन्दी में किया जाए और उन्होंने संक्षेप में बताया कि जम्मू नगर राजभाषा कार्यान्वयन समिति के माध्यम से पत्राचार में वृद्धि सुनिश्चित् हुई है, जो लक्ष्य से अधिक है जबकि हिन्दी प्रशिक्षण/टंकण लक्ष्य से भी अधिक है साथ ही उन्होंने प्रशंसा व्यक्त करते हुए कहा, ''कि हिन्दी भाषी क्षेत्रों से भी जम्मू 'ग' क्षेत्र में स्थित नराकास में महत्वपूर्ण कार्य सम्पन्न हो रहे हैं। इसके लिए उन्होंने अध्यक्ष महोदय का आभार सहित धन्यवाद किया। इस दौरान उन्होंने कई केन्द्रीय कार्यालयों/बैंकों/उपक्रमों का राजभाषा निरीक्षण भी किया और उन्होंने पाया कि राजभाषा कार्यान्वयन बेहतर ढंग से निष्पादित किए जा रहे हैं। राजभाषा प्रबंधन एवं कार्यान्वयन के लिए महत्वपूर्ण सुझाव दिए''।

श्री ए.के.मोटा, मुख्य प्रबंधक, पंजाब नेशनल बैंक, क्षेत्रीय कार्यालय, जम्मू ने अपने विचार व्यक्त करते हुए कहा, ''कि नगर राजभाषा कार्यान्वयन समिति एक महत्वपूर्ण मंच है जिसके माध्यम से नगर के सभी सदस्य कार्यालयों को राजभाषा नीति के कार्य सम्पन्न करने में महत्वपूर्ण सहयोग प्राप्त होता है। गत वर्षों में हमने अनुभव किया है कि हमारे क्षेत्रीय कार्यालय के माध्यम से त्रिकुटा गृह पत्रिका, कम्प्यूटर के माध्यम से हिन्दी में कार्य करने की क्षमता में वृद्धि हुई है और मैं डॉ. अमर सिंह, सदस्य-सचिव, नराकास, जम्मू के द्वारा समय-समय पर सभी सदस्य कार्यालयों में हिन्दी के कार्यक्रम आयोजित करने में उनका विशेष सहयोग प्राप्त हो रहा है।

श्री ए.के.तथई, आयकर आयुक्त, जम्मू/श्रीनगर ने अपने विचार व्यक्त करते हुए कहा कि आज इस बैठक में हिन्दी के कार्यान्वयन पर चर्चा हुई और हम सबका यह राष्ट्रीय दायित्व है कि हिन्दी की प्रगति एवं विकास के लिए हर सम्भव प्रयास जारी रहें, ताकि हिन्दी के कार्य करने की प्रगति हो उन्होंने कहा कि हिन्दी हमारे सरल अभिव्यक्ति की भाषा है इसका प्रयोग व प्रसार करना हमारा संबैधानिक दायित्व बनता है और इसकी कार्य प्रकृति को बढ़ाने के लिए हम सतत प्रयासरत् रहेंगे।

बैठक में आयकर आयुक्त जम्मू/श्रीनगर श्री ए.के.तथई स्मृति चिन्ह प्रदान करते हुए ।

संस्थान के वरिष्ठ वैज्ञानिक एवं अध्यक्ष, नराकास जम्मू डॉ. एस.सी.तनेजा ने सभागार में उपस्थित नगर के कार्यालय प्रमुखों एवं अन्य गणमान्य व्यक्तियों का अपने संस्थान की ओर से व नराकास मंच की ओर से सबका हार्दिक स्वागत करते हुए अपने अध्यक्षीय संबोधन में कहा, ''कि समिति के माध्यम से ज्ञानवार्ता हिन्दी पत्रिका का प्रकाशन जिसमें आप सबके सहयोग से प्रकाशित हो रही है यह हमारी समिति की एक उपलब्धि है साथ ही सभी सदस्य कार्यालयों में कम्प्यूटर के माध्यम से हिन्दी कार्य की क्षमता में दिन-प्रतिदिन वृद्धि हो रही है। गत वर्ष संसदीय समिति द्वारा नगर के कई केन्द्रीय कार्यालयों का राजभाषा निरीक्षण सफलतापूर्वक किया गया। आगे भविष्य के लिए भी अन्य कार्यालयों में निरीक्षण किया जा सकता है। हिन्दी एक सरल, सहज भाषा है और प्रयोग की दृष्टि से संबाद पूर्ण भाषा है, कहानी, काव्य, छोटे-छोटे वाक्य उपवाक्य, सरलतम शैली में अभिव्यक्ति का माध्यम बना सकते हैं। पावर ग्रिड कारपोरेशन, जम्मू व एनएचपीसी, क्षेत्र-।, जम्मू के सहयोग से अखिल भारतीय कवि सम्मेलन का आयोजन किया गया। इसके अतिरिक्त आयकर आयुक्त, जम्मू व आयुक्त सीमा शुल्क एवं केन्द्रीय उत्पाद शुल्क, जम्मू के सौजन्य से कम्प्यूटर प्रशिक्षण कार्यक्रम आयोजित किया, इस सहयोग के लिए हम उनका धन्यवाद करते हैं। यदि अन्य सदस्य कार्यालय भी इस प्रकार का सहयोग करते रहे ताकि राजभाषा की प्रगति में आशा के अनुकूल वृद्धि संभव हो सके।

नराकास बैठक को संबोधित करते डॉ. एस.सी.तनेजा

अन्त में संस्थान के वरि. हिन्दी अधिकारी एवं सदस्य-सचिव, नराकास, जम्मू डॉ. अमर सिंह ने अध्यक्ष महोदय का आभार व्यक्त करते हुए कहा कि डॉ. एस.सी.तनेजा ने इस बैठक के लिए अपना महत्वपूर्ण समय दिया, उनके इस योगदान के लिए हम उनका हृदय से आभार सहित धन्यवाद किया। श्री एक.के. तथई, आयकर आयुक्त, जम्मू/श्रीनगर जिन्होंने इस बैठक के लिए अपना बहुमूल्य समय दिया उनके इस कीमती समय के लिए उनका बहुत-बहुत आभार व्यक्त करते है। श्री ए.के.मोटा, मुख्य प्रबंधक, पंजाब नेशनल बैंक, क्षेत्रीय कार्यालय, जम्मू ने भी अपना कीमती समय निकाल कर इस बैठक में उपस्थित हुए हम उनका आभार सहित धन्यवाद करते हैं। नगर के सभी कार्यालय प्रमुख, इस अवसर पर उपस्थित हुए सभी गणमान्य व्यक्ति एवं प्रिन्ट व इलैक्ट्रानिक मीडिया दूरदर्शन के सभी संवाददाताओं का आभार व्यक्त किया। संस्थान के सभी संकाय सदस्यों का जिन्होंने इस बैठक के आयोजन में अपना योगदान दिया और सहयोग प्रदान किया उन सबका धन्यवाद किया।

स्वतंत्रता दिवस के पावन अवसर पर संस्थान के निदेशक डॉ. राम विश्वकर्मा ने ध्वजारोहण किया और सबको हार्दिक शुभकामनाएं एवं बधाई देते हुए कहा कि यह ऐतिहासिक दिन हमें स्वतंत्रता आन्दोलन के हजारों परवानों की महान कुर्बानियों की याद दिलता है। हम उन देश भक्तों, शहीदों तथा देश की रक्षा में शहीद हुए सेना के जवानों व देश के नागरिकों को श्रद्धासुमन अर्पित करते है। जिन्होंने देश की सीमाओं पर रक्षा करते हुए अपनी जॉन कुर्बान कर दी है मेरा उन्हें शत्-शत् प्रणाम।

15 अगस्त, 1947 को आज से 65 वर्ष पहले हम आज़ाद हुए थे। यह हमारी आजादी का विशेष महत्वपूर्ण एवं गौरवशाली दिन है। क्योंकि 26 जनवरी, 1930 को रावी नदी के तट पर नेहरूजी की अध्यक्षता में पूर्व स्वतंत्रता प्राप्ति का प्रस्ताव कांग्रेस के अधिवेशन में पास हुआ था। हमें स्वाधीन हुए 65 वर्ष हो गये हैं। अब यह समृद्ध भारत है, हमने इन 65 वर्षो में क्या पाया क्या खोया? हमें आगे और प्रगति के लिए आत्म मन्थन करना होगा, बहुत सारी उपलब्धियां हमने हासिल की है। देश की सुरक्षा के लिए भारत मजबूती के साथ आगे बढ़

ध्वजारोहण करते हुए संस्थान के निदेशक डॉ. राम विश्वकर्मा एवं स्टॉफ सदस्यगण ोहण

रहा है फिर भी हमारी सीमाएं सुरक्षित नहीं है यह हमारे लिए चिन्ता का विषय है।

आगे भी हमें निरन्तर प्रगति के लिए प्रयास करने होंगे। हमें जो आजादी मिली है उसे और व्यापक बनाने की आवश्यकता है, आजादी हमें कितनी कुर्बानियों से प्राप्त हुई। आजादी हमारे देश की एकता, अखण्डता आज जो स्वतंत्रता हम महसूस कर रहे हैं उसके पीछे हमारे देश-वासियों की एक जुटता ही है। मुझे अपने नये विकसित संगठित भारत पर गर्व है। क्योंकि ग्लोबलाइजेशन के इस दौर में हमारा भरत देश निरन्तर नयी ऊँचाईयों को छू रहा है। इन सभी उपलब्धियों का श्रेय उन ग्रेट इंडियंस को जाता है जिन्होंने अनेक कठिनाइयों का सामना करते हुए भारत को आज सफलता के इस सोपान तक पहुँचाया है। यदि आप में कमिटमेन्ट होगा तो आप बिना किसी मुश्किल से कार्य करते रहेंगे। स्वतंत्रता आन्दोलन सिखाता है कि हमें 'सेल्फ डिपेंडेंट्स' आत्म निर्भर बनना है। आपको याद होगा कि गाँधी जी ने 'नमक तोड़ो' आन्दोलन चलाकर पूरे देश में आत्म निर्भरता का जो सन्देश दिया था, उससे पूरा ब्रिटिश साम्राज्य हिल गया था। इसलिए खुद को बुलन्द बनाएं जिन्दगी में आत्म-निर्भरता ही सच्ची ताकत है। इस अवसर पर उन्होंने अपने संस्थान की वैज्ञानिक उपलब्धियों को संक्षेप में व्यक्त किया। इस दौरान आर. आर.एल.हाई स्कूल के बच्चों द्वारा सांस्कृतिक कार्यक्रम प्रस्तुत किए गए।

देश में सैद्धान्तिक शोध में स्थिति ठीक है लेकिन प्रयोगात्मक शोध में हम अभी बहुत पीछे हैं। इस क्षेत्र में अभी बहुत कुछ किया जाना बाकी है। प्राइज इन ऑनर जैसे बहुत से राष्ट्रीय और अन्तर्राष्ट्रीय अवार्ड जीतने हैं। हमारे रिसर्च का उद्देश्य पुरस्कार पाना नहीं है। शोध में अपना ज्ञान बढ़ाने, देश की सेवा करने और अपने आनन्द के लिए है। अतः इस ऐतिहासिक अवसर पर मैं जाति, वर्ग, भाषा, धर्म और क्षेत्र के तुच्छ भेद-भाव से ऊपर उठकर शान्ति, समृद्धि और प्रगति के मार्ग पर चलते हुए राष्ट्रीय एकता व खण्डता को मजबूत करने के लिए सभी को एकजूट होने का हम संकल्प लेते हैं।

भारतीय समवेत औषध संस्थान, जम्मू में 03.09.2012 से 14.09.2012 तक हिन्दी सप्ताह, 2012 का आयोजन।

गणतंत्र दिवस के अवसर पर आर.आर.एल.हाई स्कूल के बच्चे द्वारा नृत्य प्रस्तुत करते हुए

संस्थान में दिवस/सप्ताह के दौरान प्रतियोगिता में भाग लेते हुए प्रतियोगीगण।

संघ की राजभाषा हिन्दी में सरकारी कामकाज तथा हिन्दी के प्रति रूचि जागृति करने के उद्देश्य से संस्थान में दिनांक 03 सितम्बर, 2012 से 14 सितम्बर, 2012 के दौरान हिन्दी सप्ताह का आयोजन किया गया। जिसमें निबन्ध लेखन, श्रुतलेख, स्टॉफ सदस्यों को सामान्य ज्ञान प्रतियोगिता, राजभाषा एवं विज्ञान प्रश्नोत्तरी, अनुवाद/टिप्पण एवं प्रारूपण प्रतियोगिता, अन्तरविभागीय भाषण प्रतियोगिता, हिन्दी कार्यशाला आदि प्रतियोगिताएं आयोजित की गयीं। इस दौरान हिन्दी के प्रयोग एवं प्रगति की दिशा में विभिन्न प्रतियोगिताओं में संस्थान के 300 स्टॉफ सदस्यों ने प्रतियोगी के रूप में प्रतिभागिता की, जिससे उनकी कार्य प्रकृति और उनके कार्य संस्कृति में इज़ाफा निश्चित् हुआ है। समारोह की अध्यक्षा संस्थान के निदेशक डॉ. राम विश्वकर्मा ने की और मुख्य अतिथि के रूप में प्रो. नीलम सराफ, ''डीन अकादमिक शैक्षणिक कार्य'' जम्मू विश्वविद्यालय, जम्मू मुख्य अतिथि थी। प्रथम दृष्टिया मुख्य अतिथि का पुष्प गुच्छ से स्वागत संस्थान निदेशक डॉ. राम विश्वकर्मा जी ने किया। इस अवसर पर विजयी प्रतियोगियों को नकद राशि के पुरस्कार तथा प्रमाण पत्र प्रदान किए। इस अवसर पर श्री ओम प्रकाश, प्रशासनिक अधिकारी, डॉ. आर.के.रैणा, अध्यक्ष पी. एम.ई.प्रभाग, श्री उपेन्द्र कुमार, वित्त एवं लेखा अधिकारी, श्री रमेश कुमार रैणा, वित्त एवं लेखा अधिकारी, श्री अशोक कुमार, भण्डार एवं क्रय अधिकारी तथा इलैक्ट्रॉनिक मीडिया के सभी संवाददाता तथा अन्य गणमान्य व्यक्ति उपस्थित थे। उपस्थित सज्जनों का स्वागत डॉ. अमर सिंह, वरि. हिन्दी अधिकारी एवं सदस्य-सचिव, नराकास, जम्मू ने किया। इस अवसर पर भारत सरकार, गृह मंत्रालय के गृहमंत्री का संदेश श्री ओम प्रकाश, प्रशासनिक अधिकारी द्वारा पढ़ा गया ।

विजयी प्रतियोगियों को 24.09.2012 को पुरस्कार प्रदान किये गये जिनके नाम निम्न प्रकार हैं:-

1. निबंध लेखन प्रतियोगिता:-

   श्री सुनील कुमार-प्रथम, श्री कमलेश सिंह-द्वितीय, कु0 रश्मि शर्मा- द्वितीय, श्री विनोद कुमार मीणा-तृतीय, श्रीमती सुनीता आनन्द-तृतीय ।

2. श्रुतलेख प्रतियोगिता:-

   श्री राकेश सिंह बिसेन-प्रथम, श्री कमलेश सिंह-द्वितीय, डॉ. अनिल कुमार त्रिपाठी-तृतीय।

3. सामान्य ज्ञान प्रतियोगिता (कक्षा 5 से 8 तक के बच्चों के लिए):-

   मास्टर अन्वय सिंह, आर.आर.एल.हाई स्कूल, जम्मू-प्रथम, मास्टर शोनिक गुप्ता, के.सी.इंटरनेशनल स्कूल, जम्मू-द्वितीय, मास्टर अजीत कुमार, आर.आर.एल.हाई स्कूल, जम्मू-तृतीय

4. राजभाषा एवं विज्ञान प्रश्नोत्तरी:-

   श्री रोहित शर्मा-प्रथम, कु0 समीक्षा शर्मा-द्वितीय, श्री अभिनव शर्मा-तृतीय, कु0 रीता कुमारी-तृतीय

5. अनुवाद/टिप्पण एवं प्रारूपण प्रतियोगिता:-

   श्री राकेश सिंह बिसेन-प्रथम, कु0 हरविन्दर कौर-द्वितीय, श्री सुनील कुमार-तृतीय ।

6. अन्तर्विभागीय भाषण प्रतियोगिता:-

   कु0 रश्मि शर्मा, भारतीय समवेत औषध संस्थान, जम्मू - प्रथम

   कु0 नेहा धर, भारतीय समवेत औषध संस्थान, जम्मू - द्वितीय

   श्री अशोक कुमार दीक्षित, वरि. प्रबंधक, श्री गांधी सेवा सदन, जम्मू - द्वितीय

   कु0 रजनी शर्मा, भारतीय समवेत औषध संस्थान, जम्मू - तृतीय

   श्री वीरेन्द्र कुमार, सहायक कमाण्डेंट, केन्द्रीय रिजर्व पुलिस बल (रेंज) कूटा, जम्मू - सांत्वना

   श्री कैलाश चन्द्र मठपाल, निरीक्षक (हिन्दी), फ्रांटियर मुख्यालय, सीमा सुरक्षा बल, जम्मू - सांत्वना

संस्थान के निदेशक व नगर राजभाषा कार्यान्वयन समिति, जम्मू के अध्यक्ष डॉ. राम विश्वकर्मा को वर्ष 2010-2011 में नगर जम्मू के केन्द्रीय कार्यालयों/बैंकों/उपक्रमों में राजभाषा विभाग, गृह मंत्रालय से राजभाषा नीति के श्रेष्ठ निष्पादन के लिए प्रथम पुरस्कार दिया गया साथ ही भारतीय समवेत औषध संस्थान, जम्मू को राजभषा नीति के श्रेष्ठ निष्पादन के लिए राजभाषा विभाग से द्वितीय पुरस्कार शील्ड एवं प्रमाण-पत्र सचिव नराकास जम्मू डॉ. अमर सिंह ने प्राप्त किया। अखिल भारतीय राजभाषा संस्थान, देहरादून से संस्थान के निदेशक, नराकास के अध्यक्ष के रूप में श्री सम्मान में शील्ड प्रदान की गयी तथा डॉ. अमर सिंह, वरि. हिन्दी अधिकारी को भी राजभाषा शिल्पी सम्मान में शील्ड प्रदान की गयी।

संस्थान को राजभाषा नीति के श्रेष्ठ निष्पादन के लिए वर्ष 2010-2011 में राजभाषा विभाग द्वारा शील्ड एवं प्रमाण-पत्र।

मुख्य अतिथि प्रो. नीलम सराफ ने अपने ओजस्वी भाषण में कहा कि हिन्दी के प्रयोग व प्रगति के लिए हमें अपनी मानसिकता बदलनी होगी तथा हिन्दी एक सरल, सरस, सुबोध भाषा है जो दुनिया के लगभग सारे देशों में बोली के रूप में बोली जाती है। हिन्दी लगभग सारे चैनलों, दूरदर्शन और प्रिन्ट मीडिया की प्रमुख भाषा है। भारत का प्रत्येक व्यक्ति इसका प्रयोग करने में पूर्णत: सक्षम है।

पुरस्कार वितरण समारोह में धन्यवाद प्रस्ताव करते हुए श्री रमेश कुमार रैणा, वित्त एवं लेखा अधिकारी।

संस्थान के वरि. वैज्ञानिक डॉ. आर.के.रैणा ने अपने संबोधन में कहा कि हिन्दी का प्रयोग सभी संस्थानों तथा देश के सभी नागरिकों के लिए सर्वाधिक प्रयोग की भाषा है। हमें इसका प्रयोग रोजमर्रा के कार्यों में करना चाहिए। तत्पश्चात् सभी विजयी प्रतियोगियों को पुरस्कार एवं प्रमाण-पत्र निदेशक महोदय एवं मुख्य अतिथि ने अपने कर-कमलों से प्रदान किये। धन्यवाद प्रस्ताव संस्थान के श्री रमेश कुमार रैणा, वित्त एवं लेखा अधिकारी ने किया ।

नगर राजभाषा कार्यान्वयन समिति, जम्मू की छमाही बैठक दिनांक 18 दिसम्बर, 2012 को सायं 3.30 बजे भारतीय समवेत औषध संस्थान, जम्मू के कान्फ्रेंस हॉल में सम्पन्न।

भारत सरकार, गृह मंत्रालय, राजभाषा विभाग के निर्देशानुसार नगर राजभाषा कार्यान्वयन समिति, जम्मू की छमाही बैठक दिनांक 18 दिसम्बर, 2012 को भारतीय समवेत औषध संस्थान, जम्मू के कान्फ्रेंस हॉल में आयोजित हुई। बैठक की अध्यक्षता संस्थान के निदेशक एवं नराकास अध्यक्ष डॉ. राम विश्वकर्मा ने की। इस अवसर पर मुख्य अतिथि श्री शैलेश कुमार सिंह, उप निदेशक, भारत सरकार, गृह मंत्रालय, राजभाषा विभाग, उत्तर क्षेत्रीय कार्यान्वयन कार्यालय-1

नराकास बैठक में उपस्थित सदस्यों को संबोधित करते हुए संस्थान के निदेशक एवं नराकास अध्यक्ष डॉ. राम विश्वकर्मा।

(दिल्ली), व श्री राकेश कुमार, उप निदेशक, भारत सरकार, गृह मंत्रालय, राजभाषा विभाग, क्षेत्रीय कार्यान्वयन कार्यालय (उत्तर), गाजियबाद से भी बैठक में उपस्थित हुए, श्री राजेश पुरी, आयुक्त, सीमा शुल्क एवं केन्द्रीय उत्पाद शुल्क, जम्मू, श्री ए.के.तथई, आयुक्त, आयकर कार्यालय, जम्मू, श्री आर.एन.मीना, डी.टी. एम., उत्तर रेलवे, जम्मू, श्री बी.डी.बोहरा, महाप्रबंधक, नवार्ड बैंक, दिल्ली, श्री चन्द्रमोहन, महाप्रबंधक एन.एच.पी.सी.सलाल परियोजना, रियासी, संस्थान के वरि. वैज्ञानिक डॉ. आर.के रैणा तथा नगर जम्मू के केन्द्रीय कार्यालयों/बैंकों/उपक्रमों से पधारे सभी कार्यालय अध्यक्ष/वरि. हिन्दी अधिकारी/हिन्दी अधिकारी/राजभाषा अधिकारी/नोडल अधिकारी/हिन्दी अनुवादक व प्रिन्ट एवं इलैक्ट्रॉनिक मीडिया के सभी संवाददाता उपस्थित थे। बैठक में अधिकारियों/कर्मचारियों की कुल संख्या 80 प्रतिशत से अधिक थी। जिसमें कार्यालय अध्यक्षों की संख्या 75 प्रतिशत थी।

सर्वप्रथम बैठक में उपस्थित सज्जनों का स्वागत डॉ. अमर सिंह, वरि. हिन्दी अधिकारी एवं सचिव, नराकास, जम्मू ने किया। उन्होंने अपने स्वागत संबोधन में कहा, ''कि इस बैठक में प्रथम अप्रैल, 2012 से 30 सितम्बर, 2012 के दौरान आपके कार्यालय में राजभाषा हिन्दी में किये गये कार्यो की समीक्षा तथा इससे संबंधित आपके कार्यालयों में उत्पन्न समस्याओं पर चर्चा की जाएगी। जिसके अन्तर्गत धारा 3(3) का हम सबको अनुपालन सुनिश्चित करना चाहिए। यही संविधान की मूलभावना के अनुरूप होगा। सभी भारतीय भाषाएं देश की एकता की प्रतीक हैं। भारतीय संविधान में जो प्रावधान किये गये हैं इसी के अनुसार हमें आदेशों/अनुदेशों का पालन करना चाहिए और राष्ट्रपति जी के संकल्पों का सम्मान करना चाहिए। संघ के विभिन्न राजकीय प्रयोजनों में इसके प्रगामी प्रयोग को बढ़ावा देने के लिए राजभाषा विभाग प्रति वर्ष एक वार्षिक कार्यक्रम जारी करता है, जिसके अनुसार हम कार्यालयों में राजभाषा के कार्य सम्पन्न करते हैं। चूंकि सरकारी कामकाज में मूल टिप्पण और प्रारूपण के लिए हिन्दी का ही प्रयोग किया जाए।''

तत्पश्चात् बैठक में उपस्थित सदस्यों के परिचय के साथ ही बैठक की कार्रवाई आरम्भ हुई। सचिव, ने गत बैठक के कार्यवृत्त पर चर्चा के दौरान कहा कि सम्माननीय सदस्यों की कोई प्रतिक्रिया, सुझाव अथवा आपत्ति हो तो वे अपने विचार रखें लेकिन माननीय उपस्थित सदस्यों की ओर से कोई आपत्ति एवं प्रतिक्रिया न मिलने पर सचिव ने अध्यक्ष महोदय के अनुमोदन से गत बैठक के कार्यवृत्त की पुष्टि की।नराकास, जम्मू के सदस्य कार्यालयों द्वारा उनकी गृह पत्रिकाएं प्रकाशित की गयी है, जिसमें (1) नराकास, जम्मू की गृह पत्रिका 'ज्ञानवार्ता' अंक-3, (2) पंजाब नेशनल बैंक क्षेत्रीय कार्यालय, जम्मू की गृह पत्रिका 'त्रिकुटा' अंक-8, (3) एन.एचपी.सी. क्षेत्र-।, जम्मू कार्यालय द्वारा गृह पत्रिका 'त्रिकुटा समाचार', (4) पावर ग्रिड कारपोरेशन, पारेषण प्रणाली, क्षेत्र-।।, जम्मू कार्यालय द्वारा गृह पत्रिका 'तवी प्रवाह' अंक-10, (5) सीमा शुल्क एवं केन्द्रीय उत्पाद शुल्क आयुक्त, जम्मू-श्रीनगर द्वारा राजभाषा गृह पत्रिका 'ताज़-ए-हिन्द' अंक-1 (6) प्रसार

संस्थान के निदेशक एवं अध्यक्ष, नराकास डॉ. राम विश्वकर्मा एवं नराकास जम्मू के सदस्यगण राजभाषा गृह पत्रिका ''ज्ञानवार्ता'' के तृतीय अंक का विमोचन करते हुए।

संस्थान को वर्ष 2011-2012 के लिए राजभाषा नीति के श्रेष्ठ निष्पादन हेतु नराकास जम्मू द्वारा प्रथम पुरस्कार प्रदान करते हुए आयुक्त, श्री राजेश पुरी।

भारती, रेडिया कश्मीर, जम्मू की गृह पत्रिका 'तविषी', अंक-1 (7) मुख्य महाप्रबंधक, भारतीय दूरसंचार निगम लिमिटेड, जम्मू द्वारा राजभाषा गृह पत्रिका 'चिनारवाणी' आदि पत्रिकाएं निरन्तर प्रकाशित की जा रही है।

संस्थान के निदेशक एवं अध्यक्ष, नराकास डॉ. राम विश्वकर्मा ने नराकास जम्मू की छमाही राजभाषा गृह पत्रिका ''ज्ञानवार्ता'' के तृतीय अंक का विमोचन किया गया। इस अवसर पर अनेक गणमान्य व्यक्ति उपस्थित थे। प्रसन्नता की बात यह है कि 'ज्ञानवार्ता' राजभाषा पत्रिका को पंजीकृत कर लिया गया है, जिसकी पंजीयन संख्या ISSN 2320-2998 है इससे लेखक लाभान्वित होंगे।

अध्यक्ष महोदय ने वर्ष 2011-2012 के लिए राजभाषा नीति के श्रेष्ठ निष्पादन के लिए जिन सदस्य कार्यालयों को पुरस्कार प्रदान किये गये उनके नाम इस प्रकार हैः- (1) डॉ. राम विश्वकर्मा, निदेशक, भारतीय समवेत औषध संस्थान, जम्मू (2) श्री राजेश पुरी, आयुक्त, सीमा शुल्क एवं केन्द्रीय उत्पाद शुल्क, जम्मू (3) श्री ए.के.तथई, आयुक्त आयकर, आयकर कार्यालय, जम्मू/श्रीनगर (4) श्री गुरेन्दर जीत सिंह, पुलिस महानिरीक्षक, केन्द्रीय रिजर्व पुलिस बल, जम्मू सेक्टर मुख्यालय, जम्मू (5) श्री आर.एन.मीणा, मंडल यातायात प्रबंधक, उत्तर रेलवे, जम्मू (6) श्री अशोक गुप्ता, उप महाप्रबंधक, पंजाब नेशनल बैंक (क्षेत्रीय कार्यालय) जम्मू (7) श्री अजीत कुमार जैन, उप महाप्रबंधक, भारतीय स्टेट बैंक (प्रशासनिक कार्यालय), जम्मू (8) श्री सुरेश कनौजिया, सहायक महाप्रबंधक, आई. डी.बी.आई.बैंक, ग्रिड भवन, रेल हेड काम्पलेक्स, जम्मू (9) श्री एस.सी.रावड़ा, मुख्य महाप्रबंधक, राष्ट्रीय कृषि और ग्रामीण विकास बैंक (नवार्ड), क्षेत्रीय कार्यालय, जम्मू (10) कार्यपालक निदेशक, पावर ग्रिड कारपोरेशन ऑफ इंडिया लिमिटेड, जम्मू (11) कार्यपालक निदेशक, एन.एच.पी.सी.लिमिटेड, क्षेत्रीय कार्यालय (क्षेत्र-1), जे.डी.काम्पलेक्स, जम्मू (12) श्री शबीर मुज़ाहिद, निदेशक, भारतीय प्रसारण निगम, दूरदर्शन केन्द्र, जम्मू (13) श्री अशोक कुमार, वरिष्ठ मंडल प्रबंधक, दि ओरिएण्टल इंश्योरेंश कम्पनी लि., मंडलीय कार्यालय, जम्मू आदि सदस्य कार्यालयों को पुरस्कार एवं प्रमाण-पत्र प्रदान किये गये। तत्पश्चात् राजभाषा नीति के श्रेष्ठ निष्पादन एवं अपने कार्यालय में श्रेष्ठ कार्य करने हेतु समिति के राजभाषा अधिकारियों/अनुवादकों/ नोडल अधिकारियों को अध्यक्ष महोदय ने मेरिट प्रमाण-पत्र प्रदान किए ।

बैठक में राजभाषा नीति कार्यान्वयन पर चर्चा एवं सदस्यों की प्रतिक्रियाएं उनके महत्वपूर्ण सुझाव जो इस प्रकार हैः-

श्री शैलेश कुमार सिंह, उपनिदेशक, भारत सरकार, गृह मंत्रालय, राजभाषा विभाग, क्षेत्रीय कार्यान्वयन कार्यालय दिल्ली अपने विचार व्यक्त करते हुए कहा, ''कि नराकास जम्मू की ओर से राजभाषा पत्रिका ''ज्ञानवार्ता'' का प्रकाशन महत्वपूर्ण उपलब्धि है और राजभाषा नीति कार्यान्वयन की दिशा में उत्कृष्ट प्रयास हैं उन्होंने अध्यक्ष महोदय को इस प्रयास के लिए हार्दिक बधाई दी। उन्होंने कहा कि जम्मू नराकास राजभाषा कार्यान्वयन की दिशा में महत्वपूर्ण भूमिका अदा कर रही है। जो 'क' क्षेत्र की अपेक्षा भी उत्कृष्ट प्रयासों के ओर अग्रसर है। यहां कई कार्यालयों में अपनी गृह पत्रिकाएं प्रकाशित की हैं जिसमें पावर ग्रिड कारपोरेशन, जम्मू, पंजाब नेशनल बैंक क्षेत्रीय कार्यालय-।, जम्मू, रेडियो कश्मीर, जम्मू, मुख्य महाप्रबंधक, बीएसएनएल., जम्मू, सीमा शुल्क एवं केन्द्रीय उत्पाद शुल्क, जम्मू, एन.एच.पी.सी. क्षेत्र-। कार्यालय, जम्मू आदि के माध्यम से प्रकाशित की जा रही हैं। उन्होंने कहा कि वर्ष 2012-2013 का राजभाषा सम्मेलन अध्यक्ष, नराकास कार्यालय के सहयोग से करने का प्रस्ताव है जो मार्च, 2013 में करने का है उन्होंने यह भी कहा कि सम्मेलन के आयोजन हेतु प्रत्येक कार्यालय से सहयोग राशि देने की अपेक्षा की जिससे आवश्यक वस्तुओं की पूर्ति की जा सके। उन्होंने सभी सदस्य कार्यालयों से सम्मेलन को सफल बनाने की अपील की साथ ही उन्होंने 17.12.2012 को एक समिति का गठन अध्यक्ष महोदय के निर्देशन में किया है। जिसमें दस कार्यालयों को शामिल किया गया है।

संस्थान के निदेशक एवं अध्यक्ष, नराकास जम्मू डॉ. राम विश्वकर्मा ने सभागार में उपस्थित नगर के कार्यालय प्रमुखों एवं अन्य गणमान्य व्यक्तियों का स्वागत करते हुए अपने अध्यक्षीय संबोधन में कहा कि इस प्रकार की बैठकों का आयोजन हम सब मिलकर संयुक्त रूप से एक कार्यालय से दूसरे कार्यालय में करने का सुझाव दिया और उन्होंने अगली बैठक के लिए किसी अन्य कार्यालय में आयोजित करने पर अपनी सहमति व्यक्त की। संस्थान में हिन्दी पुस्तकों के उपलब्धता के बारे में जानकारी देते हुए

कहा कि हमने भारतीय ज्ञानपीठ से पुरस्कृत महत्वपूर्ण पुस्तकें जो इस वर्ष के दौरान प्रकाशित हुई हैं जिन्हें पुस्तकालय के माध्यम से क्रय करवायी हैं साथ ही उन्होंने सांस्कृतिक कार्यक्रम के विषय पर अपने विचार व्यक्त करते हुए कहा कि जम्मू कश्मीर कल्चरल एकैडमी के माध्यम से सांस्कृतिक कार्यक्रम के आयोजन किया गया, जो सांस्कृतिक दृष्टि से बहुत ही उत्कृष्ट है, उन्होंने राजभाषा सम्मेलन जो प्रथम मार्च, 2013 को नगर राजभाषा कार्यान्वयन समिति, भारतीय समवेत औषध संस्थान, जम्मू के सभागार में आयोजित करने पर पूर्ण सहमति व्यक्त की साथ ही उन्होंने समिति को आश्वस्त किया कि राजभाषा सम्मेलन से संबंधित कार्यक्रम की समीक्षा के लिए एक समिति गठित करने का सुझाव दिया और हर पन्द्रह दिन के बाद स्वयं इसकी समीक्षा करने को कहा। इस वर्ष लगभग समिति के सभी कार्यालयों ने बड़े बेहतर ढंग से हिन्दी दिवस/सप्ताह/पखवाड़े आदि आयोजित किए आप इसी श्रृंखला को भविष्य में भी कायम रखेंगे। गृह पत्रिका 'ज्ञानवार्ता' का तृतीय अंक आपको समर्पित है। राष्ट्रीय परिप्रेक्ष्य में सरकार के आदेशों/अनुदेशों/नियमों का पालन करना है, क्योंकि हम सरकारी नियमों के अनुपालन के लिए प्रतिबद्ध हैं। हमें आशा है कि अगले अंक में भी आप अच्छी रचनाएं एवं लेख प्रस्तुत करेंगे। सभी लेखकों, रचनाकारों, संपादक एवं संपादक मंडल को हार्दिक बधाई। हिन्दी से जुड़े स्टॉफ सदस्यों ने अपने कार्यालयों में हिन्दी के लिए अच्छे कार्य सम्पादित करने वाले

सचिव, नराकास, डॉ. अमर सिंह उपस्थित सदस्यों का आभार व्यक्त करते हुए।

हिन्दी अनुवादकों/हिन्दी अधिकारियों/राजभाषा अधिकारियों/हिन्दी सहायकों एवं अन्य हिन्दी प्रेमियों को प्रमाण-पत्र प्रदान किए जा रहे हैं और कुछ कार्यालय भी जो हिन्दी की प्रगति के लिए अच्छा वातावरण बनाए हुए हैं। हम उनका हृदय से आभार व्यक्त करना चाहते हैं और संस्थान के वरि. हिन्दी अधिकारी, डॉ. अमर सिंह ने जो इस समिति के सदस्य के रूप अपनी सेवाएं दे रहें हैं और सभी कार्यालयों के कार्यालय प्रमुखों से मिलकर समिति में हिन्दी कार्यान्वयन को दिशा देने में उनका योगदान भी सराहनीय है।

अन्त में सदस्य सचिव, डॉ. अमर सिंह ने अध्यक्ष महोदय तथा संस्थान के निदेशक डॉ. राम विश्वकर्मा जी का बैठक में महत्वपूर्ण समय देने के लिए उनके विशिष्ट योगदान के लिए उनका हृदय से आभार व्यक्त किया। बैठक में मुख्य अतिथि के रूप में राजभाषा विभाग, क्षेत्रीय कार्यान्वयन कार्यालय, दिल्ली से उपनिदेशक, श्री शैलेश कुमार सिंह ने भी अपना बहुमूल्य समय देने के लिए उनका आभार व्यक्त किया। नराकास जम्मू के सभी केन्द्रीय कार्यालयों/बैंकों/उपक्रमों के कार्यालय प्रमुखों, हिन्दी अधिकारियों/हिन्दी अनुवादकों एवं नगर के प्रिन्ट व इलैक्ट्रानिक मीडिया के सभी संवाददाताओं का आभार व्यक्त करते हुए कहा कि मीडिया का सदैव इस बैठक में सहयोग रहा है। बैठक के आयोजन में प्रबंधन के लिए संस्थान के समस्त स्टॉफ सदस्यों का आभार सहित धन्यवाद किया।

63वाँ गणतंत्र दिवस

गणतंत्र दिवस की 63वीं वर्षगांठ के पावन अवसर पर संस्थान के निदेशक डॉ. राम विश्वकर्मा सबको हार्दिक शुभकामनाएं एवं बधाई देते हुए कहा कि आज के दिन हमारे देश का संविधान लागू हुआ था। 26 जनवरी, 1950 को हमने एक अन्तर्विरोधों के जीवन में प्रवेश किया था। 26 जनवरी गणतंत्र दिवस जो आजादी को याद करने का दिन है क्योंकि इसी दिन हमारा संविधान लागू हुआ था और अंग्रेजों के समय से चले आ रहे नियम/कानूनों से हमें मुक्ति मिली थी। इस राष्ट्रीय प्रस्ताव पर चिन्तन करना होगा। हमें गणतंत्र दिवस पर कुछ नये संकल्प लेने होंगे जिन पर अमल कर आप एक अच्छे नागरिक बने रहें ताकि आप राष्ट्र निर्माण में आपकी भूमिका रहे। किसी लोकतांत्रिक/प्रजातांत्रिक देश में विधि मानव जीवन का प्रमुख आधार होता है जबकि किसी देश के कानून का ज्ञान सभी नागरिकों को हो ताकि वे अनेक प्रकार के जूल्मों से बच सकें। भारत में नई विधि व्यवस्था एवं मौलिक अधिकारों की पूर्ण स्थापना संविधान में 26 जनवरी, 1950 को लागू होने के साथ हो चुकी थी, हालाँकि उसका आंशिक रूप में प्रारम्भ 26 नवम्बर, 1949 को ही हो

गया था जब संविधान को संविधान सभा ने अधिनियमित किया था। सामाजिक, आर्थिक, न्यायायिक तथा राजनैतिक दृष्टि से भारतीय परम्परा में यह एक नये युग का सूत्र पात हुआ था, क्योंकि हमारी विधि व्यवस्था में वे काले कानून और अमानुषिक व्यवहार निषिद्ध हो गये थे, जिन्होंने आदमी की गरिमा प्रतिष्ठा तथा मान-सम्मान को नष्ट-भ्रष्ट कर दिया था।संविधान विधि का संबंध प्राय: किसी देश के शासन एवं कानून व्यवस्था से होता है। संविधान लिखित प्रारूप, प्रलेखों या नियमों, लोकाचारों, परम्पराओं और व्यवहारों पर आधारित हो सकता है। इसमें उन विविध नियमों का संग्रह होता है जिनके अनुसार उस देश की शासन व्यवस्था संचालित की जाती है। वह शासन के संरचनात्मक एवं कार्यात्मक पक्षों का विस्तृत स्वरूप तथा संगठन निर्धारित करता है।

राज्यों के कार्यों को संचालित करने वाले नियमों/कानूनों एवं सिद्धान्तों को समिष्ट कर संविधान की संज्ञा दी गयी है जो यह निश्चित् करता है कि व्यवस्था किस प्रकार हो उसके विधि अंग कौन-कौन से हों उन अंगों में परस्पर क्या संबंध तथा शक्तियां हों नागरिकों के क्या अधिकार एवं कर्तव्य हों तथा शासक एवं शासित के बीच किस तरह के संबंध हों। संविधान मुख्य धारा अथवा जीवन पद्धति को निर्धारित करने का विधिक अंग है।

जब नये संविधान का निर्माण संविधान सभा की प्रथम बैठक 9 दिसम्बर 1946 को आरम्भ हुई तब यह उम्मीद नहीं थी कि डॉ. अम्बेडकर की भूमिका इतनी सार्थक एवं निर्णायक रहेंगी जितनी की कालांतर में सिद्ध हुई। इन्हें संविधान प्रारुप (ड्राफ्ट) समिति का अध्यक्ष बनाया गया जिन्होंने नये संविधान की समस्त निर्माण प्रक्रिया में उनके विचार-विमर्श तथा मौलिक संशोधन में महत्वपूर्ण निर्णय स्वयं लिए और संविधान सभा से पारित करवाए संविधान 25 नवम्बर 1949 को बनकर तैयार हुआ तब उनके पूर्व अनेक सदस्यों ने डॉ. अम्बेडकर की बौद्धिक क्षमता, लगन, ज्ञान, सहभागिता तथा रचनात्मक भूमिका की विशेष सराहना की और उन्हें संविधान का मुख्य शिल्पकार तथा आधुनिक मनु की संज्ञा दी। नि:सन्देह डॉ. अम्बेडकर संविधान के मुख्य निर्माता निर्देशक कहे गये।

63 वें गणतंत्र दिवस पर ध्वजारोहण करते हुए संस्थान के निदेशक डॉ. राम विश्वकर्मा ।

हमारे राष्ट्रीय झण्डें में क्या अभिलाषाएं अपेक्षित हैं और राजनैतिक, सामाजिक, बौद्धिक तथा सांस्कृतिक क्षेत्रों में इन अभिलाषाओं को पूर्ण कर सके जहां अशोक चक्र कानून व्यवस्था के धर्मचक्र का प्रतिनिधित्व करता है वहीं भगवा रंग त्याग का प्रतीक है तथा हरा रंग मिट्टी पेड़-पौधों से हमारे जुड़ाव का प्रतीक है जिस पर सम्पूर्ण जीवन निर्भर है हमें आत्मानुशासन और सत्य के लिए सफेद रंग से निर्देशित होना चाहिए इसी प्रकार हम सबको संगठित एवं भावुक होकर राष्ट्र-निर्माण में योगदान देना होगा।

आज हमारा भारत बढ़ते विदेशी मुद्रा भण्डार, सूचना प्रौद्योगिकी के क्षेत्र में विज्ञान प्रगति के लिए विकसित देशों की भाँति उन्नति की दौड़ में आगे आया है वहीं व्यापार औद्योगिकीकरण और निवेश में बढ़ोत्तरी हुई है लेकिन आगे भी प्रगति की दौड़ में आगे बढ़ना है। नि:सन्देह भारत आर्थिक दृष्टि से सम्पन्न होता है तो वैज्ञानिक क्षेत्र में अनुसंधान के लिए आर्थिक ढांचे को और अधिक मजबूत

गणतंत्र दिवस के अवसर पर आर.आर.एल.हाई स्कूल के बच्चों द्वारा नृत्य प्रस्तुत करते हुए

कर सकेगा। हमें पैशन करने का काम करने का जज्बा जिसके बल पर युवा क्रांतिकारियों ने आजादी दिलाने के लिए सहयोग दिया था। आज प्रतिस्पर्दा का युग है हम प्रतियोगी बनकर सफलता प्राप्त कर सकते है हमें निराश नहीं होना चाहिए यह मूवमेन्ट हमें सिखाता है कि हमें निरन्तर प्रयास करने होंगे सूचना और प्रौद्योगिकी, कृषि, स्वास्थ, शिक्षा विज्ञान के क्षेत्र में भारत आगे बढ़ा है। हम भारत के लोग सत्यनिष्ठा पूर्वक संकल्प लें कि भारत को एक संप्रभु, समाजवादी,

पंथनिर्पेक्ष, लोकतांत्रिक, गणतंत्र में विश्वास स्थापित करें, लेकिन हमें यह भी देखना है कि संविधान के आदर्श किस रूप में वास्तविकता में रूपान्तरित हुए हैं। हमें संप्रभुता की अभिव्यक्ति सार्थक बनानी होगी। मानव मूल्यों की श्रेणी में आने वाले प्रमुख आदर्श प्रजातंत्र, न्याय, स्वतंत्रता, समानता, भाई-चारा, करूणा, मित्रता, अहिंसा, धर्म-निरपेक्षता और साहस का निर्भीकता, जो विधिक एवं प्रासंगिकता जो एक ओर संस्थागत होने की क्षमता रखते हैं तो दुसरी ओर नागरिकों के आचारण संहिता के लिए मानक भी हैं इनकी रक्षा करनी होगी। इस अवसर पर उन्होंने संस्थान की रचनात्मक प्रमुख उपलब्धियों पर विस्तार से चर्चा की और अपने महत्वपूर्ण विचार प्रस्तुत किए तथा आर.आर.एल.स्कूल के बच्चों द्वारा सांस्कृतिक कार्यक्रम प्रस्तुत किए गये।

अत: इस ऐतिहासिक अवसर पर मैं जाति, वर्ग, भाषा, धर्म और क्षेत्रीयता के तुच्छ भेद-भाव से ऊपर उठकर शान्ति, समृद्धि और प्रगति के मार्ग पर चलते हुए राष्ट्रीय एकता व अखण्डता को मजबूत करने के लिए भारतीय संविधान में प्रदत्त लोक कल्याणकारी शक्तियों को मजबूत बनाएं।

दिनांक 13-14 मार्च, 2013 तक दो दिवसीय राजभाषा सम्मेलन/भाषा कौशल/कंप्यूटर प्रशिक्षण कार्यक्रम

नगर राजभाषा कार्यान्वयन समिति, भारतीय समवेत औषध संस्थान, जम्मू के तत्वाधान में हाउसिंग एंड अर्बन डेवलपमेंट कॉरपोरेशन, क्षेत्रीय कार्यालय, जम्मू, रूरल इलेक्ट्रीफिकेशन कॉरपोरेशन लिमिटेड, आंचलिक कार्यालय, जम्मू, पंजाब नेशनल बैंक, मंडल कार्यालय, जम्मू तथा भारतीय स्टेट बैंक, प्रशासनिक कार्यालय, जम्मू के सौजन्य से दिनांक 13-14 मार्च, 2013 तक दो दिवसीय राजभाषा सम्मेलन/भाषा कौशल/कंप्यूटर प्रशिक्षण कार्यक्रम का आयोजन भारतीय समवेत औषध संस्थान, जम्मू के कान्फ्रेंस हॉल में किया गया। प्रशिक्षण कार्यक्रम की अध्यक्षता संस्थान के निदेशक एवं नराकास के अध्यक्ष डॉ. राम विश्वकर्मा ने की। इस अवसर पर श्री हरजीत कुमार, क्षेत्रीय प्रमुख, हाउसिंग एंड अर्बन डेवलपमेंट कॉरपोरेशन, क्षेत्रीय कार्यालय, जम्मू, श्री अजीत कुमार जैन, उपमहाप्रबंधक, भारतीय स्टेट बैंक, प्रशासनिक कार्यालय, जम्मू, श्री अशोक गुप्ता, उपमहाप्रबंधक, पंजाब नेशनल बैंक, मंडल कार्यालय, जम्मू, श्री राकेश सरीन, आंचलिक प्रबंधक, रूरल इलेक्ट्रीफिकेशन कारपोरेशन लिमिटेड, आंचलिक कार्यालय, जम्मू, संस्थान के वरिष्ठ वैज्ञानिक डॉ. आर.के.रैणा, श्री ओम प्रकाश, प्रशासनिक अधिकारी तथा नराकास, जम्मू के सभी सदस्य कार्यालयों के नोडल अधिकारी/वरिष्ठ राजभाषा अधिकारी/हिन्दी अनुवादक तथा प्रिन्ट एवं इलेक्ट्रॉनिक मीडिया के सभी सम्वाददाता एवं अन्य गणमान्य व्यक्ति उपस्थित थे। कार्यक्रम

दिनांक 13-14 मार्च, 2013 दो दिवसीय राजभाषा सम्मेलन/भाषा कौशल/कंप्यूटर प्रशिक्षण कार्यक्रम को संबोधित करते हुए संस्थान के निदेशक एवं अध्यक्ष, नराकास डॉ. राम विश्वकर्मा ।

का शुभारम्भ दीप प्रज्ज्वलन कर संस्थान के निदेशक एवं उनके साथ अन्य अतिथियों एवं सरस्वती वंदना गायन से श्री कृष्ण निर्मल ने कार्यक्रम का शुभारम्भ किया गया। सर्वप्रथम कार्यशाला में वक्ता डॉ. महेशचन्द्र गुप्त, सदस्य, हिन्दी सलाहकार समिति, मानव संसाधन विकास मंत्रालय, गृह मंत्रालय, विज्ञान एवं प्रौद्योगिकी मंत्रालय, भारत सरकार, नई दिल्ली एवं श्री कृष्ण निर्मल, शिक्षा अधिकारी, नई दिल्ली एवं नराकास, जम्मू के विभिन्न

निदेशक महोदय का शॉल से सम्मान करते हुए श्री हरजीत कुमार, प्रमुख हडको, जम्मू

कार्यालयों/बैंकों/उपक्रमों से आये प्रतिभागीगण श्री अमित कुमार, आई.टी. प्रबंधक, पी.एन.बी., जम्मू एवं श्री कमलेश सिंह, आई.टी. अनुभाग, आई.आई.आई.एम., जम्मू ने स्लाइड के माध्यम से यूनिकोड पर प्रशिक्षण दिया। इस कार्यक्रम के माध्यम से नगर जम्मू के केन्द्रीय कार्यालयों/बैंकों/उपक्रमों से आये अधिकारी/कर्मचारी ने प्रशिक्षण कार्यक्रम से लाभान्वित हुए।

कार्यक्रम के समाप्ति पर दिनांक 14 मार्च, 2013 को डॉ. आर.के.रैणा, मुख्य वैज्ञानिक, आई.आई.आई.एम., जम्मू व डॉ. महेशचन्द्र गुप्त ने प्रतिभागियों को अपने कर-कमलो द्वारा प्रमाण-पत्र एवं स्मृति-चिन्ह वितरित किये। इस कार्यक्रम का संचालन डॉ. अमर सिंह, सदस्य-सचिव, नराकास, जम्मू ने किया।

अन्त में धन्यवाद प्रस्ताव श्री ओम प्रकाश, प्रशासनिक अधिकारी, भारतीय समवेत औषध संस्थान, जम्मू ने प्रस्तुत किया।

श्री महेशचन्द्र गुप्त, हिन्दी सलाहकार समिति, दिल्ली को स्मृति चिन्ह प्रदान करते हुए वरिष्ठ वैज्ञानिक, डॉ. आर.के.रैणा ।

HUMAN RESOURCE

Director
Dr. Ram A Vishwakarma

Chief Scientist
Dr. S .C. Taneja
Dr. Surinder Kaul
Dr. Rajinder Parshad
Dr. R. K Raina
Dr. Y. S. Bedi
Dr. J. K. Dhar
Dr. R. K. Johri
Dr. A. K. Saxena
Dr. Sushma Koul
Dr. Suresh Chandra
Dr. R .K. Khajuria
Dr. V.K.Gupta
Mr. D.K. Sultan
Dr. Ashok Ahuja

Sr. Principal Scientist
Mr. Rajneesh Anand
M.r. R.K. Malhotra
Dr. Baldev Singh

Principal Scientist
Dr. Dilip Manikrao Mondhe
Mr. Abdul Rahim
Dr. Anindya Goswami
Dr. Muzamil Ahmad
Dr. J.L. Koul
Mrs. Geeta Mehta
Dr. Inshad Ali Khan
Dr. D.K. Gupta
Dr. Zabeer Ahmed
Dr. Gurdarshan Singh
Dr. Parthasarthi Das

Sr. Scientist
Dr. Rajkishore Rai
Dr. Subash Singh
Dr. P.N. Gupta
Dr. Zahoor Ahmad Parry
Dr. Asha Chaubey
Dr. Shashank Kr.Singh
Dr. Mrs Meenu Katoch
Dr. Abid Hamid Dar
Dr. Mohd Jamal Dar
Dr. Sandip B. Bharate
Dr. Asif Ali
Dr. Qazi Naveed Ahmad
Dr. Prasoon Kumar Gupta

Scientist
Dr. Shashi Bhushan
Dr. Sheikh Tasduq Abdullah
Dr. Fayaz Ahmad Malik
Dr. Dhiraj Kumar Vyas
Dr. Sumit G Gandhi
Mrs. Deepika Singh
Dr. Govind Yadav
Mr. Anil Kumar Katare
Dr. Bilal Ahamd Bhat
Dr. Qazi Parvaiz Hassan
Dr. Kursheed Ahmad Bhat
Dr. S.D. Sawant
Dr. (Mrs) Suphla Bajpai Gupta
Dr. Debaraj Mukherjee
Mr. Amit Nargotra
Dr. Payare Lal Sangwan
Dr. Syed Riyaz-Ul-Hassan
Dr.(Mrs.) Nasheeman Ashraf
Dr. Sumeet Gairola
Dr. Prashant Misra

Jr. Scientist
Dr. Parvinder Pal Singh
Dr. Bhahwal Ali Shah
Dr. Sundeep Jaglan

Principal Technical Officer
Dr. Arun Kumar
Mr. M.K.Tikoo
Dr. J.P. Sharma
Mr. Rakesh Bhasin
Dr. Bal krishan
Dr. Surjit Singh
Dr. Surrinder K. Lattoo
Mr. Prabhu Dutt
Dr. Anupurna Kaul
Dr. Anamika Khajuria
Dr. P.R.Sharma

Sr. Technical Officer (III)
Mr. RK. Thapa
Mrs. Urmila Jamwal
Mr. R.K. Khajuria

Mr. Surinder Kitchlu
Dr. Satya Narayan Sharma
Mr. Vijendra Kumar
Mr. L.R. Manhas
Mr. Chandji Raina
Mr. Shankar Lal
Dr. Kanti Rekha
Dr. Rekha Sapru
Mr. L.K. Bhan
Dr. A K Tripathi
Mrs. Suman Koul
Mr. Vinay Kumar Gupta

Sr. Technical Officer (II)
Mrs. Pinki Koul
Dr. Ajai Prakash Gupta
Mr. Rajinder Kumar

Tech Officer (I)
Mrs. Asha Bhagat
Dr. Buddh Singh
Mr. Sunil Kumar

Medical Officer
Dr. Amit Sharma
Dr. Mrs. Anju Gupta

Library Officer
Mr. Rakesh Singh Bisen

E. E (Civil)
Mr. Gurinder Pal Singh

E.E (Elect.)
Mr. Ashwani Chopra

Jr. Engr
Mr. S.N. Bharati

Technical Officer A
Mr. Jasbir Singh
Mr. Siya Ram Meena
Mr. Ajit Prabhakaran

Technical Assistant
Mr. Mahendara Kr. Verma
Mrs. Bhavna Vij
Mr. Gourav Sharma
Mr. Manish Kumar
Mr. Vijay Budania
Mr. Kamlesh Singh
Mr. Sumit Kumar
Dr. Shashid Rasool
Mr. Arvind K. Yadav
Mr. Yogesh Kumar
Mr. Amit Kumar
Mr. Brijender Koli
Mr. Rajinder Gochar
Mr. Nitin Ashok Narkhede

Sr. Technician
Mr . Sudhir Nanda
Mr. V. K. Khanna
Mr . Manoharlal Sharma
Mr. Inderjit Singh
Mr. Vijay Kumar
Mr . Ajeet Singh
Mr. Ramesh Kumar
Mr. Sardari Lal
Mrs. Raj Kumari
Mr. Nagar Singh
Mr. Kuldip Raj
Mr. Jeet Singh
Mr. Ram Rakha
Mr. Gulshan Kumar
Mr. S.k. Rattan
Mr. Ali Mohd. Hajam
Mr. Prithi Pal
Mr. Vikram Abrol
Mr Bhushan Lal
Mr. Nirmal Singh
Mr. OM Singh
Mr Parshotam Kumar
Mr T.S. Salathia
Mr. Jasbir Singh
Mr Ravinder Wali
Mrs. Kamlesh Sharma
Mrs. Manju Sambyal
Mrs. Neelam Sharma
Mr. A. K. Sharma
Mr. Parshotam Kumar
Mr. Madan Lal
Mr. Kuldeep Singh
Mr. Rajinder Kumar Gupta
Mrs. Sunita Devi
Mr. R. L. Jolly
Mr. A.K. Mehra
Mr. Vikram Bhardwaj
Mrs. Parveen Sharma
Dr. Ravinder Kour
Mrs. Shabnam Khan

Technician
Mr. Pushap Rattan
Dr. Anil Prabhakar
Mr. Ashwani Sharma
Mr. Partap Chand
Mr. S.k. Ganjoo
Mr. Samar Singh
Mrs. Kiran Koul
Mr. Satya Bhushan
Mrs. Sarla Bhat
Mr. Rajinder Kumar
Mr. Naresh Pal
Ms. Anjum Vashist
Mr. Rajesh Kumar Sahdev
Mr. Surinder Kumar
Mr. Bachitar Singh
Mr. Ashok Kumar
Mr. Kewal Singh
Mr. Kasturi Lal
Mr. Girdhari Lal

Lab Assist.
Mrs. Santosh Baigra
Mr. Dilbag Rai
Mr. Jita Ram
Mr. Shimlu Ram
Mr. Girdhari Lal
Mr. Gulam Quadir Sheikh
Mr. Chaman Lal
Mr. Bishan Kumar
Mr. Jasbir Singh
Mr. Kuldeep Kumar
Mr. Madan Lal
Mr. Moti Ram
Mr. Nasibu Ram
Mr. Sham Lal Bhagat
Mr. Sham Lal
Mr. V.P. Kohli
Mr. Balwant Raj
Mr. Hens Raj
Mr. Kartar Chand
Mr. Sham Lal
Mr. Ram Pal
Mr. Balwant Raj
Mr. Babu Ram
Mr. Dila Ram
Mr. Gudu Ram
Mr. Abid Hamid Dar
Mr. Karam Chand
Mr. Wali Wani
Mr. Mohd. Wani.
Mr. Rasool Mir
Mr. Neel Kamal
Mr. Rishi Kumar
Mr. Balwinder Singh
Mr. Manoj Kumar
Mr. Ajit Ram
Mr. Lal Chand
Mr. Om Parkash
Mr. Girdhari Lal
Mr. Abdul Ahad Sheikh
Mr. Fayaz Ahmad Dhar
Mr. Bushan Lal
Mr. Naranjan Singh
Mrs. Darshana
Mr. Nagar Lal
Mr. Kuldeep Kumar

Admn. OfficerGr(1)
Mr. Om Parkash

Finance & Accounts Officer
Mr. Upendra Kumar
Mr. R.K.Raina

Store & Purchase Officer
Mr. Ashok Kumar

Sr. Hindi Officer
Dr. Amar Singh

Hindi Officer
Dr. Rama Sharma

Section Officer
Mr. S.R. Alam
Mr. Rajesh Kumar Gupta

Section Officer(Store & purchase)
Mr. B.B. Gupta
MR. Ram Singh

Private Secretary
Mr. Ramesh Kumar

Section Officer(F & A)
Mr. Anil Gupta
Mr. Darshan Singh

Security Officer
Mr. Yashpal Singh

Assistant General Gr(1)
Mrs. Vijay Bazaz
Mr. Major Singh
Mr. Anil Kumar Gupta
Mr. Romesh Kumar Mottan
Mr. U.S. Thappa
Mrs. Kusum Bali
Mrs. Neelam Razdan
Mr. Ranjeet Kr. Gupta
Mr. Manoj Kumar
Ms. Nisha Vij
Mr. Rajinder Singh
Mrs. Kiran Dutta
Mr. Ashok Kumar

Asst.(F&A) Gr(1)
Mr. Tarsem Lal
Mr. Umesh Malhotra
Mr. H.K Gupta

Asst.(S&P) Gr(1)
Mr. Satish Sambyal
Mr. Y.K. Mishra
Mrs. Rajni Kumari

Senior Stenographer
Mr. V.K. Sharma
Mrs. Phoola Kumari

Security Asstt.
Mr. Mohan Lal
Mr Krishan Lal

Receptionist
Ms. Jyoti Prabha

Asstt. (G)Gr(1)
Mrs. Rekha Gupta
Mr. Benjamin
Mr. Mohd. Ayub Bhat

Asstt (F&A) Gr(II)
Mr. Vinod Kumar Meena
Mrs. Lovely Ganjoo.
Mrs. Saroj Mehta
Mr. Sanchit Kumar Sharma

Asstt (S&P) Gr(II)
Mr. Bua Ditta
Mr. Angrez Singh

Asstt (F&A) Gr(III)
Mr. Roshan Lal

Asstt (G) Gr(III)
Mrs. Sunita Kumari

Record Keeper
Mr. Tilak Raj-Gr.B
Mr. Amar Nath-Gr.C

Halwai
Mr. Janak Raj

Work Assist.
Mr. G. M. Mir
Mr. Milkhi Ram
Mr. Paras Ram
Mr Sham Lal
Mr. Panna Lal
Mr Rahim Mir
Mr. Jagdish Singh
Mr. Romesh Kumar
Mr. Chaman Lal
Mr. Parshotam Lal
Mr. Mohd. Farooq Bhat
Mr. Banadic Hans
Mr. Ram Lal
Mr. Ashok Kumar
Mr. Tarseem Kumar
Mr. Pawan Kumar
Mr. Rajesh k. Tandon
Mr. Moses Tegi
Mr. Girdhari Lal.
Mr Sodhagar Mal
Mr. Rashpal
Mr. Prithvi Raj
Mr. Mangal Dass
Mr. Sham Lal
Mr. Subash Chander
Mrs. Ratna
Mr. Girdhari Lal
Mr. Suram Chand
Mr. Bala Ram
Mr. Tara Chand
Mr. Rattan Lal
Mr. Sham Lal
Mr. Kala Ram
Mr. Ashok Kumar
Mrs. Satya Sharma
Mr. Bua Ditta
Mr. Kehar Singh
Mr. Sat Pal
Mrs. Ram Pyari
Mr. Seva Ram
Mr. Sodagar Lal
Mr. Madan Lal
Mr. Ram Ditta
Mr. Sodagar Mal
Mr. Krishan Chand
Mr. Noor Mohd. Dar
Mr. Ashok Kumar
Mr. Munna
Mr. Dev Raj
Mr. Surinder Kumar
Mr. Ashok Kumar
Mr. Karnail Chand
Mr. Bachan Lal
Mr. Kali Das
Mr.Daleep Raj
Mr. Sham Lal
Mr.Sodagar Lal
Mrs Ram Pyari.

CSIR-IIIM

सीएसआइआर–भारतीय समवेत औषध संस्थान, जम्मू–180001 (भारत)

CSIR-INDIAN INSTITUTE OF INTEGRATIVE MEDICINE

JAMMU-180001 (INDIA)